

DISS. ETH NO. 24366

**IRON BIOFORTIFICATION OF RICE USING NOVEL STRATEGIES
ENCOMPASSING INTER- AND INTRA- CELLULAR IRON TRANSPORT AND
STORAGE**

A thesis submitted to attain the degree of
DOCTOR OF SCIENCES of ETH ZURICH
(Dr. sc. ETH Zurich)

Presented by
Ting-Ying Wu

M.Sc. in Biochemical Science and Technology,
National Taiwan University, Taiwan

Born on 12th November 1989
Citizen of Taiwan

Accepted on the recommendation of

Prof. Dr. Wilhelm Gruissem, examiner

Dr. Navreet Bhullar, co-examiner

Prof. Dr. Beat Keller, co-examiner

Prof. Dr. Samuel Zeeman, co-examiner

2017

Acknowledgements

I gratefully acknowledge Mrs. Jacqueline Imhof and the ETH research for the opportunity and funding on my PhD work.

I would like to express my appreciation to **Dr. Navreet K. Bhullar** and **Prof. Dr. Wilhelm Gruissem** for their valuable guidance and supervision. I gratefully thank Prof. Dr. Beat Keller and Prof. Dr. Samuel Zeeman for their suggestions in committee meetings.

I gratefully thank Björn Studer for his kind guidance on ICP-OES instruction and Prof. Dr. Schulin Rainer for the access of the ICP-OES machine. I acknowledge Dr. Michaela Stettler, Martina Zanella and Wuyan Wang for the experimental support. I sincerely thank Irene Zurkirchen, Doris Russenberger, Daniela Rothe, Kim Schlegel, and Serena Rigotti for their kind helps and technical supports during my PhD life. Special thanks to Julia for the German translation. Thanks to all cereal member; Kulaporn Boonyaves, Kumar Vasudevan, Simrat Pal Singh, Jonghwa Park and Meng Wang who always generously help me and bring the lively atmosphere in the laboratory and the fun moments we have during my PhD.

Thanks to Asuka, Melanie, Adrian, Ravi, Katja, Simon, Joanne, Sira, Wilfred, Johannes, Matthias, Philip, Rolf, Joel, Ezequiel, Nathalie, Emily, Devang, Julia, Glen, Sebastian, Marius, Christelle, Maria and Ima for their helps and cooperation in the laboratory and fun moments we have during Apéro, coffee break and movie night.

Last but not least, thanks to my family who always support my decision.

Summary

Micronutrient malnutrition is a widespread problem worldwide and is among one of the most critical challenges to human health today. Iron deficiency anemia (IDA) is one of the most serious micronutrient deficiencies affecting around 1.6 billion people in both developed and developing countries. Most staple crops that support the global food supply, including rice, are a poor source of iron. Possible strategies to combat IDA include iron supplementation of specific population groups at high risk, iron fortification of foods and increased food diversity. These strategies however often face implementation problems due to socio-economic and/or biological reasons. Being a sustainable and cost effective approach, biofortification holds a great potential for addressing the micronutrient malnutrition. The polished rice grains contain very little amount of iron and due to limited germplasm variability, it has not been possible to increase endosperm iron concentration in rice grains using conventional breeding. Genetic engineering approaches targeting iron uptake, transport and storage within the plants have met with varied degree of success and promising lines with increased endosperm iron concentration have been developed. Despite these reports, there is limited evidence on engineering for intracellular iron mobilization to enhance final grain iron concentration.

In this work, I evaluated the potential of genes encoding vacuolar transporters, i.e. *NATURAL RESISTANCE-ASSOCIATED MACROPHAGE PROTEIN 3 (NRAMP3)* and *VACUOLAR IRON TRANSPORTER (VIT2)* and the gene encoding a citrate transporter *FERRIC REDUCTASE DEFECTIVE 3 (FRD3)* in increasing the endosperm iron concentrations when expressed together with *NICOTINAMINE SYNTHASE (NAS)* and *FERRITIN (FER)*. The transformed rice lines expressing *Arabidopsis thaliana NRAMP3* expressed under the control of rice *Olesin 18 (Ole 18)* promoter or maize *UBIQUITIN* promoter together with constitutively expressed *AtNAS1* and endosperm-specific expression of *Phaseolus vulgaris FER (PvFER)* showed significant increases in the endosperm iron concentration. Iron concentration of up to 11.63 µg/g DW and 13.45 µg/g DW were obtained in the polished grains of transformed lines in the background of cultivars Nipponbare and IR64, respectively. These iron increases address 90% of the suggested dietary estimated average requirement (EAR) for iron in rice. Most of the transformed lines also show significant increases in the endosperm zinc concentration.

Likewise, the lines expressing a combination of *AtFRD3*, *AtNAS1* and *PvFER* or that of *AtFRD3* and *PvFER* also had increased iron and zinc concentration in the endosperm. Iron concentration up to 11.03 $\mu\text{g/g}$ DW was obtained in the polished grains of the lines expressing the combination of *AtFRD3*, *AtNAS1* and *PvFER*. Furthermore, most of the transgenic plants generated using the afore-mentioned strategies exhibited higher tolerance to iron deficient growth condition. Additionally, the *osvit2* mutant line was transformed with a construct expressing the combination of *AtNAS1* and *PvFER*, leading to a 3-fold increase in the endosperm iron concentration as compared to the *osvit2* mutants. Overall, among the tested strategies in this work, the transgenic plants expressing *AtNRAMP3* under control of *Ole 18* promoter together with constitutive expression of *AtNAS1* and endosperm-specific expression of *PvFER* exhibited highest endosperm iron concentration.

Furthermore, in order to understand the molecular mechanisms controlling grain development in rice, I evaluated the gene expression and regulatory network within different sub-regions of developing rice grains. I analyzed gene activity genome-wide in cross cells (CC), nucellar epidermis (NE), ovular vascular trace (OVT), endosperm (EN) and aleurone layer (AL) dissected using laser capture microdissection (LCM) at three distinct grain development stages. The obtained mRNA dataset offer comprehensive description of gene expression with high spatio-temporal regulation.

In summary, the findings from my PhD work demonstrate that altering the expression of genes encoding vacuolar transporters (i.e., overexpression of *AtNRAMP3* or knock out of *OsVIT2*), and the expression of gene encoding citrate transporter *AtFRD3* together with *AtNAS1* and *PvFER* significantly increase iron and zinc concentration in both polished and unpolished rice grains of transformed lines. The RNA seq dataset generated from dissected rice grain sub-regions is a useful resource for better understanding of the molecular processes involved in rice grain development.

Zusammenfassung

Spurenelement Mangelernährung ist ein weit verbreitetes, weltweites Problem und gehört heutzutage zu den bedenklichsten Herausforderungen der humanen Gesundheit. Eisenmangel ist eine der schlimmsten Mangelernährungen, die 1,6 Milliarden Menschen, sowohl in Industrie- wie auch in Entwicklungsländern, betrifft. Die meisten Grundnahrungsmittel der globalen Nahrungsversorgung, Reis miteingeschlossen, sind schlechte Eisenquellen. Mögliche Strategien um Eisenmangelanämie zu bekämpfen sind Eisenergänzung von Bevölkerungsgruppen mit besonders hohem Risiko, Eisenanreicherung der Nahrung und eine Erhöhung der Nahrungsdiversität. Bei diesen Strategien gibt es jedoch Probleme bei der Implementierung aus sozio-ökonomischen und/oder biologischen Gründen. Biofortifikation, ein nachhaltiger und kostengünstiger Lösungsansatz, hat ein grosses Potential um die Spurenelement Mangelernährung zu bekämpfen. Polierte Reiskörner enthalten sehr kleine Mengen an Eisen und auf Grund der geringen Variabilität des Genpools war es nicht möglich die Eisenkonzentration im Endosperm mit konventioneller Züchtung zu erhöhen. Gentechnische Lösungsansätze zur Steigerung der Eisenaufnahme, -transport und -speicherung in der Pflanze hatten unterschiedliche Grade an Erfolg und es konnten vielversprechende Linien mit erhöhter Eisenkonzentration entwickelt werden. Trotz dieser Berichte gibt nur wenige Beweise für gentechnische, intrazelluläre Mobilisierung von Eisen um die Eisenendkonzentration im Korn zu erhöhen.

In dieser Arbeit habe ich das Potential von Genen, die für vaskuläre Transporter kodieren, evaluiert, wie zum Beispiel das *NATURAL RESISTANCE-ASSOCIATED MACROPHAGE PROTEIN 3 (NRAMP3)* und den *VACUOLAR IRON TRANSPORTER (VIT2)* und *FERRIC REDUCTASE DEFECTIVE 3 (FRD3)*, welches für einen Zitrattransporter kodiert, der die Eisenkonzentration im Endosperm erhöht, wenn es gleichzeitig mit der *NICOTINAMINE SYNTHASE (NAS)* und *FERRITIN (FER)*, exprimiert wird. Die transformierten Reislinien, die *NRAMP3* aus *Arabidopsis thaliana* unter der Kontrolle des Reis *Oleosin 18 (Ole 18)* oder des Mais *UBIQUITIN* Promotors exprimieren und gleichzeitig konstitutiv *AtNAS1* und Endosperm-spezifisch *Phaseolus vulgaris FER (PvFER)* exprimieren, zeigen erhöhte Eisenkonzentrationen im Endosperm. Eisenkonzentrationen von bis zu 11.63 µg/g Trockengewicht und 13.45 µg/g Trockengewicht konnten in polierten Reiskörnern von transformierten Linien der

Kultivare Nipponbare, beziehungsweise IR64, gemessen werden. Diese Erhöhung des Eisengehalts entspricht 90 % der empfohlenen durchschnittlichen Tagesdosis von Eisen in Reis. Die meisten transformierten Linien zeigen ebenfalls eine Erhöhung des Zinkgehalts im Endosperm. Gleichermassen hatten auch die Linien, die eine Kombination von *AtFRD3*, *AtNAS1* und *PvFER* oder *AtFRD3* und *PvFER* exprimieren, einen erhöhten Eisen- und Zinkgehalt im Endosperm. Eisengehalte von bis zu 11.03 µg/g Trockengewicht wurden in polierten Körnern gemessen, die eine Kombination von *AtFRD3*, *AtNAS1* und *PvFER* exprimieren. Des Weiteren zeigen transgene Pflanzen, die mit den bereits genannten Strategien hergestellt wurden, eine höhere Toleranz gegenüber Eisenarmen Wachstumsbedingungen. Zusätzlich wurde die *osvit2* Mutante mit einem Konstrukt, das eine Kombination von *AtNAS1* und *PvFER* exprimiert, transformiert, was zu einer 3-fachen Erhöhung der Eisenkonzentration im Endosperm verglichen mit der *osvit2* Mutanten, geführt hat. Insgesamt zeigten transgene Pflanzen, die *AtNRAMP3* unter der Kontrolle des *Ole 18* Promotors exprimieren und gleichzeitig konstitutiv *AtNAS1* und endosperm-spezifisch *PvFER* exprimieren, die höchsten Eisengehalte im Endosperm.

Um zusätzlich die molekularen Mechanismen, die die Kornentwicklung steuern zu verstehen, evaluierte ich die Genexpression und das regulatorische Netzwerk in den verschiedenen Geweben von sich entwickelnden Reiskörnern. Ich analysierte die genomweite Genaktivität in Cross cells, Nucellar Epidermis, Ovular Vascular Trace, dem Endosperm und der Aleuronschicht, die durch Laser-Mikrodissektion getrennt wurden in drei unterschiedlichen Entwicklungsstadien. Der entstandene mRNA Datensatz ermöglicht eine verständliche Beschreibung der Genexpression mit einer hohen räumlich-zeitlichen Regulierung.

Zusammengefasst zeigen die Ergebnisse meiner Doktorarbeit, dass durch Veränderung der Expression von Genen, die vaskuläre Transporter kodieren (zum Beispiel Überexpression von *AtNRAMP3* oder knock-out von *OsVIT2*) und Expression der Gene, die den Zitrattransporter *AtFRD3* kodieren, gemeinsam mit *AtNAS1* und *PvFER*, dass die Eisen- und Zinkkonzentration in polierten und nicht-polierten Reiskörnern von transformierten Linien erhöht ist. Der RNA-sequenz Datensatz, der von präparierten Reiskorngeweben, generiert wurde, ist eine hilfreiche Ressource für ein besseres Verständnis von molekularen Prozessen, die bei der Entwicklung des Reiskorns involviert sind.

List of abbreviations

ABC ATP BINDING CASSETTE TRANSPORTER

AHA Arabidopsis H⁺-ATPase

AL Aleurone layer

Al Aluminium

ATP adenosine triphosphate

BETL basal endosperm transfer layers

bHLH BASIC HELIX LOOP HELIX

CC cross cells

Cd cadmium

Cu copper

CRT PHYTOENE DESATURASE

cv. cultivar

DAF days after flowering

DMA DEOXYMUGINEIC ACID

DMAS DEOXYMUGINEIC ACID SYNTHASE

DNA deoxyribonucleic acid

DTF days to flowering

Em embryo

En endosperm

ETC endosperm transfer cells

Fe iron

FER FERRITIN

FIT IRON DEFICIENCY RESPONSE-LIKE IRON DEFICIENCY INDUCED
TRANSCRIPTION FACTOR

FPN FERROPORTIN

FRD FERRIC REDUCTASE DEFECTIVE

FRO FERRIC REDUCTASE OXIDASE

GLB GLOBULIN

GLUB GLUTELIN B

ICP/OES inductively coupled plasma-optical emission spectroscopy

IDE IRON DEFICIENCY-RESPONSE CIS-ACTING ELEMENT

IDEF IDE BINDING FACTOR

IREG IRON REGULATED TRANSPORTER

IRT IRON REGULATED METAL TRANSPORTER

IRO IRON DEFICIENCY-INDUCIBLE bHLH TRANSCRIPTION FACTOR

ITP IRON TRANSPORT PROTEIN

LC-MS liquid chromatography-mass spectrometry

MA mugineic acid

MAR MULTIPLE ANTIBIOTIC RESISTANCE

MATE MULTIDRUG AND TOXIC EFFLUX

MIT MITOCHONDRIAL IRON TRANSPORTER

NA nicotianamine

NAS NICOTIANAMINE SYNTHASE

NAAT NICOTIANAMINE AMINOTRANSFERASE

NAC NO APICAL MERISTEM

NB Nipponbare

NE nucellar epidermis

NP nucellar projection

NRAMP NATURAL RESISTANCE ASSOCIATED MACROPHAGE PROTEIN

OPT OLIGOPEPTIDE TRANSPORTER

PCR polymerase chain reaction

PEZ PROTOCATECHUIC ACID EFFLUXER

PIC PERMEASE IN CHLOROPLAST

PS phytosiderophore

PSY PHYTOENE SYNTHASE

qRT-PCR quantitative real time-PCR

SUT SUCROSE TRANSPORTER

TOM TRANSPORTER OF MUGINEIC ACID

VIT VACUOLAR IRON TRANSPORTER

Wb western blotting

WRKY WRKY transcription factor family

YS YELLOW STRIPE

YSL YELLOW STRIPE-LIKE

ZIF ZINC-INDUCED FACILITATOR

ZIP ZRT/IRT-RELATED PROTEIN

ZRT ZINC-REGULATED TRANSPORTER

Table of Contents

Acknowledgements	ii
Summary.....	iii
Zusammenfassung	v
List of abbreviations	vii
1. General Introduction	1
1.1 Importance of iron in plants	1
1.2 General mechanisms controlling iron acquisition in plants.....	1
1.2.1 Strategy I- Reduction-based strategy	1
1.2.2 Strategy II- Chelation-based strategy	2
1.3 Long distance iron transport in xylem and phloem.....	2
1.3.1 Xylem transport from root to shoot	3
1.3.2 Metal complexes in the xylem sap	4
1.3.3 Phloem transport within the plants.....	5
1.3.4 Metal complexes in phloem sap	6
1.4 Subcellular iron transport.....	6
1.4.1 Chloroplast	6
1.4.2 Mitochondria	8
1.4.3 Vacuole.....	8
1.5 Transcriptional regulation in strategy II plants	9
1.6 Iron biofortification in rice	11
1.7 Seed development.....	12
1.7.1 General development stages and structure in the seeds	12
1.7.2 Maize	13
1.7.3 Barley	15
1.7.4 Wheat	16
1.7.5 Rice	16
1.8 Aims of the PhD thesis.....	17
2. Targeting intra-cellular iron transport combined with efficient uptake and storage significantly increases grain iron levels in rice.....	18
2.1 Abstract.....	19
2.2 Introduction.....	20
2.3 Results	22
2.3.1 Combined expression of <i>AtNRAMP3</i>, <i>AtNAS1</i> and <i>PvFER</i> increases iron and zinc concentrations in polished rice grains.....	22
2.3.2 Grain iron concentration and gene expression are positively correlated	27

2.3.3 NFUN and NFON lines are more tolerant to iron-deficient growth conditions.....	29
2.3.4 Iron-deficiency induction of iron homeostasis-related genes is reduced in the transgenic plants	30
2.3.5 Transgenic plants do not accumulate more cadmium in grains.....	31
2.3.6 IR64 lines expressing NRAMP, NAS and FER have dietary significant levels of iron and zinc in their grains	32
2.4 Discussion	33
2.5 Material and Methods	36
2.5.1 DNA construct, rice transformation and plant growth conditions	36
2.5.2 Iron deficiency and cadmium excess treatment in hydroponic culture.....	37
2.5.3 Metal ion measurements.....	38
2.5.4 Pearl's Prussian blue staining.....	38
2.5.5 RNA extraction, cDNA synthesis and quantitative real-time PCR.....	39
2.5.6 Protein extraction and Western blotting analysis.....	39
2.5.7 Germination rate test.....	40
2.6 Conflict of interest.....	40
2.7 Author contributions	40
2.8 Acknowledgments	40
2.9 Supplementary data.....	41
3. Boosting citrate-iron translocation together with efficient uptake and storage significantly increases the endosperm iron and zinc concentrations in rice.....	50
3.1 Abstract.....	51
3.2 Introduction.....	52
3.3 Results	54
3.3.1 Generation of rice transgenic lines expressing <i>AtFRD3</i> , <i>AtNAS1</i> and <i>PvFER</i>	54
3.3.2 Concerted expression of <i>AtFRD3</i> , <i>AtNAS1</i> and <i>PvFER</i> elevated the iron and zinc concentration in the polished rice grains	56
3.3.3 Distribution of iron and zinc in shoots and roots of selected NFUF and FUF plants under iron sufficient and deficient condition.....	58
3.3.4 Endogenous iron homeostasis related genes are highly induced in the transformed plants upon iron deficiency.....	61
3.3.5 <i>AtFRD3</i> expression resulted in aluminium tolerance in rice	62
3.3.6 Transgenic plants did not accumulate more cadmium in the polished grains.....	64
3.4 Discussion	65
3.5 Material and Methods	67
3.5.1 DNA constructs, rice transformation and plant growth conditions.....	67
3.5.2 Iron deficiency and cadmium excess treatment in hydroponic culture.....	68

3.5.3 Metal ion measurements.....	69
3.5.4 RNA extraction, cDNA synthesis and quantitative real-time PCR.....	69
3.5.5 Xylem sap collection	70
3.5.6 LC-MS analysis	70
3.6 Conflict of interest.....	71
3.7 Author contributions	71
3.8 Acknowledgments	71
3.9 Supplementary data.....	72
4. Enhanced Grain Iron Accumulation in <i>osvit2</i> Lines Expressing <i>NAS</i> and <i>FER</i> Genes	78
4.1 Abstract.....	79
4.2 Introduction.....	80
4.3 Results	82
4.3.1 Transgene expression in the leaf, embryo and endosperm of NFvit2 lines	82
4.3.2 Metal profiles in the grains of NFvit2, <i>osvit2</i> and DJ plants.....	84
4.3.3 Distribution of iron and zinc in shoots and roots of NFvit2, <i>osvit2</i> and DJ plants	86
4.3.4 Chlorophyll content and endogenous gene expression in NFvit2, <i>osvit2</i> and DJ plants	88
4.4 Discussion	89
4.5 Material and Methods	92
4.5.1 DNA construct, rice transformation and plant growth conditions	92
4.5.2 Iron deficiency treatment in hydroponic culture.....	92
4.5.3 Metal ion measurements.....	93
4.5.4 RNA Extraction, cDNA synthesis and Quantitative real-time PCR	93
4.5.5 Chlorophyll extraction and measurement.....	94
4.6 Conflict of interest.....	94
4.7 Author contributions	94
4.8 Acknowledgements	94
4.9 Supplementary data.....	95
5. Genome wide analysis of the transcriptional profiles in different regions of the developing rice grains	97
5.1 Abstract.....	98
5.2 Introduction.....	99
5.3 Results	101
5.3.1 Spatio- temporal resolution of mRNA profiles during rice grain development...101	101

5.3.2	Diverse and complex regulatory network controlling grain filling in rice	105
5.3.3	Expression profiles of phytohormone biosynthesis and signaling related genes	107
5.3.4	Transporters are preferentially expressed in OVT	109
5.3.5	Novel cis-regulating elements associated to OVT and CC specific genes	113
5.4	Discussion	117
5.5	Materials and Methods.....	121
5.5.1	Plant Material and Growth Conditions	121
5.5.2	Cryostat settings, Mount slides preparation and Laser Capture Microdissection (LCM).....	121
5.5.3	RNA Extraction, pre-amplification and RNA sequencing.....	122
5.5.4	qRT-PCR validation	123
5.5.5	Data analysis.....	123
5.6	Conflict of interest.....	124
5.7	Author contributions	124
5.8	Acknowledgements	124
5.9	Supplementary data.....	125
6.	General discussion	132
6.1	Role of biofortification in combating hidden hunger	132
6.2	Metabolic engineering for improving nutritional profile of staple crops	132
6.3	New technologies suited for future biofortification strategies	133
6.3.1	Gene targeting by genome editing tools.....	133
6.3.2	Genome-wide association studies (GWAS) and OMICS studies to identify new gene targets	135
6.4	Understanding grain development by using OMICS approaches and bioinformatics tools.....	136
6.4.1	Proteomics and metabolomics	136
6.4.2	Transcriptomic data modeling and network construction.....	137
6.5	Summary of the findings of this PhD work	138
7.	References.....	139
8.	Curriculum Vitae	159

1. General Introduction

1.1 Importance of iron in plants

Plants required iron for several vital biological processes including photosynthesis and chlorophyll biosynthesis. Iron can exist in multiple redox states, alternating between Fe(II) and Fe(III), which make it feasible to form complexes with different organic compounds (Childs, 1981). However, the high reactive capability of iron also makes it toxic to the plants. It can lead to generation of hydroxyl radicals, which can harm the plant cells by causing oxidation of proteins, damage to nucleic acids, enzyme inhibition and activation of programmed cell death (Halliwell, 2006; Briat et al., 2007). On the other hand, in response to iron deficiency, plants exhibit several phenotypic changes including interveinal chlorosis in leaves and decreased root length (Schmidt, 1999; Muller and Schmidt, 2004). Thus, in order to prevent iron toxicity while benefitting from it, plants have evolved complex iron regulatory strategies to maintain iron homeostasis.

1.2 General mechanisms controlling iron acquisition in plants

1.2.1 Strategy I- Reduction-based strategy

Nongraminaceous plants such as Arabidopsis, cucumber, apple and beans release protons into the rhizosphere via H-ATPase, which lowers the soil pH and increases the solubility of iron in the soil (Santi et al., 2005; Santi and Schmidt, 2008). These ATPases belong to the *AHA* gene family in Arabidopsis. *AtAHA1*, *AtAHA2* and *AtAHA7* are all induced in root epidermis under iron deficiency condition, while *AtAHA2* is reported as a main H-ATPase to mediate release of protons into the rhizosphere (Santi and Schmidt, 2009). *AtAHA2* had the highest expression level among other *AHA* genes, and *aha2* knock out mutant exhibited reduced rhizosphere acidification under iron deficiency condition (Santi and Schmidt, 2009). After acidification by proton release, Fe(III) is reduced to Fe(II) by membrane-bound FERRIC CHELATE REDUCTASE (FRO, AtFRO2 in Arabidopsis) (Robinson et al., 1999). *FRO* expression is induced under iron deficient conditions and overexpression of *FROs* in the roots of tobacco, soybeans, and rice increases tolerance to low iron availability (Connolly et al., 2003; Vasconcelos et al., 2006; Ishimaru et al., 2007). Fe(II) is then transported by IRON-REGULATED TRANSPORTER 1 (AtIRT1) into the root epidermal cells (Eide et al., 1996). AtIRT1 is a plasma membrane divalent metal transporter belonging to the ZINC-REGULATED TRANSPORTER/IRON-REGULATED TRANSPORTER-RELATED PROTEIN family (Eide et al., 1996).

Expression of *AtIRT1* is predominant in roots and is induced under iron deficient condition, while *irt1* mutant shows severe chlorosis and loses the ability to generate seeds (Henriques et al., 2002; Varotto et al., 2002; Vert et al., 2002). *AtIRT1* also facilitates uptake of other divalent metals such as zinc, manganese, cobalt and cadmium (Korshunova et al., 1999).

1.2.2 Strategy II- Chelation-based strategy

Grasses use the chelation strategy to acquire Fe(III) from the soil. They release phytosiderophores (PS) into the rhizosphere, which chelate Fe(III) and the Fe(III)-PS complexes are then transported into the plant root cells. PSs belong to the mugineic acid (MAs) family and are synthesized through a conserved pathway from S-adenosyl-L-methionine (Shojima et al., 1990). First, S-ADENOSYL-L-METHIONINE SYNTHETASE (SAMS) converts methionine into SAM (Mori and Nishizawa, 1987). Then NICOTIANAMINE SYNTHASE (NAS) catalyzes SAM to form nicotianamine (NA). NICOTIANAMINE AMINOTRANSFERASE (NAAT) and DEOXYMUGINEIC ACID SYNTHASE (DMAS) then convert NA to deoxymugineic acid (DMA), the precursor of all other MAs (Higuchi et al., 1999; Ma et al., 1999; Takahashi et al., 1999; Bashir et al., 2006). In barley, DMA is further hydroxylated by IRON DEFICIENCY-SPECIFIC CLONE 2 and 3 (IDS2 and IDS3) to other MAs (Nakanishi et al., 2000; Kobayashi et al., 2001). MAs are secreted onto root surface by the TRANSPORTER OF MUGINEIC ACID family PS (TOM) (Nozoye et al., 2011). *OsTOM1* expression level is induced in roots under iron deficient condition and overexpression of *OsTOM1* enhances the tolerance to iron deficiency (Nozoye et al., 2011). The Fe(III)-MA complexes are transported into root cells by the YELLOW STRIPE (YS) and YELLOW STRIPE-LIKE (YSL) transporter family. YS1 is a proton-coupled symporter of Fe(III)-PS complexes and belongs to the OLIGOPEPTIDE TRANSPORTER (OPT) family (Curie et al., 2001). Rice can also take up Fe(II) by *OsIRT1*, which is induced in the roots under iron deficiency (Ishimaru et al., 2006).

1.3 Long distance iron transport in xylem and phloem

After iron is transported into the plant roots, it is further transported within the plant to different tissues. When entering the root epidermal cells, iron is bound by chelators to move symplastically to the pericycle cells, and then it is effluxed into the xylem and is loaded into the phloem.

1.3.1 Xylem transport from root to shoot

Iron is transported mainly as the Fe(III)-citrate complex in xylem. In Arabidopsis, FERRIC CHELATE REDUCTASE DEFECTIVE 3 (FRD3), which belongs to the MULTIDRUG AND TOXIC COMPOUND EXTRUSION (MATE) family of transporters, is identified as a citrate transporter that loads citrate into the xylem and thus facilitates iron transport from roots to shoots (Durrett et al., 2007). In *frd3* mutant, plants accumulated more iron in the roots whereas the xylem sap contained less iron and less citrate as compared to the wildtype (WT) control (Rogers, 2002; Durrett et al., 2007). Citrate supplementation was able to rescue the chlorosis phenotype in *frd3* mutants (Rogers, 2002; Durrett et al., 2007). AtFRD3 localizes to the plasma membrane of pericycle cells and the vascular cylinder (corresponding to its role in citrate efflux), and therefore in *frd3* mutants the iron is precipitated in the apoplast in roots and is accumulated in the vasculature around the xylem vessels (Green and Rogers, 2004). Recently, AtFRD3 has also been shown to be expressing in the Arabidopsis embryo and flower, and therefore the *frd3* mutant shows early germination defects, severe fertility defects and iron precipitation on the surface of the aborted pollen grains (Roschttardt et al., 2011). The *frd3* mutant also has reduced symplastic iron in leaves, embryo and pollen (Roschttardt et al., 2011). Taken together, these results suggest that in addition to the role in loading citrate into the root xylem for translocation of iron to the shoots, AtFRD3 is also necessary for mediating citrate release in the apoplastic space, allowing iron movement between symplastically disconnected tissues. The FRD3-LIKE 1 (FRDL1) is identified as the AtFRD3 homolog in rice, and *osfrdl1* mutant shows similar phenotype to *frd3* mutant in Arabidopsis (Yokosho et al., 2009). The *osfrdl1* mutant results in leaf chlorosis, lower leaf iron concentration, higher accumulation of zinc and manganese concentration in the leaves, and iron precipitation in the root's stele (Yokosho et al., 2009). The concentration of citrate and iron in the xylem sap was lower in *osfrdl1* mutant as compared to the WT (Yokosho et al., 2009). OsFRDL1 is localized at the membrane of pericycle cells of the roots and it shows citrate transport activity (Yokosho et al., 2009). Recently, OsFRDL1 is also shown to be highly expressed in the upper nodes of rice at the reproductive stage (Yokosho et al., 2016b). OsFRDL1 is expressed in most cells of vascular bundles and the interjacent parenchyma cell bridges of uppermost node I, as well as the vascular tissues (Yokosho et al., 2016b). The *osfrdl1* mutant exhibited decreased pollen viability and grain fertility and the iron concentration is lower in the anther and panicle in comparison to the WT (Yokosho et al., 2016b). These results show that

OsFRDL1 is required for iron distribution in roots, leaves, upper nodes, panicles and grains through solubilization of iron with citrate deposited in the apoplastic part of nodes in rice. However, the transporters that efflux iron into the xylem have not yet been identified. The possible candidate is the FERROPORTIN 1/IRON REGULATED 1 (FPN1/IREG1) in Arabidopsis for the Fe(II) efflux transporter (Morrissey et al., 2009). AtFPN1 localizes to the plasma membrane and is expressed in the stele. The *fpn1* mutant contains less chlorophyll independent of iron status (Morrissey et al., 2009), suggesting the role for AtFPN1 in effluxing the iron from the cytoplasm to the vasculature.

1.3.2 Metal complexes in the xylem sap

Metals in the xylem sap are preferentially complexed by the more acidic carboxylic acids rather than the much more basic amino acids due to the relatively acidic pH (pH=5-6.5) of the xylem sap (Harris et al., 2012). Fe(III)-Cit complex is the major form of iron complex in the xylem sap. Since the Fe:Cit ratio varies in plant xylem sap, it is likely that different form of Fe(III)-Cit species can be identified in different conditions. For example, the Fe_3Cit_3 complex is only found in the xylem samples with iron sufficient condition (above 20 μM), whereas Fe_2Cit_2 and Fe_3Cit_4 are also detected in Fe-Cit standards in different plant species (Rellan-Alvarez et al., 2010). The role of NA in long-distance iron transport in xylem sap is still not clear yet (Curie et al., 2009). In addition, it has been reported that NA may play a role in long distance transport of iron when carboxylates are in short supply, as it occurs in *frd3* mutants or the plant species with less acidic xylem sap (Schuler et al., 2012). In case of PSs, only a small amount of Fe(III)-DMA was found in the xylem sap from the roots of iron deficient wheat plants (Xuan et al., 2006). The studies of zinc species in the xylem sap were all carried out using hyper-accumulators *T. caerulescens* and *S. alfredii* (Monsant et al., 2011; Lu et al., 2013b). In all cases, although the major fraction of zinc is free hydrated Zn^{2+} ions, the remaining fraction is complexed with carboxylates such as Citrate and Malate. The Zn-His and Zn-phytate complexes are found in the roots while Zn-Mal and Zn-Cit are the major species in the shoots of *T. caerulescens* (Monsant et al., 2011). On the other hand, the Zn-NA complex has not been found in the xylem sap yet, but Zn-DMA complex is detected in press sap from roots of iron-deficient wheat plants (Xuan et al., 2006).

1.3.3 Phloem transport within the plants

Iron is transported through the phloem to have more efficient translocation in developing organs in plants and is remobilized from older to younger leaves via the phloem sap. YSL transporters are involved in the transport of Fe(II)-NA complexes in the phloem (DiDonato et al., 2004; Waters et al., 2006). There are eight YSLs in Arabidopsis. Among them, expression of *AtYSL1*, *AtYSL2* and *AtYSL3* is down regulated under iron deficient condition, and these are found in the vascular parenchyma, indicating their roles in unloading iron from the xylem (DiDonato et al., 2004; Waters et al., 2006). The *ysl1ysl3* mutant has reduced iron concentration in leaves and seeds, and has reproduction defects, suggesting that *AtYSL1* and *AtYSL3* are required for reproduction, seed development and for iron loading into the seeds (Chu et al., 2010). In case of *AtYSL2*, the major function has been found to be in the lateral movement of metals within vasculature (DiDonato et al., 2004). Among YSL members in rice, *OsYSL2* and *OsYSL15* are induced under iron deficient condition (Koike et al., 2004; Inoue et al., 2009). *OsYSL2* transports Fe(II)-NA and is expressed in the shoot phloem companion cells while *OsYSL15* transports Fe(III)-DMA and is expressed in the root vasculature, flower and developing seeds (Koike et al., 2004; Inoue et al., 2009). *OsYSL2* is suggested to be an important Fe(II)-NA transporter especially in the iron loading into rice shoots and endosperm (Ishimaru et al., 2010). *OsYSL15*, on the other hand, is suggested to be crucial for iron distribution and loading in early developmental stages in rice (Inoue et al., 2009; Lee et al., 2009a). Similarly, *OsYSL16* is expressed in the root epidermis, vascular bundles, and in cells surrounding the xylem and phloem. It transports Fe(III)-DMA but not Fe(II)-NA and is required for iron uptake, transport, and distribution in plants via the vascular bundles (Kakei et al., 2012; Lee et al., 2012b). *OsYSL18* is also reported as a Fe(III)-DMA transporter which mainly expressed in reproductive organs and phloem cells at the base of the leaf sheath (Aoyama et al., 2009).

Arabidopsis OLIGOPEPTIDE 3 (*AtOPT3*) loads iron into the phloem, facilitates iron recirculation from the xylem to the phloem, and regulates both shoots to roots iron signaling and iron redistribution from mature to developing tissues (Stacey et al., 2006; Mendoza-Cozatl et al., 2014). Recently, *AtOPT3* has been shown to be expressed in phloem and the majority of its expression is associated with minor veins of leaves and nodes of stems (Stacey et al., 2006). In rice, *OsOPT1*, *OsOPT4* and *OsOPT7* have been found to be able to complement the growth defect of the iron uptake yeast mutant, when

exogenously Fe(II)-NA was supplied (Lubkowitz, 2011). However, recent study suggested that the substrate of OsOPT7 is Fe(III)-DMA or Fe(II)-NA (Bashir et al., 2015). The OsOPT7 is induced under iron deficient condition and is expressed in roots vascular tissue, shoots, and developing seeds (Bashir et al., 2015). These results indicated that the OsOPT7 play a significant role in iron distribution in vegetative tissues and rice seeds. Additionally, an iron-binding protein the IRON TRANSPORT PROTEIN (ITP), which belongs to LATE EMBRYOGENESIS ABUNDANT (LEA) protein family, has been identified in the phloem sap of castor bean shoots, which preferentially binds to Fe(III) and contributes to phloem mediated long distance iron transport (Kruger et al., 2002).

1.3.4 Metal complexes in phloem sap

In rice phloem sap, iron has been found preferentially associated with high molecular weight molecules, such as Fe(III)-DMA (Nishiyama et al., 2012). Fe(II)-NA complex has been identified in Arabidopsis and rice phloem vascular tissues (Curie et al., 2009). However, there is no direct evidence of Fe(II)-NA in the phloem sap so far. It is likely that NA is important in iron phloem loading and iron may be transported in another form such as by iron binding proteins (Schuler et al., 2012). Several proteins that are capable to bind with iron are described in the phloem sap of *R. communis* and *L. texensis* (Kruger et al., 2002; Lattanzio et al., 2013). Zinc in the rice phloem sap is found associated with low molecular weight molecules such as Zn(II)-NA complex (Nishiyama et al., 2012). Four Zn-binding proteins are identified in the study using *L. texensis* phloem sap, but none of them are considered as good candidates for Zn transport (Lattanzio et al., 2013).

1.4 Subcellular iron transport

1.4.1 Chloroplast

Iron plays an extremely important role in chlorophyll synthesis, stabilization and photosynthesis. Hence, iron homeostasis is regulated tightly in the chloroplasts (Finazzi et al., 2015). Chloroplasts serve as a storage hub for iron, especially during early plant growth (Briat et al., 2010). The Arabidopsis FERRIC CHELATE REDUCTASE OXIDASE 7 (AtFRO7), which reduces ferric ion to ferrous ion, localizes to chloroplast envelopes and plays a significant role in maintaining iron homeostasis (Jeong et al., 2008; Jain et al., 2014). The *fro7* mutant contains less iron in chloroplast than the WT under iron deficient condition (Jeong et al., 2008). These results suggest that AtFRO7 is

required for efficient photosynthesis and for chloroplast iron acquisition in Arabidopsis young seedlings.

PERMEASE IN CHLOROPLASTS 1 (PIC1) is a transmembrane protein that localizes to the inner chloroplast envelope in Arabidopsis (Duy et al., 2007; Duy et al., 2011). The *pic1* mutant shows severe chlorosis and dwarfing due to impaired chloroplast development whereas AtPIC1 overexpressing plants show iron-overload phenotypes such as increased oxidative stress, leaf chlorosis, reduced biomass, defective flowers and seed development (Duy et al., 2011). These results suggest that AtPIC1 participates in chloroplast iron uptake and plant iron homeostasis in general. Recently, the NiCo protein is found to interact with AtPIC1. NiCo is predicted to transport nickel and cobalt and is localized to the inner envelope of the chloroplast (Eitinger et al., 2005; Duy et al., 2011). Therefore, it is suggested that PIC may bind with NiCo as part of chloroplast inner envelope translocon.

AtYSL4 and AtYSL6 have been characterized as potential plastid iron efflux transporters in Arabidopsis. Both genes are up-regulated in response to excessive iron supply and YSL6 is localized to the chloroplast envelope (Divol et al., 2013). Iron is trapped in chloroplasts of *ysl4ysl6* mutants whereas the plants overexpressing *AtYSL4* or *AtYSL6* exhibit reduced tolerance to iron deficiency and decreased chloroplast iron concentration (Divol et al., 2013). Taken together, these data suggest that these transporters play an important role in iron detoxification during plastid differentiation. However, there is no N-terminal chloroplast targeting peptide identified in AtYSL4 or AtYSL6 (Conte et al., 2013). On the contrary, the proteomics data suggested that AtYSL4 and AtYSL6 are localized to tonoplast and ER membranes (Conte et al., 2013). Therefore, the roles of AtYSL4 and AtYSL6 are still controversial and under debate.

NON-INTRINSIC ABC TRANSPORTER PROTEIN 14 in Arabidopsis (AtNAP14) is localized to chloroplast and is involved in iron transport. The iron concentration in the shoots of *nap14* mutant is dramatically increased, whereas it is approximately 50% lower than WT in the roots (Shimoni-Shor et al., 2010). The *nap14* mutant shows damage to chloroplast structures, exhibits severe growth defects, and misregulates the iron-homeostasis genes (Shimoni-Shor et al., 2010). Thus, AtNAP14 is suggested to function as part of chloroplast transporter complex and to be involved in iron homeostasis in the

chloroplast. Likewise, MULTIPLE ANTIBIOTIC RESISTANCE 1 (MAR1), which most likely transports aminoglycoside antibiotics into the plastids and is localized to chloroplasts, also plays a role in cellular iron homeostasis including iron chelation, storage and sequestration (Conte et al., 2009).

FERRITIN (FER), the iron storage protein in plants, can store up to 4500 iron atoms (Briat et al., 2010). It buffers iron levels and sequesters excess iron to protect against oxidative damage from electronic transport chain of photosynthesis. Most of the FERRITIN is localized in chloroplasts (Petit et al., 2001). AtFER1, AtFER2 and AtFER3 are localized to the plastid. AtFER2 is expressed only in the seeds, while AtFER1 and AtFER3 are expressed in the shoots and flowers (Petit et al., 2001; Ravet et al., 2009). FER degradation is necessary to release iron during seed germination (Ravet et al., 2009).

1.4.2 Mitochondria

Plant mitochondria serve as a central hub of redox regulation and energy conversion by linking metabolic pathways from different subcellular compartments. Nonetheless, transport of metals into plant mitochondria is poorly understood. Arabidopsis FRO3 and FRO8 are mitochondrial proteins that putatively participate in ferric reduction in the mitochondrial membrane and contribute to mitochondrial iron transport (Jain et al., 2014). MITOCHONDRIAL IRON TRANSPORTER (MIT) has been identified as an iron transporter that transports cytoplasmic iron into mitochondria in rice. OsMIT is essential for growth and development because the knockout mutant is lethal as it exhibited reduced chlorophyll content and significantly affected plant growth (Bashir et al., 2011; Vigani et al., 2016). The *osmit* mutant accumulates less iron in mitochondria but higher iron in leaves, resulting in iron deficiency phenotype (Bashir et al., 2011; Vigani et al., 2016). The MITOCHONDRIAL IRON REGULATED (OsMIR) protein which is localized to mitochondria also participates in the metal homeostasis in rice (Ishimaru et al., 2009). *OsMIR* is significantly upregulated under iron deficient condition, and the *osmir* mutant accumulates more than twice the amount of iron in the shoots and roots as compared to WT plants (Ishimaru et al., 2009).

1.4.3 Vacuole

The vacuole serves as a major reservoir to regulate cellular iron homeostasis. Iron content has to be tightly controlled in plant cells to avoid metal toxicity and therefore, the

excessive iron is deposited in the vacuoles for withdrawal when required. In plants, several efflux and influx transporters localizing to the vacuolar membrane have been identified. In Arabidopsis, VACUOLAR IRON TRANSPORTER 1 (VIT1) deposits cytoplasmic iron into vacuole. Iron localization in *vit1* knockout mutants in Arabidopsis has been altered significantly (Kim et al., 2006). VIT1-LIKE (VTL) proteins in Arabidopsis have been characterized recently. Among them, AtVTL1, AtVTL2 and AtVTL5 are iron transporters that localize in vacuolar membrane and participate in transferring cytoplasmic iron into vacuoles to regulate iron homeostasis (Gollhofer et al., 2014). In rice, OsVIT1 and OsVIT2 function as vacuolar transporters that mediate transport of iron, zinc and manganese (Zhang et al., 2012). OsVIT1 and OsVIT2 both localize at the vacuolar membrane, and are highly expressed in flag leaf blade and sheath, respectively (Zhang et al., 2012). Interestingly, OsVIT1 is constitutively expressed while OsVIT2 is highly responsive to iron treatments (Zhang et al., 2012). Increased iron and zinc accumulation were observed in the seeds of *osvit1* and *osvit2* mutants (Zhang et al., 2012; Bashir et al., 2013). Furthermore, AtFPN2 is also localized to the vacuole membrane and is involved in the sequestration of excessive iron into the vacuole to prevent toxicity in Arabidopsis (Morrissey et al., 2009).

NATURAL RESISTANCE ASSOCIATED MACROPHAGE PROTEINS (NRAMP) are integral membrane proteins involved in transport of iron, manganese and cadmium. Opposite to AtVIT1, AtNRAMP3 and AtNRAMP4 release iron from vacuoles to the cytoplasm under iron deficient conditions in Arabidopsis (Thomine et al., 2000; Thomine et al., 2003; Lanquar et al., 2004; Lanquar et al., 2005). AtNRAMP3 and AtNRAMP4 are up-regulated under iron deficient condition and are localized to the vacuole membrane, and root and shoot vasculature (Lanquar et al., 2005). *AtIRT1* and *AtFRO2* expression are down-regulated in Arabidopsis plants overexpressing *AtNRAMP3* gene, indicating that AtNRAMP3 remobilizes iron from the vacuole into the cytosol, which might down-regulate iron uptake related genes (Thomine et al., 2003). The *nramp3nramp4* mutant is hypersensitive to iron deficient condition and shows severe germination defects (Lanquar et al., 2005).

1.5 Transcriptional regulation in strategy II plants

IRON DEFICIENCY-RESPONSIVE CIS-ACTING ELEMENT (IDE) BINDING FACTOR 1 and 2 (IDEF1 and IDEF2) have been found to interact with IDE1 and IDE2,

respectively, inducing the expression of iron-deficiency-responsive genes in rice and barley. IDEF1 and IDEF2 are members of the ABSCISIC ACID INSENSITIVE 3/VIVIPAROUS 1 (ABI3/VP1) and NO APICAL MERISTEM (NAC), respectively (Kobayashi et al., 2003; Kobayashi et al., 2007; Ogo et al., 2008). OsIDEF1 is constitutively expressed independent of iron status. Overexpression of *OsIDEF1* in rice results in higher tolerance to iron deficiency, higher chlorophyll content and improved plant growth, while its knock down mutant shows hypersensitivity to early stages of iron deficient condition (Kobayashi et al., 2007). OsIDEF1 positively regulates the induction of iron uptake and translocation related genes including *OsIRO2*, *OsIRT1*, *OsYSL15*, *OsYSL2*, *OsNAS1* and *OsNAS2*, as well as genes encoding seed maturation protein, LEA (Kobayashi et al., 2007). Recently, OsIDEF1 has been shown to contain histidine-asparagine and proline-rich regions that function to bind divalent metals, suggesting it may be a candidate of iron sensing in rice (Kobayashi et al., 2012). However, the mechanism of the trans-activation of OsIDEF1 and how OsIDEF1 transmits a metal-binding signal to the downstream pathways is still unclear. As for OsIDEF2, knock down mutant results in misdistribution of iron between the roots and shoots, and misregulation of the expression of *OsYSL2* (Ogo et al., 2008). Additionally, OsIDEF2 regulates another subset of iron-deficiency-responsive genes, indicating that OsIDEF2 maintains a consistent regulatory pattern throughout the stages of iron deficiency (Ogo et al., 2008; Kobayashi et al., 2009). Taken together, these reports suggest that OsIDEF1 is an upstream target in iron deficiency response and OsIDEF1 and OsIDEF2 differentially regulate iron-responsive genes in rice.

The BASIC HELIX-LOOP-HELIX (bHLH) protein OsIRO2 is an essential transcription factor regulating iron uptake genes, which binds to G-box sequence, CACGTG in rice. It contains several IDE1 in the promoter region and therefore the expression is up-regulated by OsIDEF1 under iron deficient condition (Ogo et al., 2006; Ogo et al., 2007). *OsIRO2* overexpressing plants show better growth, while OsIRO2 knock down mutant leads to reduced DMA secretion and impaired growth under iron deficient condition (Ogo et al., 2007). In addition, the expression of *OsIRO2* is positively correlated with downstream genes such as *OsNAS1* and *OsNAS2* in embryos during seed development, germination and vegetative stages (Ogo et al., 2007). This suggested that the OsIRO2 plays a key role in regulation of iron homeostasis related genes. On the contrary, OsIRO3 is identified as a negative regulator of the iron deficiency response in rice (Zheng et al., 2010). It is up-

regulated in the shoots and roots under iron deficient condition. Plants overexpressing *OsIRO3* are susceptible to iron deficiency and accumulate less iron in shoots than WT plants since the genes which are usually highly up-regulated under iron deficient condition are no longer induced in these plants (Zheng et al., 2010).

OsbHLH133, another TF in bHLH family, has been found to be up-regulated under iron deficient condition in rice (Wang et al., 2013a). The *bhlh133* mutant increases iron concentration in the shoot and reduced iron concentration in the roots, while *OsbHLH133* overexpressing plants showed higher iron concentration in roots and reduced iron in the shoots and xylem sap (Wang et al., 2013a). Furthermore, the *bhlh133* mutant showed increased expression of genes involved in iron homeostasis under iron sufficient condition (Wang et al., 2013a). These findings suggested that *OsbHLH133* is also a negative regulator of iron translocation from roots to shoots.

1.6 Iron biofortification in rice

Iron deficiency is a widespread problem, which affect over 30% of the world's population. Since rice is a staple crop for nearly half of the world's population, it makes a good candidate for iron biofortification. So far several efforts have been reported to biofortify rice for increased iron in the endosperm.

Plants overexpressing *FER* accumulate more iron in the endosperm as compared to WT plants (Goto et al., 1999; Vasconcelos et al., 2003). Rice plants transformed with soybean *FER* under the control of the endosperm-specific rice *GLUTELIN-B1* promoter accumulate 3-fold more iron in the grains in comparison to the WT plants (Goto et al., 1999; Qu et al., 2005). A 2-fold increase in grain iron concentration is found in rice plants carrying *Phaseolus vulgaris FER* (Lucca et al., 2001b). The alternative approaches, such as increasing the iron uptake and iron translocation into plants, have also been considered to further increase iron concentration in the rice endosperm. The rice plants overexpressing *OsYSL2* under the control of phloem specific sucrose transporter promoter resulted in a 4.4-fold increase of iron in the polished grains, and the plants overexpressing barley *IDS3* accumulated 1.4-fold more iron in the grains (Masuda et al., 2008; Ishimaru et al., 2010). The most widely used strategy involves the overexpression of *NAS* gene. *HvNAS1* overexpression lines accumulated 2.3-fold more iron in the rice polished grains (Masuda et al., 2009). Overexpression of *OsNAS3* also increased iron accumulation up to

2.2-fold in the rice grains (Lee et al., 2009b). Moreover, transgenic plants expressing *OsNAS1* or *OsNAS2* accumulated up to 2.2-fold and 4.2-fold more iron in the polished grains than WT plants, respectively (Johnson et al., 2011). Furthermore, the rice plants expressing the combination of *FER*, *NAS* and/ or *PHYTASE* genes accumulated up to 6-fold higher iron concentration in the polished grains as compared to WT plants (Wirth et al., 2009). Overexpression of *FER*, *NAS* and *YSL2* increased the iron accumulation up to 4.4-fold in the rice grains while *FER*, *NAS* and *IDS3* overexpressing lines accumulated up to 4-fold more iron in the rice polished grains (Masuda et al., 2012; Masuda et al., 2013). In addition, the plants overexpressing *NAS*, *FER* and *IRT1* resulted in up to 5-fold higher iron concentration in the polished grains (Boonyaves et al., 2017). The transgenic rice plants expressing bean *FER* and rice *NAS* have been reported with sufficient iron and zinc concentrations in the polished grains to fulfill 30% of EAR in the human diet (Trijatmiko et al., 2016).

1.7 Seed development

1.7.1 General development stages and structure in the seeds

The seeds are the main source of staple foods, animal feed, the raw material of food and the production of biofuels industries in the world (Olsen, 2001; Sabelli and Larkins, 2009). Seed development initiates from double fertilization, in which two of the pollen sperms fuse with an egg cell and a central cell to produce embryo and endosperm, respectively (Chaudhury et al., 2001). The general structure of cereal seed usually consists of an embryo, a large endosperm and the maternal tissues. Embryo stores the genetic information for the next life cycle. It contains embryo axis and scutellum. After fertilization, the zygote undergoes an asymmetric division into a small apical cell and a large basal cell, becoming the embryo proper and the suspensor, respectively (Vernoud et al., 2005). Endosperm is the tissue where the plants store the main nutrients for seed germination. Several stages are important for endosperm development including syncytium, cellularization, differentiation and maturation (Olsen, 2004). Mature endosperm consists of aleurone layer (AL), starchy endosperm (SE), embryo surrounding region (ESR) and endosperm transfer cells (ETC) (Olsen, 2004). The SE itself contains three sub-regions, including the central starchy endosperm (CSE), the conducting zone (CZ) and the sub-aleurone (Olsen, 2004). Maternal tissues include nucellus, pericarp and seed coats, which become a barrier to protect developing seed from pathogen attack and provide a physical restraint for the embryo and endosperm (Krishnan and Dayanandan,

2003; Olsen, 2004). The nucellus provides nutrients to the cellularizing endosperm, and is progressively degenerated during seed development. It eventually becomes a single layer of nucellar epidermis (NE) and a small zone of tissue namely the nucellar projection (NP) (Olsen, 2004). The pericarp contains four vascular traces, three of which are located on the ventral side and the other one is on the dorsal side. The nutrient transport to the ovule and the developing endosperm is provided by the ventral vascular trace, which is called ovular vascular trace (OVT) (Krishnan and Dayanandan, 2003).

In order to understand the molecular mechanisms and the gene expressions within different sub-regions of the seeds, several methods have been developed to collect and separate the various tissue types precisely. Traditional sampling methods usually lead to a mixture of information because of the heterogeneous cell and tissue types present in the samples. Microdissection, however, allows either isolation of specific cell or tissue types or enrichment for particular cells or tissue of interest (Galbraith and Birnbaum, 2006). In laser capture microdissection (LCM), cells of interest are captured from tissue sections onto a transfer film with the help of an infrared laser. In laser capture microdissection, target cells are cut from tissue sections with the help of a UV laser and collected into a tube either by gravity or under the high pressure of a laser beam (Ohtsu et al., 2007; Thiel et al., 2011). These two methods are usually combined with high throughput technologies, including transcriptome, proteome and metabolomic profiling. These methods have been carried out in maize, barley, wheat and rice to have insights into the molecular mechanisms in seed development.

1.7.2 Maize

The endosperm and embryo of maize seeds have been characterized to define gene structure, alternative splicing events and specific gene expression patterns at different developmental stages (Lu et al., 2013c). The results showed that embryo and endosperm exhibit differential alternative splicing patterns. More complex alternative events were observed in embryo than in endosperm. The genes which showed alternative splicing events were involved in diverse biological processes and were highly tissue specific (Lu et al., 2013c). In general, the embryo showed more complex biological process than that in endosperm. The main function of endosperm is to provide nutrients for embryo development and therefore the genes involved in nutrient reservoir, storage protein accumulation, and carbohydrate metabolic process were found to be preferentially

expressed in the endosperm (Lu et al., 2013c; Chen et al., 2014). On the other hand, the main function of the embryo is to transfer genetic information into the next generation by cell division and cell differentiation, and thus the genes involved in chromatin regulation, nucleosome organization, and DNA packaging, as well as lipid biosynthesis genes were found to be preferentially expressed in the embryo (Lu et al., 2013c; Chen et al., 2014). In addition, almost one thousand TF were differentially expressed in the endosperm and embryo, suggesting that the regulatory network in the endosperm and embryo is complex and diverse (Lu et al., 2013c; Chen et al., 2014). For example, MADS TF family showed preferentially higher expression in the endosperm whereas TFs involved in hormone signaling such as ABI3/VP1, ARF, Aux/IAA, GRAS and ARR were up-regulated in the embryo, suggesting an important role of the hormone biosynthesis and regulation in the developing embryo. In addition, some TFs that are involved in cell differentiation and vascular development including zf-HD, MYB, ARF and HB family were found to be highly expressed in the embryo, which is corresponding to the function of preferentially expressed genes there (Lu et al., 2013c).

The following studies comprehensively profiled and analyzed the mRNA populations in different sub-regions of maize seeds including AL, basal endosperm transfer layer (BETL), ESR, SE and CSE, as well as the embryo and four maternal compartments (Nucellus, placenta-chalazal region, pericarp and vascular region of the pedicel) at 8-10 days after pollination (DAP) (Li et al., 2014; Zhan et al., 2015). The differentially expressed genes revealed the distinctive gene expression patterns between filial and maternal sub-regions throughout the seed development. Interestingly, similar biological functions such as DNA replication, cell cycle process and cell division were found in both AL and embryo differentially expressed genes, suggesting a close correlation between these two sub-regions (Zhan et al., 2015). Furthermore, gene co-expression network analysis showed that MYB-RELATED PROTEIN 1 (MRP-1) regulated the BETL specifically expressed genes that contain GATA motif in their sequence and regulated the differentiation and function of BETL (Zhan et al., 2015). The function of these genes is associated with signaling and nutrient transport, supporting the role of BETL as mediator of sugar and metabolite uptake into the developing endosperm (Zhan et al., 2015). The CSE is responsible for the storage of most starch and storage proteins in the endosperm. Consequently, CSE specific genes were found to be involved in starch biosynthesis and glycogen biosynthesis (Zhan et al., 2015). Consistent with the previous reports, the

function of embryo is related to regulation of transcription, floral organ development and response to hormones (Zhan et al., 2015).

1.7.3 Barley

The gene expressions in the NP and ETC in the barely seeds have been analyzed during seed development (Thiel et al., 2008). The NP is thought to be involved in cell differentiation, since the NP specific genes are associated with different histone genes, cell wall biosynthesis and extension genes, as well as genes involved in programmed cell death. Moreover, the NP specific genes also included those related to gibberellin (GA) synthesis and signaling, suggesting GA participated in the establishment of the cell differentiation in the NP (Thiel et al., 2008; Thiel et al., 2009). In contrast, the AP2/EREBP-like TFs and ethylene related genes are preferentially expressed in the ETC, indicating it is involved in defence mechanisms and therefore it might affect the development of barley grains (Thiel et al., 2008). In addition, genes encoding nucleotide sugar metabolism such as trehalose-6-P synthase and phosphatase are up-regulated in the ETC, suggesting it may be attributed to cell wall biosynthesis (Thiel et al., 2008). Various transporters are differentially expressed in the NP and ETC. For example, genes encoding amino acid permeases and proton-coupled cotransporters are up-regulated in the ETC while plasmalemma-intrinsic protein and tonoplast-intrinsic protein genes are up-regulated in the NP. These results indicate the important roles of NP and ETC in nutrient uptake and transport to the developing endosperm (Thiel et al., 2008; Thiel et al., 2009; Thiel et al., 2012).

Thiel et al. reported that the genes related to cell shape control and vesicle transport, as well as cell wall biosynthesis genes were activated at 5 and 7 DAP in the ETCs (Thiel et al., 2012; Thiel, 2014). These genes included those related to amino acid catabolism, C:N balances, carbohydrate oxidation, mitochondrial activity and starch degradation, which could provide respiratory energy and carbohydrates to the developing ETC (Thiel et al., 2012). In addition, the transcriptional activity of assimilate and micronutrient transporters were up-regulated at 5 and 7 DAP, suggesting ETC as the major uptake sub-region of solutes into the developing endosperm.

1.7.4 Wheat

Gillies et al., 2012 compared the differential gene expression in the endosperm and AL at different time points (Gillies et al., 2012). Their data suggested that endosperm is a main carbohydrate storage tissue, while AL additionally accumulates lipids and proteins. Genes related to RNA binding and translation factor activity were up-regulated in the endosperm as compared to those in the AL, while up-regulated genes were related to stress tolerance such as abiotic stress and redox reactions in the AL at late developmental stages (Gillies et al., 2012). Another study focused on analyzing gene expression in three different sub-types of endosperm, including SE, AL and ETC during the wheat seed development (Pfeifer et al., 2014). Their results showed that the genes preferentially expressing in whole endosperm were related to carbohydrate metabolic processes and glycolysis. AL specific genes exhibited a separate expression cluster from all other sub-regions, in which the genes were related to lipid metabolism, structural development, carbohydrate metabolic processes and amino acid biosynthesis. SE specific genes were associated to carbohydrate and saccharide metabolism, and ETC specific genes were enriched for proteolysis and defence-response genes (Pfeifer et al., 2014).

1.7.5 Rice

Rice developing embryo samples have been analyzed to identify the stage-specific gene expression associated with embryogenesis processes (Xu et al., 2012b). The genes related to metabolism, transcriptional regulation, nucleic acid replication or processing, and signal transduction were preferentially expressed in the early and middle stages of embryogenesis. Protein biosynthesis-related genes were enriched in the middle stage. On the contrary, genes responsible for starch or sucrose metabolism and protein modification were highly expressed in the middle and late stages of embryogenesis (Xu et al., 2012b). Several stage-specific TF families have been identified to be involved in the embryogenesis process. For example, the AP2 TF members were enriched in early developmental stage while the MADS-box TF members were enriched in the middle and late developmental stages (Xu et al., 2012b).

Additionally, stage-specific genes in the rice endosperms have been analyzed during grain filling (Gao et al., 2013). The genes related to ribosomes, the spliceosome and oxidative phosphorylation were highly expressed in the early and middle stages. Plant hormone, galactose metabolism and carbon fixation related genes showed a significant

increase in expression in the middle stage, while genes for defence against disease or response to stress as well as genes for starch or sucrose metabolism were highly expressed during the late stages of the endosperm development (Gao et al., 2013). The NF-YA TF family showed up-regulation in the early stage while the GRAS TF family was up-regulated in the middle stage. The Dof TF family members were expressed during all three stages, indicating that Dof TFs play a role in the storage process during endosperm development (Gao et al., 2013). Taken together, complex differentially expressed genes and transcriptional network have been reported in the embryo and endosperm of rice seeds, but a more detailed analysis on different seed sub-regions has not yet been reported.

1.8 Aims of the PhD thesis

My thesis aimed at evaluating two new strategies for iron biofortification and identifying specific gene expression profiles during rice grain development.

The two biofortification strategies included the combination of vacuolar iron transporter *AtNRAMP3* together with *NAS* and *FER*, and the combination of citrate transporter *AtFRD3* with *NAS* and *FER*, respectively. This work hypothesizes that overexpressing *AtNRAMP3* or *AtFRD3* together with *NAS* and *FER* can lead to further increases in iron concentration in the rice endosperm than previously achieved. Additionally, the expression of *AtNRAMP3* under the control of rice *Olesin 18* promoter and maize *UBIQUITIN* promoter is investigated.

In case of gene expression profiling during rice grain development, the mRNA populations from different sub-regions of the rice grain collected at different development stages are investigated. The PhD thesis was conducted with following objectives:

1. To test if the combination of *AtNRAMP3*, *AtNAS1* and *PvFER* genes lead to increased level of iron concentration in the rice endosperm in two rice cultivars.
2. To test if the combination of *AtFRD3*, *AtNAS1* and *PvFER* genes lead to increased level of iron concentration in the rice endosperm.
3. To investigate the spatiotemporal gene expression profiles in different grain sub-regions during rice grain development.

2. Targeting intra-cellular iron transport combined with efficient uptake and storage significantly increases grain iron levels in rice

Ting-Ying Wu, Wilhelm Gruissem and Navreet K. Bhullar*
Plant Biotechnology, Department of Biology, ETH Zurich, Universitaetsstrasse 2, 8092 Zurich, Switzerland

*** Corresponding author**

Dr. Navreet K. Bhullar
Plant Biotechnology,
Department of Biology
ETH Zurich (Swiss Federal Institute of Technology)
Universitaetsstrasse 2
8092 Zurich, Switzerland
bhullarn@ethz.ch

Submitted to Proceeding of the National Academy of Sciences (PNAS)

2.1 Abstract

Biofortification in staple crops is regarded as an effective and sustainable solution for reducing global micronutrient malnutrition. Rice is a staple food for more than half of the world population and therefore an important target for iron biofortification. Current strategies mainly focus on the expression of genes for iron uptake, long-distance transport and storage. Targeting intracellular iron mobilization to increase grain iron levels has not been reported. The vacuole is an important cell compartment for iron storage and the NATURAL RESISTANCE ASSOCIATED MACROPHAGE PROTEIN (NRAMP) family of transporters export iron from vacuoles to the cytosol when needed. We developed transgenic Nipponbare rice lines expressing *AtNRAMP3* under the control of the *UBIQUITIN* or rice embryo/aleurone-specific *18kDa Oleosin (Ole18)* promoter together with *NICOTIANAMINE SYNTHASE (AtNAS1)* and *FERRITIN (PvFER)*, or expressing only *AtNRAMP3* and *PvFER* together. Iron and zinc were increased close to recommended levels in polished grains of the transformed lines, with maximum levels when *AtNRAMP3*, *AtNAS1* and *PvFER* were expressed together. Cadmium levels were unchanged in polished transgenic grains relative to non-transformed control. Similar high iron and zinc levels were obtained in transgenic Indica IR64 lines expressing the *AtNRAMP3*, *AtNAS1* and *PvFER* cassette, equaling more than 90% of the recommended iron increase in rice endosperm. Our results demonstrate that targeting intracellular iron stores in combination with iron transport and endosperm storage is an effective strategy for iron biofortification. The iron levels achieved in polished IR64 grains are of dietary relevance for human health and a valuable nutrition trait for breeding programs.

Keywords: Rice, Iron biofortification, vacuolar iron, *NAS1*, *NRAMP3*, *FERRITIN*

2.2 Introduction

Iron deficiency is the most common nutritional deficiency that is widespread in developing countries but not uncommon in developed countries as well. Nearly 1.6 billion people in the world are affected by iron deficiency (Stevens et al., 2013). Diet diversification, iron supplementation and food fortification are among the recommended approaches to relieve iron deficiency. However, these approaches are often difficult to implement due to various regional socio-economic factors. Furthermore, oral iron supplementation can lead to side effects including nausea and gastric pain and could increase the severity of infectious diseases, such as malaria (Oppenheimer et al., 1986; Sazawal et al., 2006). Food fortification usually causes color and flavor changes because bioavailable iron molecules often react with other food molecules (Hurrell, 2002; Abbaspour et al., 2014). Biofortification for increasing iron in staple crops is therefore a promising strategy to overcome these constraints. Rice is the second most produced staple crop worldwide and consumed by more than half of the world population. Brown rice, which includes the aleurone layer of the seed coat (bran), is relatively rich in micronutrient content, including iron. However, to avoid rancidity during storage rice is usually polished, consequently removing the nutrient-rich bran. The polished white rice (which is mostly the endosperm of the grain) contains mainly starch and is poor in iron and other micronutrients. Most of the commercially-bred rice varieties contain only around two $\mu\text{g/g}$ iron in the endosperm (Bouis et al., 2011). It has not been possible to increase the endosperm iron concentration in rice via conventional breeding because of the limited genetic variability of endosperm iron content in the rice germplasm (Bouis et al., 2011). Genetic engineering approaches, however, were successful in increasing the iron concentration in polished rice grains (Vasconcelos et al., 2017).

The continuously developing knowledge on iron uptake, storage and translocation in rice has driven the design of iron biofortification approaches during the last few years. *FERRITIN* (*FER*), a ubiquitous protein that can bind about 4500 iron atoms in a complex (Ford et al., 1984; Harrison et al., 1991), has been used to increase iron accumulation in the rice endosperm (Goto et al., 1999; Lucca et al., 2001a; Vasconcelos et al., 2003; Oliva et al., 2014). Many laboratories also focused on strategies with potential to enhance iron uptake and translocation. Most gramineous plants acquire iron using Strategy II, which involves the biosynthesis and secretion of mugineic acids (MAs) (Shojima et al., 1990; Bashir et al., 2006; Kobayashi and Nishizawa, 2012). The MAs (specifically

deoxymugineic acid, DMA) are synthesized from S-adenosyl-L-methionine via a conserved pathway of three sequential enzymatic reactions catalyzed by NICOTINAMINE SYNTHASE (NAS), NICOTIANAMINE AMINOTRANSFERASE (NAAT) and DEOXYMUGINEIC ACID SYNTHASE (DMAS), respectively (Kobayashi and Nishizawa, 2012). Furthermore, nicotianamine (NA) produced by NAS is a primary chelator of iron in the phloem that facilitates effective iron translocation. Therefore, constitutive expression of *NAS* to increase iron uptake and translocation has been a widely-used approach for iron biofortification, with two- to 4.5-fold increased iron concentrations obtained in polished grains (Masuda et al., 2009; Johnson et al., 2011; Lee et al., 2012a). Among the other genes encoding iron transporters, *YELLOW STRIPE LIKE 2* (*OsYSL2*) and *IRON REGULATED TRANSPORTER 1* (*OsIRT1*) have also been transformed into rice either alone or in combination with genes related to MA synthesis and varied levels of iron increase were found in the rice grains (Lee and An, 2009; Ishimaru et al., 2010; Tan et al., 2015). *OsYSL2* is a long-distance transporter of NA-Fe complexes and *OsIRT1* facilitates Fe(II) uptake from the rhizosphere to root cells (Ishimaru et al., 2006; Ishimaru et al., 2010). In comparison to the single gene strategies, constructs expressing combinations of genes involved in iron transport and uptake could achieve higher endosperm iron concentrations in rice. The combination of endosperm-specific expression of *FER* and constitutive expression of *NAS* in rice resulted in a six-fold iron increase in polished grains (Wirth et al., 2009). Expression of *AtIRT1* under control of the *Medicago sativa* *EARLY NODULIN 12B* promoter in these lines could further increase the iron content in polished grains by 2.2-fold (Boonyaves et al., 2016). Indica rice lines expressing the combination of *FER* and *NAS* had a seven-fold higher iron content in the endosperm (Trijatmiko et al., 2016).

Cytosolic free Fe concentrations are very low in plant cells because most of the iron is stored in chloroplasts, mitochondria and vacuoles in non-toxic forms and used for the synthesis of Fe-heme or Fe-S clusters (Finney and O'Halloran, 2003). Vacuoles have an important function in storing excess Fe and releasing it into the cytosol when the external Fe supply is sub-optimal (Pich et al., 2001; Kim and Guerinot, 2007; Lanquar et al., 2010). In *Arabidopsis*, the vacuolar membrane located VACUOLAR IRON TRANSPORTER 1 (*AtVIT1*) is responsible for iron uptake into vacuoles (Kim et al., 2006). Oppositely, specific members of the NATURAL RESISTANCE ASSOCIATED MACHROPHAGE PROTEIN (NRAMP) family mediate the efflux of iron from the

vacuoles to the cytosol. NRAMP transporters localize to either intracellular vesicles, the vacuole or the plasma membrane depending on the plant species (Bereczky et al., 2003; Thomine et al., 2003; Lanquar et al., 2005; Takahashi et al., 2011). Arabidopsis AtNRAMP1, AtNRAMP3 and AtNRAMP4 mediate iron and cadmium transport, and *AtNRAMP1* is preferentially expressed in roots (Curie et al., 2000; Thomine et al., 2000). AtNRAMP3 and AtNRAMP4 are localized to the vacuolar membrane and their genes are induced by iron deficiency (Thomine et al., 2003; Lanquar et al., 2005; Lanquar et al., 2010). The *atnr3nr4* double mutant has defects in seed germination and early seedling development in low iron growth conditions (Lanquar et al., 2005). In wild type plants, iron-globoids disappear from vacuoles during germination but they remain in the vacuoles of the double mutant, suggesting that the mutants fail to transport iron from vacuolar globoids to the cytosol (Lanquar et al., 2005). Among the seven *NRAMP* homologs identified in rice, *OsNRAMP1* is involved in iron uptake (Curie et al., 2000) and is localized to the plasma membrane (Takahashi et al., 2011).

Utilizing vacuolar iron stores for increasing endosperm iron content has not been attempted to date. Here we demonstrate that inter- and intra-cellular iron mobilization can be effectively combined for biofortification strategies in rice. To accomplish this, we expressed *AtNRAMP3* under control of either the rice *18kDa Oleosin (Ole18)* or maize *UBIQUITIN (Ubi)* promoters together with the endosperm-specific expression of *PvFER* alone or in combination with the constitutive expression of *AtNAS1*. Most of the transgenic lines (background cv. Nipponbare) had significant increases of iron and zinc in both unpolished and polished grains, with maximum endosperm iron levels in lines expressing *AtNRAMP3*, *AtNAS1* and *PvFER* together. Importantly, expression of all three genes in the popular rice mega-variety IR64 resulted in iron concentrations equaling more than 90% of the recommended iron increase in rice grains.

2.3 Results

2.3.1 Combined expression of *AtNRAMP3*, *AtNAS1* and *PvFER* increases iron and zinc concentrations in polished rice grains

We transformed the rice cultivar Nipponbare (NB) with four constructs expressing different combination of genes, abbreviated NFUN (*pCaMV35S::AtNAS1*, *pOsGLB-1::PvFER*, *pZmUbi::AtNRAMP3*), NFON (*pCaMV35S::AtNAS1*, *pOsGLB-1::PvFER*, *pOsOle18::AtNRAMP3*), FUN (*pOsGLB-1::PvFER*, *pZmUbi::AtNRAMP3*), and FON

(*pOsGLB-1::PvFER*, *pOsOle18::AtNRAMP3*) (Fig. 1A). Together, 16 independent single insertion lines for each of the NFUN, NFON and FUN constructs, and 13 single insertion lines for the FON construct were selected and grown in subsequent generations (Fig. S1). Based on iron concentration analysis of T2 grains, we selected five or six lines for each of the four constructs with highest endosperm iron concentration for further analysis in subsequent generations (Fig. S2A). All of the NFUN and FUN lines had increased iron concentrations in polished T3 grains, ranging from 8.09 to 11.69 $\mu\text{g/g DW}$, respectively, as compared to 2.12 $\mu\text{g/g DW}$ iron in the NB control (Fig. 1B). Similarly, NFON and FON transgenic lines had increased iron concentrations in polished grains ranging from 7.64 to 12.77 $\mu\text{g/g DW}$, with NFON 16 having a more than six-fold higher endosperm iron concentration than the NB control (Fig. 1B). In unpolished grains, NFUN and NFON lines had higher increases in iron concentrations compared to FUN and FON lines, with NFON 12 unpolished grains containing 29.75 $\mu\text{g/g DW}$ iron (Fig. 1B). Together, all transgenic rice lines had significantly higher iron concentrations in unpolished grains compared to NB grains. Prussian blue staining of grains from selected NFUN and NFON lines confirmed the increased endosperm iron concentration (Fig. S2B). In addition, all NFUN and NFON lines had significantly increased zinc concentrations in polished and unpolished T3 grains, ranging from 29.68 to 45.62 $\mu\text{g/g DW}$ in polished grains as compared to 19.38 $\mu\text{g/g DW}$ in the NB control, and from 45.96 to 63.04 $\mu\text{g/g DW}$ in unpolished grains compared to 29.54 $\mu\text{g/g DW}$ in the NB control (Fig. 2). Increases in iron and zinc concentrations were positively correlated in NFON lines. Copper concentrations were variable in some lines, while most lines had reduced manganese concentrations in the grains (Fig. S3). Most transgenic plants were phenotypically similar to NB control plants and had comparable germination rates (Table 1 and Fig. S4). Some of the NFON lines, however, had higher tiller numbers than NB (Table 1). With few exceptions, six grain-quality parameters measured in the transgenic lines (grain length, grain width, chalkiness, amylose content, starch content, protein content) were similar to NB control plants (Table S1).

Together, the highest iron and zinc increases in the grains were observed in lines expressing the combination of NAS, FER and NRAMP (NFUN, NFON) as compared to the lines expressing FER and NRAMP only (FUN, FON) (Fig. 1 and Fig. 2). The higher micronutrient concentrations in the NFON lines suggest that the *Ole18* promoter is equally (and in some lines even more) effective for the expression of *AtNRAMP3*

compared to the *Ubi* promoter. Therefore, the *Ole18* promoter would be preferable for targeted and localized expression in biofortification strategies.

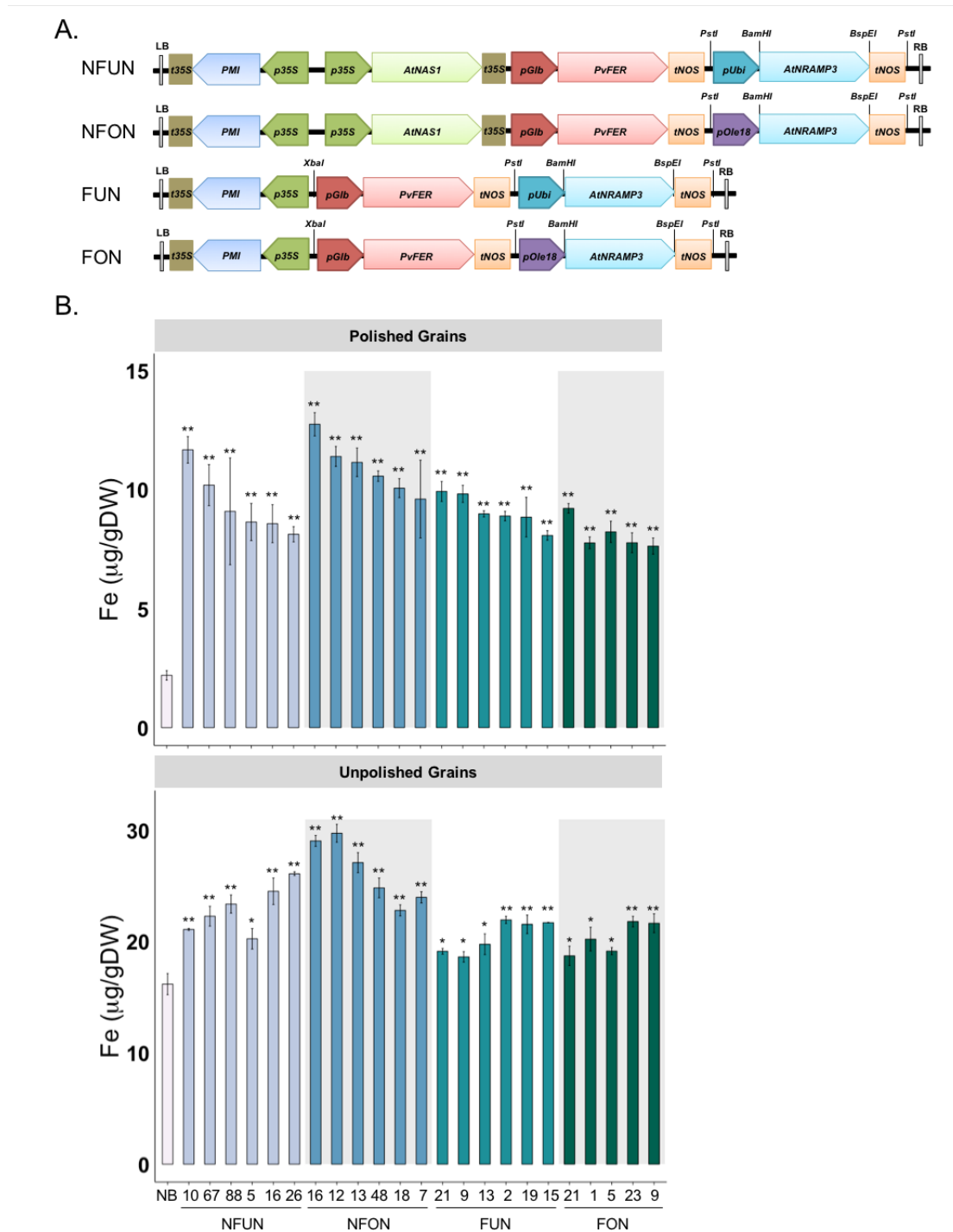


Fig. 1 Schematic representation of the gene cassettes, and iron concentrations in polished and unpolished T3 grains. (A) The design of four constructs used for transformation. LB, T-DNA left border; RB, T-DNA right border; t35S, cauliflower mosaic virus (CaMV) 35S terminator; *PMI*, *PHOSPHOMANNOSE ISOMERASE* gene; *p35S*, *CaMV35S* promoter; *pUbi*, maize *UBIQUITIN* promoter; *AtNRAMP3*, Arabidopsis *NATURAL RESISTANCE-ASSOCIATED*

MACROPHAGE PROTEIN 3 gene; *AtNAS1*, Arabidopsis *NICOTIANAMINE SYNTHASE 1* gene; *tNOS*, *NOPALINE SYNTHASE* terminator; *pGlb*, rice *GLOBULIN-1* promoter; *PvFER*, *Phaseolus vulgaris FERRITIN* gene; *pOle 18*, rice *Oleosin 18* gene promoter; BamHI, BspEI, PstI and SphI represent restriction enzyme sites. (B) Iron concentrations in polished and unpolished T3 grains of lines expressing *AtNRAMP3*, *AtNAS1* and *PvFER* or *AtNRAMP3* and *PvFER* cassettes. Values are the average of three biological replicates. NB, rice cultivar Nipponbare (control); NFUN, plants expressing *pCaMV35S::AtNAS1*, *pOsGLB-1::PvFER* and *pZmUbi::AtNRAMP3*; NFON, plants expressing *pCaMV35S::AtNAS1*, *pOsGLB-1::PvFER* and *pOsOle18::AtNRAMP3*; FUN, plants expressing *pOsGLB-1::PvFER*, and *pZmUbi::AtNRAMP3*; FON, plants expressing *pOsGLB-1::PvFER*, and *pOsOle18::AtNRAMP3*. Black asterisks indicate statistically significantly higher values calculated using Student's T-Test as compared to the NB control (*p<0.05, **p<0.01). Error bars represent standard deviation.

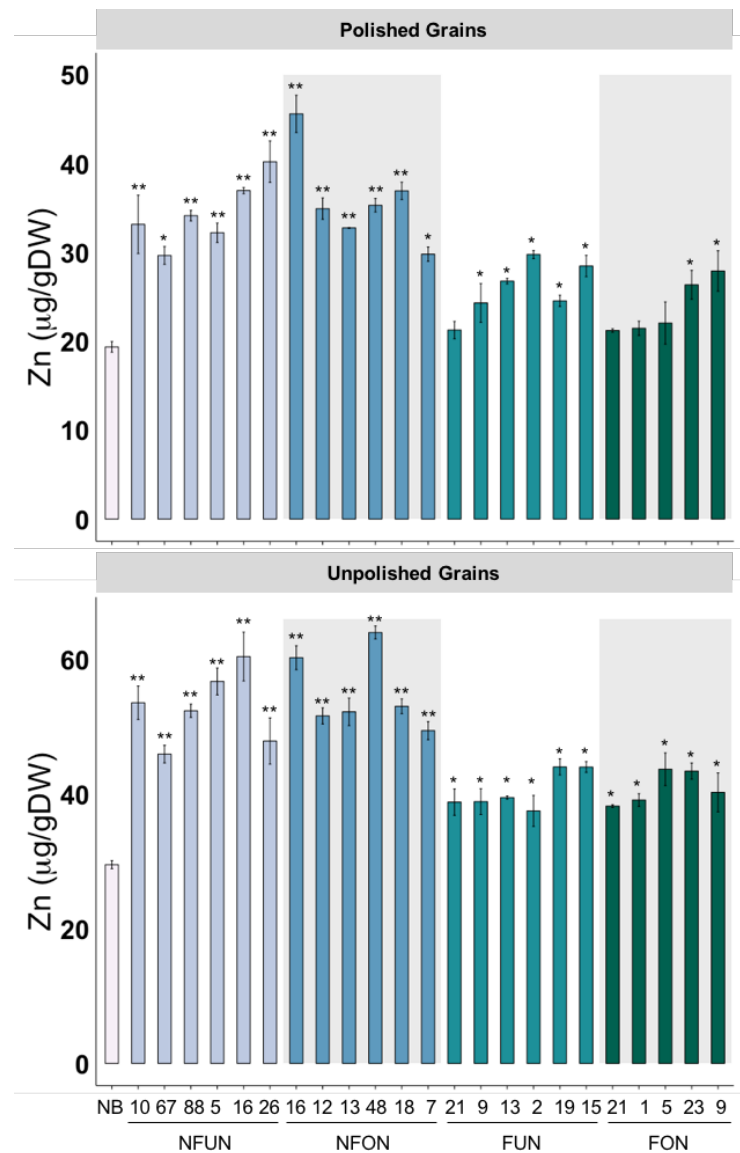


Fig. 2 Zinc concentrations in polished and unpolished T3 grains of lines expressing *AtNRAMP3*, *AtNAS1* and *PvFER* or *AtNRAMP3* and *PvFER* alone. Values are the average of three biological replicates. Black asterisks indicate statistically significantly higher values calculated using Student's T-Test as compared to the NB control (*p<0.05, **p<0.01). See Fig. 1A for the abbreviation of the gene cassettes. Error bars represent standard deviation.

Table 1 Phenotypic assessment of selected transgenic lines in T2 generation grown in the greenhouse condition. Parameters including days to flowering (DTF), soil-plant analysis development (SPAD) value, plant height, tiller number, one thousand grain weight (1000grain weight), panicle weight and panicle filling rate are presented. Values are the average of three individual plants. Panicle weight and panicle filling rate are the average of 12 panicles per line (T4 grains). Black and red asterisks indicate statistically significantly higher and lower values as compared to the NB control (*p<0.05, **p<0.01), respectively. The number that follows the ± sign is the standard deviation. See Fig. 1A for the abbreviation of the gene cassettes.

Plant line	Height (cm)	Tiller No.	SPAD	DTF	1000GrainWeight (g)	Panicle weight (g)	Grain filling (%)
NB	63.33 (±2.08)	7.67 (±1.53)	36.00 (±3.00)	81.00 (±1.00)	24.17 (±0.29)	4.49 (±0.89)	79.28 (±1.44)
NFUN							
5	59.00 (±2.00)	7.67 (±1.53)	38.00 (±1.00)	79.33 (±1.53)	25.83 (±0.76)	4.48 (±0.76)	83.88 (±1.41)*
67	61.67 (±2.31)	12.00 (±2.00)*	36.00 (±1.00)	78.33 (±1.53)	22.50 (±0.87)*	4.27 (±0.54)	82.53 (±1.09)
88	63.00 (±2.00)	11.33 (±2.08)*	38.33 (±1.53)	84.00 (±1.00)	25.33 (±0.29)	4.35 (±0.57)	72.01 (±1.47)*
26	59.00 (±2.00)	9.00 (±1.00)	38.33 (±2.08)	79.00 (±1.00)	26.17 (±0.29)	4.51 (±0.54)	85.03 (±1.11)
16	54.33 (±1.53)*	8.33 (±0.58)	39.00 (±1.00)	81.33 (±0.58)	25.33 (±0.76)	4.42 (±0.57)	83.29 (±0.98)*
10	60.67 (±1.53)	6.67 (±0.58)	38.33 (±1.15)	82.00 (±1.00)	24.33 (±0.29)	4.35 (±0.65)	80.85 (±2.01)
NFON							
7	58.33 (±1.15)	10.67 (±2.08)*	37.00 (±2.00)	78.00 (±1.00)	23.00 (±0.50)	4.65 (±0.92)	84.07 (±1.08)*
16	55.00 (±2.00)*	9.00 (±1.00)	36.67 (±2.08)	80.00 (±1.00)	24.00 (±0.50)	4.54 (±0.88)	80.04 (±1.10)
48	59.33 (±1.53)	12.00 (±1.00)*	36.67 (±0.58)	82.67 (±3.21)	23.67 (±0.76)	4.53 (±0.79)	81.60 (±1.96)
13	62.67 (±1.53)	12.00 (±2.00)*	36.67 (±2.08)	79.00 (±2.00)	24.50 (±0.50)	4.62 (±0.89)	82.17 (±0.89)
18	58.33 (±1.53)	7.33 (±1.53)	38.00 (±1.00)	81.00 (±1.00)	23.67 (±0.58)	4.57 (±0.76)	83.26 (±0.98)*
12	61.50 (±1.40)	10.00 (±1.20)*	39.00 (±2.00)	83.00 (±1.00)	23.70 (±0.58)	4.48 (±0.45)	81.97 (±1.15)
FUN							
2	61.33 (±2.08)	8.33 (±2.08)	38.67 (±1.53)	83.67 (±1.53)	25.00 (±0.50)	4.30 (±0.66)	79.02 (±1.11)
6	59.00 (±2.00)	7.33 (±1.15)	36.33 (±1.53)	80.00 (±1.00)	25.50 (±0.50)	4.77 (±1.07)	81.10 (±1.10)
16	61.00 (±1.00)	7.33 (±0.58)	38.67 (±1.53)	78.67 (±1.53)	22.83 (±0.58)	4.42 (±0.54)	79.83 (±1.21)
19	58.33 (±1.53)	7.00 (±1.00)	38.33 (±1.53)	82.33 (±1.53)	23.50 (±0.50)	4.62 (±0.67)	82.46 (±1.01)
9	59.67 (±1.53)	8.33 (±1.15)	37.86 (±0.58)	82.67 (±3.21)	24.86 (±0.50)	4.42 (±0.88)	80.16 (±1.21)
10	60.00 (±1.00)	11.33 (±1.00)*	36.67 (±1.08)	82.33 (±1.53)	23.12 (±0.58)	4.56 (±0.68)	85.84 (±1.03)*
FON							
21	59.33 (±1.00)	7.67 (±1.00)	38.67 (±1.08)	79.00 (±1.53)	22.85 (±0.58)	4.83 (±0.99)*	80.37 (±1.11)
1	58.33 (±0.53)	8.33 (±1.15)	37.33 (±0.58)	80.00 (±1.00)	24.12 (±0.50)	4.53 (±0.84)	83.19 (±1.08)*
5	57.67 (±1.53)*	7.33 (±0.58)	39.33 (±2.00)	78.00 (±1.00)	23.50 (±0.76)	4.48 (±0.57)	81.03 (±1.10)
9	59.67 (±1.53)	9.83 (±1.15)*	39.00 (±1.00)	78.67 (±1.53)	22.85 (±0.58)	4.75 (±0.91)	79.63 (±0.97)
23	58.67 (±1.53)	9.83 (±1.15)*	36.67 (±2.08)	81.00 (±1.50)	23.50 (±0.28)	4.68 (±0.89)	82.05 (±1.13)

2.3.2 Grain iron concentration and gene expression are positively correlated

The expression of the transgenes was analyzed in shoots and grains (embryo, endosperm and seed coat). As expected, *AtNAS1* was expressed in all analyzed tissues of NFUN and NFON lines, while expression of *PvFER* was detected only in the endosperm (Fig. 3A). *AtNRAMP3* was also expressed in all the tissues but more highly in shoots and embryos of NFUN and FUN transgenic lines (Fig. 3A). As expected, *AtNRAMP3* expression was restricted to the embryo and seed coat in NFON and FON lines (Fig. 3A). This was further confirmed by detection of the AtNRAMP3 protein in these specific tissues (Fig. 3B). In NFON lines, transgene expression in the embryo and endosperm was positively correlated with increased iron concentration in the polished grains, indicating a synergistic action of *NAS*, *FER* and *NRAMP* (Fig. 3C). Since constitutive ectopic expression of *AtNRAMP3* suppresses *AtIRT1* expression in Arabidopsis plants (Thomine et al., 2003), we analyzed the expression of the *AtIRT1* rice homolog *OsIRT1* in different tissues. Although the expression of *OsIRT1* was variable in different transgenic lines, we found no indication that *OsIRT1* expression was suppressed (Fig. S5).

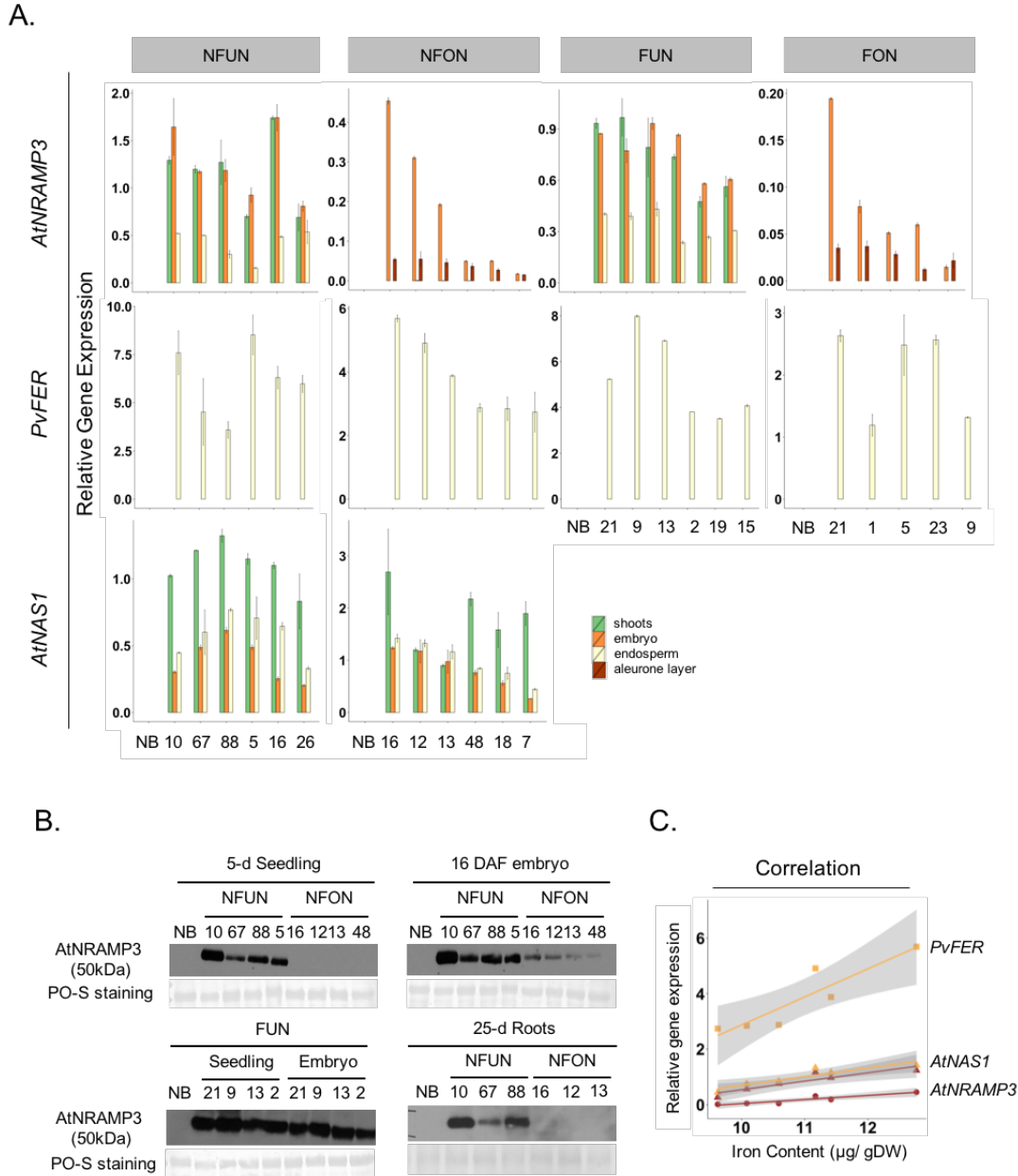


Fig. 3 Transgene expression and AtNRAMP3 protein levels in seedlings, embryo, endosperm and seed coats. (A) qRT-PCR results of *AtNAS1*, *PvFER* and *AtNRAMP3* expression level in Nipponbare control (NB) and the selected transgenic lines. (B) Western blot analysis of *AtNRAMP3* protein abundance in different tissues. Total protein extraction from NB served as a negative control. Ponceau (PO-S) staining: loading control. Individual numbers indicate independent transgenic lines. (C) Correlation between iron content and gene expression in NFN plants (lines 16, 12, 13, 48, 18, 7). Individual lines are represented by colored dots. See Fig. 1A for the abbreviation of the gene cassettes. Error bars represent standard deviation ($n = 10$ for seedlings; $n = 30$ for embryo, endosperm and seed coats, and three replications).

2.3.3 NFUN and NFON lines are more tolerant to iron-deficient growth conditions

We determined the iron and zinc distribution in the shoots and roots of selected transgenic lines for each construct when grown in iron-sufficient and iron-deficient conditions. In iron-sufficient conditions, most of the lines showed no significant increase in iron accumulation in the shoots and roots, except for NFON 16 that had a 1.5-fold higher iron concentration in shoots and 1.3-fold higher iron concentration in roots (Fig. 4A). When grown in iron-deficient conditions, most of the NFUN, NFON and FUN lines had increased iron concentrations in the shoots whereas FON lines had similar iron concentrations as NB (Fig. 4A). NFUN lines had the highest iron concentration in shoots, ranging from 1.4-fold to 1.6-fold higher than NB. The iron concentration in roots was lower in NFUN, NFON and FUN lines, with a nearly two-fold reduction in NFUN lines, while FON lines had similar root iron concentrations as NB roots (Fig. 4A). In iron-sufficient conditions, NFON and NFUN lines also had increased shoot zinc levels compared to NB, but root zinc levels were similar in all transgenic lines and the control (Fig. 4B). In contrast, in iron-deficient conditions shoot zinc concentrations were higher in NFON lines but 1.5-fold and two-fold lower in NFUN and FUN lines, respectively, compared to NB (Fig. 4B). Shoot and root fresh weight was similar for transgenic plants and NB control when grown in iron-sufficient conditions (Fig. 4 C and D). In iron-deficient growth condition, however, NFUN, NFON and FUN lines had higher shoot and root fresh weight than NB, while FON transgenic plants showed no differences (Fig. 4 C and D). These results indicate that the expression of *AtNRAMP3* and/ or *AtNAS1* facilitates efficient iron translocation from roots to shoots, leading to increased tolerance to low iron condition.

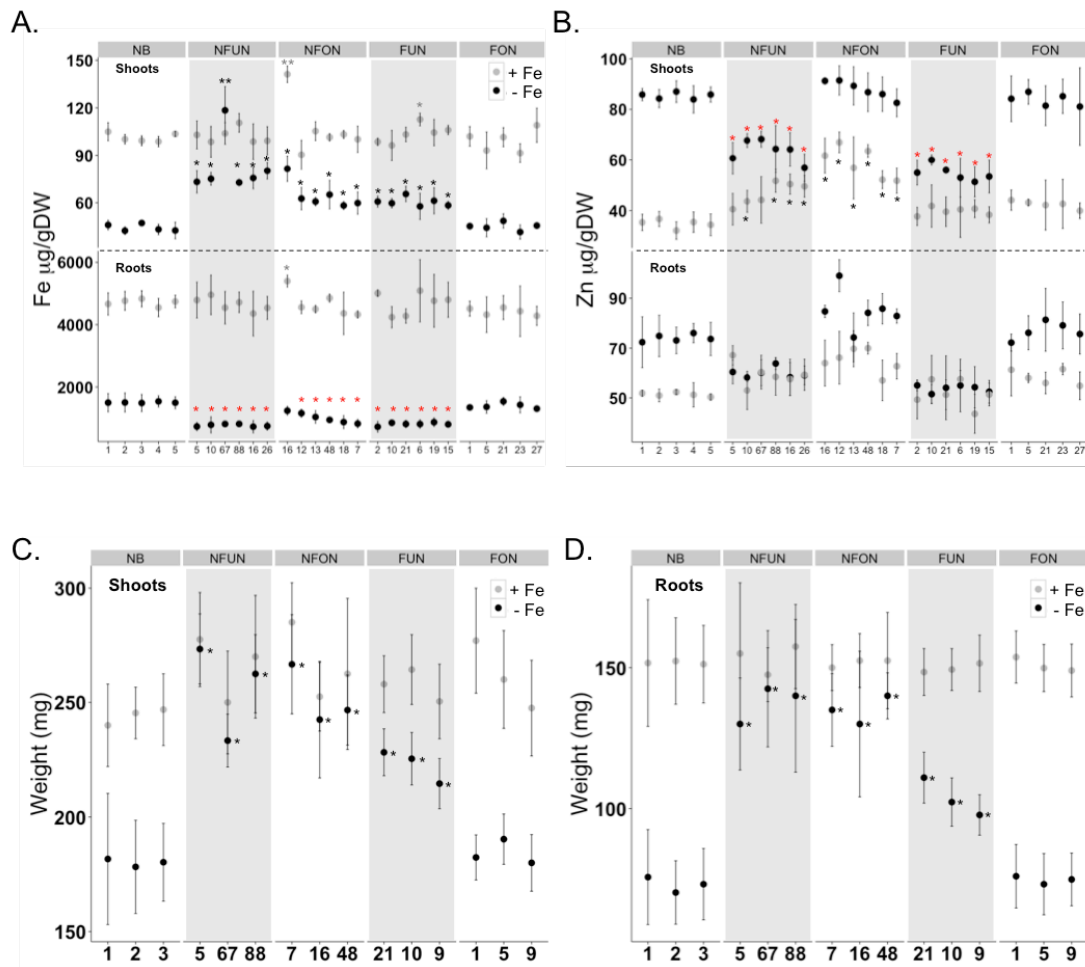


Fig. 4 Characterization of selected transgenic lines under iron sufficient and deficient growth conditions. (A) Iron and (B) zinc concentrations in shoots and roots of 28d-old seedlings. (C) Fresh weight of shoots and (D) roots. Samples were collected from 20 plants of each independent transgenic line and students' T-Test was used for statistical analysis. Black and red asterisks indicate statistically significantly higher and lower values as compared to the NB control (* $p < 0.05$, ** $p < 0.01$), respectively. See Fig. 1A for the abbreviation of the gene cassettes. Error bars represent standard deviation.

2.3.4 Iron-deficiency induction of iron homeostasis-related genes is reduced in the transgenic plants

We analyzed the expression of nine endogenous genes involved in iron homeostasis in shoots and roots of plants grown under iron-deficient and iron-sufficient conditions. These included genes encoding enzymes for NA and DMA synthesis (*OsNAS1*, *OsNAAT1*), transcription factors (*OsIDEF1*, *OsIRO2*), iron-regulated transporters and intercellular transporters (*OsIRT1*, *OsNRAMP1*, *OsYSL2*, *OsFRO1*), and ferritin (*OsFER1*). *OsNAS1*, *OsNAAT1*, *OsIRT1*, *OsNRAMP1*, *OsIDEF1* and *OsIRO2* are highly induced by iron deficiency (Ogo et al., 2007; Kobayashi et al., 2009; Wang et al., 2013b).

In iron-sufficient conditions, most of the genes were expressed at similar levels in both transgenic and NB plants, but their expression was significantly different in iron-deficient conditions (Fig. 5). In general, NB, FUN and FON plants were more sensitive to iron deficiency compared to NFUN and NFON plants in both shoots and roots. Most genes were up-regulated in both roots and shoots of NB, FUN and FON plants (Fig. 5A). Although the genes were also upregulated in NFON plants in iron-deficient conditions, their induction was significantly lower (Fig. 5B), suggesting that expression of *AtNAS1* and/ or *AtNRAMP3* allows these plants to maintain iron homeostasis also under iron deficiency. The transcription factors *OsIRO2* and *OsIDEF1* regulate the expression of *OsNAS1*, *OsNAAT1*, *OsIRT1* and *OsNRAMP1* in response to iron deficiency. The expression of these two transcription factors was not significantly changed in NFUN plants, consistent with the reduced expression of their target genes in iron-deficient conditions.

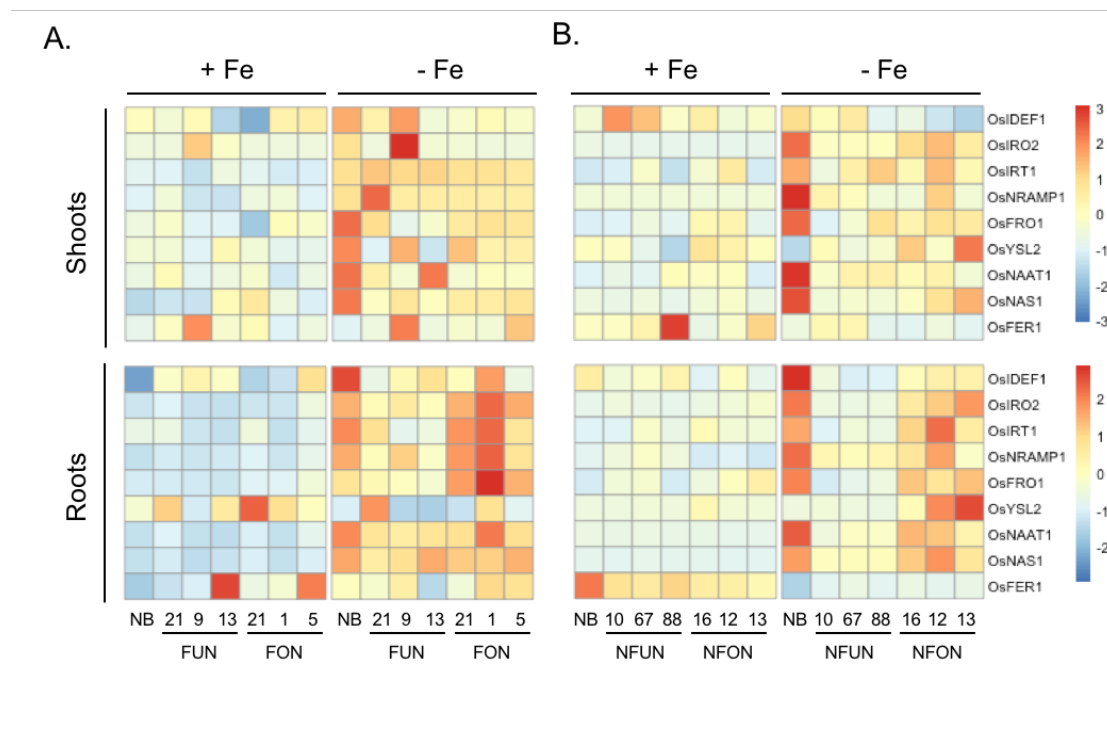


Fig. 5 Expression analysis of iron homeostasis related genes. Expression of selected endogenous genes was detected by qRT-PCR in shoots and roots of (A) FUN and FON plants and (B) NFUN and NFON plants, subjected to iron sufficient and iron deficient growth conditions. See Fig. 1A for the abbreviation of the gene cassettes.

2.3.5 Transgenic plants do not accumulate more cadmium in grains

Arabidopsis lines that overexpress *AtNRAMP3* accumulate more cadmium in leaves and roots (Thomine et al., 2000; Thomine et al., 2003). We determined cadmium

concentration in shoots, roots and grains of our transgenic rice plants grown in a hydroponic solution containing cadmium. The transgenic plants had similar cadmium concentrations compared to the NB control, ranging from 36.24 $\mu\text{g/g}$ DW to 50.00 $\mu\text{g/g}$ DW in shoots and from 1136.34 $\mu\text{g/g}$ DW to 1356.58 $\mu\text{g/g}$ DW in roots (Fig. 6). The NFON plants had significantly higher iron concentration in the shoots as compared to NB and NFUN plants (Fig. 6A). Importantly, cadmium concentrations in polished NFUN and NFON grains (2.62 to 4.9 $\mu\text{g/g}$ DW) was comparable to NB grains (4.15 $\mu\text{g/g}$ DW) (Fig. 6B). Therefore, the ectopic expression of *AtNRAMP3* in rice did not increase cadmium concentrations in the grains, shoots or roots of the transgenic plants.

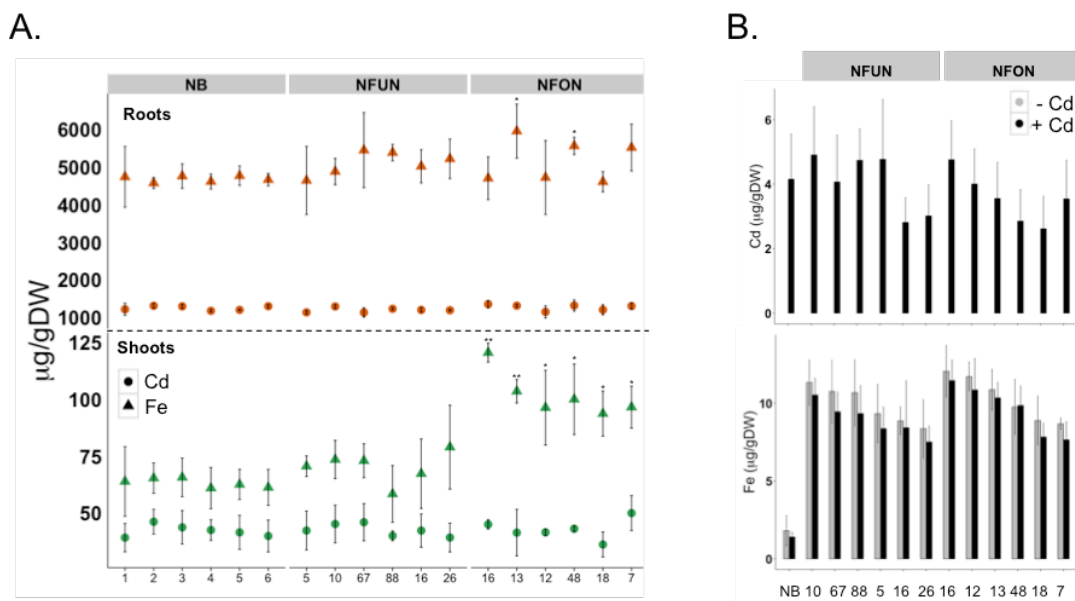


Fig. 6 Cadmium and iron accumulation in polished T4 grains, shoots and roots of T3 plants when grown in hydroponic solution containing CdCl₂. (A) Cadmium and iron content in shoots and roots of selected NFUN and NFON plants. Brown triangle, iron concentration in roots; brown circle, cadmium concentration in roots; green triangle, iron concentration in shoots; green circle, cadmium concentration in shoots. $n = 5$ and three replications. (B) Cadmium and iron content in polished grains of selected NFUN and NFON plants. Black asterisks indicate statistically significantly higher values as compared to the NB control (* $p < 0.05$, ** $p < 0.01$), respectively. See Fig. 1A for the abbreviation of the gene cassettes. Error bars represent standard deviation.

2.3.6 IR64 lines expressing NRAMP, NAS and FER have dietary significant levels of iron and zinc in their grains

Based on the results with cv. Nipponbare, we transformed Indica rice cv. IR64 with the NFON construct (*pCaMV35S::AtNAS1*, *pOsGLB-1::PvFER*, and *pOsOle 18::AtNRAMP3*; Figure 1A). Five single insertion lines were selected for further analysis (Fig. S6). The

IR64 transgenic plants had increased endosperm iron concentration of up to 13.65 $\mu\text{g/g}$ DW in the polished grains and 21.38 $\mu\text{g/g}$ DW in the unpolished grains, as compared to 2.72 $\mu\text{g/g}$ DW and 13.24 $\mu\text{g/g}$ DW iron in the polished and unpolished grains of IR64 control plants, respectively (Fig. 7A). Both polished and unpolished grains of the transgenic plants also had significantly increased zinc concentrations, with the highest zinc concentration of 48.18 $\mu\text{g/g}$ DW in the polished grains of IR64_1 (Fig. 7B). Expression of *AtNAS1* was detected in shoots, embryo and endosperm, while *AtNRAMP3* was expressed only in the embryo and *PvFER* only in the endosperm (Fig. 7C). The transgenic plants were phenotypically similar to the IR64 control in greenhouse conditions, except for IR64_12 line which had a smaller grain size (Table S2).

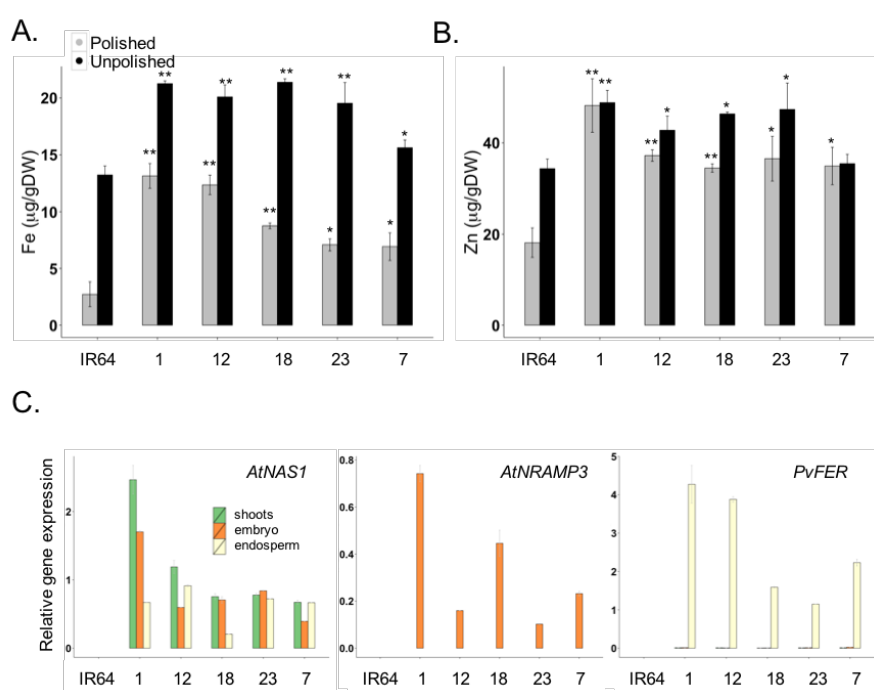


Fig. 7 Iron and zinc concentration in polished and unpolished T2 grains of Indica cv. IR64 expressing *AtNRAMP3*, *AtNAS1* and *PvFER*. (A) and (B) Values are the average of three biological replicates. IR64 (control). Numbers indicate independent single insertion lines expressing *pCaMV35S::AtNAS1*, *pOsGLB-1::PvFER* and *pOsOle18::AtNRAMP3*. Error bars represent standard deviation. (C) qRT-PCR results of *AtNAS1*, *PvFER* and *AtNRAMP3* expression levels in IR64 (control) and selected transgenic lines. Error bars represent standard deviation ($n = 10$ for shoots; $n = 30$ for embryo and endosperm, and three replications).

2.4 Discussion

Iron biofortification in rice has been variably successful in increasing endosperm iron content. In general, strategies combining multiple genes achieve higher increases in rice endosperm iron content as compared to single gene strategies. To provide 30% of the dietary estimated average requirement (EAR) rice lines containing 15 $\mu\text{g/g}$ DW iron and

28 $\mu\text{g/g}$ DW zinc in polished grains are required (Bouis et al., 2011). Transgenic rice lines reported to date have iron concentrations in the range of 6 to 19 $\mu\text{g/g}$ DW (Masuda et al., 2009; Wirth et al., 2009; Johnson et al., 2011; Trijatmiko et al., 2016). The IR64 transformed lines expressing *NAS* and *FERRITIN* reported by Trijatmiko and colleagues (Trijatmiko et al., 2016) grown under field conditions contained around 15 $\mu\text{g/g}$ DW iron in polished grains. These increases are promising, however, the best performing lines reported contain two transgene cassette copies inserted as an inverted repeat. Transgenic plants with an inverted transgene repeat could be problematic, both from a practical and regulatory point of view. First, two or more insertions of transgenes often result in epigenetic transgene silencing in subsequent plant generations (Kumpatla and Hall, 1998; Rajeevkumar et al., 2015). Second, using an inverted transgene cassette repeat in breeding programs or crop production would require a regulatory approval of uncertain, but likely negative outcome. Consequently, iron-biofortified rice lines will be most successful when containing a single-copy transgene cassette insertion for high iron concentration that is stably inherited and that can be bred efficiently into widely grown rice cultivars.

Here, we expand our biofortification strategies by combining increased iron uptake and storage with efficient intra-cellular iron mobilization. The expression of *AtNAS1* increases NA and DMA synthesis, both of which facilitate iron transport within the plants (Rellan-Alvarez et al., 2008; Aoyama et al., 2009; Alvarez-Fernandez et al., 2014). Additionally, we reasoned that expression of *AtNRAMP3* should remobilize iron from vacuole stores to the cytosol, which can then be transported to other tissues. By expressing *AtNRAMP3* under control of the *Ole18* promoter, we remobilized iron from the iron-rich aleurone layer for transport to the endosperm. The endosperm-specific expression of *PvFER* allows for effective storage of iron in the endosperm of the grains. We demonstrate that combining these genes can increase iron content more than six-fold higher in polished seeds in two major rice cultivars, Nipponbare and IR64. The transformed IR64 lines contain up to 13.65 $\mu\text{g/g}$ DW iron in polished grains, which is more than 90% of the recommended target increase of 15 $\mu\text{g/g}$ DW for rice grains. The highest zinc concentration of 48 $\mu\text{g/g}$ DW in transformed IR64 lines is equivalent to 170% of the recommended increase of 28 $\mu\text{g/g}$ DW.

Our transgenic rice lines expressing *AtNARMP3*, *AtNAS1* and *PvFER* contain higher iron and zinc concentrations in the grains compared to lines expressing *AtNRAMP3* and *PvFER* only. In NFON lines with highest iron grain concentrations, *AtNAS1* is constitutively expressed while the *AtNRAMP3* gene and *PvFER* are regulated by the rice *Ole18* and *Glb* promoters, respectively. The *Ole18* promoter directs strong expression in the embryo and aleurone layer of rice grains primarily from 7 to 17 days after flowering (DAF), whereas the *Glb* promoter is most active between 12 and 17 DAF mostly in the endosperm (Qu le and Takaiwa, 2004). The aleurone layer provides nutrients to the developing endosperm and together with the embryo and endosperm constitutes a symplast connected by plasmodesmata that allows efficient transport and distribution of nutrients during early grain filling (Zhu et al., 2003; Ishimaru et al., 2011; Thomine and Lanquar, 2011; Zhao et al., 2014). Therefore, it is likely that mobilizing iron from the vacuole to the cytosol in aleurone cells and embryo scutellum could facilitate iron transport to the endosperm. This is supported by the strong correlation between iron concentrations and transgene expression in the seed tissues of NFON lines, demonstrating that targeted expression of *AtNAS1*, *PvFER* and *AtNRAMP3* is an effective strategy for increasing iron accumulation in the endosperm. Importantly, iron mobilization as a result of *AtNRAMP3* expression did not affect growth and seed germination of the transformed plants. Endosperm zinc concentrations were also higher in most of NFUN, NFON, FUN and FON lines compared to the Nipponbare control. The highest zinc concentrations were found in NFUN and NFON lines that express all transgenes, consistent with previous reports that rice lines with high grain iron concentration, particularly those expressing *NAS*, usually have higher grain zinc concentration as well (Douchkov et al., 2005; Lee et al., 2009b; Wirth et al., 2009; Boonyaves et al., 2016).

Our results also show that expression of *AtNRAMP3* and/or *AtNAS1* in NFUN, NFON and FUN lines increase their tolerance to low iron conditions. The transgenic rice plants transport more iron from roots to shoots in iron-deficient growth conditions, similar to transgenic tobacco plants expressing *AtNAS1* that accumulated more iron in leaves in low-iron growth conditions and therefore were more tolerant to iron deficiency (Douchkov et al., 2005). High-iron biofortified rice expressing *HvNAS*, *HvNAAT* and *HvIDS3* is also more tolerant to iron deficiency conditions in hydroponic culture and calcareous soil (Masuda et al., 2013). Expression of *AtNRAMP3* alone can rescue the hypersensitive iron starvation phenotype of the Arabidopsis *atnr3nr4* double mutant

(Lanquar et al., 2005). Together, the tolerance of our transgenic lines to iron deficiency can be explained by the expression of *AtNAS1* and increased cytosolic iron availability in vegetative tissues as the result of *AtNRAMP3* expression. Similar to Arabidopsis plants expressing *AtNRAMP3* that have reduced root and shoot zinc and manganese levels in iron deficiency conditions (Thomine et al., 2003), we also found reduced zinc concentrations in NFUN and FUN plants compared to the Nipponbare control in iron deficiency conditions. However, NFON and FON plants did not differ significantly from the Nipponbare control plants in their shoot and root zinc concentrations when grown in the same conditions. This is likely due to a localized expression of *AtNRAMP3* in the NFON and FON plants.

Metal transporters often have a broader specificity, i.e. transporters facilitating the uptake of essential metal ions including Fe, Zn, Cu, and Mn may also transport heavy metal ions including cadmium (Cd). Particularly, Zn-specific transporters can co-transport Cd, and the NRAMP transporter family is known to transport Cd as well (Papoyan et al., 2007; DalCorso et al., 2010; Olsen and Palmgren, 2014). Thus, it is possible that expression of iron transporters to develop iron-biofortified rice may also cause the accumulation of non-desired toxic metals that could be detrimental to human health. The results of hydroponics experiments demonstrate that our transgenic rice lines did not have higher Cd concentrations in polished grains compared to the Nipponbare control. This supports other studies that also reported no increases in the Cd accumulation in grains of high-iron biofortified rice (Masuda et al., 2012; Trijatmiko et al., 2016).

Together, the combinatorial and targeted expression of *AtNAS1*, *AtNRAMP3* and *PvFER* is a novel and promising strategy for achieving significant iron and zinc increases in polished rice grains. The IR64 lines with highest iron concentration we report here are now important candidates for development of agronomically robust rice mega-varieties with improved nutritional benefits for human health.

2.5 Material and Methods

2.5.1 DNA construct, rice transformation and plant growth conditions

The full-length *AtNRAMP3* genomic sequence was amplified using a forward primer containing a *BamHI* site and a reverse primer with a *BspEI* site (Table S3). The fragment was subsequently inserted into the *BamHI*- and *BspEI*-digested *OsNAS2-PbskII(-)* vector

(Singh et al., 2017) to generate *pUbi::AtNRAMP3::tNOS* fragment. In parallel, the *PstI* site in the *Ubi* promoter contained in the *OsNAS2-PbskII(-)* construct was changed by a point mutation in order to use the site for subsequent cloning steps. The *pCAMBIA-1300PMI-NASFER* vector containing the *AtNAS1* and *PvFER* genes was cut at the *PstI* site and the *pUbi::AtNRAMP3::tNOS* fragment was inserted to generate the NFUN cassette. Similarly, *pOle18* promoter sequence was amplified using a forward primer containing *PstI* and *SphI* sites, and a reverse primer containing a *BamHI* site, and then inserted into *pUbi::AtNRAMP3-PbskII(-)* digested with *SphI* and *BamHI* to generate *pOle18::AtNRAMP3::tNOS*. The *pCAMBIA-1300PMI-NASFER* vector was then digested at the *PstI* site and the *pOle18::AtNRAMP3::tNOS* fragment was inserted to generate the NFON cassette. For the FUN and FON constructs, *pCAMBIA-1300PMI-NASFER* was digested at the *XbaI* and *PstI* sites to obtain the *pGlb::PvFERRITIN::tNOS* fragment, which was subsequently inserted into *pCAMBIA-1300PMI* to generate the *pCAMBIA-1300PMI-FER* vector. The *pCAMBIA-1300PMI-FER* vector was cut at the *PstI* site and the *pUbi::AtNRAMP3::tNOS* or *pOle18::AtNRAMP3::tNOS* fragments were inserted to generate the FUN or FON cassettes, respectively. These four vectors were transformed into *Oryza sativa ssp. Japonica cv. Nipponbare*, and NFON was additionally transformed into *Indica IR64* using *Agrobacterium tumefaciens* strain EHA105 (Hood et al., 1993). Transformation, selection and regeneration followed an established protocol (Nishimura et al., 2006). Candidate transformants were first screened for the presence of *AtNRAMP3*, *AtNAS1* and *PvFER* using PCR. Southern blot hybridization using digoxigenin (DIG) labeling was performed using *PmlI*-digested genomic DNA isolated from the transgenic lines to select lines with single-copy cassette insertions. The PCR-amplified *PMI* DNA fragment was used as a probe to detect the transgene cassette. The primer sequences used for cloning, sequence verification and PCR are provided in Table S3.

The plants were grown in commercial soil (Klasmann-Deilmann GmbH, Germany) under greenhouse conditions in 80% humidity at 30°C with 12h light and 60% humidity at 22°C with 12h dark. Quantification of divalent metal ions and transgene expression was conducted using T2 and T3 grains.

2.5.2 Iron deficiency and cadmium excess treatment in hydroponic culture

Transgenic and Nipponbare (NB) seeds were germinated *in vitro* for 5 days in Petri dishes on a H₂O-moistened filter paper and subsequently transferred into containers (with

tip holes) containing 400 mL hydroponic solutions for 7 days. Solutions for hydroponic growth were prepared according to established protocols (Kobayashi et al., 2005; Boonyaves et al., 2016), i.e., using 0.70 mM K₂SO₄, 0.10 mM KCl, 0.10 mM KH₂PO₄, 2.0 mM Ca(NO₃)₂, 0.50 mM MgSO₄, 10 μM H₃BO₃, 0.50 μM MnSO₄, 0.20 μM CuSO₄, 0.01 μM (NH₄)₆Mo₇O₂₄, and 0.5 μM ZnSO₄, with different iron concentrations added as Fe(III)-EDTA according to the treatment (normal condition: 100 μM; iron-deficient condition: 10 μM). For the iron-deficient condition, plants were grown in hydroponic solutions containing 10 μM Fe(III)-EDTA for 14 days. Plants grown in hydroponic solutions containing 100 μM Fe(III)-EDTA served as control. Solutions were changed every one to two days to avoid any precipitation and contamination. In case of Cd excess treatment, plants were grown in hydroponic solutions containing 50 μM CdCl₂ and shoot and root samples were collected from 21-day-old seedlings. In order to analyze grain Cd concentrations, plants were grown until maturity in a hydroponic solution containing 10 μM CdCl₂ in greenhouse conditions in 80% humidity at 30°C with 12h light and 60% humidity at 22°C with 12h dark.

2.5.3 Metal ion measurements

Grain samples were de-husked to obtain unpolished brown grains. The de-husked grains were processed using a grain polisher (Kett grain polisher ‘Pearlest’, Kett Electric Laboratory, Tokyo, Japan) for one minute. Shoot and root samples from hydroponic culture were dried at 60°C for 3 to 5 days. 200mg of each ground grains sample and 50-100 mg of root or shoot samples were boiled in 15 ml of 65% v/v HNO₃ solution at 120°C for 90 min. Three ml of 30% v/v H₂O₂ were subsequently added and continuously boiled at 120°C for 90 min. Metal concentrations were determined using inductively coupled plasma-optical emission spectroscopy (ICP-OES) (Varian Vista-MPX CCD Simultaneous ICP-OES). The wavelength used for iron, zinc, manganese and copper were 238.204, 213.857, 257.610, and 324.754 nm, respectively. The National Institute of Standards and Technology (NIST) rice flour standard 1658a was treated and analyzed in the same manner and used as internal control for every measurement. Data were analyzed using Student’s t-test. The criteria of p <0.05 and p <0.01 was used to determine statistically significant differences among the tested lines and the control.

2.5.4 Pearl’s Prussian blue staining

Rice seeds were stained as described previously (Saenchai et al., 2012). Unpolished

grains were submerged in ddH₂O overnight and then longitudinally cut with a ceramic knife (Cerastar®, Germany) in a Petri dish. The cut grains were submerged in freshly prepared Perls' Prussian blue solution (2% hydrochloric acid and 2% potassium ferrocyanide) for 10 minutes and then washed gently in distilled water for 2 minutes. Stained seeds were examined by a stereomicroscope (Keyence, VHX-1000D).

2.5.5 RNA extraction, cDNA synthesis and quantitative real-time PCR

Total RNA was extracted from roots and shoots of 5-day-old T3 generation seedlings using Trizol® reagent (Invitrogen, USA). To obtain total endosperm, embryo and seed coat RNA, whole seed coats, endosperm and embryo were separated manually from T3 rice grains at 16 DAF. Extraction buffer containing 0.15M NaCl and 1% sarcosyl was added to the ground samples followed by purification with 8M guanidine hydrochloride buffer. The RNA was treated with DNase I (Thermo Fisher Scientific Inc., USA) to remove genomic DNA contamination. First-strand cDNA was synthesized using the RevertAid™ first strand cDNA synthesis kit (Thermo Fisher Scientific Inc., USA). Quantitative RT-PCR was performed as previously described (Liu et al., 2011). In brief, qRT-PCR was performed in a 7500 Real-Time PCR System using the SYBR Green RT-PCR reagent kit following the manufacturer's protocol (Applied Biosystems, Carlsbad, CA, USA). Each reaction was run in triplicates in a volume of 20 µL with an initial denaturation step at 95°C for 10 min, followed by 40 cycles of 95°C for 15 sec and 60°C for 60 sec. Data were analysed according to the manufacturer's instructions using the 7500 System SDS Software v1.4 (Applied Biosystems). The expression level of genes of interest was normalized to the expression of rice *UBIQUITIN 5 (OsUBQ5)*.

2.5.6 Protein extraction and Western blotting analysis

Protein extraction and Western hybridization were carried out as described previously (Svozil et al., 2015). In brief, the frozen plant material was ground into a fine powder and proteins were extracted by incubation with SDS buffer containing 4% SDS, 40 mM Tris-base, 5 mM MgCl₂, and 2x protease inhibitor mix (Roche) for 20 min at room temperature (RT). Cell debris was removed by centrifugation at RT for 10 min at 16000x g. The supernatant was stored at -80°C for further use. For the Western blots, 30 µg of leaf extract and 50 µg of embryo extract were separated using SDS PAGE on 10% SDS gels. After blotting, the nitrocellulose membranes were probed with an anti-AtNRAMP3 (1:1000) antibody for 1 hr at RT and then followed by an anti-rabbit (1:5000, Roche)

antibody for 1hr at RT. After detection of the immunofluorescence signal the membranes were stained with Ponceau Red for 10 min.

2.5.7 Germination rate test

Thirty seeds of each tested line were imbibed in deionized water at RT for 2 days in the dark and then transferred to Petri dishes containing water-saturated filter paper for germination. Germination rates were scored every day. Three replications were performed using 30 seeds each time. The test was performed according to a published protocol (Yang et al., 2012a; Cheng et al., 2013) with the above modifications.

2.6 Conflict of interest

The authors declare that they have no conflict of interest.

2.7 Author contributions

NKB conceived the study, NKB and TYW designed the experiments, TYW performed the experiments, TYW, WG and NKB interpreted the data, TYW and NKB wrote the manuscript, and WG and NKB edited the manuscript. All authors have read and approved the final manuscript.

2.8 Acknowledgments

We gratefully acknowledge the support by Mrs. Jacqueline Imhof and the ETH research grants for this work to WG and NKB. We thank Prof. Rainer Schulin for providing access to ICP-OES and Björn Studer for kind assistance with metal measurements. We thank Irene Zurkirchen for the technical support in the greenhouse. We thank Wuyan Wang for assistance with analyzing grain biochemical index, and Komal Jhala and Dr. Simrat Pal Singh for assistance with IR64 transformation. We thank Dr. Sébastine Thomine (French Science Center for Scientific Research) for providing AtNRAMP3 antibody.

2.9 Supplementary data

Table S1 Grain quality assessment of selected transformed plants (T3) carrying NFUN, FNON, FUN and FON constructs as compared to the Nipponbare control. The plants were grown in the greenhouse condition prior to the analysis. Black and red asterisks indicate statistically significantly higher and lower values as compared to the NB control (*p<0.05, **p<0.01), respectively. The number that follows the ± sign is the standard deviation.

Line	Length (mm)	Width (mm)	Chalkiness (%)	Amylose content (%)	Starch content (%)	Protein content (%)
NB	5.63 (±0.12)	2.9 (±0.17)	1.5 (±0.3)	17.24 (±0.38)	83.42 (±0.75)	10.3 (±0.07)
NFUN						
10	5.54 (±0.14)	2.91 (±0.14)	1.2 (±0.3)	18.08 (±1.31)	83.57 (±0.44)	10.6 (±0.08)
67	5.46 (±0.14)	2.89 (±0.14)	1 (±0.2)	17.21 (±1.29)	81.87 (±0.69)*	10.1 (±0.09)
88	5.24 (±0.15)	2.7 (±0.16)	1.3 (±0.2)	19.29 (±1.44)	84.03 (±0.87)	11.1 (±0.14)
NFON						
16	5.48 (±0.12)	2.93 (±0.09)	2 (±0.3)	19.57 (±1.24)	82.19 (±0.73)	10.7 (±0.07)
12	5.39 (±0.12)	2.83 (±0.12)	1 (±0.2)	18.86 (±0.75)	81.73 (±0.98)*	10.3 (±0.07)
13	5.48 (±0.12)	2.88 (±0.10)	0.8 (±0.1)*	17.95 (±0.98)	83.03 (±1.03)	10.4 (±0.06)
FUN						
21	5.16 (±0.14)*	2.6 (±0.12)*	0.8 (±0.1)*	18.53 (±0.76)	82.69 (±1.12)	10.2 (±0.12)
9	5.44 (±0.10)	2.87 (±0.14)	0.8 (±0.08)*	17.44 (±1.32)	81.96 (±0.57)*	10.8 (±0.10)
13	5.45 (±0.11)	2.87 (±0.12)	0.5 (±0.1)*	17.85 (±1.21)	82.43 (±0.64)	10.7 (±0.11)
FON						
21	5.44 (±0.06)	2.93 (±0.11)	0.4 (±0.1)*	17.89 (±1.13)	81.93 (±0.73)*	10.6 (±0.14)
1	5.48 (±0.09)	2.93 (±0.08)	2.2 (±0.3)*	17.54 (±1.23)	83.03 (±0.63)	10.3 (±0.08)
5	5.49 (±0.07)	2.92 (±0.10)	0.7 (±0.2)*	17.28 (±1.17)	82.47 (±0.48)	10.3 (±0.07)

Table S2 Phenotypic assessment of selected transgenic lines from the T1 generation grown in greenhouse conditions. Parameters including days to flowering (DTF), plant height, tiller number, one thousand grain weight (1000 grain weight), grain length, grain width and grain filling are presented. Values are the average of three individual plants. Black and red asterisks indicate statistically significantly higher and lower values as compared to the NB control (*p<0.05, **p<0.01), respectively. The number that follows the ± sign is the standard deviation.

Plant line	Plant Height (cm)	Tiller No.	DTF	Grain Width (cm)	Grain Length (cm)	1000grain Weight (g)	Grain Filling (%)
IR64	82.67 (±2.52)	11.00 (±1.00)	115.33 (±2.52)	0.190 (±0.02)	0.761 (±0.05)	21.8 (±0.81)	85.00 (±2.00)
1	86.00 (±2.65)	8.00 (±1.00)*	117.00 (±3.61)	0.199 (±0.01)	0.756 (±0.05)	22.3 (±0.81)	82.03 (±0.45)
12	84.33 (±3.79)	12.00 (±2.65)	119.67 (±0.58)	0.184 (±0.02) *	0.658 (±0.04) *	15.7 (±0.58) *	79.33 (±4.04) *
18	83.33 (±1.53)	11.67 (±2.08)	116.67 (±1.53)	0.197 (±0.01)	0.800 (±0.06)	21.3 (±0.40)	81.93 (±5.37)
23	86.67 (±3.51)	11.33 (±1.53)	117.00 (±1.00)	0.199 (±0.01)	0.758 (±0.07)	21.7 (±0.93)	83.67 (±3.21)
7	84.33 (±5.13)	9.67 (±2.08)	117.33 (±2.52)	0.198 (±0.03)	0.741 (±0.04)	21.3 (±0.75)	84.67 (±2.52)

Table S3 Primer sequences used for sequence validation, cloning and qRT-PCR analysis

Primer Name	Direction	Primer sequence (5'-3')	Purpose
Ubi-mut-1	F	tcctctagagtcgaccttcagaagtaacaccaaac	cloning
	R	gtttggtgttactctgaaggctgactctagagga	
AtNRAMP-F-BamHI	F	ggatccatgccacaactcgagaac	cloning/ sequencing
AtNRAMP-R-BspEI	R	tccggatcaatgactagactccg	
Ole18-f-PstI-SphI	F	gcatgcctgcaggcaaagtattttggc	cloning/ sequencing
Ole18-BamHI	R	aaggatccgaactctgtttgatggtgtttg	
PvFer	F	gtcttcgtttatattgtctcttg	PCR/ sequencing
Ubi	R	gtaaatcccaaatccaattacc	PCR/ sequencing
35S	F	cagttcatacagagtctcttacg	PCR/ sequencing
PMI	F	ctggctaagtgtggtttct	PCR/ southern probe
	R	cgtagtgattgagagt	
AtNRAMP3-1	F	gtgtagttaaccattagctgtg	PCR/ sequencing
	R	attagctaaattacaattagaac	
AtNRAMP3-2	F	gatcaactgtttgtcacaactg	PCR/ sequencing
	R	cgatcgcccaaatgtatagtac	
qAtNRAMP3	F	gatcaactgtttgtcacaactg	qRT-PCR
	R	cgatcgcccaaatgtatagtac	
qAtNAS1	F	gcacttgagaaacacatgg	qRT-PCR
	R	tctgagagcatgagcactcc	
qPvFER	F	ggggatacgggaaaacgtaa	qRT-PCR
	R	gagcctggctaaccgcat	
OsIDEF1	F	gtcttcaggctgggatgt	qRT-PCR
	R	gggatttgttctgctgatg	
OsIRO2	F	gaaggtctcacttcactcagttca	qRT-PCR
	R	tgatcgttcctcacttctctg	
OsIRT1	F	ctcgagataggcatcgtggt	qRT-PCR
	R	gaacatctggtggaagcaca	
OsNRAMP1	F	ggaaggtggtggacgaca	qRT-PCR
	R	ggtccaatgtgggacaaaa	
OsFRO1	F	tcgccataccactgatgta	qRT-PCR
	R	ttgccttctcgatcctatg	
OsYSL2	F	gggctcctaacttgcctcc	qRT-PCR
	R	gaggggtatggaatccgitt	
OsNAAT1	F	tggagggaatccatgatga	qRT-PCR
	R	cttcattcccagcacactcc	
OsNAS1	F	cggttgagaaggcagaagagt	qRT-PCR
	R	cgatcgtccggctgttag	
OsFER1	F	ggattcgccaaattctcaa	qRT-PCR
	R	cctttctcaggatggtcgaa	
OsUBQ5	F	accacttcgaccgccactact	qRT-PCR
	R	acgcctaagcctgctggtt	

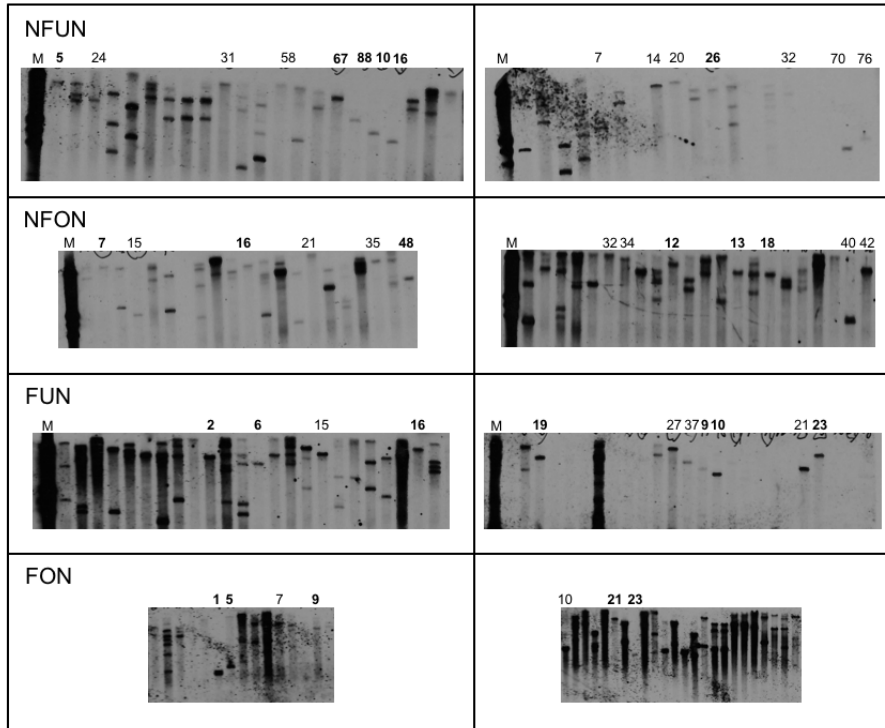


Fig. S1 Characterization of transgenic lines in T0 generation using southern hybridization. Southern hybridization analysis was performed using PMI as a probe. Numbers indicate independent transformed lines with potential single insertion of the transgene cassette.

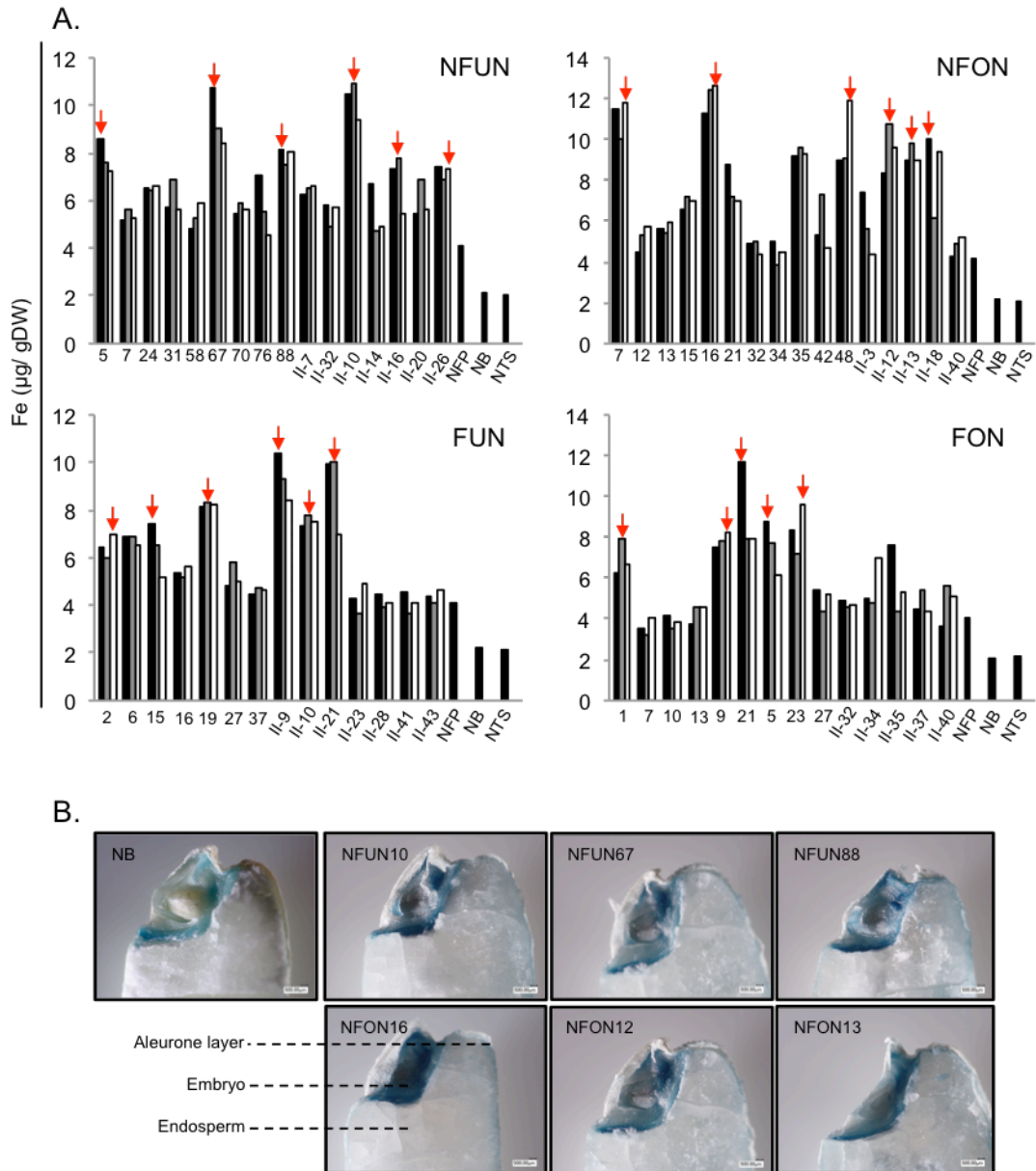


Fig. S2 Iron concentration in the polished T2 grains in all the single insertion lines carrying NFUN, NFON, FUN and FON constructs, and example of iron staining in selected NFUN and NFON plants. (A) Values are the average of two technical replicates. The bars for each line represent three individual plants. Arrows indicate the selected plants from each line for further analysis in next generation and II indicate second batch of transformation; NB, rice cultivar Nipponbare (control). See Fig. 1A for the abbreviation of the gene cassettes. (B) Grains of selected transgenic plants carrying NFUN and NFON constructs were compared to those of NB control.

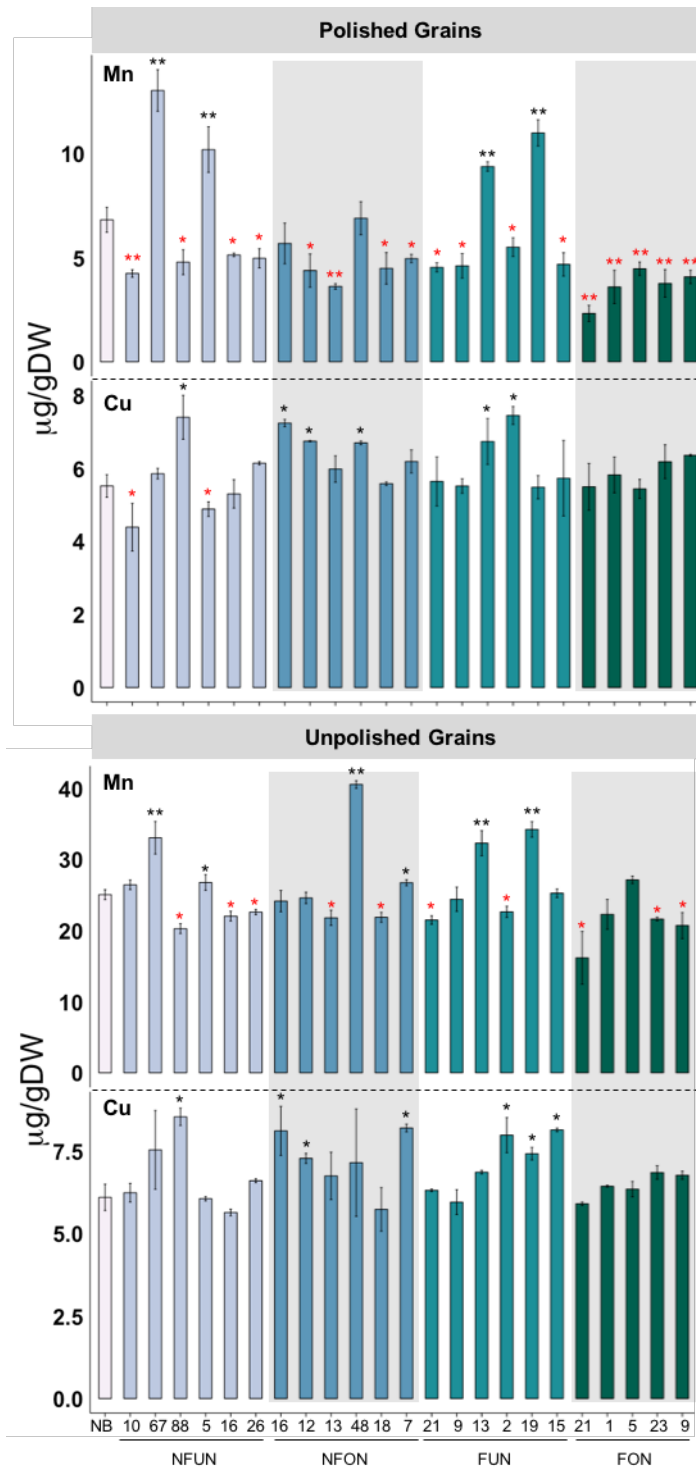


Fig. S3 Manganese and copper concentrations in polished and unpolished T3 grains expressing *AtNRAMP3*, *AtNAS1* and *PvFER* or *AtNRAMP3* and *PvFER* cassettes. Values are the average of three biological replicates. NB, Nipponbare rice control. Black asterisks indicate statistically significant higher values calculated using Student's T-Test as compared to NB control (* $p < 0.05$, ** $p < 0.01$). See Fig. 1A for the abbreviation of the gene cassettes. Error bars represent standard deviation.

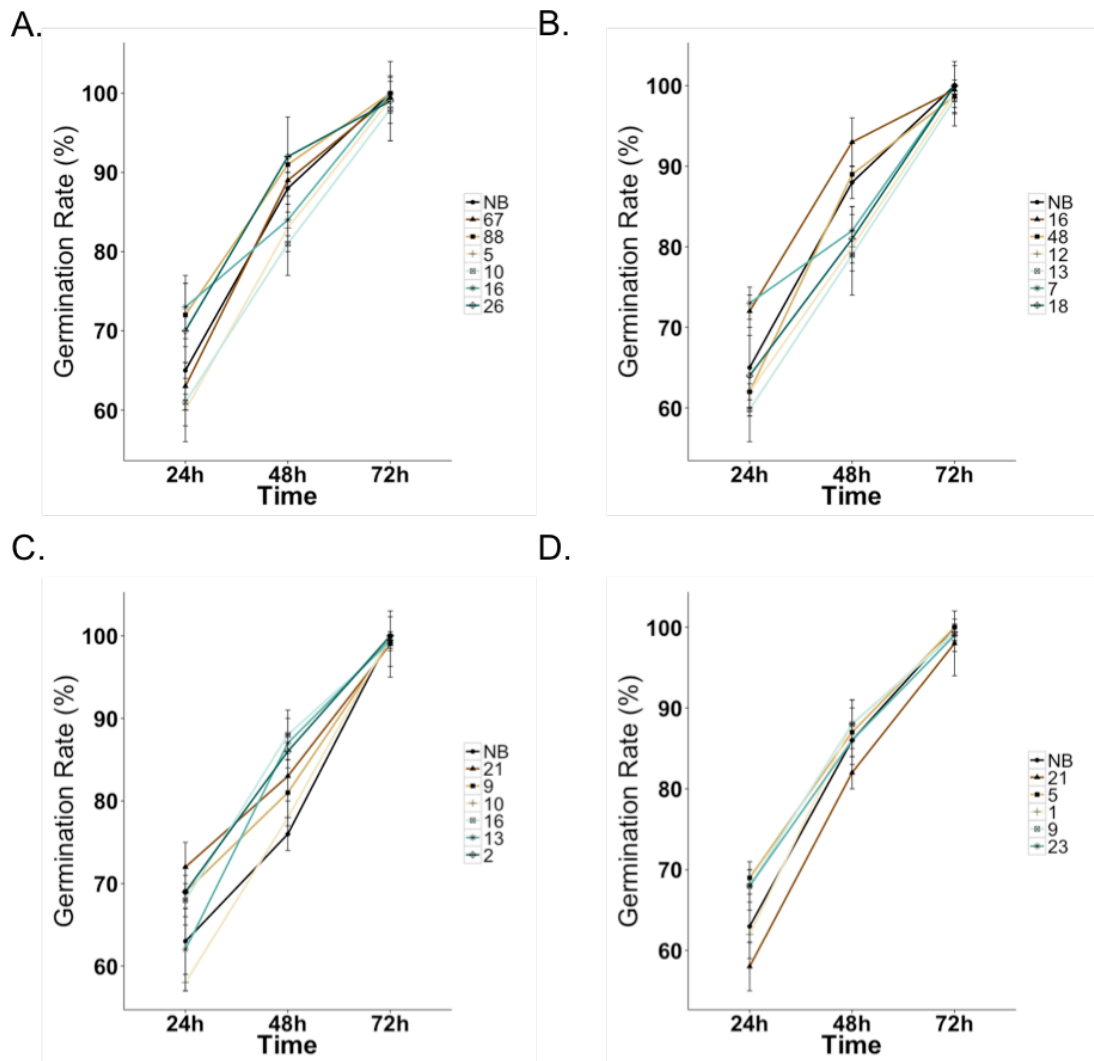


Fig. S4 Germination rate analysis of seeds from selected transgenic plants compared to the Nipponbare control. Germination rate of seeds from (A) NFUN, (B) NFON, (C) FUN and (D) FON plants at 24, 48 and 72 hours. Thirty seeds were tested in each experiment and 3 individual experiments were conducted. See Fig. 1A for the abbreviation of the gene cassettes. Error bars represent standard deviation ($n = 30$).

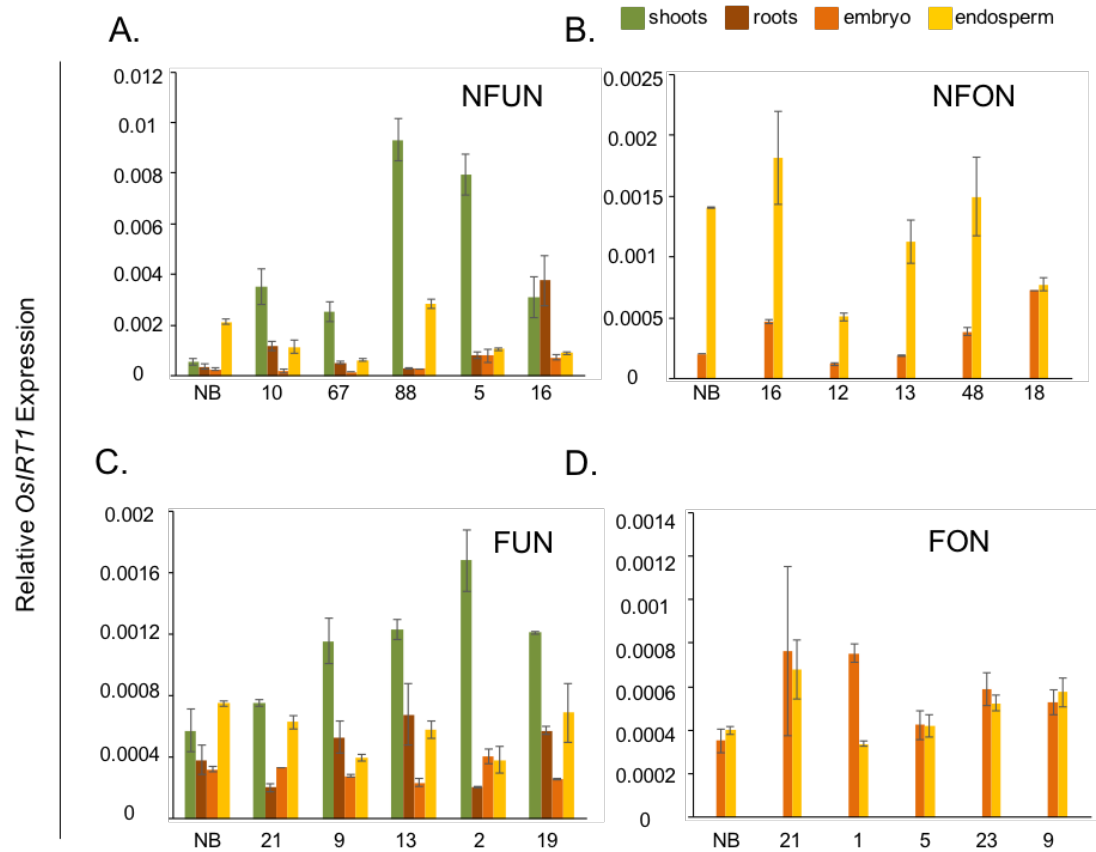


Fig. S5 Endogenous *OsIRT1* expression in shoots, roots, embryo and endosperm of selected transgenic plants. *OsIRT1* expression determined by qRT-PCR in shoots, roots, embryo and endosperm of transgenic plants expressing the (A) NFUN and (B) NFON cassettes, and in embryo and endosperm of transgenic plants expressing the (C) FUN and (D) FON cassettes. Numbers on the figure indicate independent transgenic lines. Expression values were normalized to the expression values of the rice *UBIQUITIN5* (*OsUBQ5*) gene. See Fig. 1A for the abbreviation of the gene cassettes. Error bars represent standard deviation ($n = 10$ for shoots and roots; $n = 30$ for embryo and endosperm, and three replications).

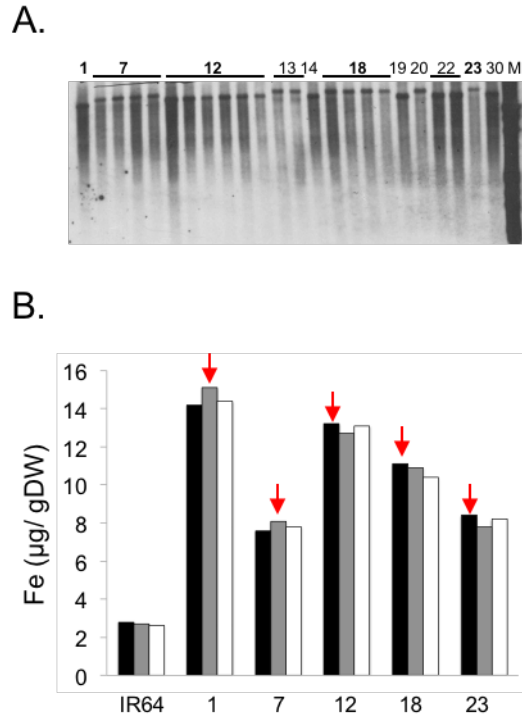


Fig. S6 Characterization of IR64 transgenic lines in T0 generation using southern hybridization and iron concentration in the polished T1 grains in the single insertion lines. (A) Southern hybridization analysis using PMI as a probe. Numbers indicate independent transformed lines with potential single insertion of transgene. (B) The bars for each line represent three individual plants. Values are the average of two technical replicates. Arrows indicate the selected plants from each line for further analysis in next generation.

3. Boosting citrate-iron translocation together with efficient uptake and storage significantly increases the endosperm iron and zinc concentrations in rice

Ting-Ying Wu, Wilhelm Gruissem and Navreet K. Bhullar*
Plant Biotechnology, Department of Biology, ETH Zurich, Universitaetsstrasse 2, 8092 Zurich, Switzerland

***Corresponding author**

Dr. Navreet K. Bhullar
Plant Biotechnology,
Department of Biology
ETH Zurich (Swiss Federal Institute of Technology)
Universitaetsstrasse 2
8092 Zurich, Switzerland
bhullarn@ethz.ch

Running title: Iron biofortification of rice

Submitted to Molecular Plant

3.1 Abstract

Iron deficiency affects around one third of the world's population. Among different approaches to overcome iron malnutrition, biofortification of staple foods is regarded as an efficient strategy. Design of biofortification approaches however rely on the understating of iron uptake and translocation mechanisms. Most iron biofortification strategies included expression of genes involved in iron uptake and storage, with only limited attention to iron translocation within the plant. FERRIC REDUCTASE DEFECTIVE 3 (FRD3) is a member of the MULTIDRUG AND TOXIN EFFLUX (MATE) family and plays an important role in xylem loading of citrate, a primary chelator of iron. The use of *FRD3* to increase grain iron levels has not been attempted so far. In this study, we expressed *AtFRD3* in combination with *AtNAS1* (NICOTIANAMINE SYNTHASE 1) and *PvFER* (FERRITIN) or with *PvFER* alone in order to improve long-distance iron transport together with efficient iron uptake and storage in the rice endosperm. The citrate and iron concentrations in the xylem sap of transgenic plants increased by 2-fold as compared to the control. Iron and zinc increased significantly in polished and unpolished rice grains, equaling more than 70% of the recommended iron increase and 140% of the recommended zinc increase in polished grains. Furthermore, the transformed plants were tolerant to iron deficiency as well as to aluminium toxicity in comparison to the control plants. Importantly, transgenic plants did not accumulate more cadmium in the polished grains. Together, these results demonstrate that boosting inter- and intra- cellular iron mobilization in combination with efficient uptake and targeted endosperm storage is an effective strategy for iron biofortification.

3.2 Introduction

Iron is an essential micronutrient for humans and plants. Iron deficiency anemia is one of the most prevalent micronutrient deficiencies, affecting around 1.6 billion people in the world (Stevens et al., 2013). Several approaches including food diversification, iron supplementation, food fortification and biofortification have been suggested to combat this issue, and among these, biofortification is regarded a sustainable and cost-effective strategy. Developing high iron biofortified crops relies on thorough understanding of iron uptake, translocation and homeostasis in plants (Vasconcelos et al., 2017). Plants require iron for several vital biological processes including photosynthesis and chlorophyll biosynthesis. However, a high reactive capability of iron can lead to generation of toxic hydroxyl radicals, which can harm the plant cells (Halliwell, 2006; Briat et al., 2007). In contrast, upon iron deficiency, plants suffer leaf chlorosis and exhibit decreased root length (Schmidt, 1999; Muller and Schmidt, 2004). Therefore, in order to prevent iron toxicity while benefitting from it, plants have evolved complex regulatory strategies to maintain iron homeostasis.

Grasses use a chelation-based strategy (also known as Strategy II) for iron uptake. Mugineic acid (MA) family phytosiderophores (PS) are released into the rhizosphere by TRANSPORTER OF MUGINEIC ACID family (TOM) (Nozoye et al., 2011). The PSs then chelate the ferric form of iron, forming PS-Fe³⁺ complexes, which are subsequently transported into the root cells by YELLOW STRIPE (YS) and YELLOW STRIPE-LIKE (YSL) transporter family (Koike et al., 2004). The PS are synthesized from S-adenosyl-L-methionine through a conserved pathway of reactions catalyzed by NICOTIANAMINE SYNTHASE (NAS), NICOTIANAMINE AMINOTRANSFERASE (NAAT), and DEOXYMUGINEIC ACID SYNTHASE (DMAS) (Kobayashi and Nishizawa, 2012). This leads to production of deoxymugineic acid (DMA), the precursor of all other MAs (Higuchi et al., 1999; Bashir et al., 2006). Rice also uses chelation based strategy for iron uptake, in addition to the direct Fe²⁺ uptake via IRON-REGULATED TRANSPORTER 1 (OsIRT1) (Ishimaru et al., 2006).

Once iron is inside the plant, different translocation mechanisms are involved in its distribution to different plant parts. Citrate and nicotianamine (NA) are main chelators of iron during inter- and intra-cellular translocation (Alvarez-Fernandez et al., 2014). NA binds to both Fe²⁺ and Fe³⁺, and YSL transporters are proposed to transport metal-NA

complexes in the phloem (DiDonato et al., 2004; Waters et al., 2006). Among rice YSLs, OsYSL2 transports Fe(II)-NA and is expressed in the shoot phloem companion cells, while OsYSL15, OsYSL16 and OsYSL18 have been shown to transport Fe(III)-DMA (Aoyama et al., 2009; Inoue et al., 2009; Kakei et al., 2012). Fe³⁺-citrate is the main form of iron in xylem (Yokosho et al., 2009; Kato et al., 2010; Rellan-Alvarez et al., 2010). Therefore, citrate has an important role in iron translocation from roots to shoots. FERRIC REDUCTASE DEFECTIVE 3 (FRD3), belonging to the multidrug and toxin efflux (MATE) family, loads citrate into the xylem in Arabidopsis (Rogers, 2002; Durrett et al., 2007). The *atfrd3* mutant could translocate iron to the central vascular cylinder of roots but failed to further transport it to the above-ground plant parts (Durrett et al., 2007). *OsFRDL1*, rice homolog of *AtFRD3*, also encodes a citrate efflux transporter (Inoue et al., 2004; Yokosho et al., 2009). *Osfrdl1* mutants exhibited leaf chlorosis, reduced iron but increased zinc and manganese concentration in the leaves, and precipitation of iron in the root stele (Yokosho et al., 2009). The *osfrdl1* mutant also had lower citrate and iron concentrations in the xylem sap. In addition to their high expression in roots, *AtFRD3* and *OsFRDL1* also express in reproductive organs, indicating their importance in seed development and distribution of iron to the grains (Inoue et al., 2004; Roschzttardtz et al., 2011; Yokosho et al., 2016b).

The iron biofortification approaches involving constitutive expression of *NAS* reported increased iron concentration in polished as well as unpolished rice grains (Masuda et al., 2009; Johnson et al., 2011; Lee et al., 2012a). Transformation of plants with *AtIRT1* could also successfully increase endosperm iron concentration in rice (Boonyaves et al., 2016; Boonyaves et al., 2017). Many of these approaches were combined with the endosperm specific expression of *FERRITIN (FER)*, encoding an iron storage protein. The strategies combining genes facilitating iron uptake and storage in a single locus resulted in higher iron concentration increases (Nakanishi et al., 2000; Wirth et al., 2009; Masuda et al., 2012; Masuda et al., 2013; Trijatmiko et al., 2016) as compared to single gene strategies. Only few studies extended the focus to genes relating to long distance internal iron translocation. Transgenic plants expressing *OsYSL2* under the control of *SUCROSE TRANSPORTER 1* promoter alone or combined with *HvNAS1* and *GmFER* showed significantly increased iron concentration in the polished grains (Ishimaru et al., 2010; Masuda et al., 2012). Despite various studies highlighting an important role of

FRD3 in internal iron translocation, engineering plants with *FRD3* with an aim to increase grain iron concentrations has not been attempted so far.

In this study, we generated transgenic plants expressing the combination of *AtFRD3*, *AtNAS1*, and *PvFER*, or that of *AtFRD3* and *PvFER* together. The transgenic lines showed a significant increase in iron and zinc concentrations in both the unpolished and polished rice grains. Additionally, the transformed lines showed tolerance to low iron and aluminium toxicity, and did not accumulate more cadmium in the polished grains in comparison to the control plants.

3.3 Results

3.3.1 Generation of rice transgenic lines expressing *AtFRD3*, *AtNAS1* and *PvFER*

Rice cv. Nipponbare (NB) was transformed with two different constructs i.e., NFUF (*pCaMV35S::AtNAS1*, *pOsGLB-1::PvFER*, and *pZmUbi::AtFRD3*) and FUF (*pOsGLB-1::PvFER*, and *pZmUbi::AtFRD3*). Ubiquitin promoter driven expression of *AtFRD3* was combined with the *CaMV35S* promoter driven constitutive expression of *AtNAS1* and the endosperm-specific expression of *PvFER* under the control of *GLOBULIN-1* promoter (NFUF), or the *AtFRD3* and *PvFER* were expressed together (FUF). In total, 23 and 11 single transgene insertion lines expressing NFUF and FUF constructs, respectively, were selected and grown subsequently to the T2 generation (Supplemental Figure 1). Based on preliminary iron concentration analysis, we selected five or six lines for each of the construct with highest endosperm iron to obtain T3 generation (Supplemental Figure 2). The transgenic plants were phenotypically similar to NB plants, with the exception of slightly higher tiller numbers and slightly lower plant heights observed in some of the NFUF transgenic plants (Table 1 and Supplemental Table 1).

Expression of *AtNAS1* and *AtFRD3* were detected in shoots, roots, embryo and endosperm of the transformed lines, whereas the expression of *PvFER* was only detected in the endosperm (Figure 1A). Furthermore, NFUF and FUF plants showed up to 2-fold higher citrate concentration in the xylem sap as compared to the NB control (Figure 1B). The expression levels of *AtNAS1* and *AtFRD3* were positively correlated in shoots and roots of the NFUF plants. These results suggested that expression of *AtFRD3* could lead to elevated citrate levels in rice xylem sap, as well as that the *AtNAS1* and *AtFRD3* appear to express synergistically in the transformed lines (Figure 1A).

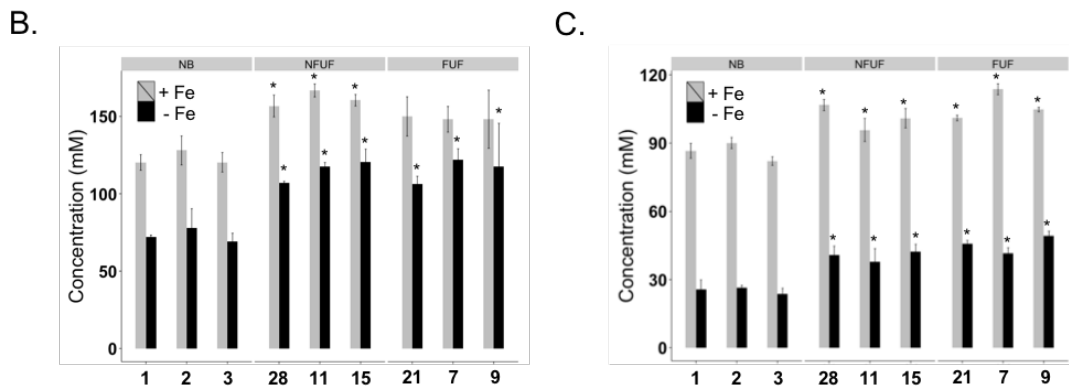
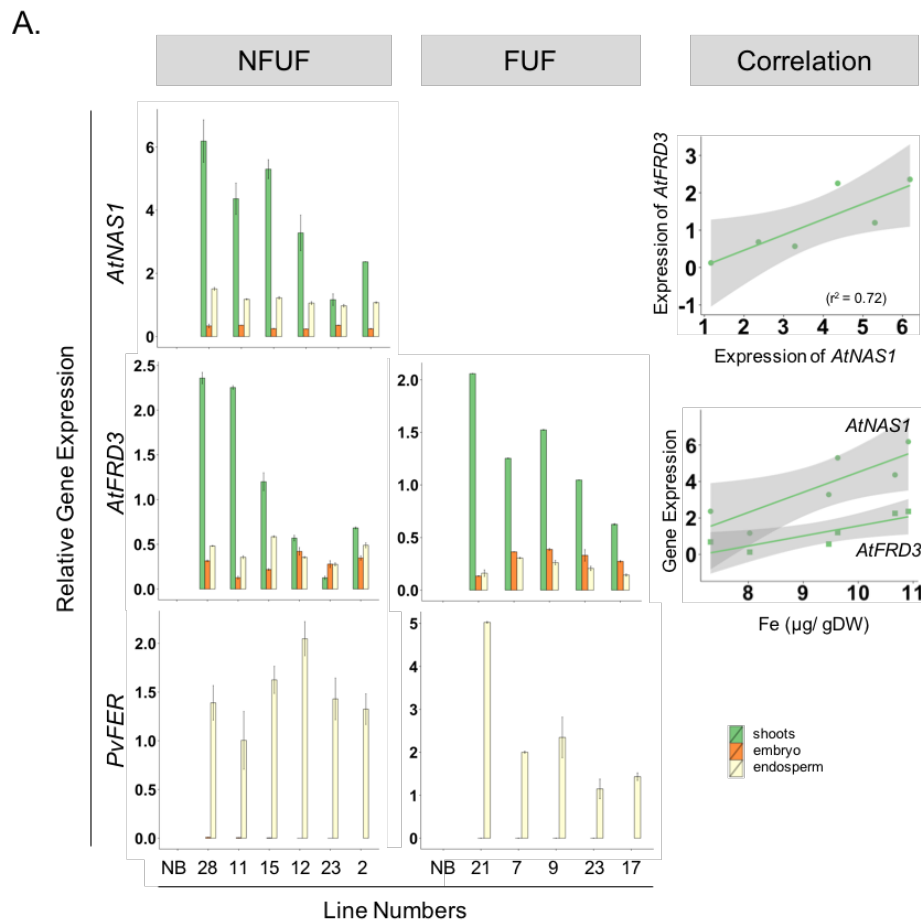


Figure 1 Transgene expression in seedlings, embryo, endosperm, and citrate and iron concentration in xylem sap. (A) *AtNAS1*, *PvFER* and *AtFRD3* expression level in the selected transgenic lines and in Nipponbare control (NB), and the correlation between iron concentration and transgene expression in NFUF plants (lines 28, 11, 15, 12, 23, 2). Individual lines are represented by colored dots. **(B)** Citrate and **(C)** Iron concentration in the xylem sap of selected transgenic lines and NB under iron deficient and iron sufficient growth condition. Black asterisks indicate statistically significantly higher values calculated using Student's T-Test as compared to the NB control ($*p < 0.05$). Number of seedlings processed per sample = 10; Number of embryos, endosperm and xylem sap processed per sample = 30, and three replications of the experiment contribute the data. Error bars indicate the standard deviation (SD) of independent replicates.

Table 1 Phenotypic assessment of selected transgenic lines in T3 generation under green house condition. Observation parameters including days to flowering (DTF), soil-plant analysis development (SPAD) value, plant height, tiller number, one thousand grain weight (1000grain weight) and grain filling rate. Values are the average of three individual replicates. Black and red asterisks indicate statistically significantly higher and lower values as compared to the NB control, respectively (* $p < 0.05$). Data is presented as mean \pm SD.

Plant line	Height (cm)	Tiller number	SPAD	DTF	1000GrainWeight (g)	Grain filling (%)
NB	63.33 (± 2.08)	7.67 (± 1.53)	36.00 (± 3.00)	81.00 (± 1.00)	24.17 (± 0.29)	82.44 (± 0.58)
NFUF						
28	55.33 (± 1.15)*	7.00 (± 1.00)	37.00 (± 1.00)	80.00 (± 1.00)	25.83 (± 0.29)	82.58 (± 1.41)
11	54.00 (± 1.00)*	9.67 (± 2.08)*	36.67 (± 0.58)	77.67 (± 1.53)	23.83 (± 0.29)	83.53 (± 1.09)
15	58.67 (± 1.53)	7.67 (± 0.58)	36.67 (± 2.08)	78.33 (± 1.53)	24.33 (± 0.58)	82.43 (± 0.29)
12	61.67 (± 0.58)	10.33 (± 1.53)*	36.33 (± 1.53)	78.00 (± 1.00)	24.33 (± 0.29)	80.03 (± 2.09)
23	57.67 (± 1.53)	7.67 (± 2.08)	36.67 (± 2.52)	78.00 (± 2.00)	24.33 (± 0.58)	83.29 (± 0.98)
2	55.00 (± 1.00)*	7.33 (± 0.58)	38.33 (± 1.53)	81.67 (± 1.53)	24.00 (± 0.50)	82.13 (± 1.11)
FUF						
21	58.33 (± 1.00)	9.67 (± 1.00)*	37.58 (± 1.53)	81.33 (± 1.00)	25.22 (± 0.40)	82.17 (± 0.98)
9	60.00 (± 1.00)	8.00 (± 1.00)	38.67 (± 1.53)	81.00 (± 1.00)	24.83 (± 1.04)	81.07 (± 0.19)
7	59.33 (± 2.08)	5.67 (± 0.58)	39.67 (± 1.53)	80.00 (± 1.00)	24.00 (± 0.50)	80.58 (± 2.18)
23	61.00 (± 1.00)	6.67 (± 1.00)	37.33 (± 0.58)	79.67 (± 1.00)	25.04 (± 0.29)	82.19 (± 1.44)
17	58.67 (± 2.08)	7.33 (± 1.53)	39.58 (± 1.00)	80.33 (± 0.58)	24.87 (± 0.58)	81.13 (± 1.15)

3.3.2 Concerted expression of *AtFRD3*, *AtNAS1* and *PvFER* elevated the iron and zinc concentration in the polished rice grains

All of the NFUF and FUF transgenic lines had increased iron concentrations in the polished grains, ranging from 6.88 to 11.08 $\mu\text{g/g}$ DW, as compared to 2.05 $\mu\text{g/g}$ DW in the NB control (Figure 2). Iron increases were also observed in the unpolished grains of NFUF and FUF transgenic lines, although NFUF lines had comparatively higher iron concentrations ranging between 22.31 to 26.74 $\mu\text{g/g}$ DW in comparison to 17.2 $\mu\text{g/g}$ DW in the NB control (Figure 2). Zinc concentrations in polished and unpolished grains of NFUF transgenic plants were also significantly increased, ranging from 29.27 to 40.09 $\mu\text{g/g}$ DW in polished grains as compared to 16.39 $\mu\text{g/g}$ DW in the NB control, and from 43.77 to 64.73 $\mu\text{g/g}$ DW in unpolished grains compared to 26.54 $\mu\text{g/g}$ DW in the NB control. In the FUF transgenic plants only slight increases of zinc were observed, within the range of 25.72 to 28.03 $\mu\text{g/g}$ DW in the polished grains and of 33.05 to 36.19 $\mu\text{g/g}$ DW in the unpolished grains (Figure 3). The manganese and copper concentrations in

grains of the transformed plants and the NB control did not vary significantly, apart from few exceptions (Supplemental Figure 3). A positive correlation between endosperm iron concentration and *AtFRD3* expression as well as citrate concentration was observed in some of the NFUF and FUF plants (Figure 1). These results suggest that iron translocate efficiently through xylem sap in the transformed plants and is then subsequently transported to the rice endosperm.

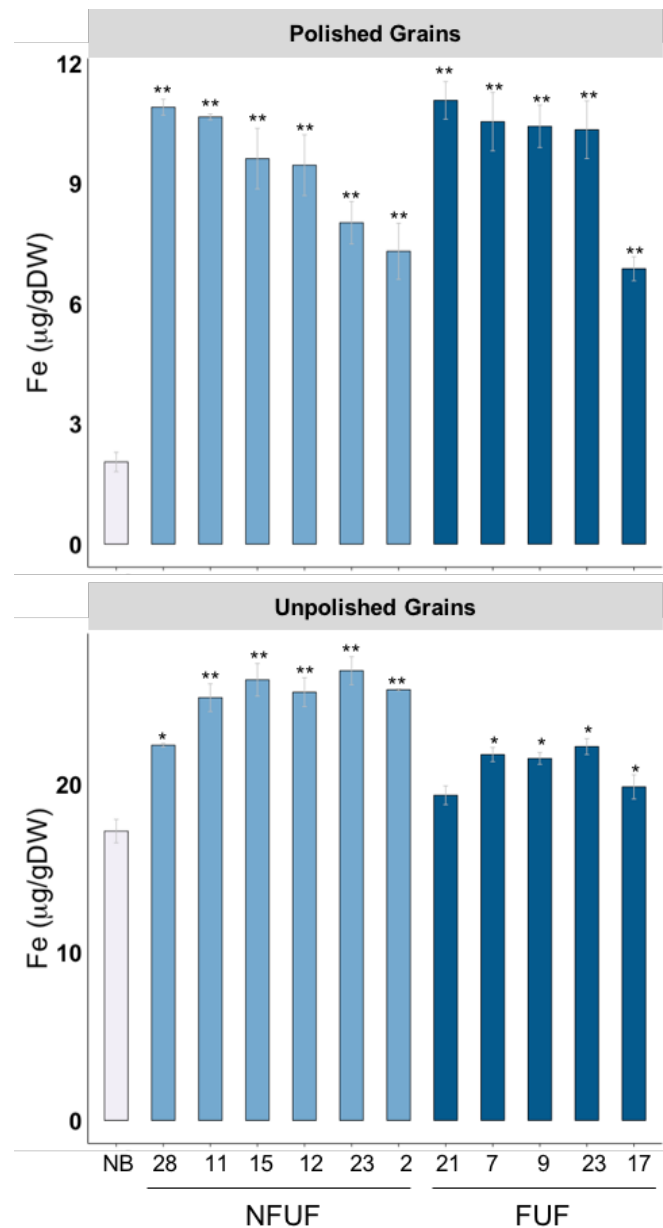


Figure 2 Iron concentration in the polished and unpolished T3 grains expressing *AtFRD3*, *AtNAS1* and *PvFER* (NFUF) or those expressing *AtFRD3* and *PvFER* genes (FUF). Values are the average of three biological replicates. NB, rice cultivar Nipponbare (control); NFUF, plants expressing *pCaMV35S::AtNAS1*, *pOsGLB-1::PvFER*, and *pZmUbi::AtFRD3*; FUF, plants expressing *pOsGLB-1::PvFER*, and *pZmUbi::AtFRD3*. Black asterisks indicate statistically

significantly higher values calculated using Student's T-Test as compared to the NB control (* $p < 0.05$, ** $p < 0.01$). Error bars indicate the SD of independent replicates.

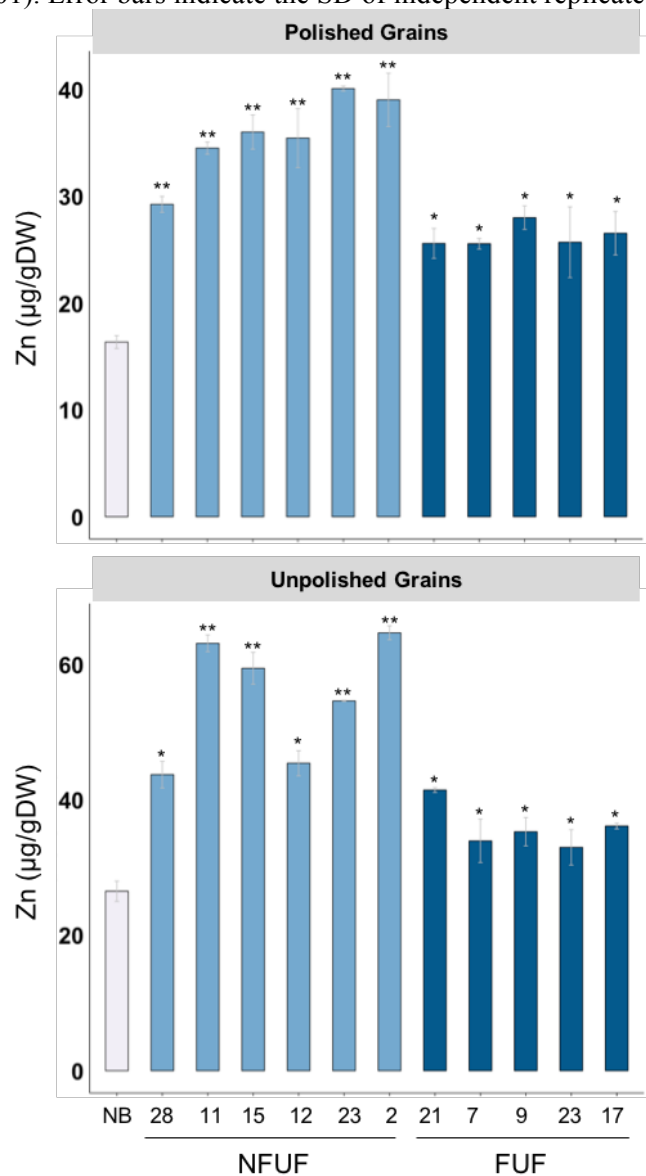


Figure 3 Zinc concentration in the polished and unpolished T3 grains expressing *AtFRD3*, *AtNAS1* and *PvFER* or those expressing *AtFRD3* and *PvFER* genes. Values are the average of three biological replicates. NB, rice cultivar Nipponbare (control). Black asterisks indicate statistically significantly higher values calculated using Student's T-Test as compared to the NB control (* $p < 0.05$, ** $p < 0.01$). See Figure 2 for the abbreviation of the gene cassettes. Error bars indicate the SD of independent replicates.

3.3.3 Distribution of iron and zinc in shoots and roots of selected NFUF and FUF plants under iron sufficient and deficient condition

The distribution of iron and zinc to shoots and roots was determined in the selected NFUF and FUF lines when grown in iron sufficient and deficient conditions. In iron sufficient condition, iron levels increased in shoots of all of the transgenic lines with up to 1.5-fold increase in NFUF 28, while only two of the NFUF lines exhibited higher root iron

concentration as compared to NB control (Figure 4A). Most of the NFUF and FUF lines also showed increased iron concentration in shoots in iron deficient condition (Figure 4A). Among them, NFUF 2 had the highest shoot iron concentration, with up to 1.9-fold higher iron than the NB control. In iron deficiency, root iron concentration of NFUF and FUF transgenic plants was lower as compared to the NB control, with almost 2-fold decrease in NFUF lines (Figure 4A). Significant iron increases were also observed in the xylem sap of NFUF and FUF transgenic plants as compared to NB control in both iron deficient and sufficient conditions (Figure 1C). In addition, root and shoot fresh weight of three selected NFUF and FUF transgenic plants was recorded. In iron sufficient condition, shoot fresh weight was significantly higher in the NFUF plants than that of FUF plants and NB control. The root fresh weight showed no significant difference between transgenic plants and NB control in iron sufficient condition, while NFUF and FUF transgenic plants had higher shoot and root fresh weight than that of NB control in iron deficiency condition (Figure 4B and 4C). These results suggest that expression of *AtFRD3* and/ or *AtNAS1* together facilitated efficient iron translocation from roots to shoots, leading to increased tolerance to iron deficient growth condition. Most of the NFUF and FUF transgenic lines had increased shoot and root zinc levels with up to 1.5-fold change in comparison to the NB control in iron sufficient condition. In contrast, in iron deficient condition, the root and shoot zinc concentrations were similar to that of NB control, with exception of NFUF 12 (Supplemental Figure 4A). The root and shoot manganese concentrations did not vary significantly between NFUF, FUF and NB plants (Supplemental Figure 4B).

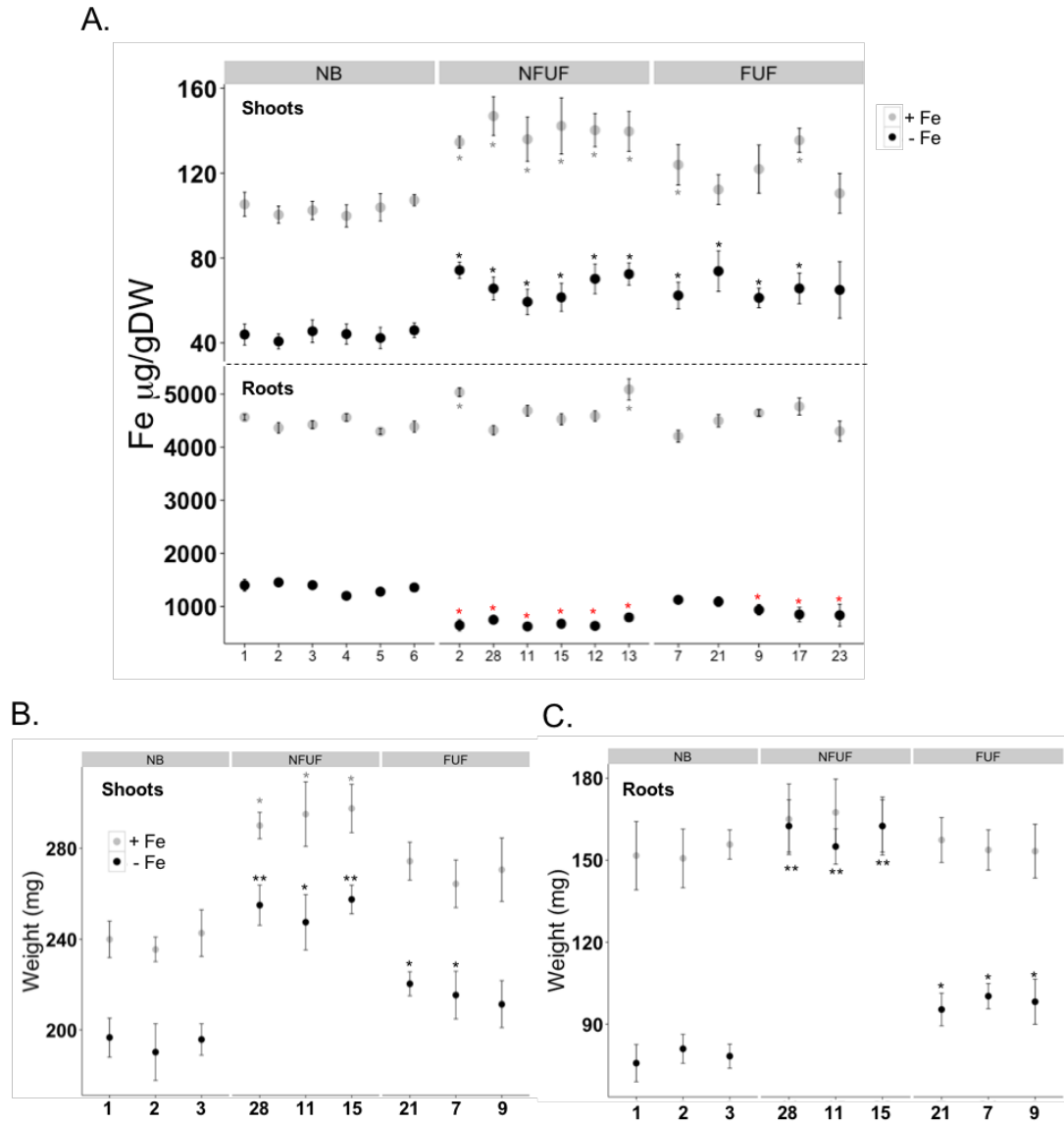


Figure 4 Characterization of selected transgenic lines under iron sufficient and deficient growth condition. (A) Iron concentration in shoots and roots of 28d-old seedlings in iron sufficient and deficient condition. Twenty plants corresponding to each independent line were screened. **(B)** and **(C)** Fresh weight of shoots and of roots, respectively. Samples were collected from 20 plants corresponding to each independent line, and the experiment was repeated three times. Student's T-Test was used for statistical calculation. Black and red asterisks indicate statistically significantly higher and lower values as compared to the NB control, respectively (* $p < 0.05$, ** $p < 0.01$). Error bars indicate the SD of independent replicates.

3.3.4 Endogenous iron homeostasis related genes are highly induced in the transformed plants upon iron deficiency

We analyzed the expression of 10 endogenous genes involved in iron homeostasis in iron deficient and sufficient conditions (Figure 5). The studied genes included those encoding enzymes for NA and DMA synthesis (*OsNAS1*, *OsNAAT1*), transcription factors (*OsIDEF1*, *OsIRO2*), iron-regulated transporters and intercellular transporters (*OsIRT1*, *OsNRAMP1*, *OsYSL2*, *OsFRO1*, *OsFRDL1*), and ferritin (*OsFER1*). *OsNAS1*, *OsNAAT1*, *OsIRT1*, *OsNRAMP1*, *OsIDEF1* and *OsIRO2* are highly induced by iron deficiency (Ogo et al., 2007; Kobayashi et al., 2009; Wang et al., 2013b). In line with this, most of the tested genes were highly induced in the shoots of NB control in iron deficiency as compared to the iron sufficient condition, except for *OsIDEF1* whose expression remained stable. On the contrary, these genes were relatively less induced in the shoots of NFUF and FUF transgenic plants in iron deficiency (Figure 5A and 5B). The expression pattern of these genes was variable in the roots. Most of the genes had elevated expression in the NFUF and FUF roots as compared to NB control in iron deficient condition, whereas the gene expression did not vary significantly in iron sufficient condition. Overall, the transgenic plants did not vary drastically from the control plants under sufficient iron supply. However, under iron deficiency, most of the tested iron homeostasis related genes exhibited variably induced expression in the roots but not in the shoots of the transformed plants. These results indicate a concerted action of different transporters in conferring iron deficiency tolerance in transformed plants.

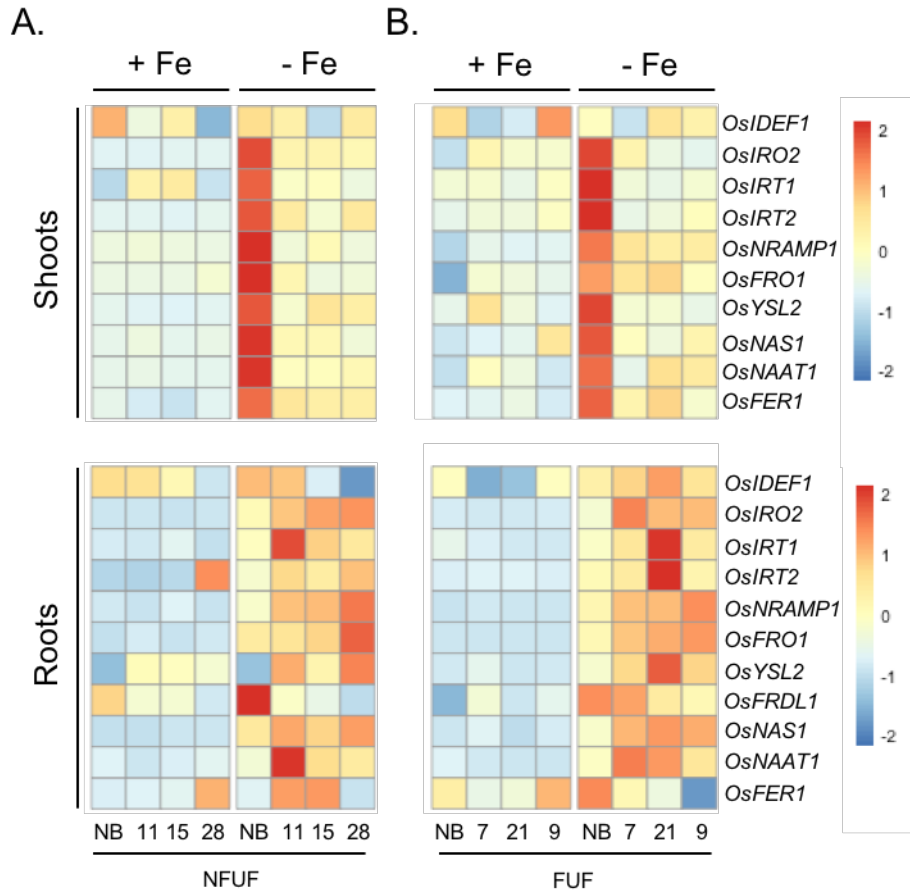


Figure 5 The expression of selected iron homeostasis related genes in shoots and roots under iron sufficient and deficient condition. Selected genes expression detected by qRT-PCR in shoots and roots of A. NFUF plants and B. FUF plants. The genes expression was normalized to the expression of rice *UBIQUITIN 5* (*OsUBQ5*).

3.3.5 *AtFRD3* expression resulted in aluminium tolerance in rice

Rice secretes citrate from the roots in response to aluminium (Al) toxicity (Yokosho et al., 2011). Ectopically expressing *AtFRD3* conferred increased tolerance to Al, but there was no difference in the Al-induced secretion of citrate from the roots between the *osfrdl1* knockout mutant and the control plants (Durrett et al., 2007; Yokosho et al., 2009). To investigate whether expressing *AtFRD3* has an effect on the Al-induced secretion of citrate and on growth of Al-treated roots in rice, we compared citrate secretion and relative root elongation between selected transgenic plants and NB control. The NFUF and FUF plants showed significantly elongated roots as compared to the NB control after exposure to Al for 24 h (Figure 6A and 6B). Higher amount of Al-induced secretion of citrate was detected in NFUF and FUF root exudates as compared to the NB root exudates (Figure 6C and 6D). These results suggest that *AtFRD3* further enhanced the Al-

induced secretion of citrate from rice roots and consequently, contributes to Al-toxicity tolerance in the transformed plants.

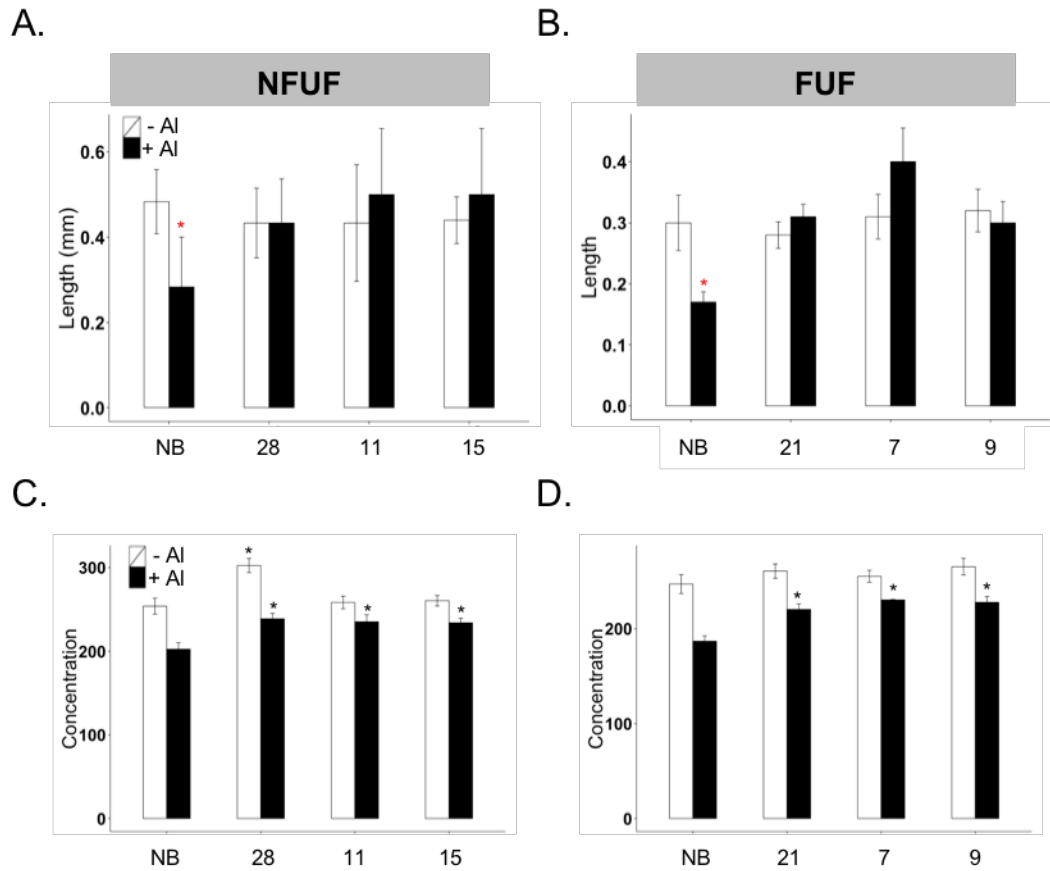


Figure 6 Root elongation and citrate concentration in root exudates of Al treated plants. (A) and (B) Roots of twenty selected transgenic plants corresponding to each independent line were measured by ruler at 0 and 24 h, respectively. **(C)** NFUF and **(D)** FUF root exudates were collected after 24 h treatment and citrate concentration was analyzed by LC-MS. Black and red asterisks indicate statistically significantly higher and lower values as compared to the NB, respectively (* $p < 0.05$). Error bars indicate the SD of independent replicates.

3.3.6 Transgenic plants did not accumulate more cadmium in the polished grains

Cadmium (Cd) also binds to citrate, and translocation of Cd from roots to shoots via xylem and phloem is critical for Cd accumulation in the rice grains (Uraguchi et al., 2009; Kato et al., 2010). Therefore, we determined Cd concentration in grains of our transgenic plants when grown on hydroponic solution containing Cd. Cd concentration in the polished NFUF and FUF grains was comparable to that of NB control grains. The Cd concentration of up to 4.05 $\mu\text{g/g}$ DW was measured in polished grains of the NB control plants, while Cd in polished grains of NFUF and FUF plants ranged between 3.78 to 4.4 $\mu\text{g/g}$ DW (Figure 7). This data suggested that expression of *AtFRD3* did not result in higher accumulation of Cd in the grains of the transformed plants.

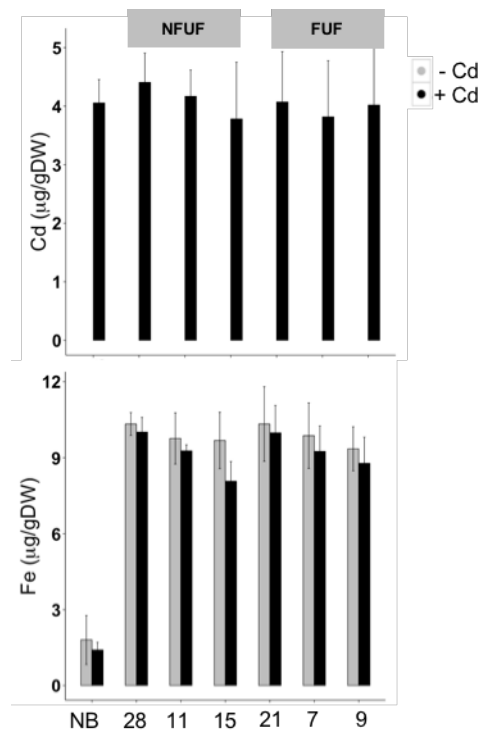


Figure 7 Cadmium and iron accumulation in polished T4 grains when grown in hydroponic solution containing CdCl_2 . Cadmium and iron concentration in polished grains of selected NFUF and FUF plants. Error bars indicate the SD of independent replicates.

3.4 Discussion

More than three billion people consume rice as a staple food globally, particularly in the countries with medium to high prevalence of iron and zinc deficiencies. Suggested approaches to mitigate iron deficiency anemia include iron supplementation, iron fortification and dietary diversification. Due to economic, cultural, and/or regional issues, however, these approaches are not always successfully implemented (Mayer et al., 2008). Biofortification of staple crops is therefore considered as an appropriate strategy. Promising increases for some micronutrients could be achieved through conventional breeding, however the improvement for iron content has not been possible in rice grains. Engineering for high-iron biofortified rice has proven to be successful in the recent years. Several studies reported development of high-iron biofortified rice lines, with iron concentrations ranging from 6 to 19 $\mu\text{g/g}$ DW in the polished grains (Johnson et al., 2011; Masuda et al., 2012; Trijatmiko et al., 2016; Boonyaves et al., 2017). Most of these studies focused on engineering rice with genes involved in iron uptake and storage, and only a few focusing on iron translocation within the plant. We expanded our iron biofortification strategies to include a focus on iron translocation within xylem (by including *AtFRD3*) together with efficient iron uptake (*AtNAS1*) and storage in the endosperm (*PvFER*). The overexpression of *AtNAS1* is expected to increase DMA secretion as well as increased NA concentration in the roots and shoots of transgenic rice plants, thus contributing to enhanced iron uptake and transport. The endosperm specific expression of *PvFER* ensures iron storage in the grains. The transformed plants developed with this novel strategy showed increased endosperm iron concentration of up to 5.3-fold. Transgenic plants expressing *AtFRD3*, *AtNAS1* and *PvFER* have higher iron and zinc concentrations in the grains as compared to the lines expressing *AtFRD3* and *PvFER*, particularly NFUF 28 and NFUF 23. Iron is reported to be transported into the grains from mature leaves via phloem and via xylem-to-phloem transport in the nodes at early grain-filling stage (Bashir et al., 2010; Sperotto et al., 2012; Ariga et al., 2014; Yamaji and Ma, 2014; Yoneyama et al., 2015). In rice plants, iron in the xylem is mainly bound to citrate, while a small amount also binds to DMA (Nishiyama et al., 2012; Alvarez-Fernandez et al., 2014). Furthermore, it was reported that *AtFRD3* is involved in promoting iron nutrition between symplastically-disconnected tissues (Roschzttardtz et al., 2011). It is therefore conceivable that increased Fe-citrate concentration in xylem sap in the transgenic plants, because of *AtFRD3* expression, leads to increased mobilization of iron and eventual transport to the grains. At the same time, the *AtNAS1* expression could

facilitate higher concentrations of Fe-NA and Fe-MA in the phloem sap. The concerted expression of both these genes, together with Fe storage function of *PvFER*, is expected to contribute to higher endosperm iron content in the transformed rice grains.

The expression of *NAS* gene often leads to concurrent zinc increases in addition to the expected iron increases in the grains (Douchkov et al., 2005; Lee et al., 2009b; Wirth et al., 2009; Boonyaves et al., 2016). Most of our NFUF lines also had higher zinc levels in the grains. Though zinc is transported mainly in free form, certain amount of zinc in rice tends to chelate with NA in the phloem sap and with DMA in the xylem sap (Xuan et al., 2006; Nishiyama et al., 2012). The *NAS* expression in rice also increases the expression of zinc transporter encoding genes, including *OsZIP1*, *OsZIP3*, *OsZIP4* and *OsNAS3* (Wang et al., 2013b). It is therefore not surprising that the expression of *AtNAS1* leads to higher grain zinc concentrations in addition to the increases in grain iron concentrations.

The *AtFRD3* and/ or *AtNAS1* expressing NFUF and FUF plants exhibited increased tolerance to low iron availability as well as to Al toxicity. These plants apparently transported more iron from roots to shoots, evident from increased shoot iron concentration as compared to the NB control. Similarly, tobacco plants expressing *AtNAS1* accumulated more iron in the leaves in low iron condition and exhibited tolerance to iron deficiency (Douchkov et al., 2005). The high iron biofortified rice lines, expressing *HvNAS1*, *HvNAAT-A* and *-B*, and *HvIDS3* from a single construct, also showed low iron tolerance when grown in hydroponic culture or calcareous soil (Masuda et al., 2013). A varied expression of iron homeostasis related endogenous genes, particularly in iron deficiency condition, indicate that the transgenes trigger a coordinated response of these genes to combat iron deficiency stress in the transformed plants.

Al toxicity inhibits root growth and leads to reduced uptake of water and nutrients, significantly limiting crop production (Kochian et al., 2004; Kochian et al., 2005). Secretion of citrate and malate by roots to chelate Al is a well-known mechanism to counteract Al toxicity (Ma et al., 2001). Expression of *AtFRD3* in Arabidopsis and barley increased Al tolerance in comparison to the control plants (Durrett et al., 2007; Zhou et al., 2014). The NFUF and FUF plants had increased root elongation rates when subjected to Al treatment and the roots released more citrate as compared to the NB control. These results demonstrate that heterologous expression of *AtFRD3* could increase the Al

toxicity tolerance in rice by enhancing citrate efflux from the roots. Similar to Al, Cd could have a negative impact on plant growth and ultimately also on human health. Analysis on 69 diverse rice cultivars revealed a strong correlation between root-to-shoot Cd translocation via xylem sap and Cd accumulation in the shoots and grains (Uraguchi et al., 2009). Other studies also reported correlation of Cd concentration in the phloem sap with the grain Cd concentration in several rice cultivars (Kato et al., 2010). Since Cd can also bind citrate in both xylem and phloem sap (Senden et al., 1995; Uraguchi et al., 2009; Kato et al., 2010), it is likely to have increased Cd accumulation in the plants expressing *AtFRD3*, which led to higher citrate concentration in the xylem sap. Based on the analysis on hydroponically grown plants with Cd treatment, we could confirm that the NFUF and FUF plants did not accumulate more Cd in the polished grains as compared to the NB control.

In summary, the rice plants expressing *AtFRD3*, *AtNAS1* and *PvFER* have significantly increased iron and zinc but not Cd concentration in the grains, and these plants show increased tolerance to iron deficiency and Al toxicity. Importantly, the concerted expression of the three transgenes does not affect the phenotypic growth of the plants, as observed in the greenhouse. These results support that enhancing citrate loading to the xylem, coupled with increased NA and DMA production as well as endosperm storage of iron is a good strategy for iron biofortification in target crops.

3.5 Material and Methods

3.5.1 DNA constructs, rice transformation and plant growth conditions

The full-length *AtFRD3* genomic sequence was amplified using a forward primer containing a *BamHI* site and a reverse primer with *BspEI* site. The whole fragment was subsequently inserted into the *BamHI* and *BspEI* digested *OsNAS2-PbskII(-)* vector (Singh et al., 2017) to generate *pUbi::AtFRD3::tNOS* fragment. In parallel, the *PstI* site in the *Ubi* promoter contained in the *OsNAS2-PbskII(-)* construct was changed by a point mutation in order to use *PstI* site for subsequent cloning steps. The *pCAMBIA-1300PMI-NASFER* vector (Provided by Dr. S. P. Singh, Singh et al., 2017, in press) was cut at *PstI* site and the fragment of *pUbi::AtFRD3::tNOS* was inserted to generate the NFUF cassette. For the FUF construct, *pCAMBIA-1300PMI-NASFER* was digested at *XbaI* and *PstI* sites to obtain the *pGlb::PvFERRITIN::tNOS* fragment, which was then subsequently

inserted into *pCAMBIA-1300PMI* to generate the *pCAMBIA-1300PMI-FER* vector. The *pCAMBIA-1300PMI-FER* vector was cut at the *PstI* site and the *pUbi::AtFRD3::tNOS* was inserted to generate the FUF cassette. These vectors were transformed into *Oryza sativa ssp. Japonica cv. Nipponbare* using *Agrobacterium tumefaciens* strain EHA105 (Hood et al., 1993). Transformation, selection and regeneration were conducted according to the established protocol described previously (Nishimura et al., 2006). Candidate transformants were first screened for the presence of *AtFRD3*, *AtNAS1*, and *PvFER* by PCR. Southern blot hybridization using digoxigenin (DIG) labeling was performed using *PmlI*-digested genomic DNA isolated from the transgenic lines to select the lines with single-copy cassette insertion. The PCR-amplified *PMI* DNA fragment was used as a probe to detect the transgene cassettes. The primer sequences used in cloning, sequence verification and PCR are provided in Supplemental Table 2. Selected transgenic plants together with Nipponbare control were grown in commercial soil (Klasmann-Deilmann GmbH, Germany) under greenhouse conditions in 80% humidity at 30°C with 12h light and 60% humidity at 22°C with 12h dark. Quantification of divalent metals and transgene expression was conducted on plants in the T2 and T3 generations.

3.5.2 Iron deficiency and cadmium excess treatment in hydroponic culture

Transgenic and NB seeds were germinated *in vitro* for five days in petri dishes on a H₂O-moistened filter paper and subsequently transferred into containers (with tip holes) containing 400 mL hydroponic solutions for seven days. Solutions for hydroponic system were prepared according to the established protocols, i.e., using 0.70 mM K₂SO₄, 0.10 mM KCl, 0.10 mM KH₂PO₄, 2.0 mM Ca(NO₃)₂, 0.50 mM MgSO₄, 10 μM H₃BO₃, 0.50 μM MnSO₄, 0.20 μM CuSO₄, 0.01 μM (NH₄)₆Mo₇O₂₄, and 0.5 μM ZnSO₄, with different iron concentrations added as Fe(III)-EDTA according to the treatment (normal condition: 100 μM; iron-deficient condition: 10 μM). For the iron-deficient condition, plants were grown in hydroponic solutions containing 10 μM Fe(III)-EDTA for 14 days. Plants grown in hydroponic solutions containing 100 μM Fe(III)-EDTA served as control. Solutions were changed every one to two days to avoid any precipitation and contamination. To obtain the grains from cadmium treated plants, plants were grown till maturity in a hydroponic solution containing 10 μM CdCl₂ in green house conditions in 80% humidity at 30°C with 12h light and 60% humidity at 22°C with 12h dark.

3.5.3 Metal ion measurements

Grain samples were de-husked to obtain unpolished brown grains. The de-husked grains were processed with a grain polisher (Kett grain polisher ‘Pearlest’, Kett Electric Laboratory, Tokyo, Japan) for one min. Shoot and root samples from hydroponic culture were dried at 60°C for three to five days. 200 mg of each ground grains sample, 50-100 mg of tissue samples and 50 µL of xylem sap samples were boiled in 15 ml of 65% v/v HNO₃ solution at 120°C for 90 min. Three ml of 30% v/v H₂O₂ were subsequently added and continuously boiled at 120°C for another 90 min. Metal concentrations were determined using inductively coupled plasma-optical emission spectroscopy (ICP-OES) (Varian Vista-MPX CCD Simultaneous ICP-OES). The wavelength used for iron, zinc, manganese and copper were 238.204, 213.857, 257.610, and 324.754, respectively. The National Institute of Standards and Technology (NIST) rice flour standard 1658a was treated and analyzed in the same manner and used as internal control for every measurement. Data were analyzed using Student’s T-Test. The criteria of $p < 0.05$ and $p < 0.01$ was used to determine statistically significant differences among the tested lines and the control.

3.5.4 RNA extraction, cDNA synthesis and quantitative real-time PCR

Total RNA was extracted from roots and shoots of five-day-old T3 generation seedlings using Trizol® reagent (Invitrogen, USA). To obtain total endosperm and embryo RNA, endosperm and embryo were separated manually from T3 rice grains at 16 DAF. Extraction buffer containing 0.15M NaCl and 1% sarcosyl was added to the ground samples followed by purification with 8M guanidine hydrochloride buffer. The RNA was treated with DNase I (Thermo Fisher Scientific Inc., USA) to remove genomic DNA contamination. First-strand cDNA was synthesized using the RevertAid™ first strand cDNA synthesis kit (Thermo Fisher Scientific Inc., USA). Quantitative RT-PCR was performed as previously described (Liu et al., 2011). In brief, qRT-PCR was performed in a 7500 Real-Time PCR System using the SYBR Green RT-PCR reagent kit following the manufacturer’s protocol (Applied Biosystems, Carlsbad, CA, USA). Each reaction was run in triplicates in a volume of 20 µL with an initial denaturation step at 95°C for 10 min, followed by 40 cycles of 95°C for 15 sec and 60°C for 60 sec. Data were analyzed according to the manufacturer’s instructions using the 7500 System SDS Software v1.4 (Applied Biosystems). The expression level of genes of interest was normalized to the expression of rice *UIBUITIN 5* (*OsUBQ5*).

3.5.5 Xylem sap collection

Transgenic and NB seeds were germinated *in vitro* for five days on H₂O-moistened filter paper placed in petri dishes and subsequently transferred into containers (with tip holes) containing 400 mL hydroponic solutions for seven days. The plants were then grown in hydroponic solution for two weeks with iron sufficient (100 μM Fe(III)-EDTA) or deficient (10 μM Fe(III)-EDTA) supply. The nutrient solution was renewed before collecting xylem sap. After six hours of solution renewal, plants were decapitated 3 cm above the roots, and xylem sap was collected with a micropipette from the cut end for one to two hrs. The first drop of xylem sap was discarded to reduce cellular contamination. The xylem sap was then stored at -80 °C for further analysis.

3.5.6 LC-MS analysis

Quantitative analysis of citrate and malate was performed as previously described (Seung et al., 2016). In brief, 50 μL of xylem sap samples were extracted using chloroform-methanol. Extracted metabolites were dried in a vacuum centrifuge, dissolved in water and filtered through a 0.2 μm cellulose membrane. Samples were analyzed using a UHPLC-MS/MS.

3.5.7 Evaluation of Al tolerance and root exudate collection

Al treatment was followed as previously described (Ma et al., 2002), with slight modification. In brief, seeds were soaked in deionized water overnight and then germinated on filter paper moistened with 0.5 mM CaCl₂ (pH 4.5) solution. The solution was renewed daily for four days. After four days of growth (at 25°C), similar sized seedlings were selected and were exposed to 0.5 mM CaCl₂ (pH 4.5) containing 0 or 50 μM AlCl₃ in a one-liter plastic container for 24 h. Root length was measured before and after Al treatment. Twenty seedlings from NFUF, FUF and NB plants were screened, and the experiment was repeated three times. To analyze citrate secreted from rice roots, root exudates from NFUF, FUF and NB plants were collected. Seeds were germinated on H₂O-moistened filter paper placed in petri dishes and five-day-old seedlings were transferred into hydroponic solutions for another five days (hydroponic solutions were prepared as explained above). After pre-culture for 10 days, roots were placed in 0.5 mM CaCl₂ (pH 4.5) solution overnight and then exposed to 0.5 mM CaCl₂ (pH 4.5) solution

containing 50 μM AlCl_3 . Root exudates were collected after 24 h and were stored at -80°C for further analysis.

3.6 Conflict of interest

The authors declare that they have no conflict of interest.

3.7 Author contributions

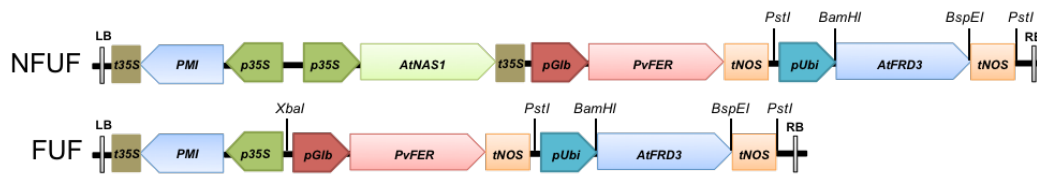
NKB conceived the study, NKB and TYW designed the experiments, TYW performed the experiments, TYW, WG and NKB interpreted the data, TYW and NKB wrote the manuscript, and WG and NKB edited the manuscript. All authors have read and approved the final manuscript.

3.8 Acknowledgments

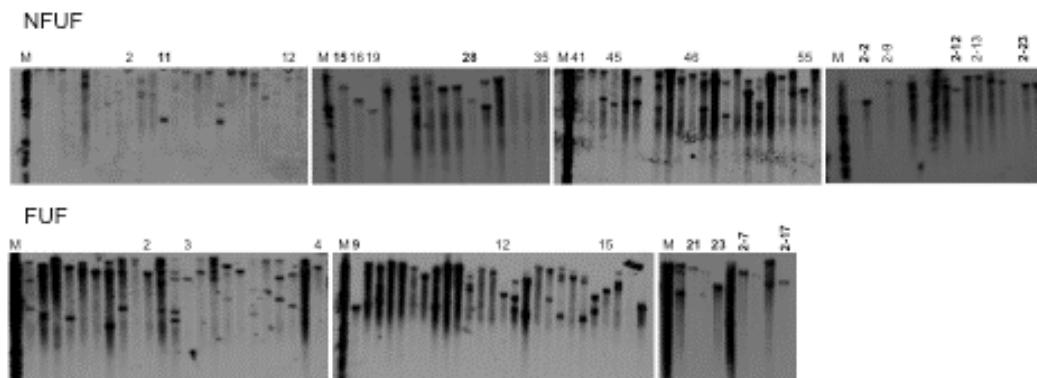
We gratefully acknowledge the support by Mrs. Jacqueline Imhof and the ETH research grants for this work to WG and NKB. We thank Prof. Rainer Schulin for providing access to ICP-OES and Björn Studer for the kind assistance with metal measurements. We thank Irene Zurkirchen for the technical support in the greenhouse. We thank Martina Zanella and Dr. Michaela Fischer-Stettler from Prof. Samuel C. Zeeman's lab for assisting with LC-MS analysis.

3.9 Supplementary data

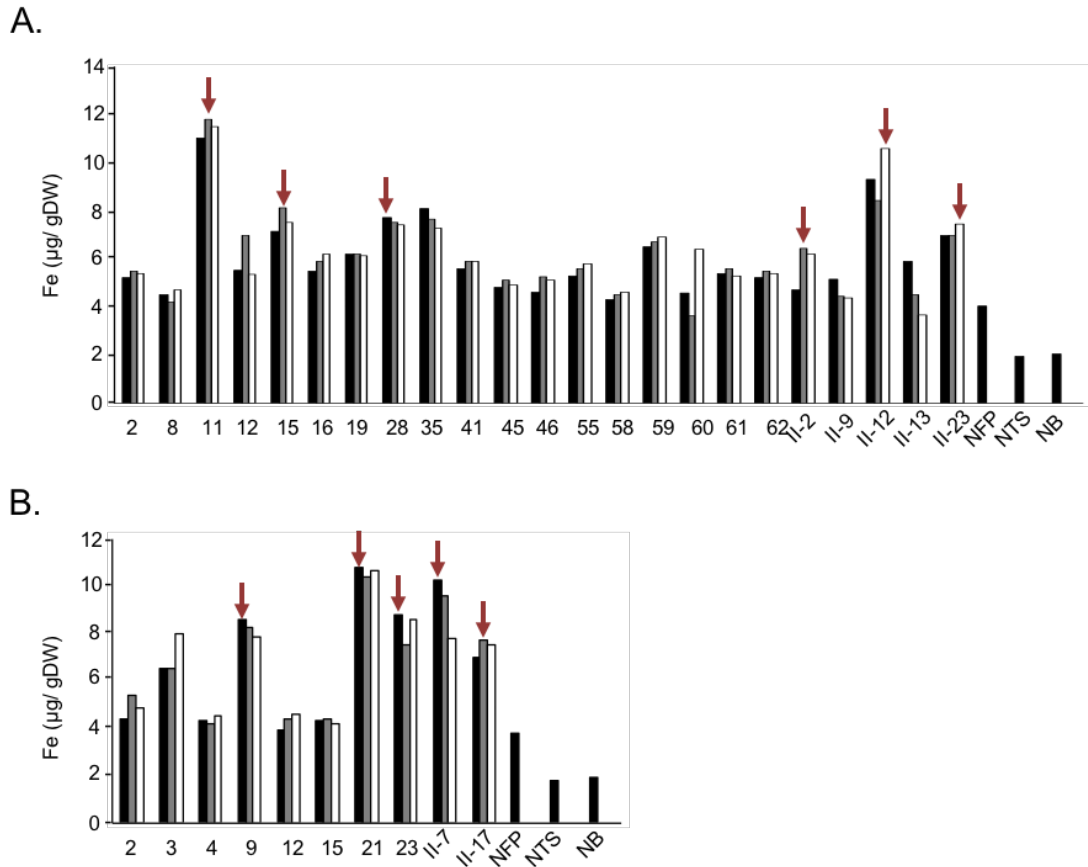
A.



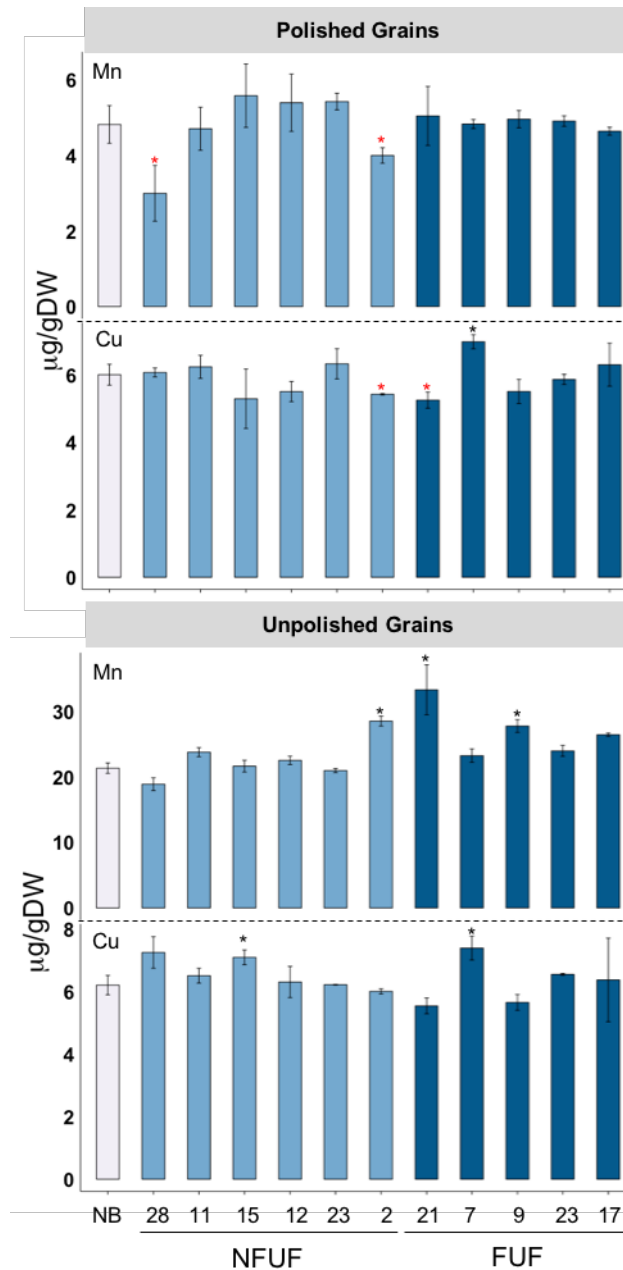
B.



Supplementary Figure 1 Schematic representation of the transformation cassettes, and characterization of transgenic lines in T0 generation using southern blotting. (A) LB, T-DNA left border; RB, T-DNA right border; t35S, cauliflower mosaic virus (CaMV) 35S terminator; *PMI*, *PHOSPHOMANNANOSE ISOMERASE* gene; *p35S*, *CaMV35S* promoter; *pUbi*, *Zea Maize UBIQUITIN* promoter; *AtFRD3*, Arabidopsis *FERRIC REDUCTASE DEFECTIVE 3* gene; *AtNAS1*, Arabidopsis *NICOTIANAMINE SYNTHASE 1* gene; *tNOS*, *NOPALINE SYNTHASE* terminator; *pGlb*, rice *GLOBULIN-1* promoter; *PvFER*, *Phaseolus vulgaris FERRITIN* gene; BamHI, BspEI, PstI and SphI are restriction enzyme sites. **(B)** Southern hybridization analysis using *PMI* as a probe. Numbers indicate independent transformed lines with potential single insertion of transgene.

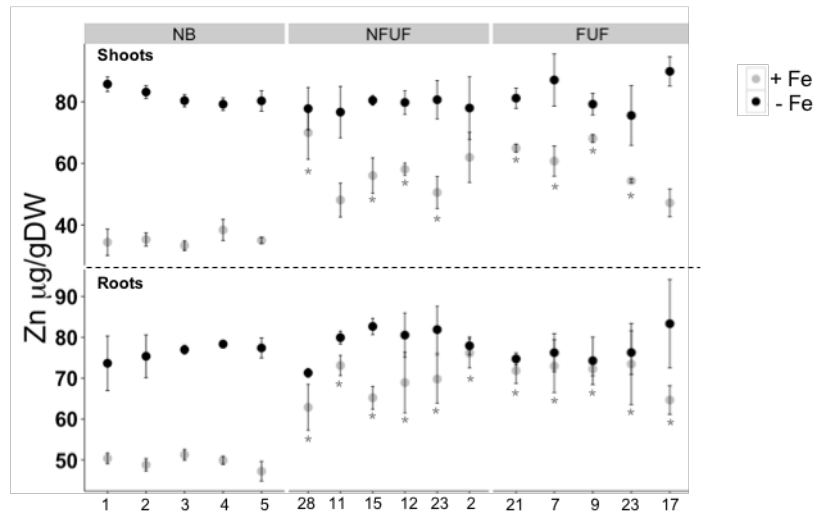


Supplementary Figure 2 Iron concentration in the polished T2 grains in all single insertion lines carrying NFUF and FUF constructs. (A) NFUF and (B) FUF plants. Values are the average of two technical replicates. The bars for each line represent three individual plants. Arrows indicate selected plants from each line for further analysis in T3 generation and II indicate second batch of transformation. NB, rice cultivar Nipponbare (control). See Figure 2 for the abbreviation of the gene cassettes.

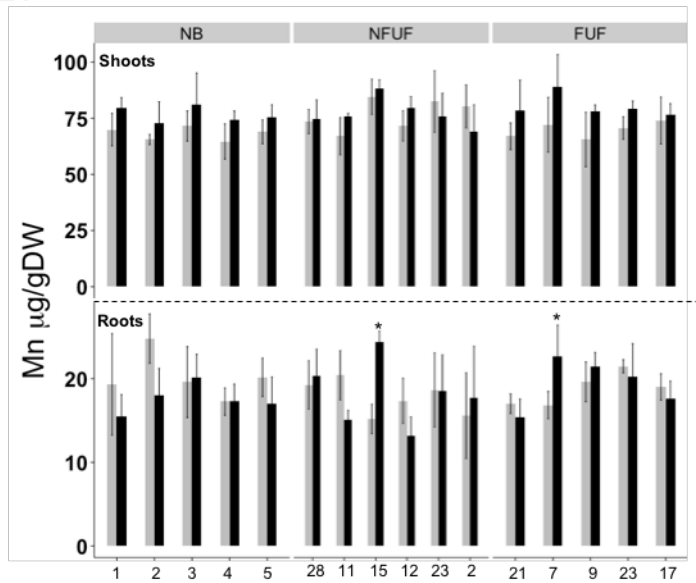


Supplementary Figure 3 Manganese and Copper concentration in the polished and unpolished T3 grains expressing *AtFRD3*, *AtNAS1* and *PvFER* (NFUF) or *AtFRD3* and *PvFER* genes (FUF). Values are the average of three biological replicates. NB, Nipponbare rice control. Black and red asterisks indicate statistically significantly higher and lower values calculated using Student's T-Test as compared to the NB control, respectively (* $p < 0.05$). Error bars indicate the SD of independent replicates.

A.



B.



Supplementary Figure 4 Zinc and manganese concentration in shoots and roots of selected transgenic lines under iron sufficient and deficient condition. (A) Zinc and (B) Manganese concentration in shoots and roots of 28d-old seedlings of transgenic plants. Samples were collected from 20 plants corresponding to each independent line and Student's T-Test was used for statistical calculation. Black asterisks indicate statistically significantly higher values as compared to the NB control (*p<0.05). Error bars indicate the SD of independent replicates.

Supplementary Table 1 Grain quality assessment of selected transformed plants carrying NFUF and FUF constructs as compared to the Nipponbare control. The plants were grown in the greenhouse condition prior to the analysis. Black and red asterisks indicate statistically significantly higher and lower values as compared to the NB control (*p<0.05), respectively. Data is presented as mean \pm SD.

Line	Length (mm)	Width (mm)	Chalkiness (%)	Amylose content (%)	Starch content (%)	Protein content (%)
NB	5.53 (\pm 0.10)	2.83 (\pm 0.13)	1.2 (\pm 0.3)	17.62 (\pm 1.24)	82.78 (\pm 0.54)	11.2 (\pm 0.12)
NFUF						
11	5.52 (\pm 0.05)	2.99 (\pm 0.10)	0.8 (\pm 0.07)	17.97 (\pm 0.76)	83.71 (\pm 0.47)	11.1 (\pm 0.11)
15	5.44 (\pm 0.07)	2.97 (\pm 0.05)	0.9 (\pm 0.06)	17.74 (\pm 0.43)	82.36 (\pm 0.86)	10.6 (\pm 0.12)
28	5.45 (\pm 0.10)	2.94 (\pm 0.11)	1.3 (\pm 0.1)	17.44 (\pm 0.76)	83.29 (\pm 0.74)	10.5 (\pm 0.09)
FUF						
21	5.5 (\pm 0.11)	2.88 (\pm 0.08)	0.7 (\pm 0.08)*	18.53 (\pm 1.57)	82.16 (\pm 0.44)	10.5 (\pm 0.07)
1	6 (\pm 0.10)*	2.92 (\pm 0.08)	1.5 (\pm 0.05)	17.35 (\pm 1.20)	81.93 (\pm 0.65)	10.7 (\pm 0.14)
9	5.9 (\pm 0.11)	2.95 (\pm 0.12)	0.5 (\pm 0.07)*	17.82 (\pm 1.56)	82.45 (\pm 0.47)	10.4 (\pm 0.14)

Supplementary Table 2 Primer sequences used for sequence validation, cloning and qRT-PCR analysis in this study

Primer Name	Direction	Primer sequence (5'-3')	Purpose
AtFRD3-F-BamHI	F	ggatccatgacgaaactggtgatg	cloning/ sequencing
AtFRD3-R-BspEI	R	tccggactaggaagatgaaggatg	
PvFer	F	gtcttcgtttatattgctcttg	PCR/ sequencing
Ubi	R	gtaaatcccaaatccaattacc	PCR/ sequencing
35S	F	cagttcatcacagagtctcttacg	PCR/ sequencing
AtNAS1	F	gacgtggtaactcggttgfgatc	PCR/ sequencing
Pmi	F	gtaactgctgagaaccttccac	PCR/ sequencing
Glb	F	gccccaccatttttaattcattc	PCR/ sequencing
PMI	F	ctggctaagtgggtttct	PCR/ southern probe
	R	cgtgatggtgattgagagt	
AtFRD3-1	F	caaccagccacagcaacctccag	PCR/ sequencing
	R	gtcctctctcctttttattcg	
AtFRD3-2	F	gtgcttcgtctagggatcatcg	PCR/ sequencing
	R	ccttcacgtacacaacaacaatc	
AtFRD3-3	F	gtatggttaactctctcttc	PCR/ sequencing
	R	gcaacagcagtcactttgttat	
AtFRD3-4	F	tatgcacactatataactatg	PCR/ sequencing
	R	gtaaaggcccaattaaataacc	
qAtFRD3	F	gtatggttaactctctcttc	qRT-PCR
	R	gcaacagcagtcactttgttat	
qAtNAS1	F	gcacttggagaaacacatgg	qRT-PCR
	R	tctgagagcatgacactcc	
qPvFER	F	ggggatacgggaaacgtaa	qRT-PCR
	R	gagcctggctaaccgcat	
OsIDEF1	F	gtcttcaggctgggatgt	qRT-PCR
	R	gggatttgtgtctgctgatg	
OsIRO2	F	gaaggcttctcacttcactgattca	qRT-PCR
	R	tgatcgttcttcaactctctg	
OsIRT1	F	ctcgagataggcatcgtggt	qRT-PCR
	R	gaacatctggtggaagcaca	
OsNRAMP1	F	ggaagggtggtggacgaca	qRT-PCR
	R	ggtccaatgtgggacaaaaa	
OsFRO1	F	tcgccataccacctgatgta	qRT-PCR
	R	ttgccctcctgatcctatg	
OsYSL2	F	gggctccttaacttgcttcc	qRT-PCR
	R	gaggggtatggaatccgttt	
OsNAAT1	F	tggagggatccatgatga	qRT-PCR
	R	cttcattcccagcacactcc	
OsNAS1	F	cggttgagaagcagaagagt	qRT-PCR
	R	cgatcgtccggctgttag	
OsFER1	F	ggattcggcaaatctcaa	qRT-PCR
	R	cccttctcaggatggtcgaa	
OsFRDL1	F	tcaccaatgctaaggcctgc	qRT-PCR
	R	aaccacggaaaacacctg	
	F	accacttcgaccgccactact	

4. Enhanced Grain Iron Accumulation in *osvit2* Lines Expressing *NAS* and *FER*

Genes

Ting-Ying Wu, Wilhelm Grissemer and Navreet K. Bhullar*
Plant Biotechnology, Department of Biology, ETH Zurich, Switzerland

***Correspondence**

Dr. Navreet K. Bhullar
Plant Biotechnology,
Department of Biology
ETH Zurich (Swiss Federal Institute of Technology)
Universitaetsstrasse 2
8092 Zurich, Switzerland
bhullarn@ethz.ch

4.1 Abstract

Nearly one-third of the world's population suffer from iron deficiency anemia. Among the approaches to address this deficiency, the development of biofortified staple food crops with increased iron in the edible parts is a promising strategy. Genetic engineering approaches have been the most successful ones in iron biofortifying the major cereals, including wheat and rice. Rice VACUOLAR IRON TRANSPORTER (VIT) mediates the transport of iron, zinc and manganese into the vacuoles. The rice *osvit* mutants were previously reported to accumulate 1.8-fold higher iron in the unpolished and polished grains as compared to the cultivar Dongjin (genetic background). We transformed the *osvit2* mutant line with the combination of *PvFERRITIN* (*PvFER*) under the control of endosperm specific promoter and constitutively expressed Arabidopsis *NICOTINAMINE SYNTHASE 1* (*AtNAS1*). The iron concentration in T3 polished and unpolished grains of transgenic plants (NFvit2) were up to 3-fold higher and 2-fold higher than that in the *osvit2* mutants, respectively. Moreover, the NFvit2 transgenic plants accumulated 1.4-fold higher zinc in the polished T3 grains as compared to the *osvit2* mutants. The iron and zinc concentration in the shoots and roots of NFvit2 lines did not vary significantly as compared to the *osvit2* mutants and DJ plants under sufficient iron supply. However, an increase of iron and zinc concentration was observed in the shoots of NFvit2 lines under iron deficiency condition. Correspondingly, elevated transcript levels for the genes encoding different iron transporters, including *OsYSL2* and *OsYSL15*, and for genes involved in NA metabolism, were detected in the shoots and roots of NFvit2 lines as compared to the *osvit2* mutants under iron deficiency. Our results demonstrate that the introduction of *AtNAS1* and *PvFER* into *osvit2* mutants could successfully increase the iron and zinc concentrations in the *osvit2* transformed grains.

4.2 Introduction

Iron deficiency is one of the most prevalent micronutrient deficiencies, affecting around 1.6 billion people worldwide. Several interventions have been suggested to tackle this issue, including increased dietary diversification, supplementation and fortification (Stevens et al., 2013). Due to socioeconomic and regional issues, these strategies are often unsuccessful. Biofortification of staple crops is therefore considered as an appropriate and effective strategy (Mayer et al., 2008). However, developing crops with increased micronutrient concentrations is challenging because plants tightly regulate metal ion homeostasis. Iron uptake, translocation and storage within plants is controlled by complex network of transporters, regulatory factors and storage proteins. In general, cereal crops use chelation-based strategy to acquire iron from soil. They release phytosiderophores (PS) that form complexes with Fe(III) which are subsequently transported back into the roots via YELLOW STRIPE-LIKE 2 (YSL2) (Koike et al., 2004; Ishimaru et al., 2010). All PSs that belong to mugineic acid (MA) family are synthesized from S-adenosyl-L-methionine through a conserved pathway catalyzed by NICOTINAMINE SYNTHASE (NAS), NICOTIANAMINE AMINOTRANSFERASE (NAAT) and DEOXYMUGINEIC ACID SYNTHASE (DMAS) (Kobayashi and Nishizawa, 2012). Rice, which is an important target for iron biofortification, utilizes both strategy I and II for iron acquisition. The IRON-REGULATED TRANSPORTER 1 (OsIRT1) have been reported to mediate Fe (II) acquisition in rice (Ishimaru et al., 2006). The genetic engineering strategies used to develop high iron biofortified rice so far, focused primarily on increasing PS biosynthesis, overexpressing iron transporter encoding genes and engineering *FERRITIN* (*FER*) expression into the rice endosperm. For example, constitutive expression of *NAS* has led to 2-to 4-fold iron increases in the polished rice grains (Johnson et al., 2011; Lee et al., 2012a). Transformation of barley genes involved in PS biosynthesis into rice plants resulted in enhanced tolerance to low iron conditions and 1.4-fold increased iron in the grains as compared to the wild type (WT) control (Masuda et al., 2009). The overexpression of *OsYSL15* controlled by *ACTIN* promoter in rice resulted in 1.2-fold higher iron concentration in the grains (Lee et al., 2009a). The transgenic rice expressing *OsYSL2* under the control of *SUCROSE TRANSPORTER* promoter exhibited a 4-fold iron increase in the endosperm (Ishimaru et al., 2010). The transformation of *AtIRT1* driven by *MsENOD12B* promoter in rice led to a 4-fold increase of iron in the polished grains (Boonyaves et al., 2016). Rice *GLOBULIN*

or *GLUTELIN* promoter driven expression of *FER* could elevate iron concentrations up to 2- and 3.7-fold, respectively (Goto et al., 1999; Vasconcelos et al., 2003).

The constructs expressing combination of genes responsible for effective iron transport and storage could achieve higher increases in the endosperm iron content compared to most single gene strategies. Rice expressing *FER* under the control of endosperm specific promoter and constitutively expressed *NAS* could lead to a 6-fold increase of iron in the polished grains (Wirth et al., 2009). Similarly, the expression of *FER* controlled by endosperm specific promoter together with a constitutive expression of *NAS* in an *Indica* rice cultivar IR64 resulted in 7-fold higher iron content in the polished grains (Trijatmiko et al., 2016). In addition, the overexpression of barley *NASI*, *OsYSL2* and soybean *FER* from a single construct increased iron content by 3.4- and 6-fold in polished grains of a Myanmar and a Japanese rice cultivar, respectively (Masuda et al., 2012; Aung et al., 2013). Overexpression of multiple genes involved in MA production together with the endosperm specific expression of *FER* increased the iron in polished grains of rice by 4-fold (Masuda et al., 2012). The concerted expression of *AtIRT1* under the control of its native promoter together with constitutive expression of *AtNAS1* and endosperm specific expression of *PvFER* in rice led to a 4-fold higher iron content in the polished grains (Boonyaves et al., 2017).

The iron biofortification strategies have not explored the potential of inter- and intracellular iron transporters to a greater extent. Vacuolar sequestration of iron is an important mechanism in regulating iron homeostasis. Several genes have been identified to regulate iron trafficking between cytosols and vacuoles. Among them, VACUOLAR IRON TRANSPORTER 1 (*AtVIT1*) in *Arabidopsis* transports cytoplasmic iron into vacuole (Kim et al., 2006). *VIT1* is highly expressed in developing seeds and therefore the iron localization in *vit1* mutant has been altered significantly (Kim et al., 2006). *VIT1*-LIKE (*VTL*) proteins in *Arabidopsis* have been characterized recently (Gollhofer et al., 2014). *AtVTL1*, *AtVTL2* and *AtVTL5* are iron transporters that localize in vacuolar membrane and play important roles in transferring cytoplasmic iron into vacuoles, and contribute to iron homeostasis regulation in plants (Gollhofer et al., 2014). Overexpressed *AtVIT1* in the starchy roots of cassava under control of patatin promoter led to a 3-4 times higher iron in the storage roots of transgenic plants (Narayanan et al., 2015). The *AtVIT1* expressing transgenic cassava also showed 4 and 16 times higher iron concentration in

their young stem and stem base tissues, respectively (Narayanan et al., 2015). However, young leaves of *AtVIT1* transgenic plants exhibited iron deficiency phenotype such as interveinal chlorosis of leaves and lower iron concentration when compared with the WT plants (Narayanan et al., 2015). These results suggested that overexpressing the *AtVIT1* in cassava altered the partitioning of iron between source and sink tissues.

In rice, OsVIT1 and OsVIT2 function as vacuolar transporters that mediate transport of iron, zinc and manganese (Zhang et al., 2012). OsVIT1 and OsVIT2 both localize to the vacuolar membrane and are highly expressed in flag leaf blade and sheath, respectively (Zhang et al., 2012). *OsVIT1* is constitutively expressed while *OsVIT2* is highly responsive to iron treatments. It was also reported that the *OsVIT2* expression increased in early grain filling stage (3-10 DAF) and decreased in late grain filling stage (14-28 DAF) in embryo, ovary and endosperm, while its expression did not change during pistil development (Zhang et al., 2012). These results supported that OsVIT2 plays a critical role in transporting iron and zinc from leaves to seeds. Functional disruption of *OsVIT1* and *OsVIT2* led to increased iron and zinc accumulation in rice seeds and a corresponding decrease of iron in the source organ flag leaves (Zhang et al., 2012).

In this study, we combined the expression of *AtNAS1* and *PvFER* under the control of a constitutive promoter and an endosperm specific promoter, respectively, into single construct and transformed into the *osvit2* mutants with high endosperm iron. We also evaluated the performance of transgenic plants when grown on different external iron supplies. Our results showed a significant increase of iron content in polished and unpolished grains of transgenic plants (NFvit2 lines) as compared to the *osvit2* mutants and DJ plants, and the transformed plants also showed better growth in low iron conditions.

4.3 Results

4.3.1 Transgene expression in the leaf, embryo and endosperm of NFvit2 lines

Fifteen single transgene insertion lines were selected using southern hybridization in T0 generation and subsequently grown for next generation in the green house (Supplementary figure 1C). Five out of 15 single insertion lines with highest iron increases in T2 seeds were grown to T3 generation (Supplementary figure 1D). The selected transgenic lines were analyzed for transgene expression in embryo, endosperm

and leaves using qRT-PCR (Figure 1). All NFvit2 lines showed *AtNAS1* expression in leaves, embryo and endosperm (Figure 1A). *PvFER* was specifically expressed in the endosperm of NFvit2 transgenic plants and its expression was not detected in the embryo and leaves (Figure 1B). The expression of *OsVIT2* was also analyzed and no expression was detected in NFvit2 transgenic plants as well as *osvit2* mutants, while a moderate expression was detected in the DJ control plants (Figure 1C). The expression of *OsVIT1* did not show significant difference in the NFvit2 plants as compared to the *osvit2* mutants or DJ plants (Figure 1D).

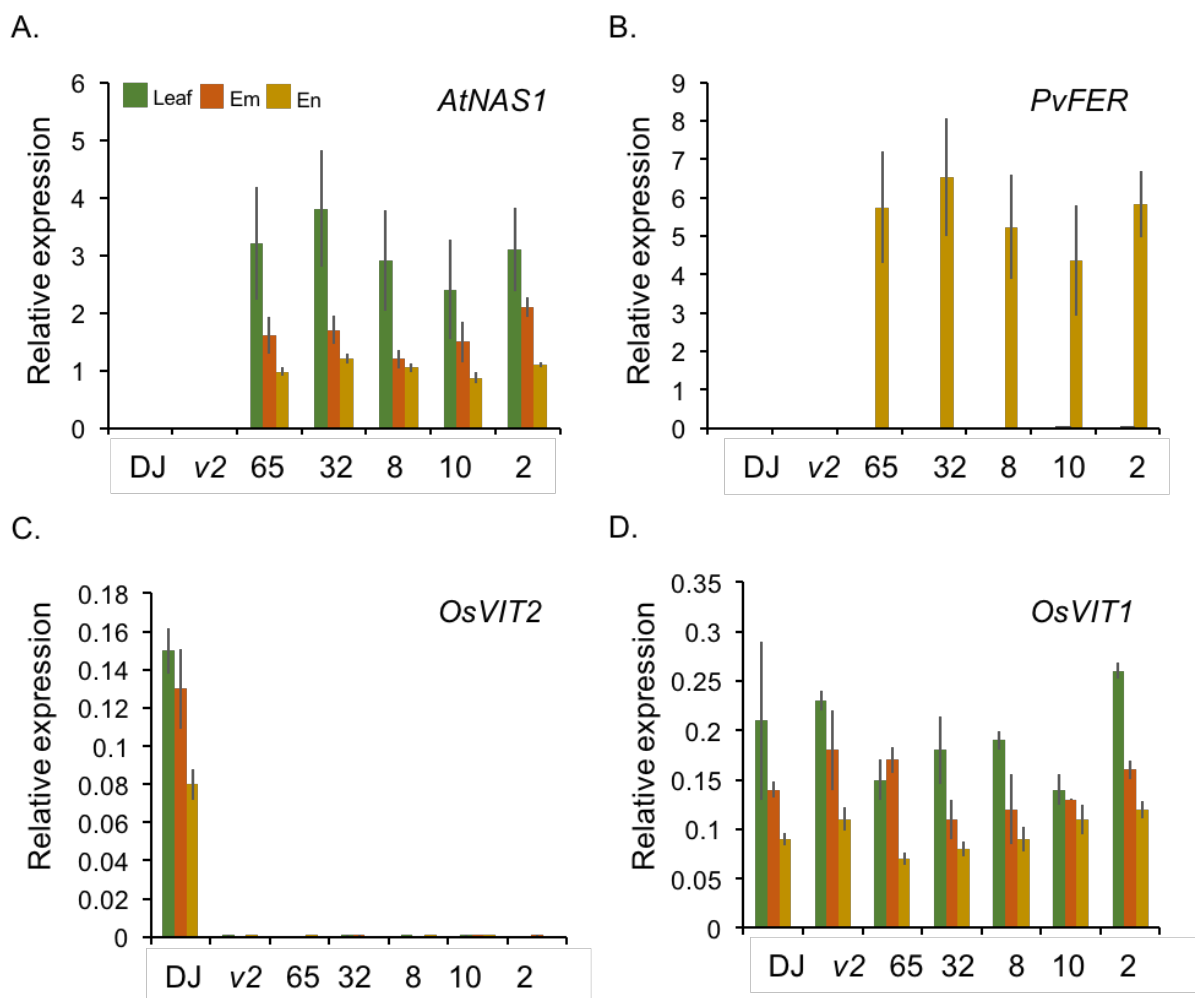


Figure 1 Transgene expression in seedlings, embryo, and endosperm. qRT-PCR results for expression of A. *AtNAS1*, B. *PvFER*, C. *OsVIT2* and D. *OsVIT1* in cultivar Dongjin (DJ), *osvit2* mutants (v2) and independent transgenic NFvit2 lines. Number of seedlings processed per sample =10; Number of embryos and endosperm processed per sample=30.

4.3.2 Metal profiles in the grains of NFvit2, *osvit2* and DJ plants

Iron concentration was significantly increased in the T3 polished seeds of all the evaluated transgenic plants, ranging between 5.2 and 8.3 $\mu\text{g/g DW}$, as compared to 1.5 $\mu\text{g/g DW}$ in DJ plants and 2.8 $\mu\text{g/g DW}$ in *osvit2* mutants (Figure 2A). The iron concentration in the unpolished grains ranged from 20.4 to 30.3 $\mu\text{g/g DW}$ in the transgenic plants as compared to 16.3 $\mu\text{g/g DW}$ in cultivar DJ and 22.4 $\mu\text{g/g DW}$ in *osvit2* mutants, respectively (Figure 2A). The *osvit2* mutants have 1.4-fold higher zinc concentration in the polished grains (29.8 $\mu\text{g/g DW}$) as compared to the DJ plants (21.3 $\mu\text{g/g DW}$) (Figure 2B). The zinc concentration was further increased in the polished grains of NFvit2 transgenic plants, ranging between 31.3 and 40.4 $\mu\text{g/g DW}$ (Figure 2B). Similarly, the zinc concentration in the unpolished grains of *osvit2* mutants (40.1 $\mu\text{g/g DW}$) was 1.3-fold higher than that in DJ plants (30.3 $\mu\text{g/g DW}$), and the zinc concentration in the NFvit2 lines further increased to 42.3-45.8 $\mu\text{g/g DW}$ (Figure 2B). Except in one line, the copper and manganese concentration did not show significant difference in the polished and unpolished grains of NFvit2 transgenic plants in comparison to the *osvit2* mutants (Figure 2C and 2D). Phenotypic performance of the NFvit2 lines was similar to that of *osvit2* mutants and DJ plants with regard to days to flowering (DTF), 1000 grain weight (1000GW), and grain filling rate, while some variation was observed in case of plant height and tiller number (Table 1).

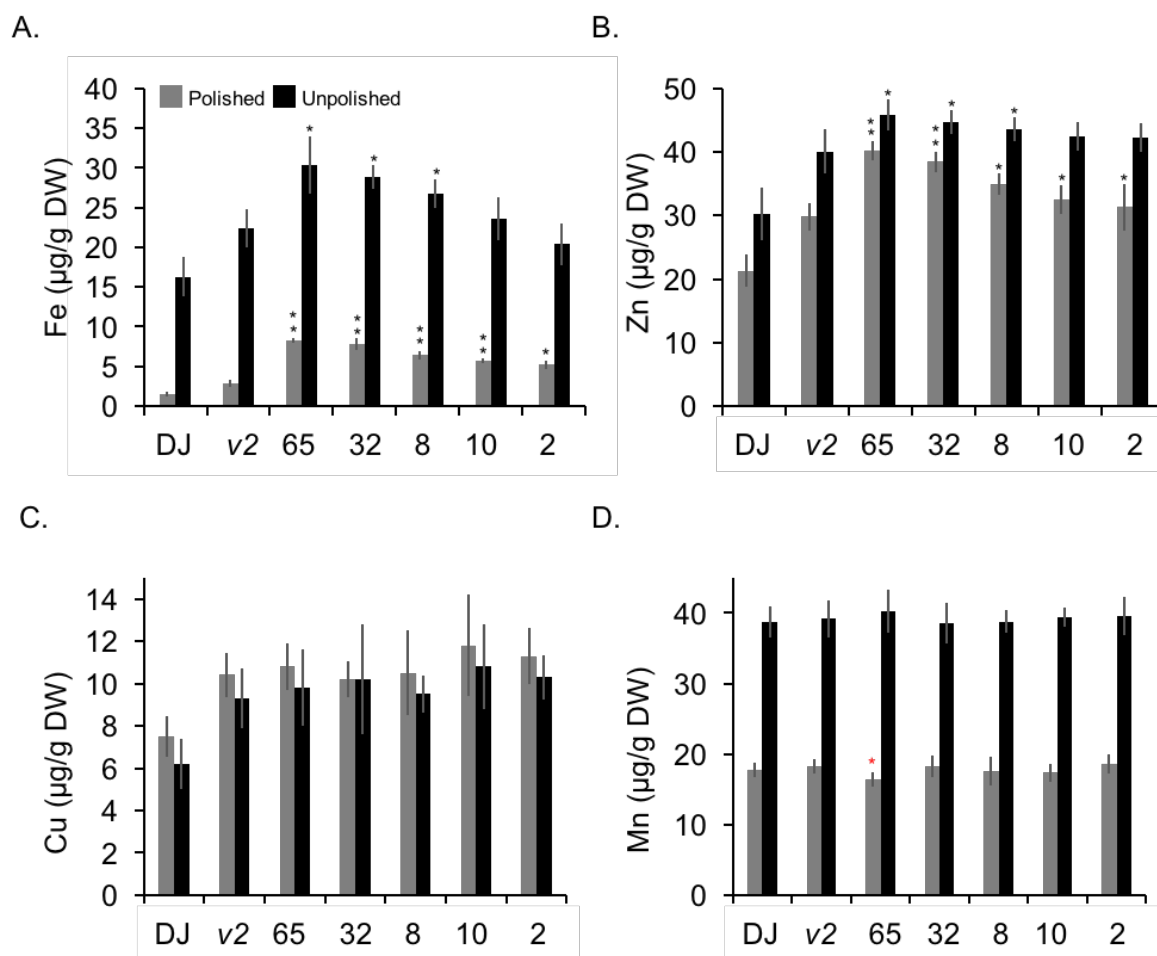


Figure 2 Metal concentration in the polished and unpolished T3 grains. Concentration of A. Fe, B. Zn, C. Cu and D. Mn in polished and unpolished grains. Values are the average of three biological replicates. DJ, cultivar Dongjin; v2, *osvit2* mutants, numbers indicate independent transgenic lines. Black and red asterisks indicate statistically significantly higher and lower values calculated using Student's T-Test as compared to *osvit2* mutants (*p<0.05, **p<0.01).

Table 1 Phenotypic assessment of selected transgenic lines in T2 generation under greenhouse condition. Observation parameters including days to flowering (DTF), plant height, tiller number, grain filling rate and one thousand grain weight (1000grain weight) are presented. Values are the average of three individual plants. Black and red asterisks indicate statistically significantly higher and lower values as compared to *osvit2* mutants (*v2*), respectively.

Plant line	Height (cm)	Tiller No.	DTF	1000GrainWeight (g)	Grain filling rate (%)
DJ	57.67 (±1.08)	9.67 (±1.00)	80.45 (±1.53)	23.45 (±0.45)	82.5 (± 0.98)
<i>v2</i>	58.67 (±1.53)	10.33 (±0.58)	81.67 (±1.00)	24.33 (±0.29)	85.15 (±2.14)
NFvit2					
65	62.33 (±0.58)*	9.33 (±2.08)	79.33 (±1.53)	22.67 (±0.58)	81.73 (±2.21)
32	52.67 (±2.08)*	10.67 (±1.00)	81.33 (±2.08)	23.58 (±0.29)	82.58 (±1.05)
8	58.45 (±1.53)	5.33 (±1.53)*	81.67 (±0.58)	24.67 (±1.00)	83.45 (±1.04)
10	59.67 (±1.00)	7.67 (±1.00)	82.15 (±1.53)	22.45 (±0.29)	85.33 (±0.96)
2	65.33 (±1.08)*	3.67 (±2.08)*	80.67 (±1.00)	21.67 (±1.04)*	80.33 (±1.25)

4.3.3 Distribution of iron and zinc in shoots and roots of NFvit2, *osvit2* and DJ plants

The iron concentration in the shoots of tested NFvit2 lines was comparable to DJ plants and *osvit2* mutants under iron sufficient condition, whereas significant iron increases were observed in the NFvit2 lines under iron deficient condition, with up to 1.9-fold increase in the line NFvit2-8 (Figure 3A). Likewise, the iron concentration in the roots of the NFvit2 lines was comparable to the *osvit2* mutants and DJ plants under iron sufficient condition (Figure 3A). However, when grown under iron deficient condition, a significant decrease in root iron was observed in four of the five NFvit2 lines as compared to the *osvit2* mutants, i.e. NFvit2-65, -32, -8, and -10 (Figure 3B). With few exceptions, the zinc concentration in the shoot and roots of NFvit2 lines did not differ significantly from the *osvit2* mutants and DJ plants under iron sufficient condition (Figure 3B). Whereas the zinc concentration in the shoots and roots was significantly higher in three of the NFvit2 lines (NFvit2-65, -32, and -8) as compared to the *osvit2* mutants under iron deficient condition (Figure 3B).

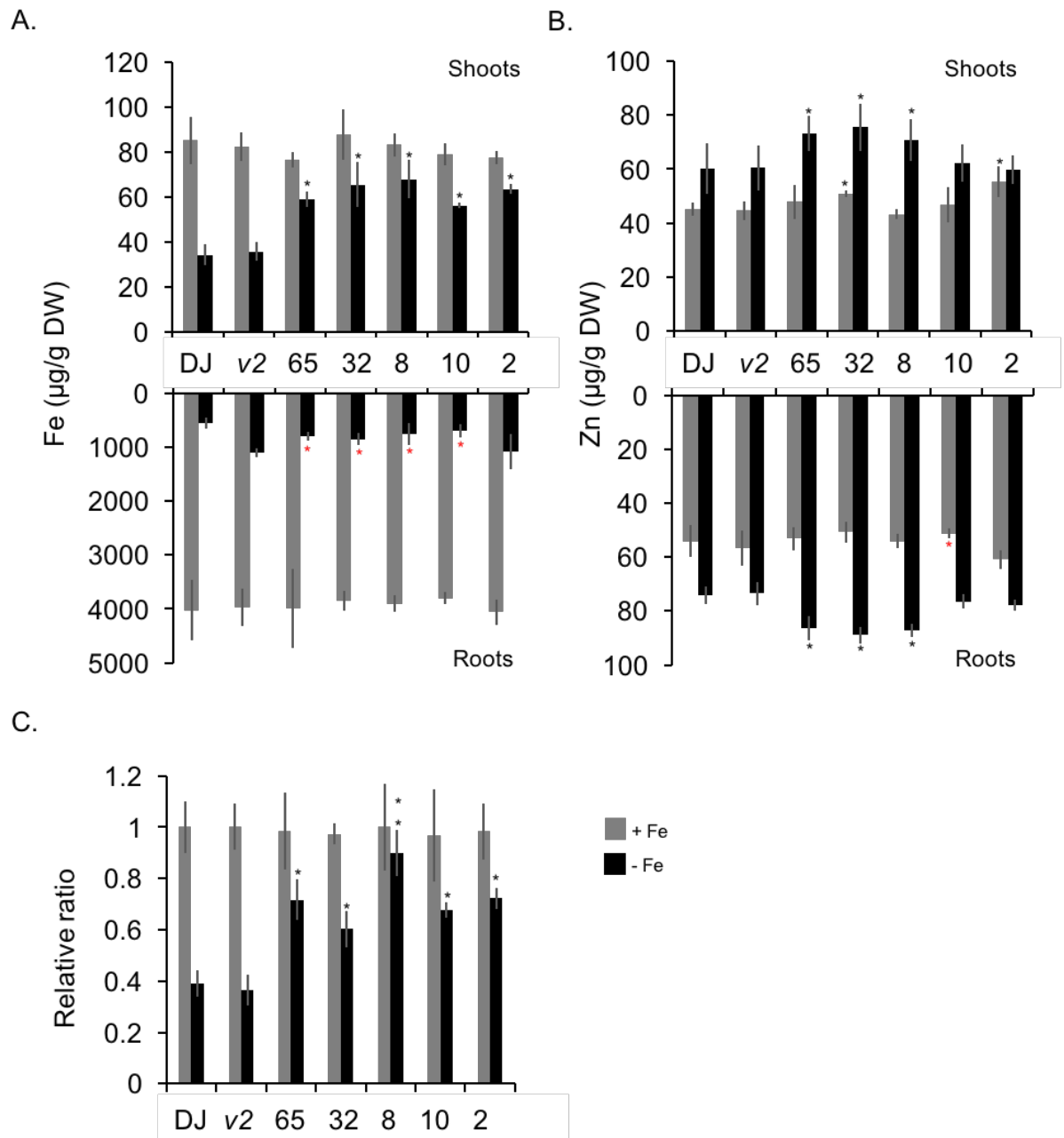


Figure 3 Characterization of selected transgenic lines under iron sufficient and deficient growth condition. A. Iron and B. Zinc concentration in shoots and roots of 28d-old seedlings in iron sufficient and deficient condition. C. Relative chlorophyll content compared between iron sufficient and deficient condition. DJ, cultivar Dongjin; v2, *osvit2* mutants, numbers indicate independent transgenic lines. Samples were collected from 20 plants corresponding to each independent line and Student's T-Test was used for statistical calculation. Black and red asterisks indicate statistically significantly higher and lower values as compared to *osvit2* mutants (*p<0.05, **p<0.01).

4.3.4 Chlorophyll content and endogenous gene expression in NFvit2, *osvit2* and DJ plants

Chlorophyll content was compared between selected NFvit2 lines, *osvit2* mutants and DJ control plants when grown under iron deficient and sufficient conditions (Figure 3C). The chlorophyll content did not show significant difference between NFvit2, *osvit2* and DJ plants under iron sufficient condition (Figure 3C). In iron deficient condition, however, *osvit2* mutants and DJ plants exhibited significantly less chlorophyll content as compared to NFvit2 selected lines (Figure 3C). The NFvit2 lines showed 72-90% of chlorophyll content under iron deficient condition compared to that under iron sufficient condition, whereas *osvit2* mutants and DJ plants showed only 38-42% of chlorophyll content under iron deficient condition compared to that under iron sufficient condition. These results suggest that overexpression of *AtNAS1* in transgenic plants conferred higher tolerance to low iron condition.

Additionally, the expression of seven endogenous iron homeostasis related genes was compared between NFvit2 lines, *osvit2* mutants and DJ control plants when grown under iron deficient and sufficient conditions. Corresponding to previous report on *osvit2* mutants (Zhang et al., 2012), the expression of iron uptake, translocation and transport related genes including *OsIRT1*, *OsNAS1*, *OsNAS3*, *OsNAAT1*, *OsYSL15*, *OsYSL2* and *OsVIT1* did not alter in *osvit2* mutants compared to DJ plants under either iron sufficient or deficient conditions (Figure 4). The expression of these genes in the NFvit2 lines was comparable to *osvit2* mutants and DJ plants under iron sufficient condition (Figure 4). In contrast, the expression of these selected genes was significantly higher in NFvit2 transgenic plants in comparison to *osvit2* mutants and DJ plants under iron deficient condition (Figure 4).

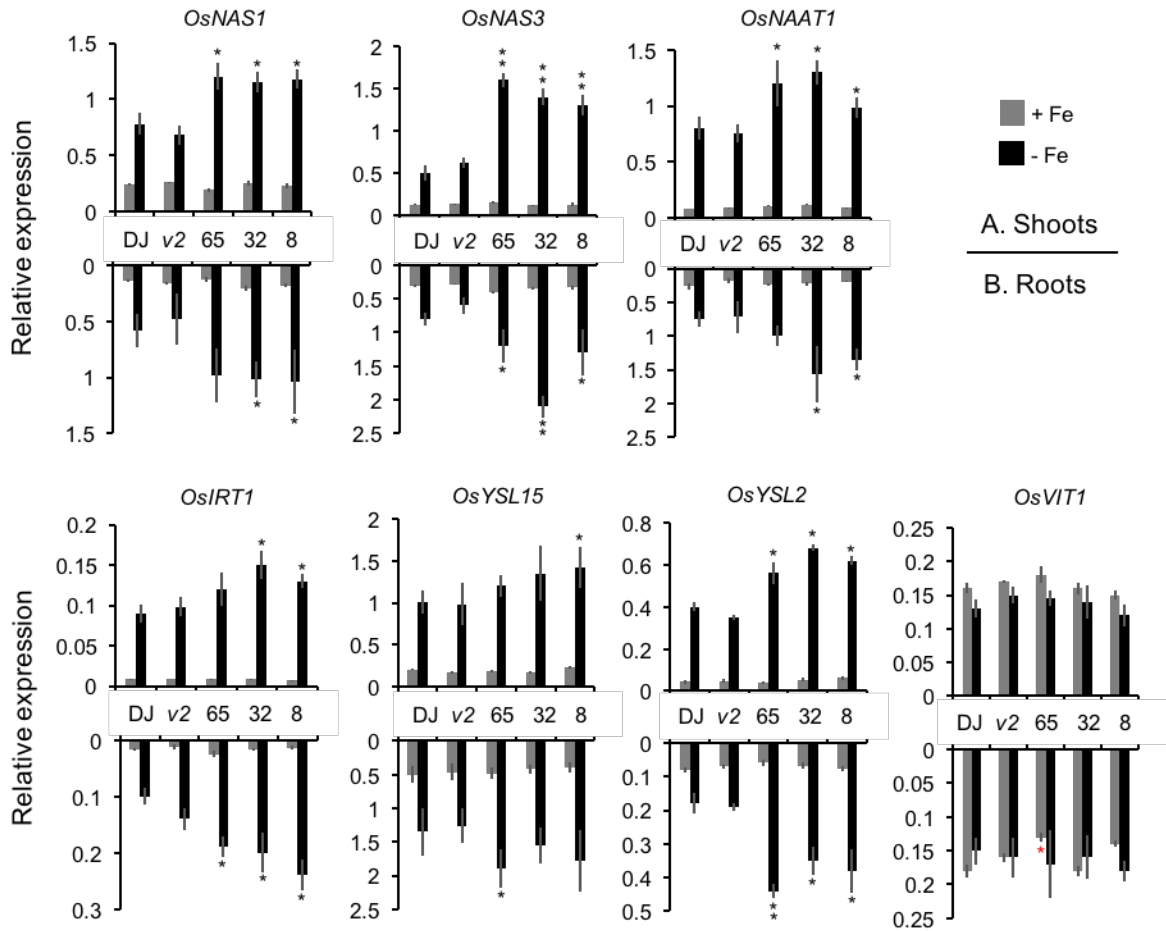


Figure 4 Expression of iron homeostasis related genes in shoots and roots under iron sufficient and deficient growth condition. Expression of selected genes was detected by qRT-PCR in A. shoots and B. roots of transgenic plants, *osvit2* mutants (*v2*) and cultivar Dongjin (DJ). Samples were collected from 20 plants corresponding to each independent lines and Student's T-Test was used for statistical calculation. Black and red asterisks indicate statistically significantly higher and lower values as compared to *osvit2* mutants (* $p < 0.05$, ** $p < 0.01$). The expression was normalized to the expression of rice *UBIQUITIN 5* (*OsUBQ5*) gene.

4.4 Discussion

Rice is the second largest produced cereal in the world and the most important grain with regard to human nutrition providing one fifth of the calories consumed worldwide. However, rice is a poor source of micronutrients. Polished grains of mega rice varieties provide only around 2 $\mu\text{g/g}$ DW of iron and conventional breeding has not been successful in improving the endosperm iron content in rice due to limited variability for endosperm iron concentration in the rice germplasm (Meng et al., 2005; Bouis et al., 2011). Therefore, various genetic engineering strategies have been tested to increase iron concentration in the rice polished grains. In this work, we explored the potential of further increasing the endosperm iron levels in *osvit2* rice mutants by transforming with

AtNAS1 and *PvFER*. The NFvit2 transgenic plants had up to 3.0-fold iron increase in the polished grains, with the highest line containing 8.3 µg/g DW iron as compared to the *osvit2* mutants. The zinc concentration was also elevated up to 1.4-fold in the polished grains of transgenic plants in comparison to the *osvit2* plants. The higher iron and zinc concentration in the *osvit2* grains as compared to the DJ control are in agreement with the previous reports on *osvit2* lines (Zhang et al., 2012; Bashir et al., 2013). The study by Zhang et al., 2012 highlighted the role of *OsVIT2* in mediating metal allocation between source and sink organs (Zhang et al., 2012). Therefore, it is conceivable that transforming the *osvit2* lines with *AtNAS1* and *PvFER* could further elevate the endosperm iron and zinc levels. Iron needs to be effectively transported from the roots to the shoots via xylem, and then between cells, particularly under iron deficient condition. The principal chelators known to bind iron include citrate, NA and DMA (Aoyama et al., 2009; Kakei et al., 2012). DMA functions to acquire iron from the rhizosphere and to chelate iron in both xylem and phloem (Aoyama et al., 2009). High concentrations of DMA have been detected in phloem sap indicating its role in long distance iron transport (Aoyama et al., 2009). Likewise, NA is biosynthesized by *OsNAS1*, *OsNAS2* and *OsNAS3* in rice and functions to facilitate iron translocation within the plants (Inoue et al., 2003). Several YSL family members are involved in transporting these iron complexes. Among them, OsYSL15 could transport Fe(III)-DMA complexes and is involved in internal iron translocation, while OsYSL2 could transport Fe(II)-NA complexes but not Fe(III)-DMA (Koike et al., 2004; Inoue et al., 2009). The overexpression of *NAS* facilitates the production of NA and DMA, and eventually increases the uptake and transport of PS-Fe(III) and as well as zinc. The overexpression of *NAS* in rice has also been previously reported to induce the expression of zinc transporter encoding genes, including *OsZIP1*, *OsZIP3*, *OsZIP4* and *OsNAS3*, which could explain the higher zinc concentration in the transgenic plants (Wang et al., 2013b).

The iron and zinc concentrations in the shoots of *osvit2* mutants were reported to be significantly lower than that of DJ plants by Bashir et al., 2013, while these metal concentrations in *osvit2* plants were comparable to DJ plants in the study by Zhang et al., 2012 under iron sufficient condition (Zhang et al., 2012; Bashir et al., 2013). Our data showed that the iron and zinc concentrations were similar between the shoots of *osvit2* mutants and DJ plants under iron sufficient condition. It is likely that the plant materials

from different age and growth conditions resulted in the disagreement of results in these three studies. On the contrary, the iron and zinc concentration in the roots of *osvit2* and DJ plants were quite comparable between these three studies. Corresponding with the increased iron and zinc concentration in the shoots of NFvit2 lines under iron deficiency, the NFvit2 lines also showed higher chlorophyll content as compared to *osvit2* mutants and DJ plants. Transgenic tobacco plants overexpressing *AtNAS1* accumulated more iron, zinc and other metals in the leaves under iron deficiency and exhibited increased tolerance to iron deficient growth condition (Douchkov et al., 2005). Similarly, NFP rice (transgenic plants overexpressing *AtNAS1* and *PvFER*) produced more NA and DMA under iron deficient condition (Wirth et al., 2009). It is expected that *NAS* overexpression in NFvit2 transgenic plants also enhanced the production of NA and DMA, and thus, increased the accumulation of iron and zinc in shoots when plants experienced iron deficiency. This observation is further supported by the induced expression of iron homeostasis related genes in NFvit2 plants when grown on iron deficient condition. The expression of these genes showed no obvious change in *osvit2* mutants and DJ plants. Similar observation has also been previously reported for NFP rice where the expression level of *OsNAS1*, *OsNAS3*, and *OsDMAS1* was higher in roots and shoots as compared to the non-transgenic sibling (NTS) control under iron deficient condition (Wang et al., 2013b). These findings also support the higher chlorophyll content in NFvit2 plants under iron deficiency as compared to the *osvit2* and DJ plants.

In summary, our work showed that a targeted expression of the proteins required for iron uptake, transport (NAS) and storage (FER), and disrupted expression of transporter required for iron transportation into vacuole (VIT2) could together lead to increased iron and zinc concentration in the polished rice grains. However, given the over-accumulation of cadmium in grains of *osvit2* mutant grown in polluted paddy soil (Zhang et al., 2012) and over-accumulation of heavy metals in some of the NAS expressing transgenic plants (Antosiewicz et al., 2014), further evaluation of *NFvit2* plants would yield valuable information.

4.5 Material and Methods

4.5.1 DNA construct, rice transformation and plant growth conditions

pCAMBIA-1300PMI-NASFER vector was transferred into *osvit2* mutants, i.e., into the *OsVIT2* T-DNA knock out lines in *Oryza sativa ssp. Japonica cv. Dongjin* (DJ) background (Jeong et al., 2006), using *Agrobacterium tumefaciens* strain EHA105 (Hood et al., 1993). Transformation, selection and regeneration were conducted according to a previously reported protocol (Nishimura et al., 2006). Putative transformants were first screened for the presence of *AtNAS1*, and *PvFER* by PCR. Southern blot hybridization by digoxigenin (DIG) labeling was conducted on *PmlI* digested genomic DNA of the transgenic lines to select the lines with a single copy transgene insertion. *PMI* fragment amplified by PCR was used as a probe to detect the transgene construct. All of the primer sequences used in cloning, sequencing verification and PCR are provided in Supplementary table 1. Selected transgenic plants together with *osvit2* mutants and DJ plants were grown on commercial soil (Klasmann-Deilmann GmbH, Germany) under greenhouse conditions i.e., 80% humidity/30°C/12h light and 60% humidity/22°C/12h dark. Quantification of divalent metals and transgene expression was conducted on plants in the T2 and T3 generations. Seeds of *osvit2* mutants and DJ plants were generously provided by Prof. Jiming Gong from Chinese Academy of Sciences (China) and by International Rice Research Institute (Philippines), respectively.

4.5.2 Iron deficiency treatment in hydroponic culture

Seeds of transgenic plants, *osvit2* mutant and *cv. DJ* were germinated *in vitro* for 5 days on moist filter paper in the petri dishes and subsequently transferred into boxes containing 400 mL hydroponic solutions for 7 days. For iron deficient condition, plants were continuously grown in hydroponic solutions containing 10 μ M Fe(III)-EDTA for 14 days, while plants grown in hydroponic solutions containing 100 μ M Fe(III)-EDTA served as a control condition with sufficient iron supply. Solutions for hydroponic system were prepared according to the protocols, using 0.70 mM K₂SO₄, 0.10 mM KCl, 0.10 mM KH₂PO₄, 2.0 mM Ca(NO₃)₂, 0.50 mM MgSO₄, 10 μ M H₃BO₃, 0.50 μ M MnSO₄, 0.20 μ M CuSO₄, 0.01 μ M (NH₄)₆Mo₇O₂₄, and 0.5 μ M ZnSO₄, with different iron concentrations added as Fe(III)-EDTA according to the treatment (normal condition: 100 μ M; iron-deficient condition: 10 μ M). Solutions were changed every one to two days to avoid any precipitation and contamination. All plants were maintained in growth chamber with 60% humidity and 16h/ 8h light/ dark cycle.

4.5.3 Metal ion measurements

Grain samples were de-husked to obtain unpolished brown grains. In order to obtain polished grains, the de-husked grains were processed with a grain polisher (Kett grain polisher ‘Pearlest’, Kett Electric Laboratory, Tokyo, Japan) for 1 min. Shoot and root samples from hydroponic culture were dried at 60°C for 3 to 5 days. 200mg of each ground grain sample were boiled in 15 ml of 65% v/v HNO₃ solution at 120°C for 90 min. Three ml of 30% v/v H₂O₂ was subsequently added, and boiling was continued at 120°C for another 90 min. Metal concentrations were determined using inductively coupled plasma-optical emission spectroscopy (ICP-OES) (Varian Vista-MPX CCD Simultaneous ICP-OES). The wavelength used for iron, zinc, manganese and copper were 238.204, 213.857, 257.610, and 324.754, respectively. The National Institute of Standards and Technology (NIST) rice flour standard 1658a was treated and analyzed in the same manner and used as internal control for every measurement. Data were analyzed using Student’s T-Test. The criteria of $p < 0.05$ and $p < 0.01$ was used to determine statistically significant differences among the tested lines and the control.

4.5.4 RNA Extraction, cDNA synthesis and Quantitative real-time PCR

Total RNA was extracted from roots and shoots of 5-day-old seedlings in T3 generation using Trizol[®] reagent (Invitrogen, USA). To obtain total endosperm and embryo RNA, endosperm and embryo were separated from rice grains at 16 DAF. Extraction buffer containing 0.15M NaCl and 1% sarcosyl was added into the ground samples followed by purification with 8M guanidine hydrochloride buffer. The RNA was treated with DNase I (Thermo Fisher Scientific Inc., USA) to remove genomic DNA contamination. First-strand cDNA was synthesized by RevertAid[™] first strand cDNA synthesis kit (Thermo Fisher Scientific Inc., USA). Quantitative RT-PCR was performed as previously described (Liu et al., 2011). In brief, qRT-PCR was performed in a 7500 Real-Time PCR System using the SYBR Green RT-PCR reagent kit following the manufacturer’s protocol (Applied Biosystems, Carlsbad, CA, USA). Each reaction was run in triplicates in a volume of 20 mL with an initial denaturation step at 95 °C for 10 min, followed by 40 cycles of 95 °C for 15 s and 60 °C for 60 s. Data were analyzed according to the manufacturer’s instructions using the 7500 System SDS Software v1.4 (Applied Biosystems). The expression level of genes of interest was normalized to the expression of rice *UBIQUITIN 5 (OsUBQ5)* or rice *ACTIN 1 (OsACT1)* genes.

4.5.5 Chlorophyll extraction and measurement

Leaf number third were collected from DJ, *ostiv2* and NFvit2 plants grown in iron sufficient and deficient condition for 10 days. Pigment extraction was performed as previously described (Hu et al., 2013). In brief, around 20 mg of leaves from each sample were harvested and were frozen in liquid nitrogen for further pigment extraction. Pigments were extracted by immersing ground leaves in 1 mL of ice cooled organic solvent (80% Acetone and 20% 0.2 M Tris-HCl, pH=8) and incubated at 4°C for 24 hr in the dark. The microtubes containing the homogenized samples were centrifuged at full speed for 5 min at 4°C. The resulting supernatant was analyzed by spectrometer in optical density at 663 nm.

4.6 Conflict of interest

The authors declare that they have no conflict of interest.

4.7 Author contributions

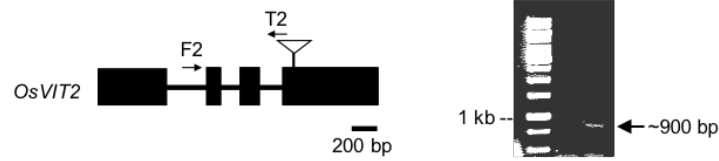
NKB conceived the study, NKB and TYW designed the experiments, TYW performed the experiments, TYW, WG and NKB interpreted the data, TYW and NKB wrote the manuscript, and WG and NKB edited the manuscript. All authors have read and approved the final manuscript.

4.8 Acknowledgements

We gratefully acknowledge the support by Mrs. Jacqueline Imhof and the ETH research grants for this work to WG and NKB. We thank Prof. Rainer Schulin for providing access to ICP-OES and Björn Studer for the kind assistance with metal measurements. We thank Irene Zurkirchen for the technical support in the greenhouse. We thank Prof. Jiming Gong from Chinese Academy of Sciences, China for providing us the seeds for *osvit2* mutant line and the International Rice Research Institute, Philippines for providing us the seeds of cultivar Dongjin.

4.9 Supplementary data

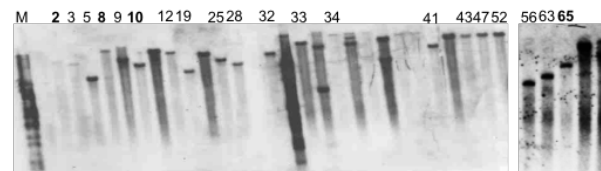
A.



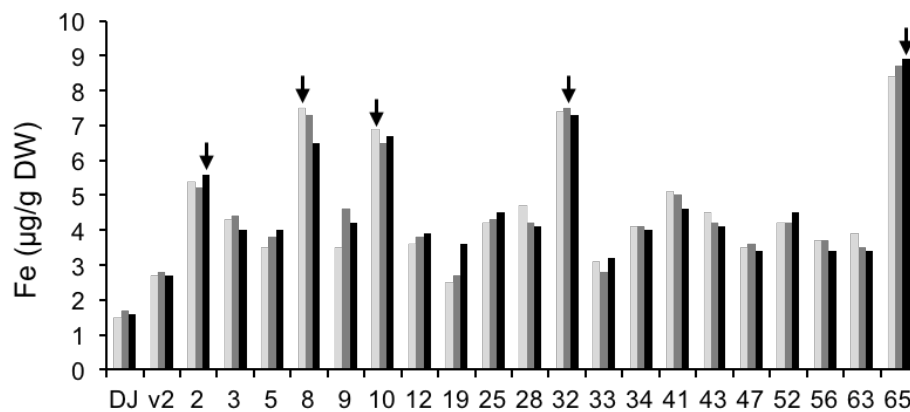
B.



C.



D.



Supplementary figure 1. Confirmation of *osvit2* mutants, schematic representation of the transformation vector, characterization of transgenic lines in T0 generation using southern blotting and iron concentration in T2 polished grains A. Genotyping of *osvit2* mutants using specific primers on T-DNA site. B. Transformation construct. LB, T-DNA left border; RB, T-DNA right border; t35S, cauliflower mosaic virus (CaMV) 35S terminator; *PMI*, *PHOSPHOMANNOSE ISOMERASE* gene; *p35S*, *CaMV35S* promoter; *AtNAS1*, Arabidopsis *NICOTIANAMINE SYNTHASE 1* gene; *tNOS*, *NOPALINE SYNTHASE* terminator; *pGlb*, rice *GLOBULIN-1* promoter; *PvFER*, *Phaseolus vulgaris FRRITIN* gene C. Southern hybridization analysis using *PMI* as a probe. Numbers indicate independent transformed lines with potential single insertion of transgene. D. Iron concentration in all single insertion lines. Values are the average of two technical replicates. The bars for each line represent three individual plants. Arrows indicate selected plants from each line for further analysis in T3 generation.

Supplementary table 1 Primer sequences used for sequence validation, cloning and qRT-PCR analysis in this study

Primer Name	Direction	Primer sequence (5'-3')	Purpose
F2	F	actaca agcacgcagcaaac	genotyping
T2	R	cgfegtgaatggcatcgtttgaa	genotyping
PvFer	F	gtcttcgtttatattgctcttg	PCR/ sequencing
Ubi	R	gtaaatcccaaatccaattacc	PCR/ sequencing
35S	F	cagttcatacagagtctcttacg	PCR/ sequencing
AtNAS1	F	gacgtggttaactcgggtgtgatc	PCR/ sequencing
Pmi	F	gtaactgctgagaaccttccac	PCR/ sequencing
Glb	F	gccccaccatttttaattcattc	PCR/ sequencing
PMI	F	ctggctaattgggtgtttct	PCR/ southern probe
	R	cgtgatgtgattgagagt	
qAtNAS1	F	gcacttggagaaacacatgg	qRT-PCR
	R	tctgagagcatgagcactcc	
qPvFER	F	ggggatacgggaaaacgtaa	qRT-PCR
	R	gagcctggctaaccgcat	
OsIRT1	F	ctcagatagggatcgtggt	qRT-PCR
	R	gaacatctggtggaagcaca	
OsYSL2	F	gggctccttaacttcttcc	qRT-PCR
	R	gagggtatggaatccgttt	
OsNAAT1	F	tggagggaatccatgatga	qRT-PCR
	R	cttcattcccagcactcc	
OsNAS1	F	cggttgagaaggcagaagagt	qRT-PCR
	R	cgatcgtccggctgtag	
OsNAS3	F	gtgatcaactccgtcatc	qRT-PCR
	R	tcagt ctcatcatgggaaaaa	
OsYSL15	F	actggtac cctgcaaacatac	qRT-PCR
	R	gcaatgatgcttagcaagaag	
OsVIT1	F	tcctcaagcttgctcgaacttcat	qRT-PCR
	R	atggcgt tctgtgctgtggagata	
OsVIT2	F	ggctgcaggcatcc aagtaaatgt	qRT-PCR
	R	cactacaagcacgcagcaaacg ta	
OsACT1	F	tggaaagctgcgggtatccat	qRT-PCR
	R	tactcagccttgcaatccaca	
OsUBQ5	F	accactcgaccgccactact	qRT-PCR
	R	acgcctaagcctgctggtt	

5. Genome wide analysis of the transcriptional profiles in different regions of the developing rice grains

Ting-Ying Wu, Marlen Müller, Wilhelm GUISSEM and Navreet K. Bhullar*
Plant Biotechnology, Department of Biology, ETH Zurich (Swiss Federal Institute of Technology), Zurich, Switzerland

***Correspondence**

Dr. Navreet K. Bhullar
Plant Biotechnology,
Department of Biology
ETH Zurich (Swiss Federal Institute of Technology)
Universitaetsstrasse 2
8092 Zurich, Switzerland
bhullarn@ethz.ch

5.1 Abstract

Rice is an important food source for humans worldwide. Due to the nutritional and agricultural significance of rice grain, a number of studies addressed various aspects of grain development and grain filling. Nevertheless, the molecular processes underlying grain filling are not yet completely revealed. We profiled gene activity genome-wide in cross cells (CC), nucellar epidermis (NE), ovular vascular trace (OVT), endosperm (EN) and aleurone layer (AL) dissected using laser captured microdissection (LCM) at three distinct grain development stages. The obtained mRNA datasets offer comprehensive description of gene expression with high spatio-temporal regulation. Comparison between different tissues reveals their similar and unique functions, respectively. The expression patterns of hormone and transporter encoding genes signify an important role of OVT in nutrient transportation during grain development. Gene co-expression network prediction on OVT specific genes identified several distinct and common development specific transcription factors. Further analysis of enriched DNA sequence motifs upstream of OVT specific genes identified known and novel motifs relevant to grain development. Taken together, the obtained data is a useful resource for better understanding of the molecular processes involved in rice grain development.

5.2 Introduction

Rice (*Oryza sativa* L.) is the second most consumed staple crop worldwide, with nearly 3.5 billion people depending on rice as a staple food. Dependency on rice is extensive in the Asian countries, where rice provides nearly 20% of the daily caloric intake (Colman, 2004). These facts make rice grain an important model to understand the regulatory networks and molecular processes controlling grain development and grain filling.

Seed development in monocots varies significantly from that in dicots. The rice grains have been anatomically characterized to comprise distinct tissues, namely embryo, endosperm, nucellar epidermis, cross-cells, ovular vascular trace and aleurone layer (Krishnan and Dayanandan, 2003). Endosperm (EN) comprises the major storage tissue for starch, and contributes to the nourishment of the developing embryo. Nucellar Epidermis (NE), which differentiates from maternal tissues at around five days after flowering (DAF), is known to support the endosperm development. Aleurone layer (AL) differentiates from the endosperm at about 8-10 DAF and is characterized to be richer in nutrients as compared to the endosperm. Cross-Cells (CC) generate and transport photosynthates into the endosperm and could be well differentiated from other tissues because of their distinct green color. Ovular Vascular Trace (OVT) facilitates transfer of nutrients to the endosperm and to the developing embryo. The anatomical studies during the past have provided a detailed overview of rice grain morphology during development (Krishnan and Dayanandan, 2003). More recently, studies have taken advantage of transcriptomic approaches to gain an insight of the molecular processes associated with the anatomical and physiological changes during rice seed development (Zhu et al., 2003; Xu et al., 2012b).

RNA sequencing (RNA-seq) is being widely utilized for studying the transcriptomic changes in response to stresses as well as to understand processes underlying plant development. To date, several studies reported transcriptomic analysis of seeds to identify important genes and regulators expressed at different developmental stages and/or in specific tissues. To date, most comprehensive study on spatiotemporal gene network during seed development was conducted in *Arabidopsis* (*Arabidopsis thaliana*) by using a combination of laser-capture microdissection (LCM) and microarray analysis (Le et al., 2010; Belmonte et al., 2013). Thirty-one sub-regions including embryo, suspensor,

micropylar, peripheral, chalazal and seed coat were isolated in preglobular, globular and heart stages, which represented different developmental and morphogenesis stages. This work identified chalazal as a unique sub-region that was highly enriched for seed-specific genes related to hormone biosynthesis and ubiquitin-dependent protein catabolism. In monocots, most of the studies focused on crop grains, including wheat, barley, maize and rice, and mostly studied one-two tissues at a time (Gillies et al., 2012; Thiel et al., 2012; Gao et al., 2013; Li et al., 2014). In wheat, the EN and AL sub-regions were compared at 06, 09, and 14 days post-anthesis by using RNA-seq (Gillies et al., 2012) to address the differences in gene expression and metabolic processes. The genes that preferentially expressed in EN were associated with carbohydrate storage, while the genes preferentially expressed in AL were related to lipid and protein metabolisms. The mapping of spatio-temporally expressed genes to the three homeologous genomes A, B, D revealed cell-type and stage dependent genome dominance (Pfeifer et al., 2014). Similarly, the studies on different sub-regions of maize (*Zea mays*) and barley (*Hordeum vulgare*) seeds have indicated complex and novel regulatory networks in various cell types (Krishnan and Dayanandan, 2003; Lu et al., 2013c; Li et al., 2014; Zhan et al., 2015). The genes up-regulated in the endosperm transfer cells (ETCs) and basal endosperm transfer layer (BETL) were related to hormone regulation, carbohydrate metabolisms and transport activities, highlighting their significant roles in endosperm development (Zhan et al., 2015). In rice seeds, embryo and endosperm regions are the ones among the most studied for gene expression patterns (Xu et al., 2012b; Xue et al., 2012; Gao et al., 2013). The expression patterns of hormone biosynthesis related genes and the complex transcription factor networks explained the morphological and physiological function of these sub-regions. Additionally, a distinct spatial and temporal expression patterns of genes involved in starch biosynthetic pathway have been identified in the endosperm (Zhu et al., 2003).

Despite the afore-mentioned studies, the gene activity and regulatory patterns in several crucial sub-regions of the rice grain are still under-explained. Therefore, we studied five sub-regions of rice grains including EN, CC, NE, OVT and AL at three different time points using a combination of LCM and RNA sequencing approaches. The RNA sequence analysis revealed the molecular mechanisms and regulatory patterns in these specific tissues, providing a comprehensive dataset serving as a foundation for further basic researches as well as in advanced biotechnological applications.

5.3 Results

5.3.1 Spatio- temporal resolution of mRNA profiles during rice grain development

Gene expression was studied in five sub-regions of the developing rice grains, including CC, NE, OVT, EN and AL collected at 4, 8 and 16 DAF. These time points were selected based on the literature information on differentiation of the main cell types (Krishnan and Dayanandan, 2003). NE is differentiated into a single layer cell at around 4 DAF, while the enlarged cells and thickenings of NE are noticed at 8 DAF (Krishnan and Dayanandan, 2003). CC are visible as greenish cell layer from 4 DAF to 16 DAF. OVT locates in the ventral side of the endosperm, in conjunction with NE (Krishnan and Dayanandan, 2003). EN cells are gradually developing and enlarging through 4 to 16 DAF, and the outer layer of EN cells differentiate into AL at about 16 DAF.

The RNA sequence reads were quality checked and over 20000 genes were assembled and detected as statistically significant (reads higher than 10, $p < 0.001$). The genes specific to each sub-region and grain development stages were compared by Hierarchical clustering and principal component analysis (PCA). The biological replicates from individual sub-regions clustered together and the PCA collectively identified 79% variance in our dataset (Figure 1, Supplementary Figure 1). The dataset was further analyzed to segregate tissue-specific and stage-specific genes. The genes with a preferentially higher expression level (with the highest number of reads, $p < 0.001$) in a particular sub-region or at a particular developmental time point were assigned to be tissue-specific and stage-specific differentially expressed genes (DEGs), respectively. In total, 10037 DEGs were identified. In order to further characterize the sub-region and stage specific genes, gene ontology (GO) analysis on DEGs by PlantGSEA (Yi et al., 2013) was conducted. Significantly overrepresented GO terms and metabolic pathways ($p < 0.01$) were chosen for further comparison. Additionally, a set of selected genes were also validated for expression by quantitative PCR (qPCR) (Supplementary Figure 2).

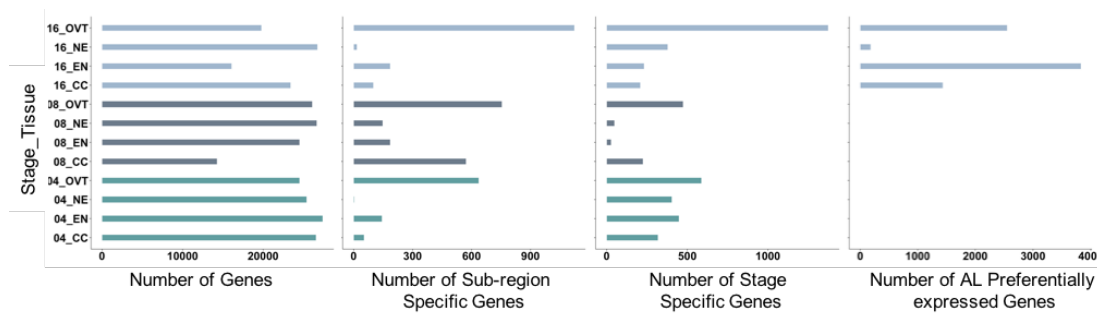


Figure 1. Differentially expressed genes in different sub-regions and developmental stages of the rice grains. Number of total counts detected in different sub-regions, number of RNAs preferentially expressed in a specific sub-region or time point are presented. NE: Nucellar Epidermis; CC: Cross Cells; OVT: Ovular Vascular Trace; EN: Endosperm; AL: Aleurone Layer.

Tissue-specific differentially expressed genes. In OVT, 635 and 753 DEGs were identified at 4 and 8 DAF, respectively. The most significantly enriched GO categories for these genes are iron binding, transporter, transcriptional activity, and phytohormone biosynthesis and signaling. Among the 1123 DEGs that were identified as OVT specific at 16 DAF, the over-represented GO categories included protein translation, ribosomal activity, protein folding and macromolecular metabolic process (Figure 2A, Supplementary Figure 3A and Supplementary Table 1). In the EN specific set of genes, 143, 186, and 185 DEGs were identified at 4, 8 and 16 DAF, respectively. The enriched GO terms for EN specific genes were associated with metabolism and providing energy, such as starch and glucose metabolism, glycolysis, transportation, and protein and lipid metabolism. The glycogen biosynthesis and microtubule-associated genes were also highly expressed at 4 and 8 DAF in EN, suggesting that endosperm cells are still enlarging and developing (Figure 2B and Supplementary Table 1). In case of NE, 1 DEG at 4 DAF, 147 DEGs at 8 DAF, and 16 DEGs at 16 DAF were identified. The enriched GO terms for the 8 DAF NE specific DEGs included transferase, metabolic activity, transcription, and coenzyme binding endorsing the role of NE to support EN development (Figure 2C). In line with the suggested role of CC, the overrepresented GO terms among the 53, 572, and 99 DEGs identified in CC at 4, 8 and 16 DAF, respectively, included photosynthesis, transporter activity, binding, catalytic activity, and metabolic processes (Figure 2D and Supplementary Table 1). Since AL was only collected at 16 DAF, we performed pairwise comparison on AL with CC, EN, NE, and OVT at 16 DAF, and 1438, 3829, 178, and 2550 DEGs were identified as differentially expressed, respectively. Genes associated with macromolecule metabolism, amino acid metabolism, secondary metabolism, and lipid metabolism as well as vitamin B biosynthesis and transport were expressed in AL. These data suggest an important role of AL in synthesis and transport of

nutrients during grain filling in rice. Additionally, some stress responsive genes were also identified among the AL specific DEGs (Figure 2E, Supplementary Figure 3B and Supplementary Table 2).

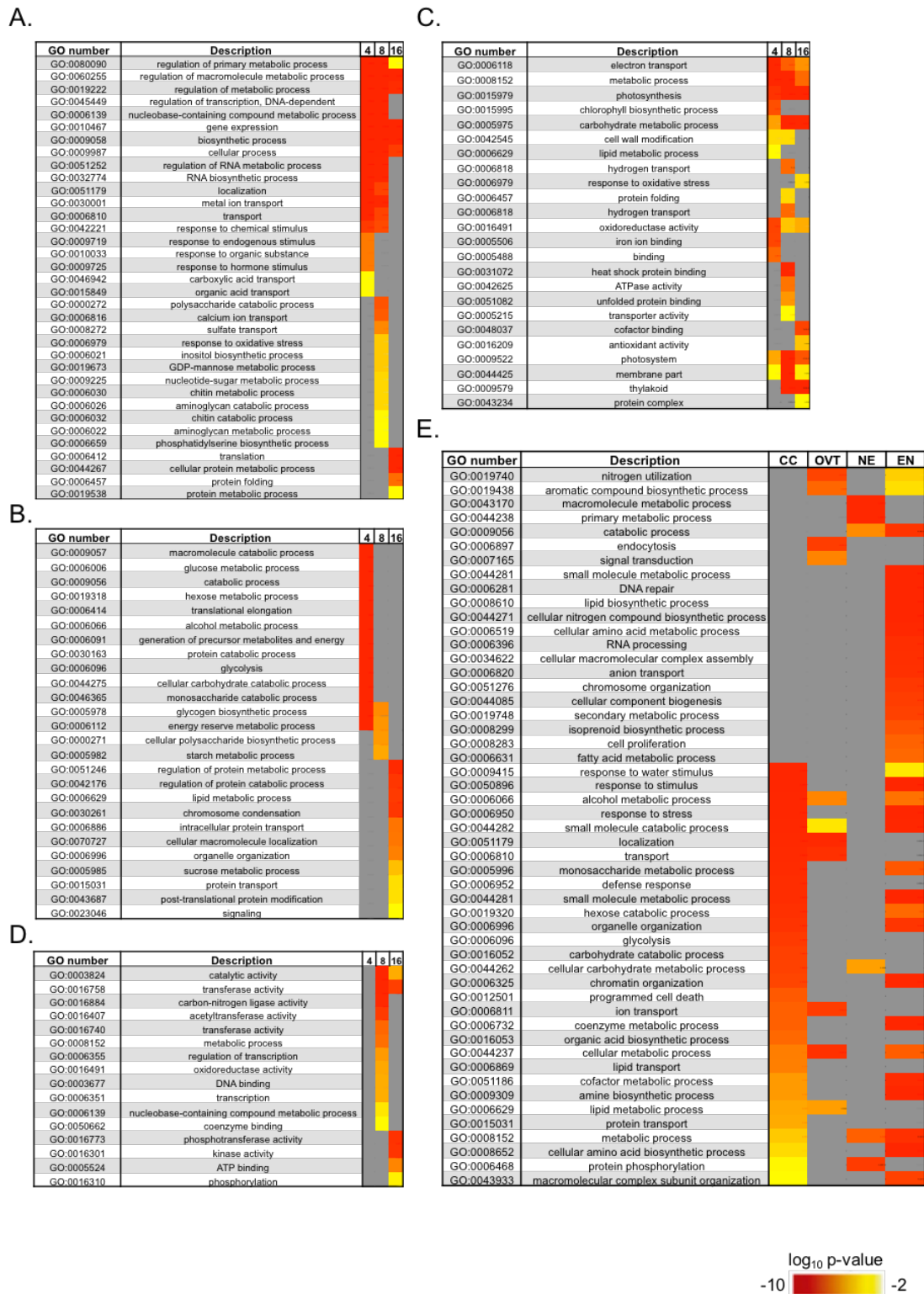
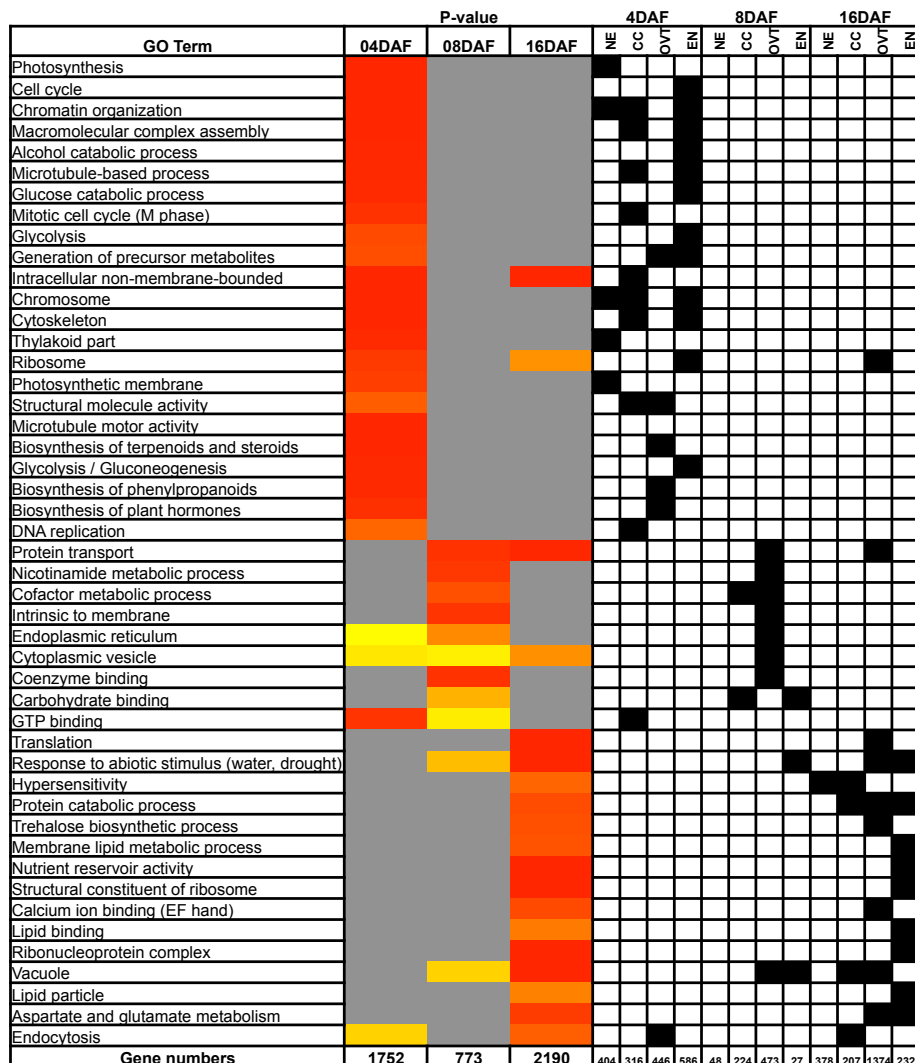


Figure 2. Gene Ontology (GO) analysis of the DEGs in different sub-regions at 4, 8 and 16 Days after flowering (DAF) of the rice grains. Significantly ($p < 0.01$) overrepresented GO terms

in (A) OVT, (B) CC, (C) EN, (D) NE and (E) AL are shown as heatmaps. OVT: Ovular Vascular Trace; CC: Cross Cells; EN: Endosperm; NE: Nucellar Epidermis and AL: Aleurone Layer.

Stage-specific differentially expressed genes. Among the DEGs, 1752 DEGs at 4 DAF, 773 DEGs at 8 DAF, and 2190 DEGs at 16 DAF were identified as growth stage specific (Fig. 1). The genes in 4DAF-specific set were related to chromatin assembly, DNA replication, cell mitosis and division in NE, EN and CC, and to hormone regulation and glycolysis in OVT. The 8DAF-specific genes were related to major CHO metabolism and transporter activity in OVT and EN. Over-represented GO categories of stage-specific gene sets indicate a transition into translation, protein biosynthesis, establishing protein localization and secondary metabolism, especially in CC, OVT and EN at 16DAF (Figure 3), which is consistent with previous studies on seed maturation (Gillies et al., 2012).



log₁₀ P-value
-10 -2

Figure 3. GO analysis of the DEGs at 4, 8 and 16 DAF of the rice grains. Significantly ($p < 0.01$) overrepresented GO at 4, 8 and 16 DAF are shown as heatmap. OVT: Ovular Vascular Trace; CC: Cross Cells; EN: Endosperm and NE: Nucellar Epidermis.

5.3.2 Diverse and complex regulatory network controlling grain filling in rice

Transcription factors (TFs) are important regulators of the gene expression. In order to explore the role of TFs in rice grain development, we surveyed about 1500 TFs expressed in rice genome and out of these 470 TFs were expressed differentially in our data set (Figure 4A, and Supplementary Table 3). OVT specific DEGs had the maximum number of TF encoding genes, comprising 21.3%, 21.5% and 15.5% of them at 4, 8 and 16 DAF, respectively (Figure 4B). Diverse types of TF encoding genes were found as differentially expressed, although the majority of these OVT specific TFs belonged to bHLH and MYB families (Figure 4C). Several of these TF family members, such as ABI3/VP1, ARF, Aux/IAA, B3, ARR and GRAS, play an important role in hormone regulation. Additionally, the TFs known for their role in vascular development, cell growth regulation and differentiation, such as MYB, SBP, MADS, NAC, bZIP and HB family were also differentially expressed in the OVT. Growth stage specific differences in TF profiles were also observed. The genes belonging to MADS and bZIP families showed higher expression at 4 and 8 DAF; while those in MYB, HB and WRKY had elevated expression at 16 DAF in the OVT (Figure 4D). Following OVT, CC specific dataset showed higher proportion of TFs as compared to NE, EN and AL specific sets, especially at 8 DAF (13%) (Figure 4E). The enriched TF families included WRKY, HB and Zinc finger, most of which are known to be involved in seed development (Figure 4E). Chi-square test showed that zinc-finger and AP2-ERF families were overrepresented in CC at 4 and 8 DAF (Supplementary Table 3). In addition, nine TFs were highly expressed in EN at 16 DAF, and most of these are reported to be involved in seed maturation or germination. Two AP2-like ethylene-responsive transcription factors (*Os04g0653600* and *Os05g0437100*) and three Heat Shock Transcription Factors (*Os02g0232000*, *Os06g0553100* and *Os10g0419300*) had higher expression level in the AL sub-region (Supplementary Table 3). *OsWRKY71* (*Os02g0181300*) also had highest expression level in AL, as also previously reported (Zhang et al., 2004). These data suggest that the reprogramming events in the developing rice grains comprise a complex coordination of different TFs in each sub-region and at different developmental time points.

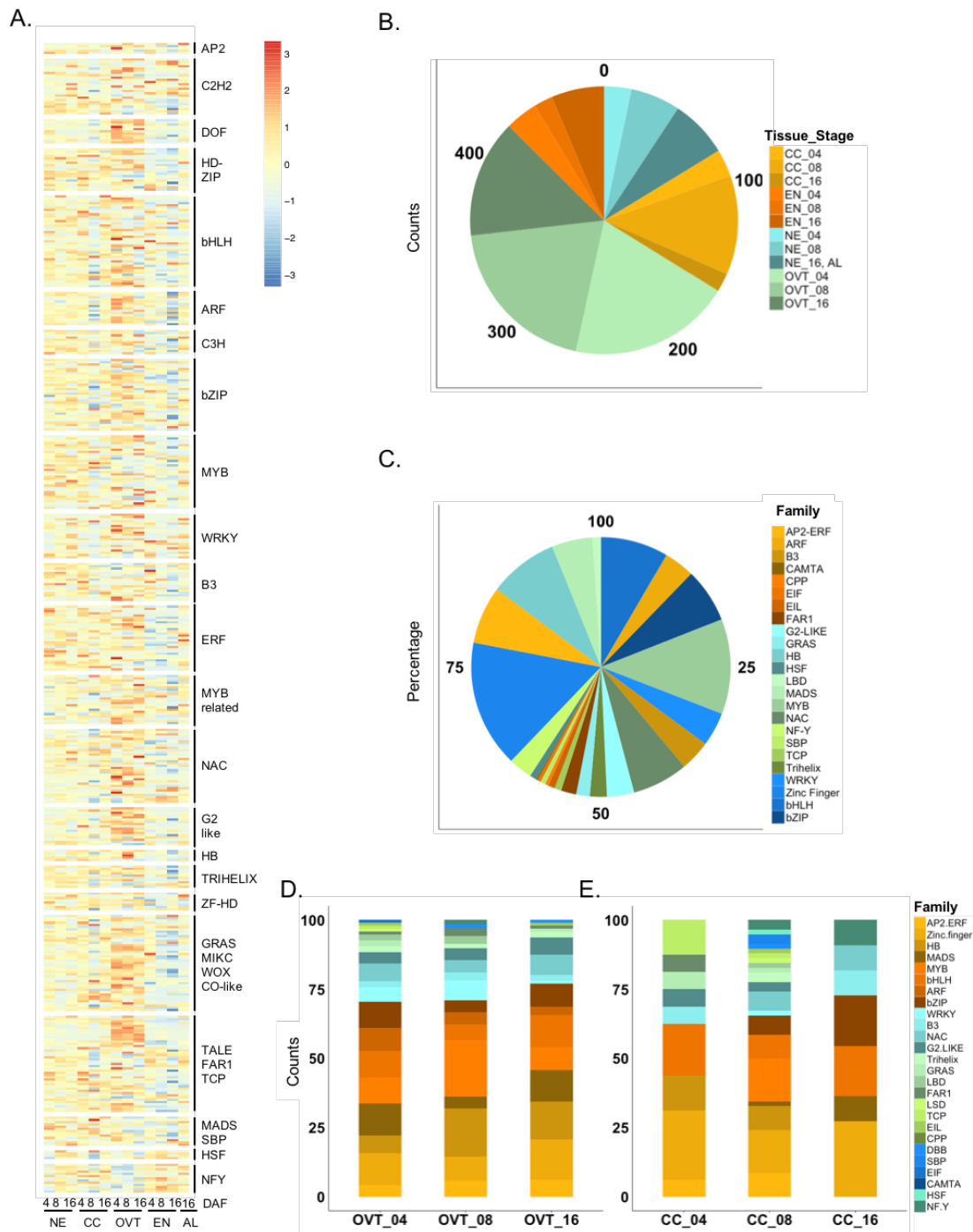


Figure 4. Analysis of differentially expressed genes encoding for transcription factors (TFs). A. Overview of heatmap for all differentially expressed TF encoding genes. B. Percentage of differentially expressed TF encoding genes in different sub-regions and at different growth stages in the developing rice grains. C. Distribution of TF families among the differentially expressed TF encoding genes in current data set. D. Distribution of TF families in ovular vascular trace (OVT) at different growth stages. E. Distribution of TF families in cross cells (CC) at different growth stages.

5.3.3 Expression profiles of phytohormone biosynthesis and signaling related genes

Since plant hormones are crucial in grain development, we studied the expression of genes related to auxin (IAA), Gibberellin (GA), Brassinosteroid (BR), cytokine (CK), Abscisic acid (ABA) and ethylene (ET) metabolism and biosynthesis. In general, BR, CK and GA related genes had higher expression level at 4 and 8 DAF in all sub-regions. The genes related to IAA had relatively stable expression in OVT during the 4 and 8 DAF, but exhibited slightly decreased expression at 16 DAF (Figure 5, Supplementary Figure 4A and 4B, and Supplementary Table 4).

IAA biosynthesis genes, including *OsYUCCA7*, *OsYUCCA4*, *OsASAI* and *OsASA2* (Mano and Nemoto, 2012) exhibited higher expression in OVT at 4 and 8 DAF, with a slight decrease in expression at 16 DAF. Genes encoding the IAA transporters and related TFs, such as *Aux/IAA*, were expressed higher in OVT at 4 and 8 DAF. The IAA signaling genes however were highly expressed in the AL as compared to the EN at 16 DAF (Figure 5A). GA20ox is a key enzyme in GA biosynthesis (Fleet and Sun, 2005) and among GA20ox encoding genes in rice, *Os1g09300* had higher expression level in OVT at 4 DAF. Notably, the expression levels of GA related genes were relatively low in EN at every time point (Supplementary Figure 4A). CK biosynthesis related genes including *OsRR2* and *OsRR6* (Hirano et al., 2008) were also preferentially expressed in the OVT at 8 DAF (Figure 5B). Only few BR biosynthesis related genes were differentially expressed in our data sets. Among them, *OsDWARF* (*Os03g0602300*), which encodes a brassinosteroid biosynthetic enzyme, C-6 oxidase, and is involved in seed development and panicle elongation (Mori et al., 2002), was differentially expressed in CC and OVT sub-regions at 8 and 16 DAF. Several of the BR signaling related genes were found as differentially expressed, especially in the OVT sub-region. *OsCYP* genes involved in BR pathways and known for regulating seed size (Wu et al., 2008), were expressed highly in the OVT at 4 and 8 DAF (Figure 5C). ABA biosynthesis genes exhibited higher expression in the AL and the EN sub-regions; while the ABA signaling related genes were preferentially expressed in the AL sub-region at 16 DAF (Figure 5D). This result is in a good agreement with previous reports, in which genes involved in ABA biosynthesis and signaling, including *NCED*, *AAO*, *bZIP* and *PP2C* (*HVA*), were enriched in the EN in late developmental stages (Xue et al., 2012) (Figure 5D). The expression pattern of ethylene (ET) signal transduction genes was quite stable during 4, 8 and 16 DAF

(Supplementary Figure 4B). The expression of ethylene responsive TF genes was preferentially low in EN at 16 DAF.

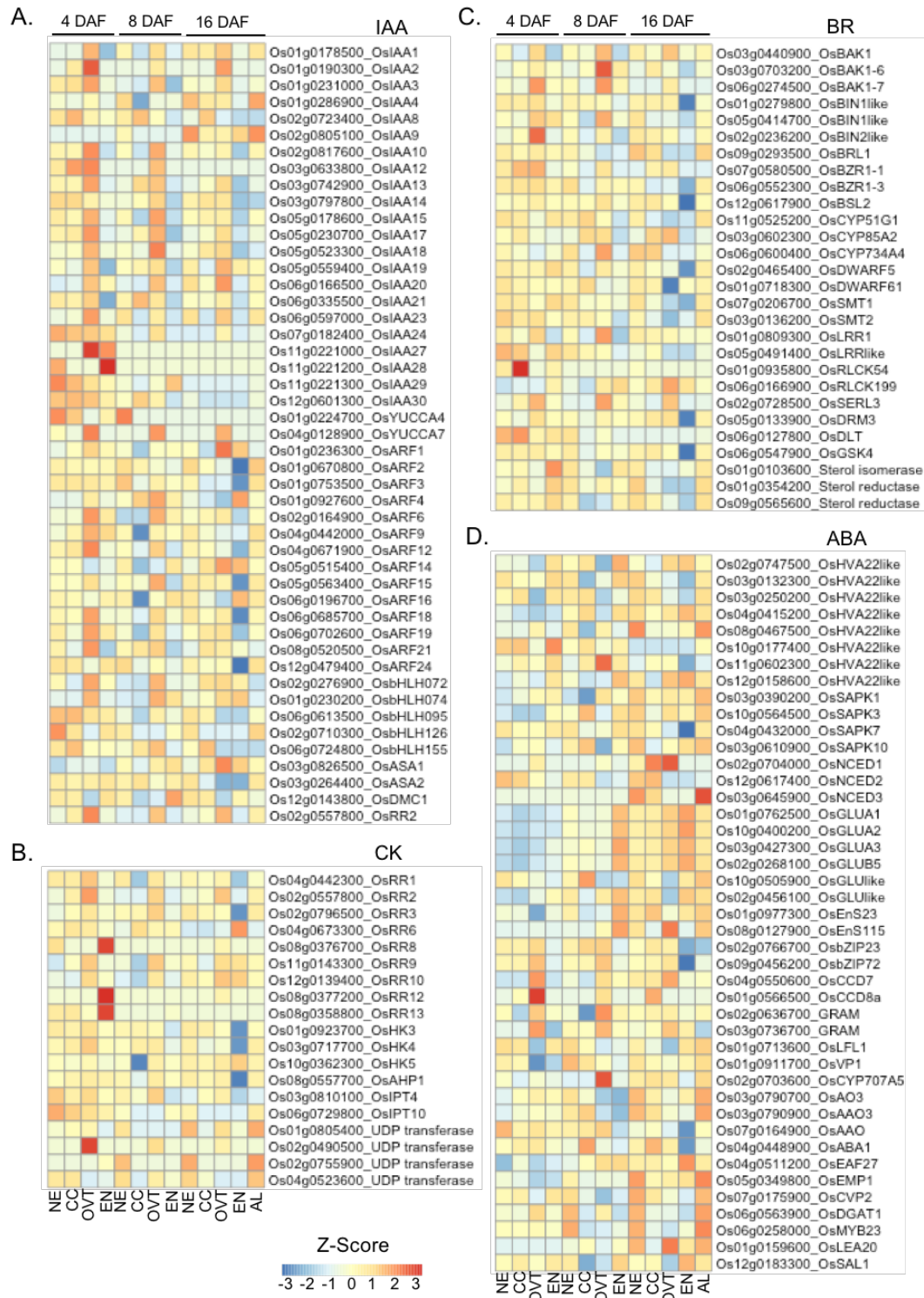


Figure 5. Expression profiles of differentially expressed genes related to hormone metabolism and transport in rice grain sub-regions. A. Genes related to auxin (IAA) biosynthesis, signaling and transporters. B. Genes related to cytokinin (CK) metabolism, transporters and receptors. C. Genes related to brassinosteroids (BR) metabolism, transporters and signaling. D. Genes related to abscisic acid (ABA) signaling. The gene-normalized signal

intensities are shown in the heat maps using Z-Scores. DAF: Days after flowering; NE: Nucellar Epidermis; CC: Cross Cells; OVT: Ovular Vascular Trace; EN: Endosperm; AL: Aleurone Layer.

5.3.4 Transporters are preferentially expressed in OVT

In order to gain an insight into the nutrient transport route in the rice grain, we extracted the list of genes encoding different transporters from MapMan and examined their expression patterns in our set of differentially expressed genes. Overall, the expression level of genes encoding nutrient transporters, including ATPase, sugar, nitrate and sulfate transporters, was preferentially higher in OVT, CC, and NE at 4 and 8 DAF. The expression level of genes encoding amino acid and protein transporters was higher at 16 DAF in OVT, CC and AL. The EN had a general low expression level of these genes as compared to the other tissues (Figure 6, Supplementary Figure 4C and 4D, and Supplementary Table 5).

P and V type of ATPases showed the highest expression at 8 DAF in OVT and CC. Three of these genes expressed higher in CC at 8 DAF and among these, *Os03g0183900* is a plasma membrane H⁺ ATPase that is specifically expressed in seeds (Baxter et al., 2003). Seven of these genes exhibited higher expression levels in the OVT at 4 and 8 DAF (Figure 6A). Most of these genes encode for vacuolar ATP synthase and phospholipid transporting ATPase (Figure 6A). Genes encoding sugar transporters had higher expression level at 4 and 8 DAF in EN, while their expression decreased at 16 DAF in EN but increased in AL (Figure 6C). We also found several sugar transporter encoding genes to preferentially express in OVT at 4 and 8 DAF. Six putative sugar transporters showed higher expression at 4 DAF in the OVT, including *Os02g0229400*, *Os04g0453400*, *Os04g0453200*, *Os03g0197100*, *Os11g0135300*, and *Os03g0101300* (Figure 6C), supporting that OVT plays a significant role in transporting sugars and nutrients to the developing EN and embryo. Three putative genes encoding sugar transporters (*Os03g0594400*, *Os12g0132500*, and *Os04g0511400*) had highest expression level at 4 DAF in EN. The expression of known sucrose transporter encoding genes including *OsSUT1*, *OsSUT2*, *OsSUT3*, *OsSUT4* and *OsSUT5* (Zhu et al., 2003) was stable at 4, 8 and 16 DAF in all the sub-regions. Most of the genes encoding amino acid transporters (Zhao et al., 2012), including *OsAAP2*, *OsAAP3*, *OsAAP5*, *OsAAP6*, and *OsAAP7*, showed preferentially high expression in OVT but not in EN at 4, 8 and 16 DAF (Supplementary Figure 4C). However, the *OsCAT11*, *OsATL6* and *OsPROT2* showed an increased expression in EN at 16 DAF (Supplementary Figure 4C). The genes

encoding nitrate, phosphate and sulfate transporters were preferentially expressed in OVT at 4 and 8 DAF but preferentially expressed in NE, CC and AL at 16 DAF (Supplementary Figure 4D). For example, HIGH AFFINITY NITRATE TRANSPORTER (Feng et al., 2011) *OsNAR2.1* expressed highly in OVT at 4 DAF (Supplementary Figure 4D). *OsPHO1;2* and *OsPHO1;1*, which tightly regulate phosphate loading into xylem in rice and regulate plant fitness (Secco et al., 2010; Jabnune et al., 2013), were enriched in OVT at 8 DAF and in CC at 16 DAF, respectively. *OsSULT3;3* and *OsSULT3;4*, which showed highest expression level in AL at 16 DAF and in OVT at 8 DAF, respectively, are known to be induced by heavy metal stress (Buchner et al., 2004; Kumar et al., 2011) (Supplementary Figure 4D). Sulfate transporter *OsSULT3;5* was the only gene which showed highest expression level in EN at 16 DAF in our data set (Supplementary Figure 4D).

The expression of genes encoding iron and zinc related transporters, such as NRAMP, ABC, HMA and ZIP (Kobayashi and Nishizawa, 2012); (Lanquar et al., 2005) was higher at 4 and 8 DAF, but significantly decreased at 16DAF (Figure 6D, Figure 7 and Supplementary Table 5 and 6). EN exhibited the lowest metal transporter gene expression level, while most of the genes expressed higher in AL at 16 DAF (Figure 6D). Expression of *NRAMP* gene family including *OsNRAMP1*, *OsNRAMP2*, *OsNRAMP3* and *OsNRAMP5* was higher in OVT and CC but lower in EN at 4 and 8 DAF (Figure 6D). Similarly, a selection of HMA family genes showed significantly higher expression level in OVT at 4 and 8 DAF, and in NE and AL at 16 DAF (Figure 7B). Among the ZIP family genes, *OsZIP4* and *OsZIP7* showed higher expression level in OVT at 4 and 8 DAF, while *OsZIP3* showed highest expression in EN (Figure 6D). Genes related to iron acquisition and transport such as *OsFRDL2* (Yokosho et al., 2016a), *OsOPT*, *OsYS* and *OsCOPT3* also expressed higher in OVT and CC at 4 and 8 DAF (Figure 6B and 6D and Figure 7C).

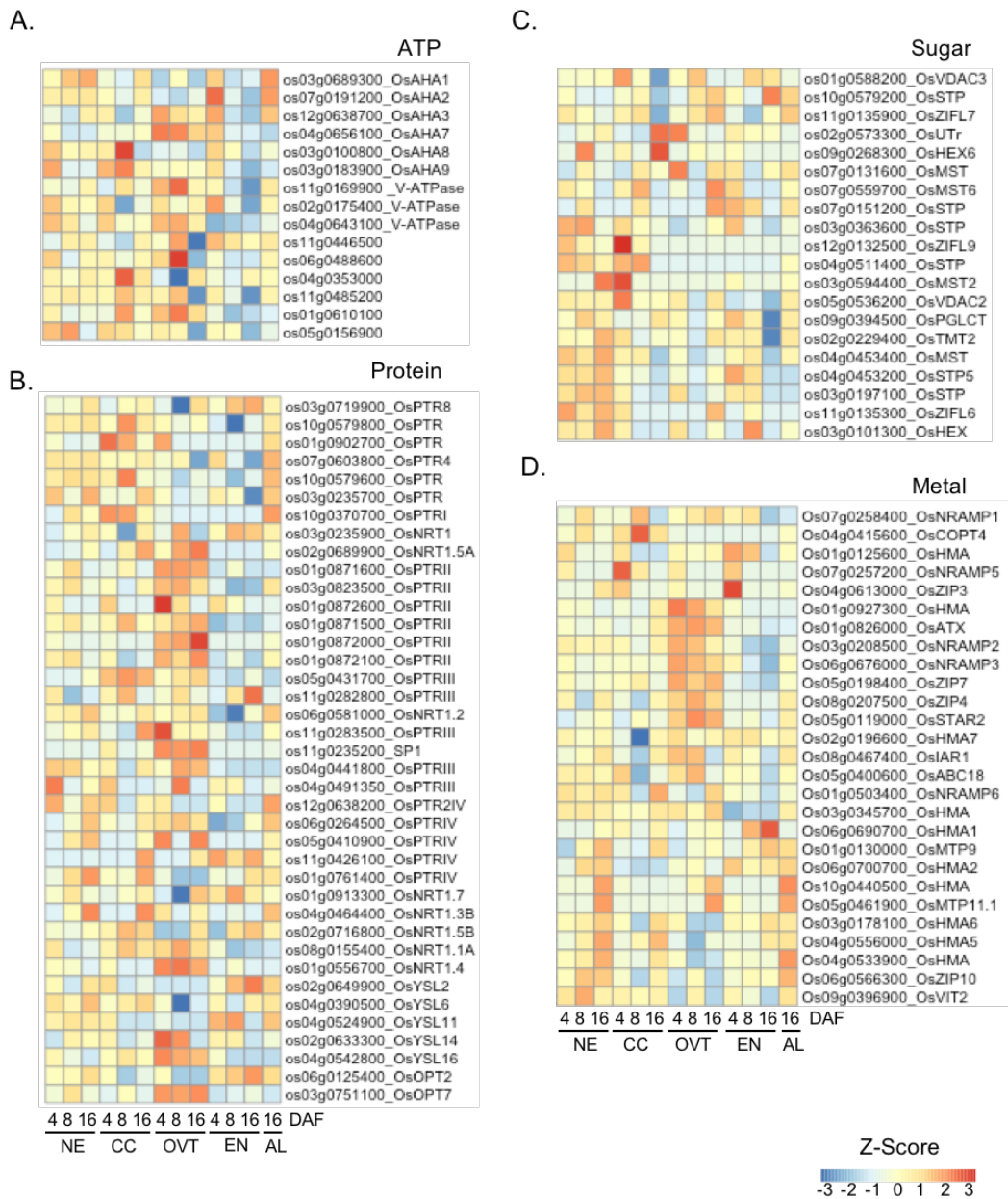


Figure 6. Expression profiles of differentially expressed genes related to transporters. A. Genes involved in ATP synthesis and transport. B. Genes involved in protein transport. C. Genes involved in metal transport. D. Genes involved in sugar transport. The gene-normalized signal intensities are shown in the heat maps using Z-Scores. DAF: days after flowering; NE: Nucellar Epidermis; CC: Cross Cells; OVT: Ovular Vascular Trace; EN: Endosperm; AL: Aleurone Layer.

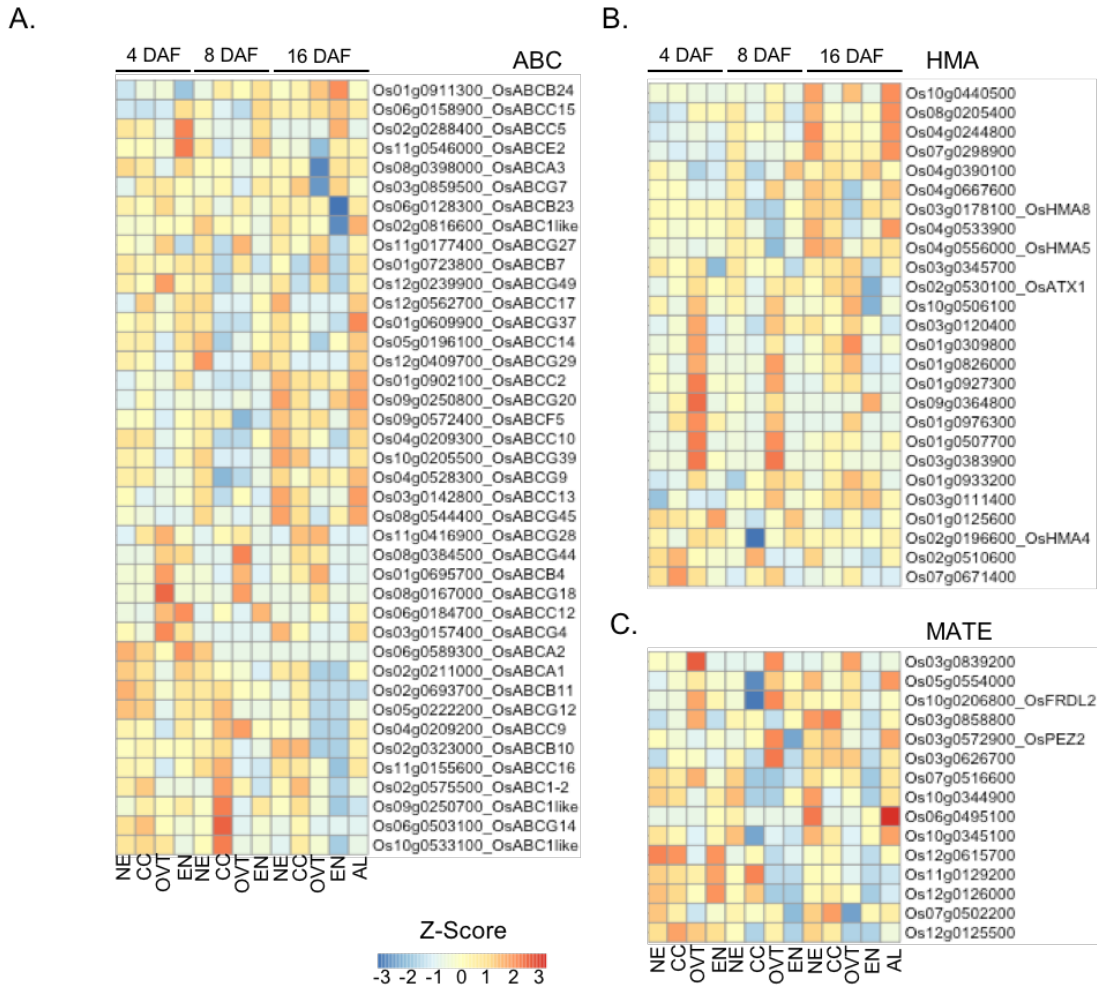


Figure 7. Expression profiles of differentially expressed genes related to ATP-binding cassette (ABC), heavy metal ATPase (HMA) and multidrug and toxic compound extrusion (MATE) families. A. Expression pattern of genes from ABC family. B. Expression pattern of genes from HMA family C. Expression pattern of genes from MATE family. The gene-normalized signal intensities are shown in the heat maps using Z-Scores. DAF: days after flowering; NE: Nucellar Epidermis; CC: Cross Cells; OVT: Ovular Vascular Trace; EN: Endosperm; AL: Aleurone Layer.

5.3.5 Novel cis-regulating elements associated to OVT and CC specific genes

Since a significant number of genes differentially expressed in OVT and CC were related to transcription factors as indicated by GO analysis, we performed promoter analysis to identify known and/or unknown regulatory motifs in the promoter or the coding regions of these OVT and CC specific genes. We searched up to 1000bp upstream and 1000bp downstream from ATG site for novel or known motifs and analyzed the sequences using MEME database and JASPAR plant database. Several common motifs were identified among the OVT and CC specific DEGs. For example, MADS binding region SOC1 and PI were found in OVT and CC at 4, 8 and 16 DAF. In addition, high mobility group box HMG-I/Y and zinc finger binding motif id1 were also enriched in our dataset during all three development stages. In addition to the common motifs, several tissue-specific motifs were also identified. Of note, ABI3 (GCATG), a binding site of ABI/VP3 transcription factor related to auxin signaling, and BES1 (CACGTG) motif, related to BR signaling transduction were enriched only in OVT specific genes at 8DAF, suggesting an important role of phytohormone related transcription factors in early grain filling. At 16 DAF, MYB (GGTnGGT) and SBP (GTAC) were enriched motifs in OVT but no motifs specific to CC were detected as enriched at this development stage (Table 1). We also identified a novel motif “GGAGGA” in OVT specific genes. From the analysis using GO-MEME (Buske et al., 2010) and cross comparison with other plant species, it is likely that this motif is involved in transporter and hormone regulation. Another motif “GCCGCC” was also identified as unique, but a high GC content motif is suggested to be commonly found in rice gene promoters (Lenka et al., 2009; Lenka et al., 2011). We did not detect any novel motifs in CC specific genes. In the downstream regions of OVT and CC specific genes, we found motif “GCATGC” as enriched in OVT specific genes at 4 and 8 DAF, and motif “CCTCC” enriched in CC specific genes at 8 DAF. We compared these two motifs with known motifs using TOMTOM (Gupta et al., 2007) software. “GCATGC” was similar to BR signaling associated regulatory element BES1 and “CCTCC” was similar to MYB regulatory elements (Table 1).

A.

B.

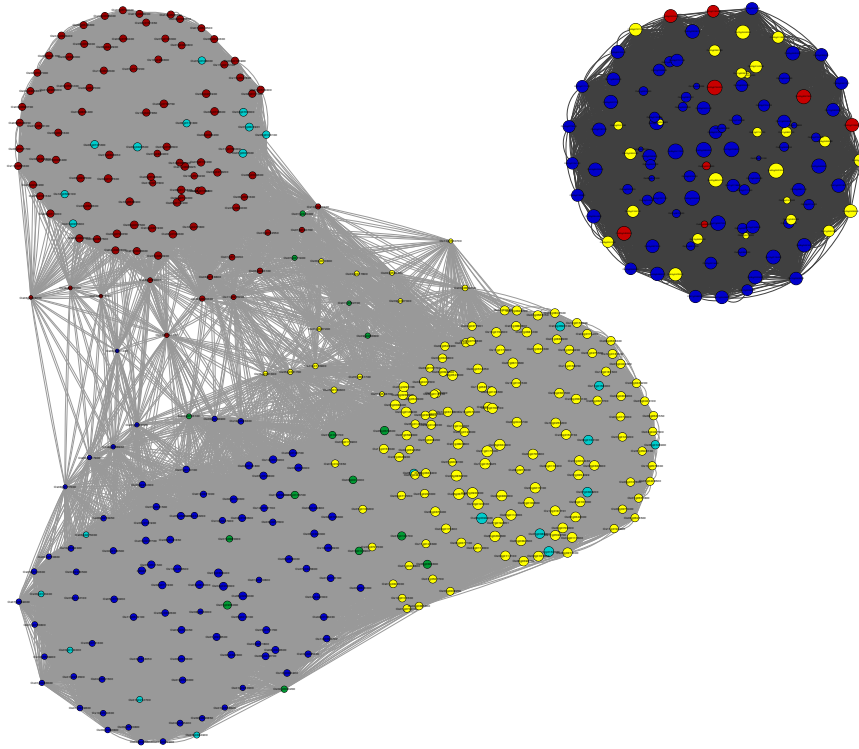
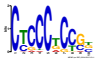



Figure 8. Co-expression analysis for OVT and CC specific genes in different stages of rice grain development. Co-expression dataset of A. OVT and B. CC specific genes were analysed and a graphic view produced using Cytoscape is presented. Blue: OVT_04, Yellow: OVT_08, Red: OVT_16, Green: bridge TF, and Light blue: central TF

The co-expression analysis grouped the OVT specific genes into three subsets (Figure 8A). The 4DAF and 8DAF specific OVT genes interacted more with each other; while 16 DAF specific genes formed a distinct subset, suggesting a phase change in OVT at 16 DAF. Additionally, TFs divided into two groups in co-expression analysis of OVT specific genes. One group of TFs resided among the 4 and 8 DAF subsets, suggesting their role in regulating the gene network of OVT at early stages of grain development. Most of transporters assigned to the individual nodes, indicating that distinct transporters might be required for specific developmental stages. The co-expression network of CC specific genes grouped as one subset, indicating a closer function of these genes at all three developmental stages i.e., 4, 8 and 16 DAF (Figure 8B). Several TFs related to growth regulation, cell wall growth and flowering time were identified in between of two subsets. Among these TFs, *OSH15* (*Os07g0129700*) is known to affect the architecture of internodes, resulting in dwarf plants (Sato et al., 1999) and *OsMADS15* (*Os07g0108900*) is required to ensure sexual reproduction in rice (Wang et al., 2010). On the other hand, *Hd-1* (*Os06g0275000*), which is identified within the node of OVT at 8 DAF, was shown as a zinc-finger domain TF regulating panicle development in rice (Yano et al., 2000). The TFs involved in secondary cell wall formation, namely CesA and Myb TFs family ((Hirano et al., 2013a; Hirano et al., 2013b) were also identified in OVT specific gene network.

Table 1. Summary of overrepresented motifs identified from the MEME analysis

ID	NAME	Family	Adjusted p-value					
			04OVT	08OVT	16OVT	04CC	08CC	16CC
MA0554.1	SOC1	MADS	1.88E-08	0.00000226	0.00000403	0.00000475	0.000216	-
MA0045.1	HMG-I/Y	HMG	0.0000841	0.00735	0.0144	0.000641	0.00315	-
MA0120.1	id1	BetaBetaAlpha-zinc finger	0.000278	0.0145	0.016	0.0164	-	-
MA0559.1	PI	MADS	0.0189	0.0339	0.000101	-	0.00984	-
MA0123.1	abi4	AP2-MBD like	-	0.024	-	-	-	-
MA0549.1	BES1	Helix-Loop-Helix	-	0.0345	-	-	-	-
MA0581.1	LEC2	ABI3VP1	-	0.0416	0.015	-	-	-
MA0552.1	PIL5	Helix-Loop-Helix	-	0.0445	-	-	-	-
MA0548.1	AGL15	MADS	-	0.0469	-	-	-	-
MA0082.1	squamosa	MADS	-	0.019	-	-	-	-
MA0564.1	ABI3	ABI3VP1	-	0.00899	-	-	-	-
MA0578.1	AtSPL8	SBP	-	-	0.00567	-	-	-
MA0558.1	FLC	MADS	-	-	0.0143	0.0217	0.0217	-
MA0576.1	AtMYB84	Myb	-	-	0.0176	-	-	-

Logo	Region	E-value	Tissue	Stage
	1000bp upstream	2.00E-02	OVT	08,16DAF
	1000bp downstream	4.50E-03	OVT	04,08DAF

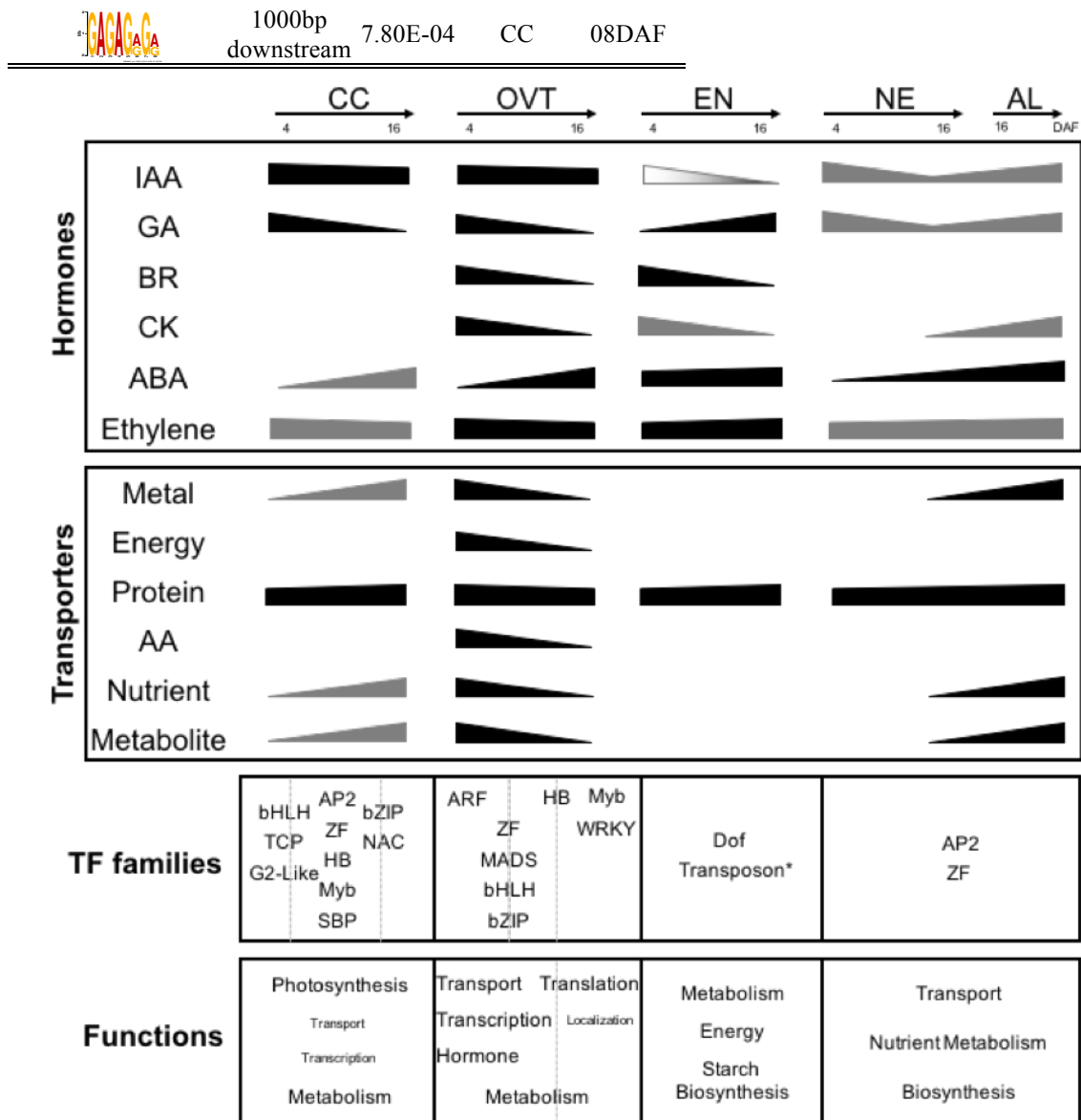


Figure 9. Summary of Spatio-temporal regulation in different tissues during grain development. Changes in hormone-regulated genes and in the genes encoding transporters in CC, OVT, EN, NE and AL are summarized. Enriched TF families in different sub-regions during different developmental stages are presented.

5.4 Discussion

Seeds provide around 70% of the human caloric intake worldwide and store the genetic information for the plant's next life cycle. Therefore, understating the gene expression in developing seeds will help us identify the crucial regulators. Several transcriptomic studies have characterized gene expression in different sub-regions of grains in various crops(Thiel et al., 2012; Pfeifer et al., 2014; Zhan et al., 2015). However, most earlier reports focused only on embryo and endosperms in rice(Xu et al., 2012b; Gao et al., 2013), and the molecular processes in different sub-regions of the grain are still unclear. We made a comprehensive analysis on developing rice grains dissected into different important sub-regions and identified several tissue- and stage-specific genes. The summary of our findings is presented in Figure 9. This data will serve as a valuable resource for understanding the complexity of gene expression during rice grain development.

GO analysis revealed common and unique stage-specific and sub-region specific genes indicating distinct and shared spatio-temporal features associated to rice grain development. These observations are consistent with previous morphological and molecular studies (Krishnan et al., 2001; Krishnan and Dayanandan, 2003; Zhu et al., 2003; Xu et al., 2012b; Xue et al., 2012). Endosperm transfer cells (ETC) of barley and wheat are specific cells differentiated from aleurone and are suggested to transfer different kinds of solutes such as hormones, amino acids, sugars, micronutrients and waters to the endosperm(Offler et al., 2003; Thiel et al., 2012), which are important for grain filling and grain quality (Jia et al., 2011; Sun et al., 2012; Xu et al., 2012a). Most of the divalent metal transporter encoding genes, including *HMA*, *ZIP*, *YSL*, *NRAMP*, *MTP*, and *VIT* families have been found to respond to alterations of zinc and iron concentrations in ETCs of barley grains(Tauris et al., 2009). Additionally, auxin, glucose, ethylene and reactive oxygen species are reported to initiate signal cascades leading to the development of ETC (Thiel et al., 2012). Some reports also suggested that the rice OVT has similar functions as ETC (Krishnan and Dayanandan, 2003; Li et al., 2008b). Minerals and nutrients are unloaded into the rice grain from the OVT, which contains both phloem and xylem cells, into the aleurone and endosperm(Lu et al., 2013a; Zhao et al., 2014). Our RNA sequence data supports these observations, as the genes related to hormones and different transporters are enriched in the OVT region at 4 and 8 DAF of grain development. For example, the metal transporter encoding genes including *NRAMP*,

HMA, and *ZIP* families as well as IAA regulators were preferentially expressed in OVT at 4 and 8 DAF. Similar trend is observed for ethylene-associated genes in OVT at 4 and 8 DAF in our data set.

Although EN and AL share several metabolic pathways, our data also indicated distinct processes in EN and AL, respectively. Genes specific to AL are involved in secondary metabolism, lipid metabolism, and protein processing, while the EN specific genes are involved in starch synthesis, sugar metabolism and energy reservoir pathway. At 16 DAF, most genes were expressed at a lower level in the EN as compared to the AL, suggesting an important function of AL in providing nutrition and energy to the developing grains. Similar to our findings on the EN specific genes, another study on the transcriptomic analysis of rice endosperm at 6 DAF and 10 DAF reported genes involved in amino sugar and nucleotide sugar metabolism to be enriched (Gao et al., 2013). In case of wheat, AL and EN genes involved in transport, definition of cell structure, cell differentiation, lipid metabolic process and nitrogen compound metabolic process were reported to be differentially expressed (Gillies et al., 2012; Pfeifer et al., 2014). Furthermore, the transcripts promoting rapid accumulation of carbohydrate and other storage macromolecules were frequently detected in wheat EN, including carbohydrate metabolic processes, generation of precursor energy and macromolecule biosynthetic process (Gillies et al., 2012; Pfeifer et al., 2014). These observations are also in line with our analysis on DEGs specific to AL and EN. It has been suggested previously that the concentration of Zn, K, Ca and Fe are much higher in AL than in EN in the grains (Iwai et al., 2012; Lu et al., 2013a; Zhao et al., 2014). We also found the expression of genes encoding Zn, Mn, Cu and Fe transporters to be relatively higher in AL as compared to that in EN. Together, these observations suggest that both OVT and AL sub-regions contribute significantly to nutrient transport in the developing rice grains and indicate relatively conserved molecular mechanism controlling grain filling and development in monocots (Sreenivasulu and Wobus, 2013).

Coordination of different phytohormones is important for seed development. The information on expression patterns of different hormone related genes in individual grain sub-regions are rather limited in crops. It has been suggested that high concentration of auxin is present throughout the seed developmental phases. IAA is also known to provide positional signaling during AL development in maize seeds (Forestan et al., 2012). The

pattern of cytokine is opposite from auxin. CK has a prominent role during the early developmental phase, decreasing gradually during seed maturation (Locascio et al., 2014). In addition, CK related genes have been reported to have higher expression in maternal tissue, especially in the ETC in maize and wheat seeds. Similar to CK, the highest concentration of BR is observed at the beginning of seed development, with gradual decrease during seed maturation (Jiang and Lin, 2013). GA is more dynamic, showing fluctuations corresponding to early and late developmental stages, respectively, while ABA concentration is higher during seed maturation (Seo et al., 2006; Liu et al., 2013). In barley, ABA metabolism is reported to be enriched in EN and AL at 16 and 25 DAF (Seiler et al., 2011), while CK and GA metabolism were enriched at 8 and 16 DAF (Thiel et al., 2012). In our dataset, genes related to auxin biosynthesis and signal transductions had higher expression level in OVT at 4 and 8 DAF, with a slight decrease at 16 DAF. Likewise, the genes involved in BR and CK signaling showed higher expression in OVT and CC in early developmental stages. The genes associated with ABA have higher expression in EN and AL in the late developmental stage (16 DAF), which is consistent with the observation in barley (Seiler et al., 2011). These data suggested a key role of OVT in hormone regulation and nutrient transportation to the developing grain (Kanno et al., 2010; Locascio et al., 2014). Our data, together with previous reports (Seiler et al., 2011; Locascio et al., 2014), also suggest that the role and regulation of phytohormones is largely conserved during grain filling in monocots, though characteristic differences exist.

The analysis of stage-specific genes suggested that the genes expressing preferentially higher at 4 and 8 DAF are related to photosynthesis, major metabolism and protein translation; while genes expressing higher at 16 DAF are related to protein, lipid and fatty acid metabolism and stress response. Similar metabolic changes in developing rice seeds have been reported via a shotgun proteomics analysis (Lee and Koh, 2011). This suggests that the putative metabolic changes that we anticipate from the RNA-seq data are in good agreement with the observations made at the protein level (Sun et al., 2012). So far only few genes have been fully characterized with their known roles associated to rice grain development. Among them, *OsMADS29* (*Os02g0170300*) which regulates the degradation of nucellus and nucellar projections in rice has been shown to have higher expression level in early developmental stages (3 to 6 DAF) in nucellus and nucellar projections, while its expression is low in endosperm with further decrease in endosperm expression at 8 DAF (Yang et al., 2012b; Yin and Xue, 2012). *OsGIF1* (*Os04g0413500*)

encodes a cell-wall invertase required for carbon partitioning during early grain filling stages (3 to 15 DAP) (Wang et al., 2008) and has been shown to localize in OVT. We identified that *OsMADS29* and *OsGIF1* were preferentially expressed in OVT at 4 and 8 DAF, and expressed at very low level in EN at 4, 8 and 16 DAF.

Higher number of genes encoding TFs are differentially expressed in the early grain developmental stages, indicating a relatively complex regulation in this stage as compared to that in a relatively mature grain. We observed that MADS, ARF, HB and ARR-B TFs are enriched in OVT, and MYB and NAC TFs are enriched in CC at 4, 8 DAF. Most of the known motifs from MEME prediction also belonged to the MADS, ABI3VP1 and MYB families, which is consistent with the analysis of enriched TF families in OVT and CC. In EN, the most abundant TF families are MYB, MADS, NAC and NF-Y. The bZIP TFs were mainly expressed in AL and EN in our data set, which is consistent with the previous studies proposing that bZIP TFs are expressed in the aleurone cells and the EN and bind to ABRE to mediate the ABA-induced transcription (Xue et al., 2012). Similarly, in maize endosperm, bZIP, MADS, NAC, MYB and SBP were reported as enriched TF families, and most of them are associated with seed development (Lu et al., 2013c; Zhan et al., 2015). In Arabidopsis, the known seed-specific transcription families include MADS, ARR-B TFs, and bZIP TFs (Le et al., 2010; Khan et al., 2014a; Khan et al., 2014b). In the funiculus, which anchors the seed to the maternal plants and is the only direct route for nutrient transport to the seeds in Arabidopsis, MYC is hypothesized to be responsible for auxin response (Khan et al., 2015). In barley, bZIP and MYB TFs are abundantly present during the transition from grain maturation to germination; while ARF and AUX/IAA TF family members are preferentially expressed in the embryo of germinating grains (Sreenivasulu et al., 2008; Thiel et al., 2012; Zhang et al., 2016a). These reports, together with our findings, suggest the afore-mentioned TF families to be important in grain development and also that several of the regulators of seed development are conserved in monocots. Additionally, these studies also revealed novel transcription factors whose functions are yet unknown. For example, in our data *OsWRKY109* (*Os05g0129800*) showed highest expression in OVT at 4 DAF, but its biological function and regulatory network are yet unclear. Nevertheless, the differentially expressed TF genes provide informative clues on the regulatory network controlling rice grain development.

Together, our dataset provides a comprehensive overview of molecular mechanisms controlling rice grain development at a finer scale providing detailed expression profiles in vital sub-regions of the grain. The information on tissue- and stage-specific genes and regulatory factors could serve as a foundation resource for future functional genomics studies on rice grain development and grain filling.

5.5 Materials and Methods

5.5.1 Plant Material and Growth Conditions

The rice plants (*Oryza sativa* cv. Nipponbare) were grown in hydroponic solutions maintained at 28°C. Solutions for the hydroponic system were prepared as previously described (Wang et al., 2013b). Rice grains were collected at 04, 08 and 16 days after flowering, were dehusked and were immediately frozen by placing the collection tubes in liquid nitrogen.

5.5.2 Cryostat settings, Mount slides preparation and Laser Capture Microdissection (LCM)

Three grains were used for each sample preparation. Cryostat was set to specific conditions with the knife at -18°C and specimen at -20°C. Thirty µm of trim and 10 µm of fine trim were used. Two to three rice grains from the same developing stage, i.e. 4, 8 or 16 DAF, were mounted in the mold with optimal cutting temperature compound (O.C.T compound). The samples with mold were incubated at -20°C for 5 min. The fixed samples were then removed from the mold for further dissection.

One drop of 70% ethanol was added with 100µm pipette onto the membrane slide, and the liquid was distributed over the entire area on the slide. The slide was put upside down and touched shortly with the ethanol until it was soaked and warmed in 70% ethanol solution. The slide was attached to the membrane surface of the microscope and was immediately placed back to the cryostat, further drying was allowed for 20 min and finally, the samples were processed with the LCM.

PALM Laser capture microdissection settings were set to 65-75% of energy and focus. After Köhler-Illumination was done, the lens were changed to 10x or 20x objective. The cut tissues were catapulted in eppendorf cap and then the eppendorf tube was unmounted

from microscope. 350µl RLT Buffer from Qiagen RNeasy Micro Kit was added to the cap and tube, vortexed for 5 min and incubated at room temperature (RT) for 5 min.

5.5.3 RNA Extraction, pre-amplification and RNA sequencing

The RNA extraction was done with the Qiagen RNeasy Micro Kit following manufacturer's instruction manual. All RNA samples were adjusted to a concentration of 100pg/µl prior to pre-amplification step. Pre-amplification for the Illumina sequencing was done with the Clontech SMARTer Ultra Low kit following the user's manual with slight modification. In brief, the RNA samples were subjected to first strand cDNA synthesis, followed by 15 cycles of Long distance (LD) PCR. The PCR amplified cDNA was subsequently purified by immobilization on AMPure XP beads for 15 min at RT, resuspended in 15 µl nuclease-free water and stored at -20°C for further experiments and library preparation.

Three biological replicates for each tissue were sequenced at the Functional Genomics Center Zurich (FGCZ). Correlation coefficients of two biological replicates between tissues ranged from 0.85 to 0.9, indicating that the results were highly reproducible. The biological replicates with poor quality were removed, and therefore leaving 28 samples in total for detailed analysis (NE_4DAF(3), OVT_4DAF(3), CC_4DAF(2), EN_4DAF(1), NE_8DAF(3), OVT_8DAF(2), CC_8DAF(1), EN_8DAF(2), NE_16DAF(3), OVT_16DAF(1), CC_16DAF(2), EN_16DAF(2), AL_16DAF(3)). The TruSeq SR Cluster Kit v4-cBot-HS (Illumina, Inc, California, USA) was used for cluster generation using 8 pM of pooled normalized libraries on the cBOT. Sequencing were performed on the Illumina HiSeq 2500 single end 126 bp using the TruSeq SBS Kit v4-HS (Illumina, Inc, California, USA).

Threshold for data analysis were chosen to be $p < 0.001$ and RNA-seq reads higher than 10. For a pair-wise comparison, gene expression level change higher than 2-fold and p -value < 0.05 were chosen. Reads were aligned with the STAR aligner (Dobin et al. 2012) to the cv. Nipponbare reference genome IRGSP1.0 (Tanaka et al., 2008) Gene expression counts were computed with R/Bioconductor. Differential expression was assessed with the Bioconductor packages edgeR (Robinson et al. 2010). Genes were considered as differentially expressed if the p -value was below 0.01 and the expression fold-change was greater than 2.

5.5.4 qRT-PCR validation

Reverse transcription was performed using Superscript-III Reverse Transcriptase (Invitrogen, Carlsbad, USA). The diluted cDNA samples were used as templates for RT-PCR and real-time PCR. The internal control genes used for RT-PCR were rice *UBIQUITIN 5 (OsUBQ5)* and *ELONGATION FACTOR 1-ALPHA (OsEF-1 α)*. Real-time PCR were performed using SYBR Premix Ex Taq (Takara, Dalian, China) on a Rotor-Gene 3000 (Corbett Research, QIAGEN, Hilden, Germany) detection system and software, according to the manufacturer's instructions. The primers used for qPCR validation are provided in Supplementary Table 7.

5.5.5 Data analysis

The enriched GO categories of subregion or stage-specific DEGs were analyzed in PlantGSEA (Yi et al., 2013) (The Plant GeneSet Enrichment Analysis, <http://structuralbiology.cau.edu.cn/PlantGSEA/>). Fisher test and cut-off for FDR-adjusted p-value<0.01 was used to screen the GO term enrichment. The significantly changed metabolic pathway analysis was carried out using KEGG (Tanabe and Kanehisa, 2012) server (Kyoto Encyclopedia of Genes and Genomes, <http://www.genome.jp/kegg/>) with the threshold of p-value<0.01. The functional gene set was annotated by TIGR (Rice Genome Annotation, <http://rice.plantbiology.msu.edu/index.shtml>) and RiceDB (<http://ricedb.plantenergy.uwa.edu.au/>). The categories of transcription factors were downloaded from PlantTFDB (<http://planttfdb.cbi.pku.edu.cn/>) for further analysis. DEGs were also assigned and visualized using MapMan v3.6. Default parameters were used and the background of mapping was TIGR7 rice protein and IPR Interpro.

Motif analysis was conducted using the MEME (Bailey et al., 2009) (Multiple EM for motif elicitation, <http://meme.nbcr.net/meme/>) Suite analyzing tools. 1000bp upstream or downstream from translational start site ATG of DEGs was extracted from RAPDB (<http://rapdb.dna.affrc.go.jp/>). Over-represented cis-motifs of a width of 6-10 nucleotides were selected. The enriched known motifs were analyzed in AME (McLeay and Bailey, 2010) (Analysis of Motif Enrichment) tools by JASPAR plants database with the threshold of p-value<0.05.

Gene co-expression analysis was performed as described previously (Coman et al., 2014). In brief, the Pearson correlation coefficients between DEGs were calculated. The analysis was visualized in Cytoscape (Cline et al., 2007).

5.6 Conflict of interest

The authors declare that they have no conflict of interest.

5.7 Author contributions

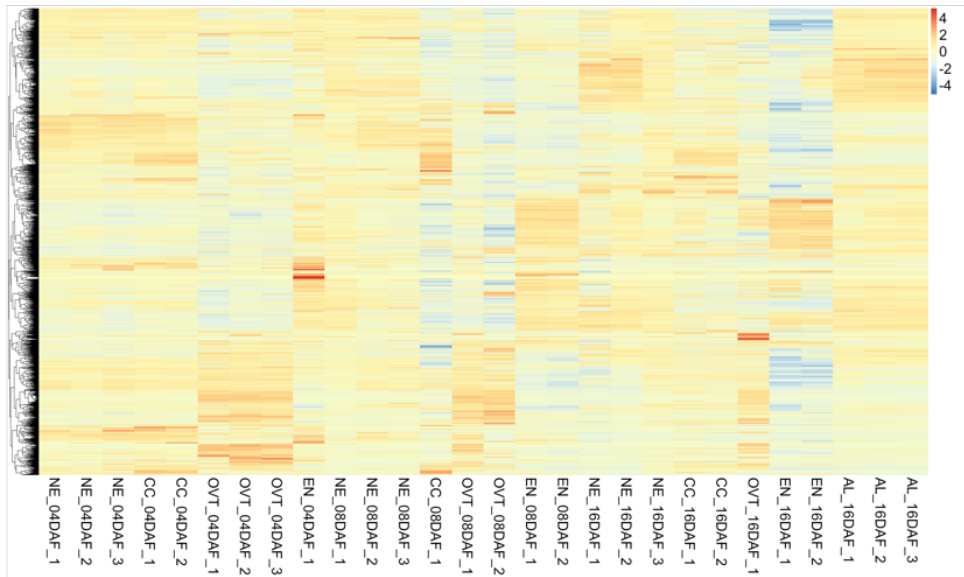
NKB and WG conceived the study, TYW and MM performed the experiments, TYW analyzed the RNA-sequencing data, TYW and NKB wrote the manuscript, and WG and NKB edited the manuscript.

5.8 Acknowledgements

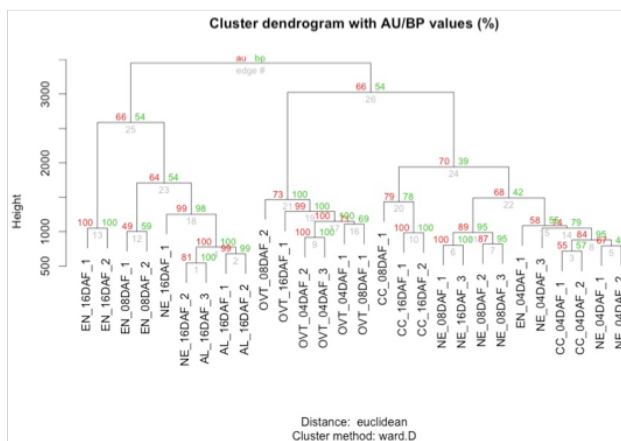
We gratefully acknowledge the ETH research grants for this work to WG and NKB. We thank Irene Zurkirchen for the technical support in the greenhouse. We thank Dr. Hubert Rehrauer and Catharine Aquino from the Functional Genomics Center Zurich (FGCZ) for the support in RNA sequencing and quality processing of RNA seq data.

5.9 Supplementary data

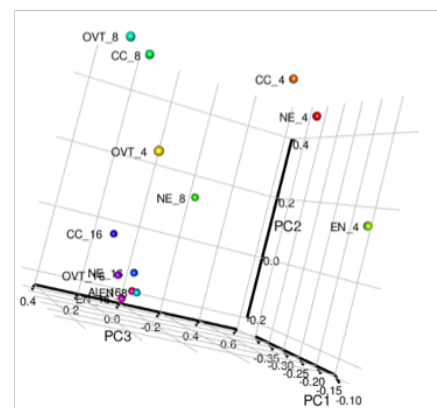
A.



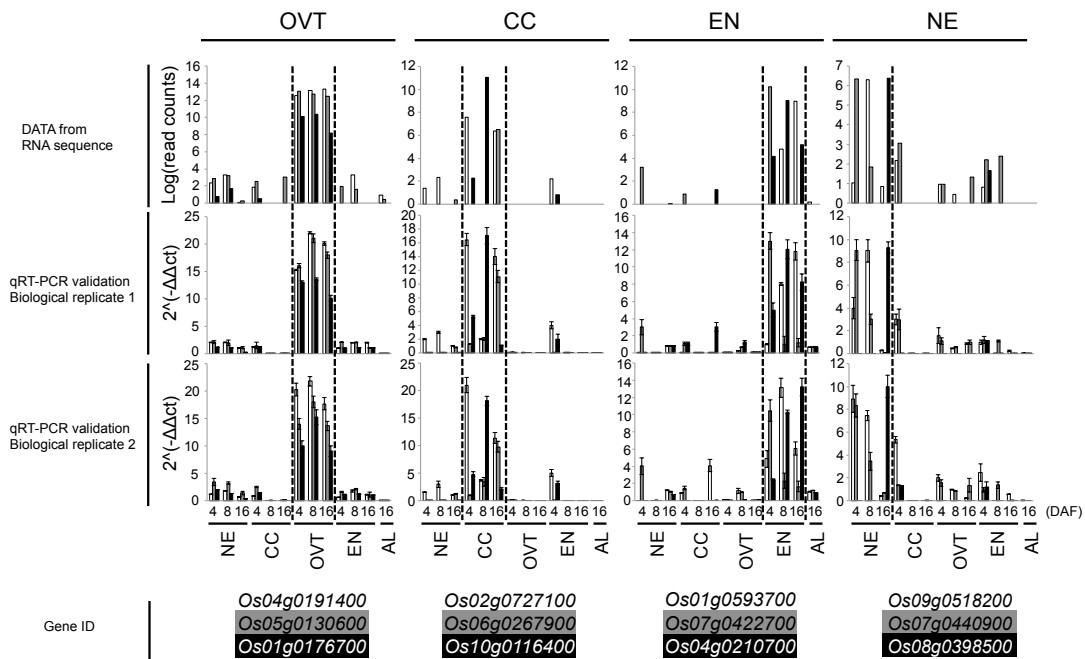
B.



C.

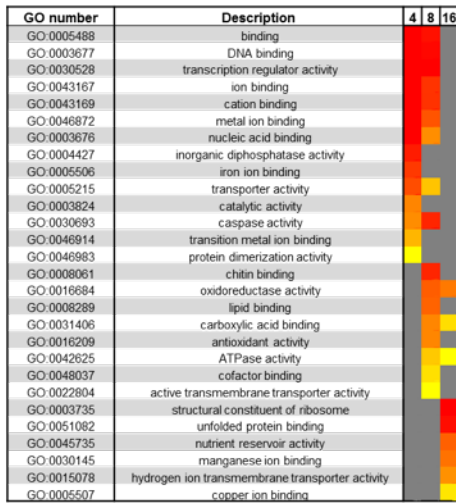


Supplementary Figure 1. Summary of differentially expressed genes and principle component analysis (PCA) for each rice grain sub-region and time point. A. Overview of differentially expressed genes by heatmap for NE, CC, OVT, EN and AL at 4, 8, and 16 DAF. B. Hierarchical clustering for NE, CC, OVT, EN and AL at 4, 8, and 16 DAF with different biological replicates. C. PCA of sub-regions. Principle components through one to three collectively represent 79% of the variance in the dataset. NE: Nucellar Epidermis; CC: Cross Cells; OVT: Ovular Vascular Trace; EN: Endosperm; AL: Aleurone Layer.

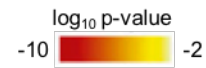
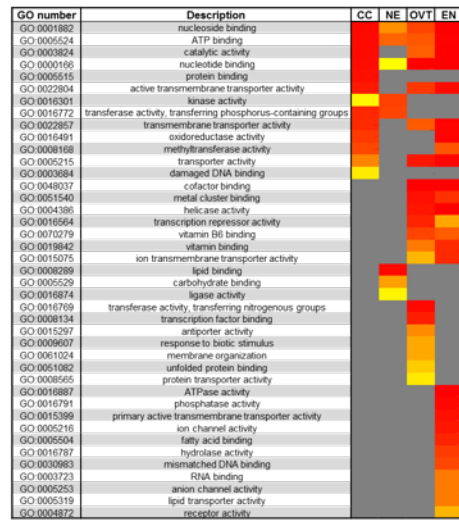


Supplementary Figure 2. qRT-PCR validation of sub-region specific genes. Top three genes from each sub-region were chosen from the list of DEGs. Values are the average of three technical replicates. Data from two biological replicates are shown. The error bars are from three technical replicates. The expression was normalized to the expression of rice *UBIQUITIN 5* (*OsUBQ5*) gene. NE: Nucellar Epidermis; CC: Cross Cells; OVT: Ovular Vascular Trace; EN: Endosperm.

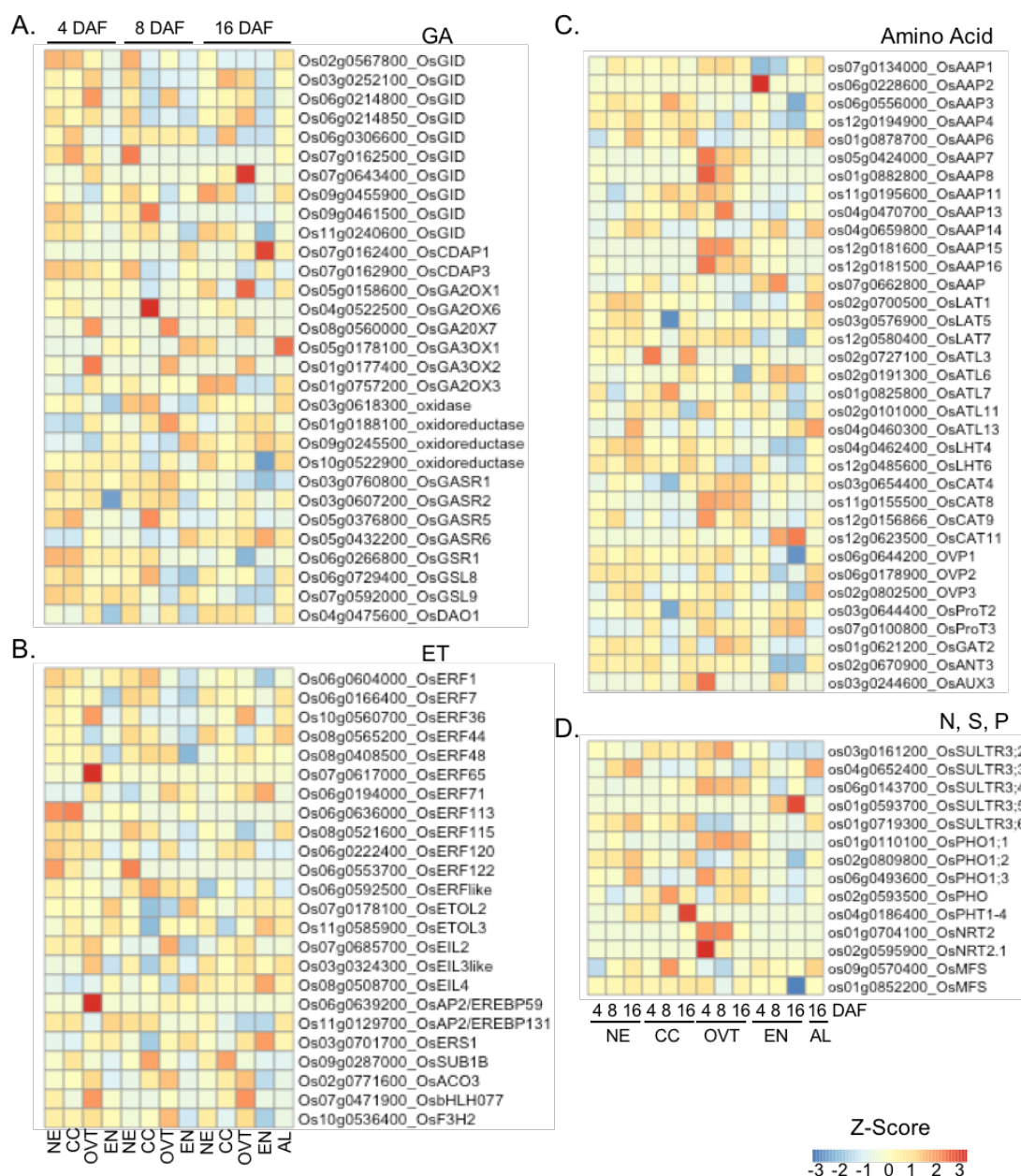
A.



B.



Supplementary Figure 3. Gene Ontology (GO) analysis for molecular function of the DEGs in ovular vascular trace (OVT) at 4, 8 and 16 Days after flowering (DAF), and aleurone layer (AL) of the rice grains. Significantly ($p < 0.01$) overrepresented GO terms in (A) OVT at 4, 8 and 16DAF and (B) AL as compared to CC, NE, OVT and EN are shown as heatmaps. NE: Nucellar Epidermis; CC: Cross Cells and EN: Endosperm.



Supplementary Figure 4. Expression profiles of differentially expressed genes related to hormone metabolism and transporters in rice grain sub-regions. A. Genes related to gibberellin (GA) biosynthesis, signaling and transporters. B. Genes related to ethylene (ET) metabolism, transporters and receptors. C. Genes related to amino acid transport. D. Genes involved in nitrate (N), sulfate (S) and phosphate (P) transport. The gene-normalized signal intensities are shown in the heat maps using Z-Scores. DAF: days after flowering; NE: Nucellar Epidermis; CC: Cross Cells; OVT: Ovular Vascular Trace; EN: Endosperm; AL: Aleurone Layer.

Supplementary Table 1. Kyoto Encyclopedia of Genes and Genomes (KEGG) analysis for OVT, CC and EN. The overrepresented pathways are shown by p-values <0.05

KEGG pathway	No.	p-value
OVT		
Biosynthesis of secondary metabolites	osa01110	4.16E-05
Metabolic pathways	osa01100	2.78E-05
Amino sugar and nucleotide sugar metabolism	osa00520	3.29E-05
Glycolysis / Gluconeogenesis	osa00010	6.70E-05
Starch and sucrose metabolism	osa00500	7.61E-05
CC		
Phenylalanine metabolism	osa00360	1.09E-03
Phenylpropanoid biosynthesis	osa00940	1.94E-03
Plant hormone signal transduction	osa04075	3.51E-03
Biosynthesis of secondary metabolites	osa01110	0.0962
Ribosome	osa03010	6.28E-31
Oxidative phosphorylation	osa00190	1.09E-04
Protein processing in endoplasmic reticulum	osa04141	2.23E-03
Pentose phosphate pathway	osa00030	8.80E-03
Glycerophospholipid metabolism	osa00564	0.0186
Endocytosis	osa04144	0.0195
Metabolic pathways	osa01100	0.031
Spliceosome	osa03040	0.0459
EN		
Photosynthesis	osa00195	1.91E-14
Metabolic pathways	osa01100	5.74E-07
Glycerophospholipid metabolism	osa00564	0.0138
Biosynthesis of secondary metabolites	osa01110	0.0375
Porphyrin and chlorophyll metabolism	osa00860	0.04
Ascorbate and aldarate metabolism	osa00053	1.32E-03
Carbon fixation in photosynthetic organisms	osa00710	5.32E-03

Supplementary Table 2. KEGG analysis for the AL. The overrepresented pathways are shown by p-values <0.05

KEGG pathway	No.	p-value
Biosynthesis of secondary metabolites	osa01110	3.93E-05
Metabolic pathways	osa01100	5.59E-05
Glycolysis / Gluconeogenesis	osa00010	2.70E-03
Ubiquinone biosynthesis	osa00130	2.75E-03
Carbon fixation in photosynthetic organisms	osa00710	4.59E-03
Protein processing in endoplasmic reticulum	osa04141	5.95E-03
RNA degradation	osa03018	9.37E-03
Phosphatidylinositol signaling system	osa04070	0.0114
Pyruvate metabolism	osa00620	0.0137
Glutathione metabolism	osa00480	0.0262
Fatty acid biosynthesis	osa00061	4.21E-03
Steroid biosynthesis	osa00100	0.0109
Carotenoid biosynthesis	osa00906	0.0142
Glycerolipid metabolism	osa00561	0.0178
RNA transport	osa03013	0.0351
Mismatch repair	osa03430	8.10E-06
DNA replication	osa03030	1.75E-05
Ascorbate and aldarate metabolism	osa00053	2.15E-03
Amino sugar and nucleotide sugar metabolism	osa00520	2.33E-03
Oxidative phosphorylation	osa00190	0.0209
N-Glycan biosynthesis	osa00510	0.0214
Ribosome biogenesis in eukaryotes	osa03008	0.0226
Plant-pathogen interaction	osa04626	0.0259
Phenylpropanoid biosynthesis	osa00940	0.0335
Sulfur metabolism	osa00920	0.0339
Plant hormone signal transduction	osa04075	0.0459

Supplementary Table 7. qPCR primers used in this study

GeneID	Primer Name	Direction	Primer sequence (5'-3')
Os04g0191400	O1	F	CTGTCACTGGAACAGCCTCA
		R	GTTTCATCTGGCTGTTGTGGA
Os05g0130600	O2	F	GGCGAGCTCACTTCTTGTC
		R	ACTTGGGCGCCTTTGGTT
Os01g0176700	O3	F	CACGTCTCGAGGAAGAGAGG
		R	CCGATGTTCTTCACCGGTAT
Os02g0727100	C1	F	GACCTGGAGCAGAGTTGGAG
		R	GAGCAGAGGAAGTCGTGGAG
Os06g0267900	C2	F	AATACACGTCGGCCTTATCG
		R	TGCACGTTGTAATGGCAA AT
Os10g0116400	C3	F	ATTCTTGGTGGTTCGACTGG
		R	GGACTTGATGGATGGCAAGT
Os09g0518200	N1	F	CAACGACAGAGGGGTTGAGT
		R	CCATGAACTCCTTGCTCCTC
Os07g0440900	N2	F	GCAAGAAGGAATCCCAACTG
		R	GGTGGTCATCTCACGGATCT
Os08g0398500	N3	F	AGCCAAGGAACATCACAAGG
		R	CCTTCTTCTCCTTGCCCTTC
Os01g0593700	E1	F	TGCTTCCTCATCTTCCTCGT
		R	ATATCGAGCTCGGGTTGATG
Os07g0422700	E2	F	AACCAAGGACGCTTTCAAGA
		R	CGTAAGTTCGGCTCCTTCTG
Os04g0210700	E3	F	GACCATAATGTTCCGTGAAGG
		R	TCTGGAAACCCCTCAAATGT
Os03g0234200	UBQ5	F	ACCACTTCGACCGCCACTACT
		R	ACGCCTAAGCCTGCTGGTT

6. General discussion

6.1 Role of biofortification in combating hidden hunger

Hidden hunger, or malnutrition, is a major health problem worldwide, and it has negative impacts on economic development, especially in the developing countries. Several strategies including industrial fortification and supplementation have been suggested in order to overcome malnutrition, but these require a sustainable industrial processing, access to health care and significant investment. In this regard, biofortification has emerged as a promising strategy to combat the problem of malnutrition. Biofortification relies on the biosynthesis or physiological capacity of plants to accumulate the target nutrients via the use of improved agronomic practices, conventional breeding and/or biotechnology. It is a sustainable, targeted and cost-effective approach to reach the populations where supplementation and other strategies are difficult to implement (Meenakshi et al., 2010).

6.2 Metabolic engineering for improving nutritional profile of staple crops

Metabolic engineering involves the engineering of metabolic pathways by altering the expression of one or several genes associated to the trait of interest (Farre et al., 2014). Several staple crops have been metabolically engineered for improving the nutrient content in their edible parts. For example, β -carotene, a pro-vitamin A, biofortified crops have been developed by transforming target plants with a combination of genes. In rice, maize and wheat, plants were transformed with *PHYTOENE SYNTHASE (PSY)* and *PHYTOENE DESATURASE (CRTI)* which resulted in a significant increase of carotenoids in the seeds (Ye et al., 2000; Paine et al., 2005; Cong et al., 2009; Naqvi et al., 2009). Expression of *1-DEOXYXYLULOSE-5-PHOSPHATE SYNTHASE (DXS)* in combination with bacterial *PHYTOENE SYNTHASE CRTB* also led to a significant increase of carotenoids in cassava (Sayre et al., 2011). Overexpression of genes involved in Vitamin E (α -tocopherol) biosynthesis including *HOMOGENTISATE GERANYLGERANYL TRANSFERASE* and bacterial *PREPHENATE DEHYDROGENASE* resulted in an increase of tocopherols in soybean and canola seeds (Karunanandaa et al., 2005; Tavva et al., 2007). In case of vitamin B1, the overexpression of two thiamin biosynthesis genes, *4-METHYL-5-BETA-HYDROXYETHYLTHIAZOLE PHOSPHATE SYNTHASE* and *4-AMINO-2-METHYL-5-HYDROXYMETHYLPYRIMIDINE PHOSPHATE SYNTHASE*, increased thiamin concentration up to 5-fold in unpolished

rice grains (Dong et al., 2016). Likewise, overexpression of two genes related to biosynthesis of vitamin B6 *de novo* in plants, namely *PDX1* and *PDX2*, resulted in significantly increased bioavailable vitamin B6 in the cassava roots (Li et al., 2015). Increases of folate in rice and maize by introducing folate biosynthesis related genes i.e., *GTP CYCLOHYDROLASE 1 (GTPCHI)* and *AMINODEOXYCHORISMATE SYNTHASE (ADCS)* have also been reported (Storozhenko et al., 2007). Recently, the combined overexpression of *GTPCHI*, *ADCS* and a fusion between a synthetic folate-binding protein (FBP) and *BETA-CARBONIC ANHYDRASE 2* in rice led to an additional increase in folate levels and its stability (Blancquaert et al., 2015).

Most of the biofortification studies targeted to improve the concentration of a single micronutrient. However, several deficiencies often occur simultaneously in affected populations. Hence, the next step will be engineering crops with improved levels of different nutrients in a single variety. So far, there are only few examples of such an approach. A multivitamin white corn with enhanced levels of folate, β -carotene and ascorbate have been reported (Naqvi et al., 2009). More recently, multi-nutrient rice with increased levels of β -carotene, iron and zinc have been developed by transforming rice with multiple genes expressing from a single locus (Singh et al., 2017, in press). Most iron biofortification strategies, particularly those involving overexpression of *NAS* genes, resulted in accompanied zinc increases in addition to the target nutrient iron (Wirth et al., 2009; Boonyaves et al., 2017). The strategies tested in this PhD work also led to simultaneous increases of endosperm iron and zinc concentrations in the rice grains (Chapter 2, 3 and 4). It is imaginable that with the recent progress in genome editing tools coupled with targeted gene mining, development and designing of varieties simultaneously improved for multiple traits will become more practical and achievable.

6.3 New technologies suited for future biofortification strategies

6.3.1 Gene targeting by genome editing tools

The transcription activator-like effector nucleases (TALENs) and Clustered Regularly Interspaced Short Palindromic Repeats (CRISPR)/CRISPR-associated nuclease 9 (Cas9) are two promising genome editing tools that can precisely modify genes, leading to their rapid integration in smart breeding as well as in agricultural biotechnology programs (Christian et al., 2010; Jinek et al., 2012; Feng et al., 2013; Jiang et al., 2013). The double strand breaks (DSBs) introduced at target loci by CRISPR or TALEN nucleases activate

the DNA repair pathways, principally non-homologous end-joining (NHEJ) and homologous recombination (HR) (Puchta et al., 1996). NHEJ causes the disruption of gene function or point mutation, while HR causes gene replacement or targeted gene insertion (Puchta et al., 1996). TALENs are chimeric proteins made by fusing an engineered DNA binding domain with the catalytic domain of FokI endonuclease, which cleaves as a dimer (Christian et al., 2012; Cong et al., 2012). Two monomers bind opposing strands of DNA separated by a spacer, allowing FokI to dimerize and cleave DNA (Christian et al., 2012; Cong et al., 2012). On the other hand, Cas9 nuclease coupled with trans-activating crRNA (tracrRNA) can be guided by a 20-22 nt guide sequence in crRNA, which guide the nuclease to cleave non-self DNA on both strands at a specific site (Jinek et al., 2012; Jinek et al., 2013). Parts of crRNA and tracrRNA sequence can be fused in a synthetic gene to produce a single guide RNA (sgRNA) and the gRNA could be programmed to target specific sites (Jinek et al., 2012; Jinek et al., 2013). These tools have already been tested for targeted gene manipulation in maize (Nemudryi et al., 2014; Bortesi and Fischer, 2015). Phytic acid is an anti-nutrient that chelate iron and reduce its bioavailability. A low-phytate maize has been developed by reducing the expression of the *INOSITOL 1,3,4,5,6-PENTAKISPHOSPHATE 2-KINASE GENE (IPK1)* using both TALEN and CRISPR-Cas9 strategies (Shukla et al., 2009; Liang et al., 2014). In the report from Shukla *et al.* (2009), a herbicide-resistance cassette was recombined into intron 1 of *IPK1* gene, resulting in both herbicide tolerance and the alteration of the inositol phosphate profile in the developing maize seeds. It has been very challenging to create mutations in crops with complex genomes and high content of repetitive DNA, such as hexaploid wheat. The afore-mentioned genome editing tools hold a great potential to manipulate gene expression and create mutations simultaneously in the homeologous wheat genes. For example, using TALEN and CRISPR-Cas9 systems, powdery mildew resistant bread wheat has been developed by targeting mutations in three homeoalleles that encode MILDEW-RESISTANCE LOCUS (MLO) proteins (Wang et al., 2014). Likewise, altering the expression of *DENSE AND ERECT PANICLE 1* and *GASR7* in all homeologs in wheat using CRISPR-Cas9 could increase grain quantity and yield (Zhang et al., 2016c).

6.3.2 Genome-wide association studies (GWAS) and OMICS studies to identify new gene targets

GWAS is an excellent approach to discover genetic factors in a population. Once new genetic associations are identified, this information can be used to develop better biofortification strategies. For example, GWAS have revealed genes involved in plant tolerance to iron toxicity and deficiency (Li and Lan, 2015; Matthus et al., 2015). A GWAS study on Sorghum identified novel quantitative trait loci for polyphenols, which are important anti-nutritional factors for iron bioavailability (Rhodes et al., 2014). Likewise, knowledge about the proteomic and metabolic adaptations to iron deficiency in plants could allow development of crop plants tolerant to iron deficiency, and with increased iron concentration in the edible parts (Lopez-Millan et al., 2013). Several proteomic studies have been done in different plant species under iron deficient conditions in order to identify common or new regulators involved in iron homeostasis (Li et al., 2008a; Lan et al., 2011; Rodriguez-Celma et al., 2011; Hopff et al., 2013). The most commonly regulated functional categories found in different studies are carbon and nitrogen metabolism, glycolysis and TCA cycles. The metabolomics study in the roots and shoots of barley suggested that citrate and malate are two major organic acids which show higher concentration under iron deficient condition (Lopez-Millan et al., 2012). The enzyme activities of GLUCOSE-6-PHOSPHATE DEHYDROGENASE and FUMARASE were also reported to be higher in rice and barley roots under iron deficient condition, indicating the existence of carbon fixation via increased enzyme activities in the roots (Lopez-Millan et al., 2012). So far only few RNA-seq studies have been carried out in the plants grown on different iron conditions, particularly during grain filling stages. The gene expression has been analyzed in the barley Endosperm Transfer Cells (ETC) during grain filling in plants grown under excess iron condition (Darbani et al., 2015). Several components including the auxin and ethylene signaling factors, diurnal fluctuation components, retroelements, sulfur homeostasis components, mineral trafficking components, and vacuole organization factors were highlighted to be involved in the iron homeostasis maintenance (Darbani et al., 2015).

6.4 Understanding grain development by using OMICS approaches and bioinformatics tools

6.4.1 Proteomics and metabolomics

Large scale transcriptomic analysis based on RNA-seq is a widely used tool to gain overview of the gene expression network in the developing grains. However, due to post-transcriptional regulation, protein stability and post-translational modifications, transcript levels often do not correlate with protein expression. Therefore, investigation of the proteomics and metabolomics are crucial to completely reveal the main components underlying grain development. Several studies including those on whole seed, embryo and/or endosperm have revealed the reorganization and reprogramming of protein expressions during grain development (Xu et al., 2008; Liao et al., 2014; Bonnot et al., 2015; Cao et al., 2016). The differentially expressed proteins were involved in central metabolic or regulatory pathways, including carbohydrate metabolism and protein synthesis, folding and degradation. These studies provided proteomic confirmation that seed formation and development involve diverse and complicated pathways. In case of embryo proteins, phosphoproteins were suggested to play an important role in biomolecular signaling and hormonal interplay during cell division, differentiation and delineation (Qiu et al., 2016). In the endosperm, proteins mediating cell growth and morphogenesis showed higher expression in the early developmental stages, whereas proteins involved in starch synthesis and programmed cell death were reported to be up-regulated during mid and late developmental stages, respectively (Deng et al., 2013).

The grain metabolomics analysis have been done in the barley grains on different grain sub-regions during different grain filling stages (Peukert et al., 2014). Various types of oligofructans showed specific distribution patterns. Levan- and graminan-type oligofructans were synthesized in the cellularized endosperm prior to the commencement of starch biosynthesis, while during the storage phase, inulin-type oligofructans accumulated to a higher concentration in and around the nascent endosperm cavity (Peukert et al., 2014). The tight partitioning of oligofructan biosynthesis indicates the distinct functions of the various fructan types in the young endosperm prior to starch accumulation and in the ETCs that accomplish the assimilate supply towards the endosperm during the storage phase. A similar metabolite profiling study has been done in the ETCs in barley grains during different development stages (Thiel et al., 2012). High level of proline and 4-hydroxyproline (HYP) were detected in the ETCs in early

developmental stage, suggesting their requirement for the biosynthesis of proline-rich cell wall proteins and HYP-rich glycoproteins during early ETCs development.

6.4.2 Transcriptomic data modeling and network construction

The massive data generated by omics technologies require further bioinformatics analysis such as network analysis and data modeling. The omics data modeling is becoming a powerful analytical tool for understanding whole biological systems and prediction of gene functions (Yonekura-Sakakibara et al., 2013). Various networks including gene co-expression, metabolite-to-metabolite, gene-to-protein, gene-to-metabolite and protein-protein interaction have been elucidated by using omics data generated from Arabidopsis seeds (Hajduch et al., 2010; Belmonte et al., 2013; Francoz et al., 2015). For example, the protein and transcript expression data have been collected from five sequential stages of Arabidopsis seed development encompassing the period of reserve polymer accumulation. The subsequent pattern analysis on 319 protein-transcript pairs was then established by using general linear modeling. Overall, more than 56% of expression pairs showed concurrence that includes the carbohydrate metabolism pathway during seed development in Arabidopsis (Hajduch et al., 2010). In addition, transcriptional gene co-expression modules regulating seed maturation and germination in Arabidopsis have also been predicted. Fifty-four genes required for mucilage synthesis during seed maturation and release for facilitating seeds germination have been identified, which included novel transcription factor and its downstream regulatory network in different seed sub-regions (Francoz et al., 2015).

Similarly, in order to uncover the pattern of storage proteins in developing cereal seeds in response to environmental and genetic perturbation, a metabolic network in the developing endosperm of barley grains have been computationally analyzed (Grafahrend-Belau et al., 2009). The model included 25 biochemical and transport reactions across four different grain sub-regions to study grain yield and metabolic flux distribution in response to oxygen depletion and enzyme deletion (Grafahrend-Belau et al., 2009). As a result, the model provided an insight into active metabolic pathway and growth rate in different stress conditions as well as the potential role of inorganic pyrophosphate metabolism to maintain seed metabolism under oxygen deprivation. In addition, by integrating the metabolite data with the RNA-seq data at three different grain development stages, six co-regulatory networks were constructed to explore inositol

phosphates (IPs) metabolism and their interactions with other pathways in the maize (Zhang et al., 2016b). Three new target genes were identified by using co-regulatory model including genes encoding IP synthesis enzyme, IP transporter and IP co-transporter into vesicles (Zhang et al., 2016b). In this study, a gene co-expression network has been predicted for Ovular Vascular Trace (OVT) differentially expressed genes that emphasized a distinct role of OVT in micronutrient transport during the course of rice grain development (Chapter 5).

6.5 Summary of the findings of this PhD work

In this thesis, the potential of *AtNRAMP3* and *AtFRD3* in iron and zinc enhancement in rice grains have been evaluated. The results showed that the expression of *AtNRAMP3* and *AtFRD3* in combination with *NAS* and *FER* expression could significantly increase endosperm iron without any increase in the cadmium accumulation in the rice grains. Among the tested strategies, the expression of *AtNRAMP3* under the control of aleurone and embryo specific promoter Ole 18 in combination with constitutively expressed *NAS* and endosperm specifically expressed *FER* led to highest increases of iron concentration in the polished rice grains. Further characterization of the plants developed using these distinct strategies would be required in order to identify the underlying reasons for the differences in the achieved iron increases. In case of *AtFRD3* overexpressing plants, it is perhaps possible that co-expressing a citrate biosynthesis related gene together with the citrate transporter encoding gene (*AtFRD3*) could further increase the iron concentrations, by boosting citrate production in addition to an efficient transport of citrate-Fe complexes. Furthermore, preliminary analysis on transgenic plants revealed their higher tolerance to low iron growth conditions. It would also be interesting to test the performance of potential lines in cadmium contaminated rice-paddy fields or in calcareous soils. This work also evaluated the gene expression patterns in different rice grain sub-regions during grain development. Various spatiotemporal genes have been identified in different grain sub-regions, providing a valuable dataset for understating the molecular mechanisms underlying grain development. The dataset provides avenues for further studies such as functional and molecular characterization of candidate genes. With the progress made in genome editing tools, it is now possible to design better biofortification strategies involving tissue- or stage- specifically expressing constructs with precise insertion into the genome.

7. References

- Abbaspour, N., Hurrell, R., and Kelishadi, R. (2014). Review on iron and its importance for human health. *J Res Med Sci* 19:164-174.
- Alvarez-Fernandez, A., Diaz-Benito, P., Abadia, A., Lopez-Millan, A.F., and Abadia, J. (2014). Metal species involved in long distance metal transport in plants. *Front Plant Sci* 5:105.
- Antosiewicz, D.M., Barabasz, A., and Siemianowski, O. (2014). Phenotypic and molecular consequences of overexpression of metal-homeostasis genes. *Front Plant Sci* 5.
- Aoyama, T., Kobayashi, T., Takahashi, M., Nagasaka, S., Usuda, K., Kakei, Y., Ishimaru, Y., Nakanishi, H., Mori, S., and Nishizawa, N.K. (2009). OsYSL18 is a rice iron(III)-deoxymugineic acid transporter specifically expressed in reproductive organs and phloem of lamina joints. *Plant Mol Biol* 70:681-692.
- Ariga, T., Hazama, K., Yanagisawa, S., and Yoneyama, T. (2014). Chemical forms of iron in xylem sap from graminaceous and non-graminaceous plants. *Soil Sci Plant Nutr* 60:460-469.
- Aung, M.S., Masuda, H., Kobayashi, T., Nakanishi, H., Yamakawa, T., and Nishizawa, N.K. (2013). Iron biofortification of Myanmar rice. *Front Plant Sci* 4.
- Bailey, T.L., Boden, M., Buske, F.A., Frith, M., Grant, C.E., Clementi, L., Ren, J., Li, W.W., and Noble, W.S. (2009). MEME SUITE: tools for motif discovery and searching. *Nucleic Acids Res* 37:W202-208.
- Bashir, K., Inoue, H., Nagasaka, S., Takahashi, M., Nakanishi, H., Mori, S., and Nishizawa, N.K. (2006). Cloning and characterization of deoxymugineic acid synthase genes from graminaceous plants. *J Biol Chem* 281:32395-32402.
- Bashir, K., Ishimaru, Y., Itai, R.N., Senoura, T., Takahashi, M., An, G., Oikawa, T., Ueda, M., Sato, A., Uozumi, N., et al. (2015). Iron deficiency regulated OsOPT7 is essential for iron homeostasis in rice. *Plant Mol Biol* 88:165-176.
- Bashir, K., Ishimaru, Y., and Nishizawa, N.K. (2010). Iron Uptake and Loading into Rice Grains. *Rice* 3:122-130.
- Bashir, K., Ishimaru, Y., Shimo, H., Nagasaka, S., Fujimoto, M., Takanashi, H., Tsutsumi, N., An, G., Nakanishi, H., and Nishizawa, N.K. (2011). The rice mitochondrial iron transporter is essential for plant growth. *Nat Commun* 2.
- Bashir, K., Takahashi, R., Akhtar, S., Ishimaru, Y., Nakanishi, H., and Nishizawa, N.K. (2013). The knockdown of OsVIT2 and MIT affects iron localization in rice seed. *Rice* 6.
- Baxter, I., Tchieu, J., Sussman, M.R., Boutry, M., Palmgren, M.G., Gribskov, M., Harper, J.F., and Axelsen, K.B. (2003). Genomic comparison of P-type ATPase ion pumps in Arabidopsis and rice. *Plant Physiol* 132:618-628.
- Belmonte, M.F., Kirkbride, R.C., Stone, S.L., Pelletier, J.M., Bui, A.Q., Yeung, E.C., Hashimoto, M., Fei, J., Harada, M., Munoz, M.D., et al. (2013). Comprehensive developmental profiles of gene activity in regions and subregions of the Arabidopsis seed. *Proc Natl Acad Sci U S A* 110:E435-E444.
- Berezky, Z., Wang, H.Y., Schubert, V., Ganai, M., and Bauer, P. (2003). Differential regulation of nramp and irt metal transporter genes in wild type and iron uptake mutants of tomato. *J Biol Chem* 278:24697-24704.
- Blancquaert, D., Van Daele, J., Strobbe, S., Kiekens, F., Storozhenko, S., De Steur, H., Gellynck, X., Lambert, W., Stove, C., and Van Der Straeten, D. (2015). Improving folate (vitamin B-9) stability in biofortified rice through metabolic engineering. *Nat Biotechnol* 33:1076-+.

- Bonnot, T., Bancel, E., Chambon, C., Boudet, J., Branlard, G., and Martre, P. (2015). Changes in the nuclear proteome of developing wheat (*Triticum aestivum* L.) grain. *Front Plant Sci* 6.
- Boonyaves, K., Gruissem, W., and Bhullar, N.K. (2016). NOD promoter-controlled AtIRT1 expression functions synergistically with NAS and FERRITIN genes to increase iron in rice grains. *Plant Mol Biol* 90:207-215.
- Boonyaves, K., Wu, T.Y., Gruissem, W., and Bhullar, N.K. (2017). Enhanced Grain Iron Levels in Rice Expressing an IRON-REGULATED METAL TRANSPORTER, NICOTIANAMINE SYNTHASE, and FERRITIN Gene Cassette. *Front Plant Sci* 8.
- Bortesi, L., and Fischer, R. (2015). The CRISPR/Cas9 system for plant genome editing and beyond. *Biotechnol Adv* 33:41-52.
- Bouis, H.E., Hotz, C., McClafferty, B., Meenakshi, J.V., and Pfeiffer, W.H. (2011). Biofortification: A new tool to reduce micronutrient malnutrition. *Food Nutr Bull* 32:S31-S40.
- Briat, J.F., Curie, C., and Gaymard, F. (2007). Iron utilization and metabolism in plants. *Curr Opin Plant Biol* 10:276-282.
- Briat, J.F., Duc, C., Ravet, K., and Gaymard, F. (2010). Ferritins and iron storage in plants. *Bba-Gen Subjects* 1800:806-814.
- Buchner, P., Takahashi, H., and Hawkesford, M.J. (2004). Plant sulphate transporters: co-ordination of uptake, intracellular and long-distance transport. *J Exp Bot* 55:1765-1773.
- Buske, F.A., Boden, M., Bauer, D.C., and Bailey, T.L. (2010). Assigning roles to DNA regulatory motifs using comparative genomics. *Bioinformatics* 26:860-866.
- Cao, H., He, M., Zhu, C., Yuan, L.L., Dong, L.W., Bian, Y.W., Zhang, W.Y., and Yan, Y.M. (2016). Distinct metabolic changes between wheat embryo and endosperm during grain development revealed by 2D-DIGE-based integrative proteome analysis. *Proteomics* 16:1515-1536.
- Chaudhury, A.M., Koltunow, A., Payne, T., Luo, M., Tucker, M.R., Dennis, E.S., and Peacock, W.J. (2001). Control of early seed development. *Annu Rev Cell Dev Bi* 17:677-699.
- Chen, J., Zeng, B., Zhang, M., Xie, S.J., Wang, G.K., Hauck, A., and Lai, J.S. (2014). Dynamic Transcriptome Landscape of Maize Embryo and Endosperm Development. *Plant Physiol* 166:252-264.
- Cheng, X.Y., Wu, Y., Guo, J.P., Du, B., Chen, R.Z., Zhu, L.L., and He, G.C. (2013). A rice lectin receptor-like kinase that is involved in innate immune responses also contributes to seed germination. *Plant J* 76:687-698.
- Childs, C.W. (1981). Field-Tests for Ferrous Iron and Ferric-Organic Complexes (on Exchange Sites or in Water-Soluble Forms) in Soils. *Aust J Soil Res* 19:175-180.
- Christian, M., Cermak, T., Doyle, E.L., Schmidt, C., Zhang, F., Hummel, A., Bogdanove, A.J., and Voytas, D.F. (2010). Targeting DNA Double-Strand Breaks with TAL Effector Nucleases. *Genetics* 186:757-U476.
- Christian, M.L., Demorest, Z.L., Starker, C.G., Osborn, M.J., Nyquist, M.D., Zhang, Y., Carlson, D.F., Bradley, P., Bogdanove, A.J., and Voytas, D.F. (2012). Targeting G with TAL Effectors: A Comparison of Activities of TALENs Constructed with NN and NK Repeat Variable Di-Residues. *PLoS One* 7.
- Chu, H.H., Chiecko, J., Punshon, T., Lanzirrotti, A., Lahner, B., Salt, D.E., and Walker, E.L. (2010). Successful Reproduction Requires the Function of Arabidopsis YELLOW STRIPE-LIKE1 and YELLOW STRIPE-LIKE3 Metal-Nicotianamine

- Transporters in Both Vegetative and Reproductive Structures. *Plant Physiol* 154:197-210.
- Cline, M.S., Smoot, M., Cerami, E., Kuchinsky, A., Landys, N., Workman, C., Christmas, R., Avila-Campilo, I., Creech, M., Gross, B., et al. (2007). Integration of biological networks and gene expression data using Cytoscape. *Nature protocols* 2:2366-2382.
- Colman, D. (2004). World agriculture towards 2015/2030: An FAO perspective. *World Econ* 27:114-115.
- Coman, D., Rutimann, P., and Gruissem, W. (2014). A flexible protocol for targeted gene co-expression network analysis. *Methods Mol Biol* 1153:285-299.
- Cong, L., Wang, C., Chen, L., Liu, H.J., Yang, G.X., and He, G.Y. (2009). Expression of phytoene synthase1 and Carotene Desaturase crtI Genes Result in an Increase in the Total Carotenoids Content in Transgenic Elite Wheat (*Triticum aestivum* L.). *J Agr Food Chem* 57:8652-8660.
- Cong, L., Zhou, R.H., Kuo, Y.C., Cunniff, M., and Zhang, F. (2012). Comprehensive interrogation of natural TALE DNA-binding modules and transcriptional repressor domains. *Nat Commun* 3.
- Connolly, E.L., Campbell, N.H., Grotz, N., Prichard, C.L., and Guerinot, M.L. (2003). Overexpression of the FRO2 ferric chelate reductase confers tolerance to growth on low iron and uncovers posttranscriptional control. *Plant Physiol* 133:1102-1110.
- Conte, S., Stevenson, D., Furner, I., and Lloyd, A. (2009). Multiple Antibiotic Resistance in *Arabidopsis* Is Conferred by Mutations in a Chloroplast-Localized Transport Protein. *Plant Physiol* 151:559-573.
- Conte, S.S., Chu, H.H., Chan-Rodriguez, D., Punshon, T., Vasques, K.A., Salt, D.E., and Walker, E.L. (2013). *Arabidopsis thaliana* Yellow Stripe1-Like4 and Yellow Stripe1-Like6 localize to internal cellular membranes and are involved in metal ion homeostasis. *Front Plant Sci* 4.
- Curie, C., Alonso, J.M., Le Jean, M., Ecker, J.R., and Briat, J.F. (2000). Involvement of NRAMP1 from *Arabidopsis thaliana* in iron transport. *Biochem J* 347 Pt 3:749-755.
- Curie, C., Cassin, G., Couch, D., Divol, F., Higuchi, K., Jean, M., Misson, J., Schikora, A., Czernic, P., and Mari, S. (2009). Metal movement within the plant: contribution of nicotianamine and yellow stripe 1-like transporters. *Ann Bot-London* 103:1-11.
- Curie, C., Panaviene, Z., Loulergue, C., Dellaporta, S.L., Briat, J.F., and Walker, E.L. (2001). Maize yellow stripe1 encodes a membrane protein directly involved in Fe(III) uptake. *Nature* 409:346-349.
- DalCorso, G., Farinati, S., and Furini, A. (2010). Regulatory networks of cadmium stress in plants. *Plant Signal Behav* 5:663-667.
- Darbani, B., Noeparvar, S., and Borg, S. (2015). Deciphering Mineral Homeostasis in Barley Seed Transfer Cells at Transcriptional Level. *PLoS One* 10.
- Deng, Z.Y., Gong, C.Y., and Wang, T. (2013). Use of proteomics to understand seed development in rice. *Proteomics* 13:1784-1800.
- DiDonato, R.J., Roberts, L.A., Sanderson, T., Easley, R.B., and Walker, E.L. (2004). *Arabidopsis* Yellow Stripe-Like2 (YSL2): a metal-regulated gene encoding a plasma membrane transporter of nicotianamine-metal complexes. *Plant J* 39:403-414.

- Divol, F., Couch, D., Conejero, G., Roschztardt, H., Mari, S., and Curie, C. (2013). The Arabidopsis YELLOW STRIPE LIKE4 and 6 Transporters Control Iron Release from the Chloroplast. *Plant Cell* 25:1040-1055.
- Dong, W., Thomas, N., Ronald, P.C., and Goyer, A. (2016). Overexpression of Thiamin Biosynthesis Genes in Rice Increases Leaf and Unpolished Grain Thiamin Content But Not Resistance to *Xanthomonas oryzae* pv. *oryzae*. *Front Plant Sci* 7:616.
- Douchkov, D., Gryczka, C., Stephan, U.W., Hell, R., and Baumlein, H. (2005). Ectopic expression of nicotianamine synthase genes results in improved iron accumulation and increased nickel tolerance in transgenic tobacco. *Plant Cell Environ* 28:365-374.
- Durrett, T.P., Gassmann, W., and Rogers, E.E. (2007). The FRD3-mediated efflux of citrate into the root vasculature is necessary for efficient iron translocation. *Plant Physiol* 144:197-205.
- Duy, D., Stube, R., Wanner, G., and Philippar, K. (2011). The Chloroplast Permease PIC1 Regulates Plant Growth and Development by Directing Homeostasis and Transport of Iron. *Plant Physiol* 155:1709-1722.
- Duy, D., Wanner, G., Meda, A.R., von Wiren, N., Soll, J., and Philippar, K. (2007). PIC1, an ancient permease in Arabidopsis chloroplasts, mediates iron transport. *Plant Cell* 19:986-1006.
- Eide, D., Broderius, M., Fett, J., and Guerinot, M.L. (1996). A novel iron-regulated metal transporter from plants identified by functional expression in yeast. *Proc Natl Acad Sci U S A* 93:5624-5628.
- Eitinger, T., Suhr, J., Moore, L., and Smith, J.A.C. (2005). Secondary transporters for nickel and cobalt ions: Theme and variations. *Biometals* 18:399-405.
- Farre, G., Blancquaert, D., Capell, T., Van Der Straeten, D., Christou, P., and Zhu, C.F. (2014). Engineering Complex Metabolic Pathways in Plants. *Annu Rev Plant Biol* 65:187-+.
- Feng, H., Yan, M., Fan, X., Li, B., Shen, Q., Miller, A.J., and Xu, G. (2011). Spatial expression and regulation of rice high-affinity nitrate transporters by nitrogen and carbon status. *J Exp Bot* 62:2319-2332.
- Feng, Z.Y., Zhang, B.T., Ding, W.N., Liu, X.D., Yang, D.L., Wei, P.L., Cao, F.Q., Zhu, S.H., Zhang, F., Mao, Y.F., et al. (2013). Efficient genome editing in plants using a CRISPR/Cas system. *Cell Res* 23:1229-1232.
- Finazzi, G., Petroustos, D., Tomizioli, M., Flori, S., Sautron, E., Villanova, V., Rolland, N., and Seigneurin-Berny, D. (2015). Ions channels/transporters and chloroplast regulation. *Cell Calcium* 58:86-97.
- Finney, L.A., and O'Halloran, T.V. (2003). Transition metal speciation in the cell: insights from the chemistry of metal ion receptors. *Science* 300:931-936.
- Fleet, C.M., and Sun, T.P. (2005). A DELLAcate balance: the role of gibberellin in plant morphogenesis. *Curr Opin Plant Biol* 8:77-85.
- Ford, G.C., Harrison, P.M., Rice, D.W., Smith, J.M.A., Treffry, A., White, J.L., and Yariv, J. (1984). Ferritin - Design and Formation of an Iron-Storage Molecule. *Philos T Roy Soc B* 304:551-&.
- Forestan, C., Farinati, S., and Varotto, S. (2012). The maize PIN gene family of auxin transporters. *Front Plant Sci* 3.
- Francoz, E., Ranocha, P., Burlat, V., and Dunand, C. (2015). Arabidopsis seed mucilage secretory cells: regulation and dynamics. *Trends Plant Sci* 20:515-524.
- Galbraith, D.W., and Birnbaum, K. (2006). Global studies of cell type-specific gene expression in plants. *Annu Rev Plant Biol* 57:451-475.

- Gao, Y., Xu, H., Shen, Y., and Wang, J. (2013). Transcriptomic analysis of rice (*Oryza sativa*) endosperm using the RNA-Seq technique. *Plant Mol Biol* 81:363-378.
- Gillies, S.A., Futardo, A., and Henry, R.J. (2012). Gene expression in the developing aleurone and starchy endosperm of wheat. *Plant Biotechnol J* 10:668-679.
- Gollhofer, J., Timofeev, R., Lan, P., Schmidt, W., and Buckhout, T.J. (2014). Vacuolar-Iron-Transporter1-Like Proteins Mediate Iron Homeostasis in Arabidopsis. *PLoS One* 9.
- Goto, F., Yoshihara, T., Shigemoto, N., Toki, S., and Takaiwa, F. (1999). Iron fortification of rice seed by the soybean ferritin gene. *Nat Biotechnol* 17:282-286.
- Grafahrend-Belau, E., Schreiber, F., Koschutzki, D., and Junker, B.H. (2009). Flux Balance Analysis of Barley Seeds: A Computational Approach to Study Systemic Properties of Central Metabolism. *Plant Physiol* 149:585-598.
- Green, L.S., and Rogers, E.E. (2004). FRD3 controls iron localization in Arabidopsis. *Plant Physiol* 136:2523-2531.
- Gupta, S., Stamatoyannopoulos, J.A., Bailey, T.L., and Noble, W.S. (2007). Quantifying similarity between motifs. *Genome Biol* 8:R24.
- Hajduch, M., Hearne, L.B., Miernyk, J.A., Casteel, J.E., Joshi, T., Agrawal, G.K., Song, Z., Zhou, M.Y., Xu, D., and Thelen, J.J. (2010). Systems Analysis of Seed Filling in Arabidopsis: Using General Linear Modeling to Assess Concordance of Transcript and Protein Expression. *Plant Physiol* 152:2078-2087.
- Halliwell, B. (2006). Reactive species and antioxidants. Redox biology is a fundamental theme of aerobic life. *Plant Physiol* 141:312-322.
- Harris, W.R., Sammons, R.D., and Grabiak, R.C. (2012). A speciation model of essential trace metal ions in phloem. *J Inorg Biochem* 116:140-150.
- Harrison, P.M., Andrews, S.C., Artymiuk, P.J., Ford, G.C., Guest, J.R., Hirzmann, J., Lawson, D.M., Livingstone, J.C., Smith, J.M.A., Treffry, A., et al. (1991). Probing Structure-Function Relations in Ferritin and Bacterioferritin. *Adv Inorg Chem Rad* 36:449-486.
- Henriques, R., Jasik, J., Klein, M., Martinoia, E., Feller, U., Schell, J., Pais, M.S., and Koncz, C. (2002). Knock-out of Arabidopsis metal transporter gene IRT1 results in iron deficiency accompanied by cell differentiation defects. *Plant Mol Biol* 50:587-597.
- Higuchi, K., Suzuki, K., Nakanishi, H., Yamaguchi, H., Nishizawa, N.K., and Mori, S. (1999). Cloning of nicotianamine synthase genes, novel genes involved in the biosynthesis of phyto siderophores. *Plant Physiol* 119:471-479.
- Hirano, K., Aya, K., Hobo, T., Sakakibara, H., Kojima, M., Shim, R.A., Hasegawa, Y., Ueguchi-Tanaka, M., and Matsuoka, M. (2008). Comprehensive transcriptome analysis of phytohormone biosynthesis and signaling genes in microspore/pollen and tapetum of rice. *Plant Cell Physiol* 49:1429-1450.
- Hirano, K., Aya, K., Morinaka, Y., Nagamatsu, S., Sato, Y., Antonio, B.A., Namiki, N., Nagamura, Y., and Matsuoka, M. (2013a). Survey of genes involved in rice secondary cell wall formation through a co-expression network. *Plant Cell Physiol* 54:1803-1821.
- Hirano, K., Kondo, M., Aya, K., Miyao, A., Sato, Y., Antonio, B.A., Namiki, N., Nagamura, Y., and Matsuoka, M. (2013b). Identification of transcription factors involved in rice secondary cell wall formation. *Plant Cell Physiol* 54:1791-1802.
- Hood, E.E., Gelvin, S.B., Melchers, L.S., and Hoekema, A. (1993). New Agrobacterium Helper Plasmids for Gene-Transfer to Plants. *Transgenic Res* 2:208-218.
- Hopff, D., Wienkoop, S., and Luthje, S. (2013). The plasma membrane proteome of maize roots grown under low and high iron conditions. *J Proteomics* 91:605-618.

- Hu, X.Y., Tanaka, A., and Tanaka, R. (2013). Simple extraction methods that prevent the artifactual conversion of chlorophyll to chlorophyllide during pigment isolation from leaf samples. *Plant Methods* 9.
- Hurrell, R.F. (2002). Fortification: overcoming technical and practical barriers. *J Nutr* 132:806S-812S.
- Inoue, H., Higuchi, K., Takahashi, M., Nakanishi, H., Mori, S., and Nishizawa, N.K. (2003). Three rice nicotianamine synthase genes, OsNAS1, OsNAS2, and OsNAS3 are expressed in cells involved in long-distance transport of iron and differentially regulated by iron. *Plant J* 36:366-381.
- Inoue, H., Kobayashi, T., Nozoye, T., Takahashi, M., Kakei, Y., Suzuki, K., Nakazono, M., Nakanishi, H., Mori, S., and Nishizawa, N.K. (2009). Rice OsYSL15 Is an Iron-regulated Iron(III)-Deoxymugineic Acid Transporter Expressed in the Roots and Is Essential for Iron Uptake in Early Growth of the Seedlings. *J Biol Chem* 284:3470-3479.
- Inoue, H., Mizuno, D., Takahashi, M., Nakanishi, H., Mori, S., and Nishizawa, N.K. (2004). A rice FRD3-like (OsFRDL1) gene is expressed in the cells involved in long-distance transport. *Soil Sci Plant Nutr* 50:1133-1140.
- Ishimaru, Y., Bashir, K., Fujimoto, M., An, G., Itai, R.N., Tsutsumi, N., Nakanishi, H., and Nishizawa, N.K. (2009). Rice-Specific Mitochondrial Iron-Regulated Gene (MIR) Plays an Important Role in Iron Homeostasis. *Mol Plant* 2:1059-1066.
- Ishimaru, Y., Bashir, K., and Nishizawa, N.K. (2011). Zn Uptake and Translocation in Rice Plants. *Rice* 4:21-27.
- Ishimaru, Y., Kim, S., Tsukamoto, T., Oki, H., Kobayashi, T., Watanabe, S., Matsuhashi, S., Takahashi, M., Nakanishi, H., Mori, S., et al. (2007). Mutational reconstructed ferric chelate reductase confers enhanced tolerance in rice to iron deficiency in calcareous soil. *Proc Natl Acad Sci U S A* 104:7373-7378.
- Ishimaru, Y., Masuda, H., Bashir, K., Inoue, H., Tsukamoto, T., Takahashi, M., Nakanishi, H., Aoki, N., Hirose, T., Ohsugi, R., et al. (2010). Rice metal-nicotianamine transporter, OsYSL2, is required for the long-distance transport of iron and manganese. *Plant J* 62:379-390.
- Ishimaru, Y., Suzuki, M., Tsukamoto, T., Suzuki, K., Nakazono, M., Kobayashi, T., Wada, Y., Watanabe, S., Matsuhashi, S., Takahashi, M., et al. (2006). Rice plants take up iron as an Fe³⁺-phytosiderophore and as Fe²⁺. *Plant J* 45:335-346.
- Iwai, T., Takahashi, M., Oda, K., Terada, Y., and Yoshida, K.T. (2012). Dynamic changes in the distribution of minerals in relation to phytic acid accumulation during rice seed development. *Plant Physiol* 160:2007-2014.
- Jabnoue, M., Secco, D., Lecampion, C., Robaglia, C., Shu, Q., and Poirier, Y. (2013). A rice cis-natural antisense RNA acts as a translational enhancer for its cognate mRNA and contributes to phosphate homeostasis and plant fitness. *Plant Cell* 25:4166-4182.
- Jain, A., Wilson, G.T., and Connolly, E.L. (2014). The diverse roles of FRO family metalloreductases in iron and copper homeostasis. *Front Plant Sci* 5.
- Jeong, D.H., An, S., Park, S., Kang, H.G., Park, G.G., Kim, S.R., Sim, J., Kim, Y.O., Kim, M.K., Kim, S.R., et al. (2006). Generation of a flanking sequence-tag database for activation-tagging lines in japonica rice. *Plant J* 45:123-132.
- Jeong, J., Cohu, C., Kerkeb, L., Pilon, M., Connolly, E.L., and Guerinot, M.L. (2008). Chloroplast Fe(III) chelate reductase activity is essential for seedling viability under iron limiting conditions. *Proc Natl Acad Sci U S A* 105:10619-10624.

- Jia, H., Ren, H., Gu, M., Zhao, J., Sun, S., Zhang, X., Chen, J., Wu, P., and Xu, G. (2011). The phosphate transporter gene *OsPht1;8* is involved in phosphate homeostasis in rice. *Plant Physiol* 156:1164-1175.
- Jiang, W.B., and Lin, W.H. (2013). Brassinosteroid functions in Arabidopsis seed development. *Plant Signal Behav* 8.
- Jiang, W.Z., Zhou, H.B., Bi, H.H., Fromm, M., Yang, B., and Weeks, D.P. (2013). Demonstration of CRISPR/Cas9/sgRNA-mediated targeted gene modification in Arabidopsis, tobacco, sorghum and rice. *Nucleic Acids Res* 41.
- Jinek, M., Chylinski, K., Fonfara, I., Hauer, M., Doudna, J.A., and Charpentier, E. (2012). A Programmable Dual-RNA-Guided DNA Endonuclease in Adaptive Bacterial Immunity. *Science* 337:816-821.
- Jinek, M., East, A., Cheng, A., Lin, S., Ma, E.B., and Doudna, J. (2013). RNA-programmed genome editing in human cells. *Elife* 2.
- Johnson, A.A.T., Kyriacou, B., Callahan, D.L., Carruthers, L., Stangoulis, J., Lombi, E., and Tester, M. (2011). Constitutive Overexpression of the *OsNAS* Gene Family Reveals Single-Gene Strategies for Effective Iron- and Zinc-Biofortification of Rice Endosperm. *PLoS One* 6.
- Takei, Y., Ishimaru, Y., Kobayashi, T., Yamakawa, T., Nakanishi, H., and Nishizawa, N.K. (2012). *OsYSL16* plays a role in the allocation of iron. *Plant Mol Biol* 79:583-594.
- Kanno, Y., Jikumaru, Y., Hanada, A., Nambara, E., Abrams, S.R., Kamiya, Y., and Seo, M. (2010). Comprehensive hormone profiling in developing Arabidopsis seeds: examination of the site of ABA biosynthesis, ABA transport and hormone interactions. *Plant Cell Physiol* 51:1988-2001.
- Karunanandaa, B., Qi, Q.G., Hao, M., Baszis, S.R., Jensen, P.K., Wong, Y.H.H., Jiang, J., Venkatramesh, M., Gruys, K.J., Moshiri, F., et al. (2005). Metabolically engineered oilseed crops with enhanced seed tocopherol. *Metab Eng* 7:384-400.
- Kato, M., Ishikawa, S., Inagaki, K., Chiba, K., Hayashi, H., Yanagisawa, S., and Yoneyama, T. (2010). Possible chemical forms of cadmium and varietal differences in cadmium concentrations in the phloem sap of rice plants (*Oryza sativa* L.). *Soil Sci Plant Nutr* 56:839-847.
- Khan, D., Chan, A., Millar, J.L., Girard, I.J., and Belmonte, M.F. (2014a). Predicting transcriptional circuitry underlying seed coat development. *Plant Sci* 223:146-152.
- Khan, D., Millar, J.L., Girard, I.J., and Belmonte, M.F. (2014b). Transcriptional circuitry underlying seed coat development in Arabidopsis. *Plant Sci* 219-220:51-60.
- Khan, D., Millar, J.L., Girard, I.J., Chan, A., Kirkbride, R.C., Pelletier, J.M., Kost, S., Becker, M.G., Yeung, E.C., Stasolla, C., et al. (2015). Transcriptome atlas of the Arabidopsis funiculus--a study of maternal seed subregions. *Plant J* 82:41-53.
- Kim, S.A., and Gueriot, M.L. (2007). Mining iron: iron uptake and transport in plants. *FEBS Lett* 581:2273-2280.
- Kim, S.A., Punshon, T., Lanzirotti, A., Li, L.T., Alonso, J.M., Ecker, J.R., Kaplan, J., and Gueriot, M.L. (2006). Localization of iron in Arabidopsis seed requires the vacuolar membrane transporter *VIT1*. *Science* 314:1295-1298.
- Kobayashi, T., Itai, R.N., Aung, M.S., Senoura, T., Nakanishi, H., and Nishizawa, N.K. (2012). The rice transcription factor *IDEF1* directly binds to iron and other divalent metals for sensing cellular iron status. *Plant J* 69:81-91.
- Kobayashi, T., Itai, R.N., Ogo, Y., Takei, Y., Nakanishi, H., Takahashi, M., and Nishizawa, N.K. (2009). The rice transcription factor *IDEF1* is essential for the early response to iron deficiency, and induces vegetative expression of late embryogenesis abundant genes. *Plant J* 60:948-961.

- Kobayashi, T., Nakanishi, H., Takahashi, M., Kawasaki, S., Nishizawa, N.K., and Mori, S. (2001). In vivo evidence that *Ids3* from *Hordeum vulgare* encodes a dioxygenase that converts 2'-deoxymugineic acid to mugineic acid in transgenic rice. *Planta* 212:864-871.
- Kobayashi, T., Nakayama, Y., Itai, R.N., Nakanishi, H., Yoshihara, T., Mori, S., and Nishizawa, N.K. (2003). Identification of novel cis-acting elements, IDE1 and IDE2, of the barley *IDS2* gene promoter conferring iron-deficiency-inducible, root-specific expression in heterogeneous tobacco plants. *Plant J* 36:780-793.
- Kobayashi, T., and Nishizawa, N.K. (2012). Iron uptake, translocation, and regulation in higher plants. *Annu Rev Plant Biol* 63:131-152.
- Kobayashi, T., Ogo, Y., Itai, R.N., Nakanishi, H., Takahashi, M., Mori, S., and Nishizawa, N.K. (2007). The transcription factor IDEF1 regulates the response to and tolerance of iron deficiency in plants. *Proc Natl Acad Sci U S A* 104:19150-19155.
- Kobayashi, T., Suzuki, M., Inoue, H., Itai, R.N., Takahashi, M., Nakanishi, H., Mori, S., and Nishizawa, N.K. (2005). Expression of iron-acquisition-related genes in iron-deficient rice is co-ordinately induced by partially conserved iron-deficiency-responsive elements. *J Exp Bot* 56:1305-1316.
- Kochian, L.V., Hoekenga, O.A., and Pineros, M.A. (2004). How do crop plants tolerate acid soils? Mechanisms of aluminum tolerance and phosphorous efficiency. *Annu Rev Plant Biol* 55:459-493.
- Kochian, L.V., Pineros, M.A., and Hoekenga, O.A. (2005). The physiology, genetics and molecular biology of plant aluminum resistance and toxicity. *Plant Soil* 274:175-195.
- Koike, S., Inoue, H., Mizuno, D., Takahashi, M., Nakanishi, H., Mori, S., and Nishizawa, N.K. (2004). OsYSL2 is a rice metal-nicotianamine transporter that is regulated by iron and expressed in the phloem. *Plant J* 39:415-424.
- Korshunova, Y.O., Eide, D., Clark, W.G., Guerinot, M.L., and Pakrasi, H.B. (1999). The IRT1 protein from *Arabidopsis thaliana* is a metal transporter with a broad substrate range. *Plant Mol Biol* 40:37-44.
- Krishnan, S., and Dayanandan, P. (2003). Structural and histochemical studies on grain-filling in the caryopsis of rice (*Oryza sativa* L.). *J Biosciences* 28:455-469.
- Krishnan, S., Ebenezer, G.A.I., and Dayanandan, P. (2001). Histochemical localization of storage components in caryopsis of rice (*Oryza sativa* L.). *Curr Sci India* 80:567-571.
- Kruger, C., Berkowitz, O., Stephan, U.W., and Hell, R. (2002). A metal-binding member of the late embryogenesis abundant protein family transports iron in the phloem of *Ricinus communis* L. *J Biol Chem* 277:25062-25069.
- Kumar, S., Asif, M.H., Chakrabarty, D., Tripathi, R.D., and Trivedi, P.K. (2011). Differential expression and alternative splicing of rice sulphate transporter family members regulate sulphur status during plant growth, development and stress conditions. *Funct Integr Genomics* 11:259-273.
- Kumapatla, S.P., and Hall, T.C. (1998). Recurrent onset of epigenetic silencing in rice harboring a multi-copy transgene. *Plant J* 14:129-135.
- Lan, P., Li, W.F., Wen, T.N., Shiau, J.Y., Wu, Y.C., Lin, W.D., and Schmidt, W. (2011). iTRAQ Protein Profile Analysis of *Arabidopsis* Roots Reveals New Aspects Critical for Iron Homeostasis. *Plant Physiol* 155:821-834.
- Lanquar, V., Lelièvre, F., Barbier-Brygoo, H., and Thomine, S. (2004). Regulation and function of AtNRAMP4 metal transporter protein. *Soil Sci Plant Nutr* 50:1141-1150.

- Lanquar, V., Lelievre, F., Bolte, S., Hames, C., Alcon, C., Neumann, D., Vansuyt, G., Curie, C., Schroder, A., Kramer, U., et al. (2005). Mobilization of vacuolar iron by AtNRAMP3 and AtNRAMP4 is essential for seed germination on low iron. *EMBO J* 24:4041-4051.
- Lanquar, V., Ramos, M.S., Lelievre, F., Barbier-Brygoo, H., Krieger-Liszkay, A., Kramer, U., and Thomine, S. (2010). Export of vacuolar manganese by AtNRAMP3 and AtNRAMP4 is required for optimal photosynthesis and growth under manganese deficiency. *Plant Physiol* 152:1986-1999.
- Lattanzio, G., Andaluz, S., Matros, A., Calvete, J.J., Kehr, J., Abadia, A., Abadia, J., and Lopez-Millan, A.F. (2013). Protein profile of *Lupinus texensis* phloem sap exudates: Searching for Fe- and Zn-containing proteins. *Proteomics* 13:2283-2296.
- Le, B.H., Cheng, C., Bui, A.Q., Wagmaister, J.A., Henry, K.F., Pelletier, J., Kwong, L., Belmonte, M., Kirkbride, R., Horvath, S., et al. (2010). Global analysis of gene activity during Arabidopsis seed development and identification of seed-specific transcription factors. *Proc Natl Acad Sci U S A* 107:8063-8070.
- Lee, J., and Koh, H.J. (2011). A label-free quantitative shotgun proteomics analysis of rice grain development. *Proteome Sci* 9:61.
- Lee, S., and An, G. (2009). Over-expression of OsIRT1 leads to increased iron and zinc accumulations in rice. *Plant Cell Environ* 32:408-416.
- Lee, S., Chiecko, J.C., Kim, S.A., Walker, E.L., Lee, Y., Guerinot, M.L., and An, G. (2009a). Disruption of OsYSL15 Leads to Iron Inefficiency in Rice Plants. *Plant Physiol* 150:786-800.
- Lee, S., Jeon, U.S., Lee, S.J., Kim, Y.K., Persson, D.P., Husted, S., Schjorring, J.K., Kakei, Y., Masuda, H., Nishizawa, N.K., et al. (2009b). Iron fortification of rice seeds through activation of the nicotianamine synthase gene. *Proc Natl Acad Sci U S A* 106:22014-22019.
- Lee, S., Kim, Y.S., Jeon, U.S., Kim, Y.K., Schjoerring, J.K., and An, G. (2012a). Activation of Rice nicotianamine synthase 2 (OsNAS2) Enhances Iron Availability for Biofortification. *Mol Cells* 33:269-275.
- Lee, S., Ryoo, N., Jeon, J.S., Guerinot, M.L., and An, G. (2012b). Activation of Rice Yellow Stripe1-Like 16 (OsYSL16) Enhances Iron Efficiency. *Mol Cells* 33:117-126.
- Lenka, S.K., Katiyar, A., Chinnusamy, V., and Bansal, K.C. (2011). Comparative analysis of drought-responsive transcriptome in Indica rice genotypes with contrasting drought tolerance. *Plant Biotechnol J* 9:315-327.
- Lenka, S.K., Lohia, B., Kumar, A., Chinnusamy, V., and Bansal, K.C. (2009). Genome-wide targeted prediction of ABA responsive genes in rice based on over-represented cis-motif in co-expressed genes. *Plant Mol Biol* 69:261-271.
- Li, G., Wang, D., Yang, R., Logan, K., Chen, H., Zhang, S., Skaggs, M.I., Lloyd, A., Burnett, W.J., Laurie, J.D., et al. (2014). Temporal patterns of gene expression in developing maize endosperm identified through transcriptome sequencing. *Proc Natl Acad Sci U S A* 111:7582-7587.
- Li, J., Wu, X.D., Hao, S.T., Wang, X.J., and Ling, H.Q. (2008a). Proteomic response to iron deficiency in tomato root. *Proteomics* 8:2299-2311.
- Li, K.T., Moulin, M., Mangel, N., Albersen, M., Verhoeven-Duif, N.M., Ma, Q., Zhang, P., Fitzpatrick, T.B., Gruissem, W., and Vanderschuren, H. (2015). Increased bioavailable vitamin B6 in field-grown transgenic cassava for dietary sufficiency. *Nat Biotechnol* 33:1029-1032.

- Li, M., Singh, R., Bazanova, N., Milligan, A.S., Shirley, N., Langridge, P., and Lopato, S. (2008b). Spatial and temporal expression of endosperm transfer cell-specific promoters in transgenic rice and barley. *Plant Biotechnol J* 6:465-476.
- Li, W., and Lan, P. (2015). Genome-wide analysis of overlapping genes regulated by iron deficiency and phosphate starvation reveals new interactions in *Arabidopsis* roots. *BMC Res Notes* 8:555.
- Liang, Z., Zhang, K., Chen, K.L., and Gao, C.X. (2014). Targeted Mutagenesis in *Zea mays* Using TALENs and the CRISPR/Cas System. *J Genet Genomics* 41:63-68.
- Liao, J.L., Zhou, H.W., Zhang, H.Y., Zhong, P.A., and Huang, Y.J. (2014). Comparative proteomic analysis of differentially expressed proteins in the early milky stage of rice grains during high temperature stress. *J Exp Bot* 65:655-671.
- Liu, H.C., Liao, H.T., and Charng, Y.Y. (2011). The role of class A1 heat shock factors (HSFA1s) in response to heat and other stresses in *Arabidopsis*. *Plant Cell Environ* 34:738-751.
- Liu, X.D., Zhang, H., Zhao, Y., Feng, Z.Y., Li, Q., Yang, H.Q., Luan, S., Li, J.M., and He, Z.H. (2013). Auxin controls seed dormancy through stimulation of abscisic acid signaling by inducing ARF-mediated ABI3 activation in *Arabidopsis*. *Proc Natl Acad Sci U S A* 110:15485-15490.
- Locascio, A., Roig-Villanova, I., Bernardi, J., and Varotto, S. (2014). Current perspectives on the hormonal control of seed development in *Arabidopsis* and maize: a focus on auxin. *Front Plant Sci* 5.
- Lopez-Millan, A.F., Grusak, M.A., Abadia, A., and Abadia, J. (2013). Iron deficiency in plants: an insight from proteomic approaches. *Front Plant Sci* 4:254.
- Lopez-Millan, A.F., Grusak, M.A., and Abadia, J. (2012). Carboxylate metabolism changes induced by Fe deficiency in barley, a Strategy II plant species. *J Plant Physiol* 169:1121-1124.
- Lu, L., Tian, S., Liao, H., Zhang, J., Yang, X., Labavitch, J.M., and Chen, W. (2013a). Analysis of metal element distributions in rice (*Oryza sativa* L.) seeds and relocation during germination based on X-ray fluorescence imaging of Zn, Fe, K, Ca, and Mn. *PLoS One* 8:e57360.
- Lu, L.L., Tian, S.K., Zhang, J., Yang, X., Labavitch, J.M., Webb, S.M., Latimer, M., and Brown, P.H. (2013b). Efficient xylem transport and phloem remobilization of Zn in the hyperaccumulator plant species *Sedum alfredii*. *New Phytol* 198:721-731.
- Lu, X., Chen, D., Shu, D., Zhang, Z., Wang, W., Klukas, C., Chen, L.L., Fan, Y., Chen, M., and Zhang, C. (2013c). The differential transcription network between embryo and endosperm in the early developing maize seed. *Plant Physiol* 162:440-455.
- Lubkowitz, M. (2011). The Oligopeptide Transporters: A Small Gene Family with a Diverse Group of Substrates and Functions? *Mol Plant* 4:407-415.
- Lucca, P., Hurrell, R., and Potrykus, I. (2001a). Approaches to improving the bioavailability and level of iron in rice seeds. *J Sci Food Agr* 81:828-834.
- Lucca, P., Hurrell, R., and Potrykus, I. (2001b). Genetic engineering approaches to improve the bioavailability and the level of iron in rice grains. *Theor Appl Genet* 102:392-397.
- Ma, J.F., Ryan, P.R., and Delhaize, E. (2001). Aluminium tolerance in plants and the complexing role of organic acids. *Trends Plant Sci* 6:273-278.
- Ma, J.F., Shen, R.F., Zhao, Z.Q., Wissuwa, M., Takeuchi, Y., Ebitani, T., and Yano, M. (2002). Response of rice to Al stress and identification of quantitative trait loci for Al tolerance. *Plant Cell Physiol* 43:652-659.

- Ma, J.F., Taketa, S., Chang, Y.C., Iwashita, T., Matsumoto, H., Takeda, K., and Nomoto, K. (1999). Genes controlling hydroxylations of phytosiderophores are located on different chromosomes in barley (*Hordeum vulgare* L.). *Planta* 207:590-596.
- Mano, Y., and Nemoto, K. (2012). The pathway of auxin biosynthesis in plants. *J Exp Bot* 63:2853-2872.
- Masuda, H., Ishimaru, Y., Aung, M.S., Kobayashi, T., Kakei, Y., Takahashi, M., Higuchi, K., Nakanishi, H., and Nishizawa, N.K. (2012). Iron biofortification in rice by the introduction of multiple genes involved in iron nutrition. *Sci Rep* 2.
- Masuda, H., Kobayashi, T., Ishimaru, Y., Takahashi, M., Aung, M.S., Nakanishi, H., Mori, S., and Nishizawa, N.K. (2013). Iron-biofortification in rice by the introduction of three barley genes participated in mugineic acid biosynthesis with soybean ferritin gene. *Front Plant Sci* 4.
- Masuda, H., Suzuki, M., Morikawa, K.C., Kobayashi, T., Nakanishi, H., Takahashi, M., Saigusa, M., Mori, S., and Nishizawa, N.K. (2008). Increase in Iron and Zinc Concentrations in Rice Grains Via the Introduction of Barley Genes Involved in Phytosiderophore Synthesis. *Rice* 1:100-108.
- Masuda, H., Usuda, K., Kobayashi, T., Ishimaru, Y., Kakei, Y., Takahashi, M., Higuchi, K., Nakanishi, H., Mori, S., and Nishizawa, N.K. (2009). Overexpression of the Barley Nicotianamine Synthase Gene *HvNAS1* Increases Iron and Zinc Concentrations in Rice Grains. *Rice* 2:155-166.
- Matthus, E., Wu, L.B., Ueda, Y., Holler, S., Becker, M., and Frei, M. (2015). Loci, genes, and mechanisms associated with tolerance to ferrous iron toxicity in rice (*Oryza sativa* L.). *Theor Appl Genet* 128:2085-2098.
- Mayer, J.E., Pfeiffer, W.H., and Beyer, P. (2008). Biofortified crops to alleviate micronutrient malnutrition. *Curr Opin Plant Biol* 11:166-170.
- McLeay, R.C., and Bailey, T.L. (2010). Motif Enrichment Analysis: a unified framework and an evaluation on ChIP data. *BMC bioinformatics* 11:165.
- Meenakshi, J.V., Johnson, N.L., Manyong, V.M., Degroote, H., Javelosa, J., Yanggen, D.R., Naher, F., Gonzalez, C., Garcia, J., and Meng, E. (2010). How Cost-Effective is Biofortification in Combating Micronutrient Malnutrition? An Ex ante Assessment. *World Dev* 38:64-75.
- Mendoza-Cozatl, D.G., Xie, Q.Q., Akmajian, G.Z., Jobe, T.O., Patel, A., Stacey, M.G., Song, L.H., Demoin, D.W., Jurisson, S.S., Stacey, G., et al. (2014). OPT3 Is a Component of the Iron-Signaling Network between Leaves and Roots and Misregulation of OPT3 Leads to an Over-Accumulation of Cadmium in Seeds. *Mol Plant* 7:1455-1469.
- Meng, F., Wei, Y., and Yang, X. (2005). Iron content and bioavailability in rice. *J Trace Elem Med Biol* 18:333-338.
- Monsant, A.C., Kappen, P., Wang, Y.D., Pigram, P.J., Baker, A.J.M., and Tang, C.X. (2011). In vivo speciation of zinc in *Noccaea caerulescens* in response to nitrogen form and zinc exposure. *Plant Soil* 348:167-183.
- Mori, M., Nomura, T., Ooka, H., Ishizaka, M., Yokota, T., Sugimoto, K., Okabe, K., Kajiwara, H., Satoh, K., Yamamoto, K., et al. (2002). Isolation and characterization of a rice dwarf mutant with a defect in brassinosteroid biosynthesis. *Plant Physiol* 130:1152-1161.
- Mori, S., and Nishizawa, N. (1987). Methionine as a Dominant Precursor of Phytosiderophores in Gramineae Plants. *Plant Cell Physiol* 28:1081-1092.
- Morrissey, J., Baxter, I.R., Lee, J., Li, L.T., Lahner, B., Grotz, N., Kaplan, J., Salt, D.E., and Gueriot, M.L. (2009). The Ferroportin Metal Efflux Proteins Function in Iron and Cobalt Homeostasis in *Arabidopsis*. *Plant Cell* 21:3326-3338.

- Muller, M., and Schmidt, W. (2004). Environmentally induced plasticity of root hair development in arabidopsis. *Plant Physiol* 134:409-419.
- Nakanishi, H., Yamaguchi, H., Sasakuma, T., Nishizawa, N.K., and Mori, S. (2000). Two dioxygenase genes, *Ids3* and *Ids2*, from *Hordeum vulgare* are involved in the biosynthesis of mugineic acid family phytosiderophores. *Plant Mol Biol* 44:199-207.
- Naqvi, S., Zhu, C.F., Farre, G., Ramessar, K., Bassie, L., Breitenbach, J., Conesa, D.P., Ros, G., Sandmann, G., Capell, T., et al. (2009). Transgenic multivitamin corn through biofortification of endosperm with three vitamins representing three distinct metabolic pathways. *Proc Natl Acad Sci U S A* 106:7762-7767.
- Narayanan, N., Beyene, G., Chauhan, R.D., Gaitan-Solis, E., Grusak, M.A., Taylor, N., and Anderson, P. (2015). Overexpression of *Arabidopsis* VIT1 increases accumulation of iron in cassava roots and stems. *Plant Sci* 240:170-181.
- Nemudryi, A.A., Valetdinova, K.R., Medvedev, S.P., and Zakian, S.M. (2014). TALEN and CRISPR/Cas Genome Editing Systems: Tools of Discovery. *Acta Naturae* 6:19-40.
- Nishimura, A., Aichi, I., and Matsuoka, M. (2006). A protocol for *Agrobacterium*-mediated transformation in rice. *Nat Protoc* 1:2796-2802.
- Nishiyama, R., Kato, M., Nagata, S., Yanagisawa, S., and Yoneyama, T. (2012). Identification of Zn-Nicotianamine and Fe-2'-Deoxymugineic Acid in the Phloem Sap from Rice Plants (*Oryza sativa* L.). *Plant Cell Physiol* 53:381-390.
- Nozoye, T., Nagasaka, S., Kobayashi, T., Takahashi, M., Sato, Y., Sato, Y., Uozumi, N., Nakanishi, H., and Nishizawa, N.K. (2011). Phytosiderophore Efflux Transporters Are Crucial for Iron Acquisition in Gramineous Plants. *J Biol Chem* 286:5446-5454.
- Offler, C.E., McCurdy, D.W., Patrick, J.W., and Talbot, M.J. (2003). Transfer cells: cells specialized for a special purpose. *Annu Rev Plant Biol* 54:431-454.
- Ogo, Y., Itai, R.N., Nakanishi, H., Inoue, H., Kobayashi, T., Suzuki, M., Takahashi, M., Mori, S., and Nishizawa, N.K. (2006). Isolation and characterization of *IRO2*, a novel iron-regulated bHLH transcription factor in gramineous plants. *J Exp Bot* 57:2867-2878.
- Ogo, Y., Itai, R.N., Nakanishi, H., Kobayashi, T., Takahashi, M., Mori, S., and Nishizawa, N.K. (2007). The rice bHLH protein *OsIRO2* is an essential regulator of the genes involved in Fe uptake under Fe-deficient conditions. *Plant J* 51:366-377.
- Ogo, Y., Kobayashi, T., Itai, R.N., Nakanishi, H., Kakei, Y., Takahashi, M., Toki, S., Mori, S., and Nishizawa, N.K. (2008). A novel NAC transcription factor, *IDEF2*, that recognizes the iron deficiency-responsive element 2 regulates the genes involved in iron homeostasis in plants. *J Biol Chem* 283:13407-13417.
- Ohtsu, K., Takahashi, H., Schnable, P.S., and Nakazono, M. (2007). Cell type-specific gene expression profiling in plants by using a combination of laser microdissection and high-throughput technologies. *Plant Cell Physiol* 48:3-7.
- Oliva, N., Chadha-Mohanty, P., Poletti, S., Abrigo, E., Atienza, G., Torrizo, L., Garcia, R., Duenas, C., Poncio, M.A., Balindong, J., et al. (2014). Large-scale production and evaluation of marker-free indica rice IR64 expressing phytoferritin genes. *Mol Breeding* 33:23-37.
- Olsen, L.I., and Palmgren, M.G. (2014). Many rivers to cross: the journey of zinc from soil to seed. *Front Plant Sci* 5:30.
- Olsen, O.A. (2001). Endosperm development: Cellularization and cell fate specification. *Annu Rev Plant Phys* 52:233-+.

- Olsen, O.A. (2004). Nuclear endosperm development in cereals and *Arabidopsis thaliana*. *Plant Cell* 16 Suppl:S214-227.
- Oppenheimer, S.J., Gibson, F.D., Macfarlane, S.B., Moody, J.B., Harrison, C., Spencer, A., and Bunari, O. (1986). Iron supplementation increases prevalence and effects of malaria: report on clinical studies in Papua New Guinea. *Trans R Soc Trop Med Hyg* 80:603-612.
- Paine, J.A., Shipton, C.A., Chaggar, S., Howells, R.M., Kennedy, M.J., Vernon, G., Wright, S.Y., Hinchliffe, E., Adams, J.L., Silverstone, A.L., et al. (2005). Improving the nutritional value of Golden Rice through increased pro-vitamin A content. *Nat Biotechnol* 23:482-487.
- Papoyan, A., Pineros, M., and Kochian, L.V. (2007). Plant Cd²⁺ and Zn²⁺ status effects on root and shoot heavy metal accumulation in *Thlaspi caerulescens*. *New Phytol* 175:51-58.
- Petit, J.M., Briat, J.F., and Lobreaux, S. (2001). Structure and differential expression of the four members of the *Arabidopsis thaliana* ferritin gene family. *Biochem J* 359:575-582.
- Peukert, M., Thiel, J., Peshev, D., Weschke, W., Van den Ende, W., Mock, H.P., and Matros, A. (2014). Spatio-Temporal Dynamics of Fructan Metabolism in Developing Barley Grains. *Plant Cell* 26:3728-3744.
- Pfeifer, M., Kugler, K.G., Sandve, S.R., Zhan, B.J., Rudi, H., Hvidsten, T.R., Mayer, K.F.X., Olsen, O.A., and Sequencing, I.W.G. (2014). Genome interplay in the grain transcriptome of hexaploid bread wheat. *Science* 345.
- Pich, A., Manteuffel, R., Hillmer, S., Scholz, G., and Schmidt, W. (2001). Fe homeostasis in plant cells: does nicotianamine play multiple roles in the regulation of cytoplasmic Fe concentration? *Planta* 213:967-976.
- Puchta, H., Dujon, B., and Hohn, B. (1996). Two different but related mechanisms are used in plants for the repair of genomic double-strand breaks by homologous recombination. *Proc Natl Acad Sci U S A* 93:5055-5060.
- Qiu, J.H., Hou, Y.X., Tong, X.H., Wang, Y.F., Lin, H.Y., Liu, Q., Zhang, W., Li, Z.Y., Nallamilli, B.R., and Zhang, J. (2016). Quantitative phosphoproteomic analysis of early seed development in rice (*Oryza sativa* L.). *Plant Mol Biol* 90:249-265.
- Qu le, Q., and Takaiwa, F. (2004). Evaluation of tissue specificity and expression strength of rice seed component gene promoters in transgenic rice. *Plant Biotechnol J* 2:113-125.
- Qu, L.Q., Yoshihara, T., Ooyama, A., Goto, F., and Takaiwa, F. (2005). Iron accumulation does not parallel the high expression level of ferritin in transgenic rice seeds. *Planta* 222:225-233.
- Rajeevkumar, S., Anunanthini, P., and Sathishkumar, R. (2015). Epigenetic silencing in transgenic plants. *Front Plant Sci* 6.
- Ravet, K., Touraine, B., Kim, S.A., Cellier, F., Thomine, S., Guerinot, M.L., Briat, J.F., and Gaymard, F. (2009). Post-Translational Regulation of AtFER2 Ferritin in Response to Intracellular Iron Trafficking during Fruit Development in *Arabidopsis*. *Mol Plant* 2:1095-1106.
- Rellan-Alvarez, R., Abadia, J., and Alvarez-Fernandez, A. (2008). Formation of metal-nicotianamine complexes as affected by pH, ligand exchange with citrate and metal exchange. A study by electrospray ionization time-of-flight mass spectrometry. *Rapid Commun Mass Spectrom* 22:1553-1562.
- Rellan-Alvarez, R., Giner-Martinez-Sierra, J., Orduna, J., Orera, I., Rodriguez-Castrillon, J.A., Garcia-Alonso, J.I., Abadia, J., and Alvarez-Fernandez, A. (2010). Identification of a Tri-Iron(III), Tri-Citrate Complex in the Xylem Sap of Iron-

- Deficient Tomato Resupplied with Iron: New Insights into Plant Iron Long-Distance Transport. *Plant Cell Physiol* 51:91-102.
- Rhodes, D.H., Hoffmann, L., Jr., Rooney, W.L., Ramu, P., Morris, G.P., and Kresovich, S. (2014). Genome-wide association study of grain polyphenol concentrations in global sorghum [*Sorghum bicolor* (L.) Moench] germplasm. *J Agric Food Chem* 62:10916-10927.
- Robinson, N.J., Procter, C.M., Connolly, E.L., and Guerinot, M.L. (1999). A ferric-chelate reductase for iron uptake from soils. *Nature* 397:694-697.
- Rodriguez-Celma, J., Lattanzio, G., Grusak, M.A., Abadia, A., Abadia, J., and Lopez-Millan, A.F. (2011). Root Responses of *Medicago truncatula* Plants Grown in Two Different Iron Deficiency Conditions: Changes in Root Protein Profile and Riboflavin Biosynthesis. *J Proteome Res* 10:2590-2601.
- Rogers, E.E. (2002). FRD3, a Member of the Multidrug and Toxin Efflux Family, Controls Iron Deficiency Responses in *Arabidopsis*. *Plant Cell* 14:1787-1799.
- Roschzttardtz, H., Seguela-Arnaud, M., Briat, J.F., Vert, G., and Curie, C. (2011). The FRD3 citrate effluxer promotes iron nutrition between symplastically disconnected tissues throughout *Arabidopsis* development. *Plant Cell* 23:2725-2737.
- Sabelli, P.A., and Larkins, B.A. (2009). The Development of Endosperm in Grasses. *Plant Physiol* 149:14-26.
- Saenchai, C., Prom-u-thai, C., Jamjod, S., Dell, B., and Rerkasem, B. (2012). Genotypic variation in milling depression of iron and zinc concentration in rice grain. *Plant Soil* 361:271-278.
- Santi, S., Cesco, S., Varanini, Z., and Pinton, R. (2005). Two plasma membrane H⁺-ATPase genes are differentially expressed in iron-deficient cucumber plants. *Plant Physiol Bioch* 43:287-292.
- Santi, S., and Schmidt, W. (2008). Laser microdissection-assisted analysis of the functional fate of iron deficiency-induced root hairs in cucumber. *J Exp Bot* 59:697-704.
- Santi, S., and Schmidt, W. (2009). Dissecting iron deficiency-induced proton extrusion in *Arabidopsis* roots. *New Phytol* 183:1072-1084.
- Sato, Y., Sentoku, N., Miura, Y., Hirochika, H., Kitano, H., and Matsuoka, M. (1999). Loss-of-function mutations in the rice homeobox gene OSH15 affect the architecture of internodes resulting in dwarf plants. *EMBO J* 18:992-1002.
- Sayre, R., Beeching, J.R., Cahoon, E.B., Egesi, C., Fauquet, C., Fellman, J., Fregene, M., Gruissem, W., Mallowa, S., Manary, M., et al. (2011). The BioCassava Plus Program: Biofortification of Cassava for Sub-Saharan Africa. *Annu Rev Plant Biol* 62:251-272.
- Sazawal, S., Black, R.E., Ramsan, M., Chwaya, H.M., Stoltzfus, R.J., Dutta, A., Dhingra, U., Kabole, I., Deb, S., Othman, M.K., et al. (2006). Effects of routine prophylactic supplementation with iron and folic acid on admission to hospital and mortality in preschool children in a high malaria transmission setting: community-based, randomised, placebo-controlled trial. *Lancet* 367:133-143.
- Schmidt, W. (1999). Mechanisms and regulation of reduction-based iron uptake in plants. *New Phytol* 141:1-26.
- Schuler, M., Rellan-Alvarez, R., Fink-Straube, C., Abadia, J., and Bauer, P. (2012). Nicotianamine Functions in the Phloem-Based Transport of Iron to Sink Organs, in Pollen Development and Pollen Tube Growth in *Arabidopsis*. *Plant Cell* 24:2380-2400.

- Secco, D., Baumann, A., and Poirier, Y. (2010). Characterization of the rice PHO1 gene family reveals a key role for OsPHO1;2 in phosphate homeostasis and the evolution of a distinct clade in dicotyledons. *Plant Physiol* 152:1693-1704.
- Seiler, C., Harshavardhan, V.T., Rajesh, K., Reddy, P.S., Strickert, M., Rolletschek, H., Scholz, U., Wobus, U., and Sreenivasulu, N. (2011). ABA biosynthesis and degradation contributing to ABA homeostasis during barley seed development under control and terminal drought-stress conditions. *J Exp Bot* 62:2615-2632.
- Senden, M.H.M.N., Vandermeer, A.J.G.M., Verburg, T.G., and Wolterbeek, H.T. (1995). Citric-Acid in Tomato Plant-Roots and Its Effect on Cadmium Uptake and Distribution. *Plant Soil* 171:333-339.
- Seo, M., Hanada, A., Kuwahara, A., Endo, A., Okamoto, M., Yamauchi, Y., North, H., Marion-Poll, A., Sun, T.P., Koshiba, T., et al. (2006). Regulation of hormone metabolism in Arabidopsis seeds: phytochrome regulation of abscisic acid metabolism and abscisic acid regulation of gibberellin metabolism. *Plant J* 48:354-366.
- Seung, D., Lu, K.J., Stettler, M., Streb, S., and Zeeman, S.C. (2016). Degradation of Glucan Primers in the Absence of Starch Synthase 4 Disrupts Starch Granule Initiation in Arabidopsis. *J Biol Chem* 291:20718-20728.
- Shimoni-Shor, E., Hassidim, M., Yuval-Naeh, N., and Keren, N. (2010). Disruption of Nap14, a plastid-localized non-intrinsic ABC protein in Arabidopsis thaliana results in the over-accumulation of transition metals and in aberrant chloroplast structures. *Plant Cell Environ* 33:1029-1038.
- Shojima, S., Nishizawa, N.K., Fushiya, S., Nozoe, S., Irifune, T., and Mori, S. (1990). Biosynthesis of Phytosiderophores : In Vitro Biosynthesis of 2'-Deoxymugineic Acid from L-Methionine and Nicotianamine. *Plant Physiol* 93:1497-1503.
- Shukla, V.K., Doyon, Y., Miller, J.C., DeKolver, R.C., Moehle, E.A., Worden, S.E., Mitchell, J.C., Arnold, N.L., Gopalan, S., Meng, X.D., et al. (2009). Precise genome modification in the crop species Zea mays using zinc-finger nucleases. *Nature* 459:437-U156.
- Singh, S.P., Keller, B., Gruissem, W., and Bhullar, N.K. (2017). Rice NICOTIANAMINE SYNTHASE 2 expression improves dietary iron and zinc levels in wheat. *Theor Appl Genet* 130:283-292.
- Sperotto, R.A., Ricachenevsky, F.K., Waldow, V.D., and Fett, J.P. (2012). Iron biofortification in rice: It's a long way to the top. *Plant Sci* 190:24-39.
- Sreenivasulu, N., Usadel, B., Winter, A., Radchuk, V., Scholz, U., Stein, N., Weschke, W., Strickert, M., Close, T.J., Stitt, M., et al. (2008). Barley grain maturation and germination: metabolic pathway and regulatory network commonalities and differences highlighted by new MapMan/PageMan profiling tools. *Plant Physiol* 146:1738-1758.
- Sreenivasulu, N., and Wobus, U. (2013). Seed-development programs: a systems biology-based comparison between dicots and monocots. *Annu Rev Plant Biol* 64:189-217.
- Stacey, M.G., Osawa, H., Patel, A., Gassmann, W., and Stacey, G. (2006). Expression analyses of Arabidopsis oligopeptide transporters during seed germination, vegetative growth and reproduction. *Planta* 223:291-305.
- Stevens, G.A., Finucane, M.M., De-Regil, L.M., Paciorek, C.J., Flaxman, S.R., Branca, F., Pena-Rosas, J.P., Bhutta, Z.A., Ezzati, M., and Nutrition Impact Model Study, G. (2013). Global, regional, and national trends in haemoglobin concentration and prevalence of total and severe anaemia in children and pregnant and non-pregnant

- women for 1995-2011: a systematic analysis of population-representative data. *Lancet Glob Health* 1:e16-25.
- Storozhenko, S., De Brouwer, V., Volckaert, M., Navarrete, O., Blancquaert, D., Zhang, G.F., Lambert, W., and Van Der Straeten, D. (2007). Folate fortification of rice by metabolic engineering. *Nat Biotechnol* 25:1277-1279.
- Sun, S.B., Gu, M.A., Cao, Y., Huang, X.P., Zhang, X., Ai, P.H., Zhao, J.N., Fan, X.R., and Xu, G.H. (2012). A Constitutive Expressed Phosphate Transporter, OsPht1;1, Modulates Phosphate Uptake and Translocation in Phosphate-Replete Rice. *Plant Physiol* 159:1571-1581.
- Svozil, J., Grussem, W., and Baerenfaller, K. (2015). Proteasome targeting of proteins in *Arabidopsis* leaf mesophyll, epidermal and vascular tissues. *Front Plant Sci* 6.
- Takahashi, M., Yamaguchi, H., Nakanishi, H., Shioiri, T., Nishizawa, N.K., and Mori, S. (1999). Cloning two genes for nicotianamine aminotransferase, a critical enzyme in iron acquisition (strategy II) in graminaceous plants. *Plant Physiol* 121:947-956.
- Takahashi, R., Ishimaru, Y., Senoura, T., Shimo, H., Ishikawa, S., Arao, T., Nakanishi, H., and Nishizawa, N.K. (2011). The OsNRAMP1 iron transporter is involved in Cd accumulation in rice. *J Exp Bot* 62:4843-4850.
- Tan, S., Han, R., Li, P., Yang, G., Li, S., Zhang, P., Wang, W.B., Zhao, W.Z., and Yin, L.P. (2015). Over-expression of the MxIRT1 gene increases iron and zinc content in rice seeds. *Transgenic Res* 24:109-122.
- Tanabe, M., and Kanehisa, M. (2012). Using the KEGG database resource. *Current protocols in bioinformatics / editorial board, Andreas D. Baxevanis ... [et al.] Chapter 1:Unit1 12.*
- Tanaka, T., Antonio, B.A., Kikuchi, S., Matsumoto, T., Nagamura, Y., Numa, H., Sakai, H., Wu, J., Itoh, T., Sasaki, T., et al. (2008). The rice annotation project database (RAP-DB): 2008 update. *Nucleic Acids Res* 36:D1028-D1033.
- Tauris, B., Borg, S., Gregersen, P.L., and Holm, P.B. (2009). A roadmap for zinc trafficking in the developing barley grain based on laser capture microdissection and gene expression profiling. *J Exp Bot* 60:1333-1347.
- Tavva, V.S., Kim, Y.H., Kagan, I.A., Dinkins, R.D., Kim, K.H., and Collins, G.B. (2007). Increased alpha-tocopherol content in soybean seed overexpressing the *Perilla frutescens* gamma-tocopherol methyltransferase gene. *Plant Cell Rep* 26:61-70.
- Thiel, J. (2014). Development of endosperm transfer cells in barley. *Front Plant Sci* 5.
- Thiel, J., Muller, M., Weschke, W., and Weber, H. (2009). Amino acid metabolism at the maternal-filial boundary of young barley seeds: a microdissection-based study. *Planta* 230:205-213.
- Thiel, J., Riewe, D., Rutten, T., Melzer, M., Friedel, S., Bollenbeck, F., Weschke, W., and Weber, H. (2012). Differentiation of endosperm transfer cells of barley: a comprehensive analysis at the micro-scale. *Plant J* 71:639-655.
- Thiel, J., Weier, D., Sreenivasulu, N., Strickert, M., Weichert, N., Melzer, M., Czauderna, T., Wobus, U., Weber, H., and Weschke, W. (2008). Different hormonal regulation of cellular differentiation and function in nucellar projection and endosperm transfer cells: a microdissection-based transcriptome study of young barley grains. *Plant Physiol* 148:1436-1452.
- Thiel, J., Weier, D., and Weschke, W. (2011). Laser-Capture Microdissection of Developing Barley Seeds and cDNA Array Analysis of Selected Tissues. *Methods Mol Biol* 755:461-475.
- Thomine, S., and Lanquar, V. (2011). Iron Transport and Signaling in Plants. 7:99-131.

- Thomine, S., Lelievre, F., Debarbieux, E., Schroeder, J.I., and Barbier-Brygoo, H. (2003). AtNRAMP3, a multispecific vacuolar metal transporter involved in plant responses to iron deficiency. *Plant J* 34:685-695.
- Thomine, S., Wang, R., Ward, J.M., Crawford, N.M., and Schroeder, J.I. (2000). Cadmium and iron transport by members of a plant metal transporter family in *Arabidopsis* with homology to Nramp genes. *Proc Natl Acad Sci U S A* 97:4991-4996.
- Trijatmiko, K.R., Duenas, C., Tsakirpaloglou, N., Torrizo, L., Arines, F.M., Adeva, C., Balindong, J., Oliva, N., Sapasap, M.V., Borrero, J., et al. (2016). Biofortified indica rice attains iron and zinc nutrition dietary targets in the field. *Sci Rep* 6:19792.
- Uraguchi, S., Mori, S., Kuramata, M., Kawasaki, A., Arao, T., and Ishikawa, S. (2009). Root-to-shoot Cd translocation via the xylem is the major process determining shoot and grain cadmium accumulation in rice. *J Exp Bot* 60:2677-2688.
- Varotto, C., Maiwald, D., Pesaresi, P., Jahns, P., Salamini, F., and Leister, D. (2002). The metal ion transporter IRT1 is necessary for iron homeostasis and efficient photosynthesis in *Arabidopsis thaliana*. *Plant J* 31:589-599.
- Vasconcelos, M., Datta, K., Oliva, N., Khalekuzzaman, M., Torrizo, L., Krishnan, S., Oliveira, M., Goto, F., and Datta, S.K. (2003). Enhanced iron and zinc accumulation in transgenic rice with the ferritin gene. *Plant Sci* 164:371-378.
- Vasconcelos, M., Eckert, H., Arahana, V., Graef, G., Grusak, M.A., and Clemente, T. (2006). Molecular and phenotypic characterization of transgenic soybean expressing the *Arabidopsis* ferric chelate reductase gene, FRO2. *Planta* 224:1116-1128.
- Vasconcelos, M.W., Gruissem, W., and Bhullar, N.K. (2017). Iron biofortification in the 21st century: setting realistic targets, overcoming obstacles, and new strategies for healthy nutrition. *Curr Opin Biotech* 44:8-15.
- Vernoud, V., Hajduch, M., Khaled, A.S., Depege, N., and Rogowsky, P.M. (2005). Maize Embryogenesis. *Maydica* 50:469-483.
- Vert, G., Grotz, N., Dedaldechamp, F., Gaymard, F., Guerinot, M.L., Briat, J.F., and Curie, C. (2002). IRT1, an *Arabidopsis* transporter essential for iron uptake from the soil and for plant growth. *Plant Cell* 14:1223-1233.
- Vigani, G., Bashir, K., Ishimaru, Y., Lehmann, M., Casiraghi, F.M., Nakanishi, H., Seki, M., Geigenberger, P., Zocchi, G., and Nishizawa, N.K. (2016). Knocking down mitochondrial iron transporter (MIT) reprograms primary and secondary metabolism in rice plants. *J Exp Bot* 67:1357-1368.
- Wang, E., Wang, J., Zhu, X., Hao, W., Wang, L., Li, Q., Zhang, L., He, W., Lu, B., Lin, H., et al. (2008). Control of rice grain-filling and yield by a gene with a potential signature of domestication. *Nat Genet* 40:1370-1374.
- Wang, K., Tang, D., Hong, L., Xu, W., Huang, J., Li, M., Gu, M., Xue, Y., and Cheng, Z. (2010). DEP and AFO regulate reproductive habit in rice. *PLoS Genet* 6:e1000818.
- Wang, L., Ying, Y.H., Narsai, R., Ye, L.X., Zheng, L.Q., Tian, J.L., Whelan, J., and Shou, H.X. (2013a). Identification of OsbHLH133 as a regulator of iron distribution between roots and shoots in *Oryza sativa*. *Plant Cell Environ* 36:224-236.
- Wang, M., Gruissem, W., and Bhullar, N.K. (2013b). Nicotianamine synthase overexpression positively modulates iron homeostasis-related genes in high iron rice. *Front Plant Sci* 4:156.

- Wang, Y.P., Cheng, X., Shan, Q.W., Zhang, Y., Liu, J.X., Gao, C.X., and Qiu, J.L. (2014). Simultaneous editing of three homoeoalleles in hexaploid bread wheat confers heritable resistance to powdery mildew. *Nat Biotechnol* 32:947-951.
- Waters, B.M., Chu, H.H., DiDonato, R.J., Roberts, L.A., Eisley, R.B., Lahner, B., Salt, D.E., and Walker, E.L. (2006). Mutations in *Arabidopsis* Yellow Stripe-Like1 and Yellow Stripe-Like3 reveal their roles in metal ion homeostasis and loading of metal ions in seeds. *Plant Physiol* 141:1446-1458.
- Wirth, J., Poletti, S., Aeschlimann, B., Yakandawala, N., Drosse, B., Osorio, S., Tohge, T., Fernie, A.R., Gunther, D., Gruissem, W., et al. (2009). Rice endosperm iron biofortification by targeted and synergistic action of nicotianamine synthase and ferritin. *Plant Biotechnol J* 7:631-644.
- Wu, C.Y., Trieu, A., Radhakrishnan, P., Kwok, S.F., Harris, S., Zhang, K., Wang, J., Wan, J., Zhai, H., Takatsuto, S., et al. (2008). Brassinosteroids regulate grain filling in rice. *Plant Cell* 20:2130-2145.
- Xu, G., Fan, X., and Miller, A.J. (2012a). Plant nitrogen assimilation and use efficiency. *Annual review of plant biology* 63:153-182.
- Xu, H., Gao, Y., and Wang, J. (2012b). Transcriptomic analysis of rice (*Oryza sativa*) developing embryos using the RNA-Seq technique. *PLoS One* 7:e30646.
- Xu, S.B., Li, T., Deng, Z.Y., Chong, K., Xue, Y.B., and Wang, T. (2008). Dynamic proteomic analysis reveals a switch between central carbon metabolism and alcoholic fermentation in rice filling grains. *Plant Physiol* 148:908-925.
- Xuan, Y., Scheuermann, E.B., Meda, A.R., Hayen, H., von Wiren, N., and Weber, G. (2006). Separation and identification of phytosiderophores and their metal complexes in plants by zwitterionic hydrophilic interaction liquid chromatography coupled to electrospray ionization mass spectrometry. *J Chromatogr A* 1136:73-81.
- Xue, L.J., Zhang, J.J., and Xue, H.W. (2012). Genome-wide analysis of the complex transcriptional networks of rice developing seeds. *PLoS One* 7:e31081.
- Yamaji, N., and Ma, J.F. (2014). The node, a hub for mineral nutrient distribution in graminaceous plants. *Trends Plant Sci* 19:556-563.
- Yang, A., Dai, X.Y., and Zhang, W.H. (2012a). A R2R3-type MYB gene, OsMYB2, is involved in salt, cold, and dehydration tolerance in rice. *J Exp Bot* 63:2541-2556.
- Yang, X., Wu, F., Lin, X., Du, X., Chong, K., Gramzow, L., Schilling, S., Becker, A., Theissen, G., and Meng, Z. (2012b). Live and let die - the B(sister) MADS-box gene OsMADS29 controls the degeneration of cells in maternal tissues during seed development of rice (*Oryza sativa*). *PLoS One* 7:e51435.
- Yano, M., Katayose, Y., Ashikari, M., Yamanouchi, U., Monna, L., Fuse, T., Baba, T., Yamamoto, K., Umehara, Y., Nagamura, Y., et al. (2000). Hd1, a major photoperiod sensitivity quantitative trait locus in rice, is closely related to the *Arabidopsis* flowering time gene *CONSTANS*. *Plant Cell* 12:2473-2484.
- Ye, X.D., Al-Babili, S., Klotti, A., Zhang, J., Lucca, P., Beyer, P., and Potrykus, I. (2000). Engineering the provitamin A (beta-carotene) biosynthetic pathway into (carotenoid-free) rice endosperm. *Science* 287:303-305.
- Yi, X., Du, Z., and Su, Z. (2013). PlantGSEA: a gene set enrichment analysis toolkit for plant community. *Nucleic Acids Res* 41:W98-103.
- Yin, L.L., and Xue, H.W. (2012). The MADS29 transcription factor regulates the degradation of the nucellus and the nucellar projection during rice seed development. *Plant Cell* 24:1049-1065.
- Yokosho, K., Yamaji, N., Fujii-Kashino, M., and Ma, J.F. (2016a). Functional Analysis of a MATE Gene OsFRDL2 Revealed its Involvement in Al-Induced Secretion of

- Citrate, but a Lower Contribution to Al Tolerance in Rice. *Plant Cell Physiol* 57:976-985.
- Yokosho, K., Yamaji, N., and Ma, J.F. (2011). An Al-inducible MATE gene is involved in external detoxification of Al in rice. *Plant J* 68:1061-1069.
- Yokosho, K., Yamaji, N., and Ma, J.F. (2016b). OsFRDL1 expressed in nodes is required for distribution of iron to grains in rice. *J Exp Bot* 67:5485-5494.
- Yokosho, K., Yamaji, N., Ueno, D., Mitani, N., and Ma, J.F. (2009). OsFRDL1 Is a Citrate Transporter Required for Efficient Translocation of Iron in Rice. *Plant Physiol* 149:297-305.
- Yonekura-Sakakibara, K., Fukushima, A., and Saito, K. (2013). Transcriptome data modeling for targeted plant metabolic engineering. *Curr Opin Biotechnol* 24:285-290.
- Yoneyama, T., Ishikawa, S., and Fujimaki, S. (2015). Route and Regulation of Zinc, Cadmium, and Iron Transport in Rice Plants (*Oryza sativa* L.) during Vegetative Growth and Grain Filling: Metal Transporters, Metal Speciation, Grain Cd Reduction and Zn and Fe Biofortification. *Int J Mol Sci* 16:19111-19129.
- Zhan, J., Thakare, D., Ma, C., Lloyd, A., Nixon, N.M., Arakaki, A.M., Burnett, W.J., Logan, K.O., Wang, D., Wang, X., et al. (2015). RNA sequencing of laser-capture microdissected compartments of the maize kernel identifies regulatory modules associated with endosperm cell differentiation. *Plant Cell* 27:513-531.
- Zhang, R., Tucker, M.R., Burton, R.A., Shirley, N.J., Little, A., Morris, J., Milne, L., Houston, K., Hedley, P.E., Waugh, R., et al. (2016a). The Dynamics of Transcript Abundance during Cellularization of Developing Barley Endosperm. *Plant Physiol* 170:1549-1565.
- Zhang, S.J., Yang, W.Z., Zhao, Q.Q., Zhou, X.J., Jiang, L., Ma, S., Liu, X.Q., Li, Y., Zhang, C.Y., Fan, Y.L., et al. (2016b). Analysis of weighted co-regulatory networks in maize provides insights into new genes and regulatory mechanisms related to inositol phosphate metabolism. *BMC Genomics* 17.
- Zhang, Y., Liang, Z., Zong, Y., Wang, Y.P., Liu, J.X., Chen, K.L., Qiu, J.L., and Gao, C.X. (2016c). Efficient and transgene-free genome editing in wheat through transient expression of CRISPR/Cas9 DNA or RNA. *Nat Commun* 7.
- Zhang, Y., Xu, Y.H., Yi, H.Y., and Gong, J.M. (2012). Vacuolar membrane transporters OsVIT1 and OsVIT2 modulate iron translocation between flag leaves and seeds in rice. *Plant J* 72:400-410.
- Zhang, Z.L., Xie, Z., Zou, X., Casaretto, J., Ho, T.H., and Shen, Q.J. (2004). A rice WRKY gene encodes a transcriptional repressor of the gibberellin signaling pathway in aleurone cells. *Plant Physiol* 134:1500-1513.
- Zhao, F.J., Moore, K.L., Lombi, E., and Zhu, Y.G. (2014). Imaging element distribution and speciation in plant cells. *Trends Plant Sci* 19:183-192.
- Zhao, H., Ma, H., Yu, L., Wang, X., and Zhao, J. (2012). Genome-wide survey and expression analysis of amino acid transporter gene family in rice (*Oryza sativa* L.). *PLoS One* 7:e49210.
- Zheng, L.Q., Ying, Y.H., Wang, L., Wang, F., Whelan, J., and Shou, H.X. (2010). Identification of a novel iron regulated basic helix-loop-helix protein involved in Fe homeostasis in *Oryza sativa*. *BMC Plant Biol* 10.
- Zhou, G., Pereira, J.F., Delhaize, E., Zhou, M., Magalhaes, J.V., and Ryan, P.R. (2014). Enhancing the aluminium tolerance of barley by expressing the citrate transporter genes SbMATE and FRD3. *J Exp Bot* 65:2381-2390.

Zhu, T., Budworth, P., Chen, W., Provar, N., Chang, H.S., Guimil, S., Su, W., Estes, B., Zou, G., and Wang, X. (2003). Transcriptional control of nutrient partitioning during rice grain filling. *Plant Biotechnol J* 1:59-70.

8. Curriculum Vitae

Ting-Ying Wu

Nationality: Taiwan
Birthdate: 12th Nov. 1989

Education

Ph.D. Biology

Swiss Federal Institute of Technology in Zurich (ETHZ),
Zurich, Switzerland 2014- 2017

M.S. Biochemical Science and Technology

National Taiwan University, Taipei Taiwan 2011- 2013

B.S. Life Science

National Taiwan University, Taipei Taiwan 2007- 2011

Research experience

Research assistant

Agricultural Biotechnology Research Center, Academia Sinica, Taiwan 2013-2014

Publications

Research articles:

- **Wu TY**, Juan YT, Hsu YH, Wu SH, Liao HT, Fung RW, Chang YY (2013). Interplay between Heat Shock Proteins HSP101 and HSA32 Prolongs Heat Acclimation Memory Posttranscriptionally in Arabidopsis. *Plant Physiol* **161**: 2075-2084
- **Wu, T.Y.**, Kao, P., Chang, C.L., Hsu, P.H., Chou, C.H., Chang, I.,F. (2015). Phosphoproteomic profiling of microsomal fractions in leaves of Cogon grass (*Imperata cylindrica*). *Plant OMICS*
- Boonyaves K, **Wu TY**, Gruissem W, and Bhullar NK (2017). Enhanced grain iron levels in rice expressing an *IRON-REGULATED METAL TRANSPORTER*, *NICOTIANAMINE SYNTHASE* and *FERRITIN* gene cassette. *Frontier in Plant Science*, 8:130.
- **Wu TY**, Gruissem W, and Bhullar NK. Targeting intra-cellular iron transport combined with efficient uptake and storage significantly increases grain iron levels in rice. Submitted to PNAS.
- **Wu TY**, Marlen Müller, Gruissem W, and Bhullar NK. Genome-wide analysis on different regions of rice grain during grain filling stage. Manuscript in preparation
- **Wu TY**, Gruissem W, and Bhullar NK. Boosting citrate-iron translocation together with efficient uptake and storage significantly increases the endosperm iron and zinc concentrations in rice. Manuscript in preparation

Book chapter:

- Ping Kao, **Ting-Ying Wu** and Ing-Feng Chang (2011). "Decreasing of Population Size of *Imperata cylindrica* Mangrove Ecotype and Sea-Level Rising." *Global Warming Impacts- Case Studies on the Economy, Human Health and on Urban*

and National Environments, Chapter 12, ISBN: 978-953-307-785-7

Awards/ Honors

NSC Grant for bachelor research	2010-2011
Dean Award of College of Life Science	2011-2013
ETH fellowship	2014-2017
Best Poster Award in 13 rd International Symposium on Rice Functional Genomics (ISRFG)	2015